THE UNIVERSITY OF WARWICK

Library Declaration and Deposit Agreement

1. STUDENT DETAILS

Please complete the following:

Full name: Daniel E Mitchell

University ID number: 1162084

2. THESIS DEPOSIT

2.1 Under your registration at the University, you are required to deposit your thesis with the University in BOTH hard copy and in digital format. The digital copy should normally be saved as a single pdf file.

2.2 The hard copy will be housed in the University Library. The digital copy will be deposited in the University's Institutional Repository (WRAP). Unless otherwise indicated (see 2.6 below), this will be made immediately openly accessible on the Internet and will be supplied to the British Library to be made available online via its Electronic Theses Online Service (EThOS) service.
[At present, theses submitted for a Master's degree by Research (MA, MSc, LLM, MS or MMedSci) are not being deposited in WRAP and not being made available via EthOS. This may change in future.]

2.3 In exceptional circumstances, the Chair of the Board of Graduate Studies may grant permission for an embargo to be placed on public access to the thesis **in excess of two years**. This must be applied for when submitting the thesis for examination (further information is available in the *Guide to Examinations for Higher Degrees by Research*.)

2.4 If you are depositing a thesis for a Master's degree by Research, the options below only relate to the hard copy thesis.

2.5 If your thesis contains material protected by third party copyright, you should consult with your department, and if appropriate, deposit an abridged hard and/or digital copy thesis.

2.6 Please tick one of the following options for the availability of your thesis (guidance is available in the *Guide to Examinations for Higher Degrees by Research)***:**

☐ Both the hard and digital copy thesis can be made publicly available immediately

☐ The hard copy thesis can be made publicly available immediately and the digital copy thesis can be made publicly available after a period of two years (*should you subsequently wish to reduce the embargo period please inform the Library*)

☑ Both the hard and digital copy thesis can be made publicly available after a period of two years (*should you subsequently wish to reduce the embargo period please inform the Library*)

☐ Both the hard copy and digital copy thesis can be made publicly available after _____ (insert time period in excess of two years). **This option requires the prior approval of the Chair of the Board of Graduate Studies (see 2.3 above)**

The University encourages users of the Library to utilise theses as much as possible, and unless indicated below users will be able to photocopy your thesis.

☐ I **do not** wish for my thesis to be photocopied

3. GRANTING OF NON-EXCLUSIVE RIGHTS

Whether I deposit my Work personally or through an assistant or other agent, I agree to the following:

- Rights granted to the University of Warwick and the British Library and the user of the thesis through this agreement are non-exclusive. I retain all rights in the thesis in its present version or future versions. I agree that the institutional repository administrators and the British Library or their agents may, without changing content, digitise and migrate the thesis to any medium or format for the purpose of future preservation and accessibility.

4. DECLARATIONS

I DECLARE THAT:

- I am the author and owner of the copyright in the thesis and/or I have the authority of the authors and owners of the copyright in the thesis to make this agreement. Reproduction of any part of this thesis for teaching or in academic or other forms of publication is subject to the normal limitations on the use of copyrighted materials and to the proper and full acknowledgement of its source.

- The digital version of the thesis I am supplying is either the same version as the final, hard-bound copy submitted in completion of my degree once any minor corrections have been completed, or is an abridged version (see 2.5 above).

- I have exercised reasonable care to ensure that the thesis is original, and does not to the best of my knowledge break any UK law or other Intellectual Property Right, or contain any confidential material.

- I understand that, through the medium of the Internet, files will be available to automated agents, and may be searched and copied by, for example, text mining and plagiarism detection software.

- At such time that my thesis will be made publically available digitally (see 2.6 above), I grant the University of Warwick and the British Library a licence to make available on the Internet the thesis in digitised format through the Institutional Repository and through the British Library via the EThOS service.

- If my thesis does include any substantial subsidiary material owned by third-party copyright holders, I have sought and obtained permission to include it in any version of my thesis available in digital format and that this permission encompasses the rights that I have granted to the University of Warwick and to the British Library.

5. LEGAL INFRINGEMENTS

I understand that neither the University of Warwick nor the British Library have any obligation to take legal action on behalf of myself, or other rights holders, in the event of infringement of intellectual property rights, breach of contract or of any other right, in the thesis.

Please sign this agreement and ensure it is bound into the final hard bound copy of your thesis, which should be submitted to Student Reception, Senate House.

Student's signature:  Date: 17/12/2015

The Rational Design and Applications of Synthetic Antifreeze Protein Mimics

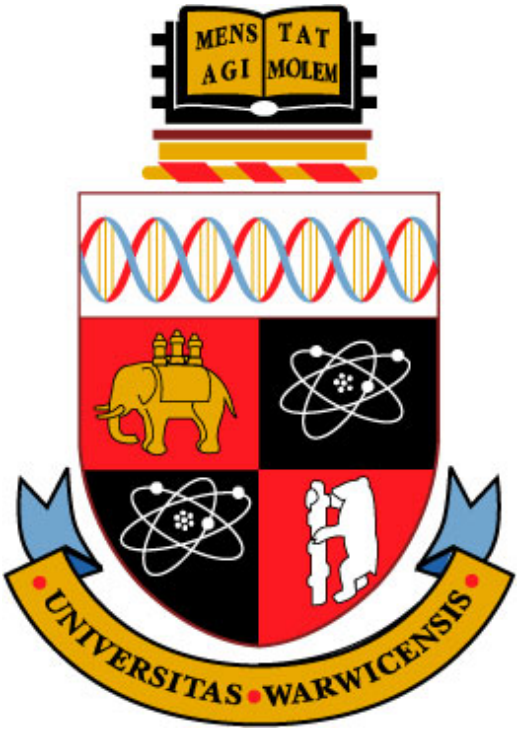

Daniel E. Mitchell

A Thesis submitted in fulfilment of the requirements
for the degree of
Doctor of Philosophy.

Molecular Organisation and Assembly of Cells
Doctoral Training Centre, University of Warwick.
September 2015.

Table of Contents

List of Figures and Schemes

List of Tables

Abbreviations

- AAT — Alanine- alanine- threonine
- ACVA — 4,4′-Azobis(4-cyanovaleric acid)
- AFGP — Antifreeze glycoprotein
- AFP — Antifreeze protein
- AR — Aggregation ratio
- AuNP — Gold nanoparticle
- B-Gal — β-Galactosidase
- BSA — Bovine serum albumin
- CD — Circular dichroism
- ConA — Concanavalin A
- CRD — Carbohydrate recognition domain
- CTA — Chain transfer agent
- DIS — Dynamic ice shaping
- DMSO — Dimethyl sulfoxide
- DPH — Diphenylhexatriene
- FTIR — Fourier transform infra-red
- Gal — Galactose
- GalNAc — *N*-Acetylgalactosamine
- GSH — Glutathione

- GO Glucose oxidase
- HEPES 4-(2-Hydroxyethyl)piperazine-1-ethanesulfonic acid
- HES Hydroxyethyl starch
- HSA Human serum albumin
- IgG Immunoglobulin G
- IR Ice recrystallization
- IRI Ice recrystallization inhibition
- ISP Ice shaping protein
- IVF *In-vitro* fertilization
- MD Molecular dynamics
- MSA Mercaptosuccinic acid
- NMR Nuclear magnetic resonance
- OSA Ovine serum albumin
- PAA Poly(acrylic acid)
- PAEMA Poly(aminoethyl methacrylate)
- PAEMA-*co*-SA anhydride Poly(aminoethyl methacrylate)-co-succinic anhydride
- PEG Poly(ethylene glycol)
- PBS Phosphate buffered saline
- PMEDS Poly([2-(methacryloyloxy) ethyl]dimethyl-(3-sulfopropyl) ammonium hydroxide)
- PMPC Poly(2-methacryloyloxyethyl phosphorylcholine)
- PMVEMA Poly(methyl vinyl ether-alt-maleic anhydride)
- PVA Poly(vinyl alcohol)

- PVP Polyvinylpyrolidone
- RAFT Reversible addition- fragmentation chain transfer
- RBCs Red blood cells
- RCA_{120} *Ricinus communis* agglutinin 120
- ROCK Rho-associated kinase
- ROS Reactive oxygen species
- SA Succinic anhydride
- SBA Soybean agglutinin
- SEC Size exclusion chromatography
- Taq Taq polymerase
- TEA Triethylamine
- TMS Tetramethylsilane
- TH Thermal Hysteresis

Acknowledgements

Firstly, I would like to thank my supervisor, Matt, for suggesting and helping me develop the project over the past three years, and who's huge enthusiasm and positivity has motivated me throughout my PhD. Secondly, thank you to Liz Fullam and Jose Gutiérrez-Marcos at life sciences for the opportunities to conduct research in their respective laboratories, and for help and advice on all things molecular biological. Thank you also to Giampiero Marconi in the Gutiérrez-Marcos group for experimental advice.

Thank you also to everyone in the Gibson group for advice, support and generally being a great group of people to work with. Especially, Tom for everything ice related, and the large amount of PVA you let me have, Dan for teaching me all about polymers, and Rob both for help with cryopreservation, and for how fast you have to run to get automatic entry into London marathon. Furthermore, I have felt privileged to work in a chemistry department equipped with such a wide range of scientific instruments, and I'd like to thank everyone who helped me make the most of these. Specifically, Ben Douglas for DSC and DLS, Kay and Raj for help with SEC, Nicola and Alison for letting me use their world class CD machines and Lijiang for his help with mass spectrometry. Without support from the EPSRC through MOAC DTC and particularly Nicola and Alison, I would not have been able to complete or even start this PhD, so thank you for everything you have done to help. Being part of MOAC

has been a wonderful experience and have enjoyed the opportunity especially the annual conference and getting to know some wonderful people.

Lastly, I would like to thank a number of friends and family who kept me sane over the last three years. Thank you to everyone at Kenilworth runners and Coventry Tri club and Warwick University Tri club for helping me get and keep fit, especially Mark and Anna, I didn't know what an Ironman was until I met you. Thanks to my friends back in Taunton also, who will be glad I'm finally nearly ready to get a proper job. I want to thank my parents for all their support and lastly my wonderful girlfriend Rhiannon for your love, support and for agreeing to proof read for me.

Declaration

The work presented in this thesis is entirely original and my own work, except where acknowledged in the text. I confirm that this thesis has not been submitted for a degree at another University.

Chapter 2 was published as:

D.E. Mitchell and M.I. Gibson, "Latent Ice Recrystallization Inhibition Activity in Non-Antifreeze Proteins; Ca^{2+} Activated Plant Lectins and Cation-Activated Antimicrobial Peptides". *Biomacromolecules*. 2015, Accepted.

Chapter 3 was published as:

D.E. Mitchell, M. Lilliman, S.G. Spain and M.I Gibson, "Quantitative study on the antifreeze protein mimetic ice growth inhibition properties of poly(ampholytes) derived from vinyl-based polymers." *Biomater. Sci.* **2014,** *2*, 1787–1795.

Chapter 4 is in revision for:

D.E. Mitchell, T. Congdon, A. Rodger, M.I. Gibson, "Gold Nanoparticle Aggregation as a Probe of Antifreeze (Glyco) Protein-Inspired Ice Recrystallization Inhibition and Identification of New IRI Active Macromolecules."

Chapter 5 is in preparation for:

D.E. Mitchell, R. Kaner, P. Scott and M.I. Gibson, "Metallohelices Mimic the Ice Recrystallization Inhibition Activity of Helical Antifreeze Proteins".

Chapter 6 was published as:

D.E. Mitchell, N.R. Cameron, M.I Gibson, "Rational, yet simple, design and synthesis of an antifreeze-protein inspired polymer for cellular cryopreservation." *Chem. Commun.* **2015**. 51, 12977-12980.

Chapter 7 is in preparation for:

D.E. Mitchell, R.C. Deller, J. Gutierrez-Marcos, M.I. Gibson, "A simple polymeric solution to the challenge of therapeutic protein storage".

Abstract

Antifreeze proteins (AFPs) and antifreeze glycoproteins (AFGPs) are proteins found in a wide variety of organisms adapted to survive in freezing temperatures. These proteins are powerful ice recrystallization inhibitors (IRI), slowing or even stopping ice crystal growth. This property is of significant interest in the area of cryopreservation due to ice recrystallization upon thawing being the limiting factor in the recovery of many biological materials. The need for reliable cryopreservation is becoming more and more necessary in many clinical areas, including regenerative and transplant medicine, and protein based therapeutics.

The identification of new protein structures and sequences is crucially to understanding this ability. To this end l-type lectins, which show sequential homology to type 2 AFPs were explored and found to possess calcium dependant IRI activity. In addition, a secondary motif, amphipathicity was investigated. As many AFPs possess separate well defined hydrophilic/ hydrophobic domains this was thought to be a property of high importance. The antimicrobial peptide nisin A, which is amphipathic, was found to also possess cation dependant IRI activity. This identification demonstrates a new approach to identifying IRI active molecules and may further enhance our understanding of the mechanisms involved. As current "gold standard" methods for identification of IRI activity are relatively slow and time consuming signifying that the discovery of new IRI molecules is a slow process. In order to increase throughput of the discovery of novel IRI active molecules a gold

nanoparticle assay was developed. Using this method serum proteins were discovered to possess weak but definite activity at higher concentrations. This is of particular interest as serum proteins such as fetal calf serum are commonly used in cryopreservation applications.

The isolation of these remarkable proteins from primary sources in significant quantities is difficult and not financially viable, while recombinant expression is complicated by glycosylation of AFGPs. Furthermore non-native proteins may cause immunogenic problems. Therefore synthetic mimetic such as polymers and small molecules are highly appealing. Using a biomimetic approach, amphipathic metallohelicies with alpha helical character similar to that of a type 1 AFP were evaluated for ice recrystallization inhibition. It was found that these metallohelices could be optimized to completely inhibit ice recrystallization, demonstrating that by creating materials which mimic AFPs similar properties can be engineered successfully. In addition, polyampholyte polymers (polymers possessing both positive and negative side chains) were synthesized, and demonstrated to possess IRI activity when the ratio of positive to negative side chains was roughly 1:1. These were then used to significantly enhance post-thaw recovery rates of red blood cells (RBCs). Polymers are appealing as they are highly tunable and can be used to mimic proteins in a wide variety of biological areas. Polyampholyte polymers and previously identified IRI polymer; polyvinyl alcohol (PVA), added to polyethylene glycol were found to be a highly efficient way of preserving proteins and antibodies under freezing conditions. The application of polyampholytes and other IRI active molecules are therefore highly attractive in the cryopreservation of a whole range of biological materials, potentially yielding widespread clinical benefits.

Chapter 1

1. Introduction

1.1. The frozen world

Ice plays an important role in a wide variety of areas, from evolutionary biology to geological weathering, to modern medicine,[1-3] due to its unique properties. Under terrestrial freezing conditions it forms a hexagonal crystal structure (ice 1h), but with up to 15 other crystalline structures are possible at higher pressures, more than any other known material.[4] There is also the phenomenon, that solid ice is less dense than liquid water unlike almost all other liquids. These unusual properties make the understanding of ice and particularly the ice-water interface extremely challenging, but vital for us to be able to explain for biotechnology, industry and fundamental science.

The prevalence of ice in many areas of the globe has lead to a wide variety of organisms evolved to thrive in areas where ice is present. As ice formation is a complex process, there is a lot we can learn from studying these life forms adapted to live in freezing conditions. The biological effect and methods by which living organisms can survive in cold temperatures have been of interest for scientific investigation for hundreds of years. Recently this interest has led to research into

areas including cryopreservation of cells and tissues,[3] treatment and prevention of cold induced injury such as frostbite[5] and protection of crops.[6] As the effect of cooling is to reduce biological degradation and extend storage time, cryopreservation has many potential applications. However, a significant challenge to storing human tissue, is that humans, and many other organisms have evolved to function at higher temperatures, with lower temperatures leading to cell damage and meaning that ice modulating materials could have a huge impact.

Many organisms including fish, beetles, plants and bacteria have been found to be able to survive temperatures below the freezing point of water, without the damaging effects caused by uncontrolled ice growth, using a variety of techniques.[7-9] The challenge is to fully understand these mechanisms and develop them for use in a variety of applications.

1.2. Cold survival methods in nature

1.2.1. Antifreeze glycoproteins

Average surface ocean temperatures at polar latitudes can drop as low as -1.9 °C presenting a stern challenge for life, yet many fish species thrive in such conditions using freeze-avoidance methods. This interesting ability was first investigated in Antarctic notothenioid fish species by DeVries and Schoolander over 45 years ago, and was found to be due to their unusual serum composition.[10-11] The fish possess higher concentrations of salts and sugars than fish found in warmer waters, but this only accounts for around 70 % of the observed freezing point depression. The other 30% was found to be due to the presence of a mixture of glycoproteins.[10, 12]

Furthermore, it was discovered that these glycoproteins depress the freezing point significantly more than would be expected from a concentration dependent colligative effect. To account for this non-colligative ability there must be some active, ice binding property associated with these glycoproteins and hence they were termed antifreeze glycoproteins (AFGPs).

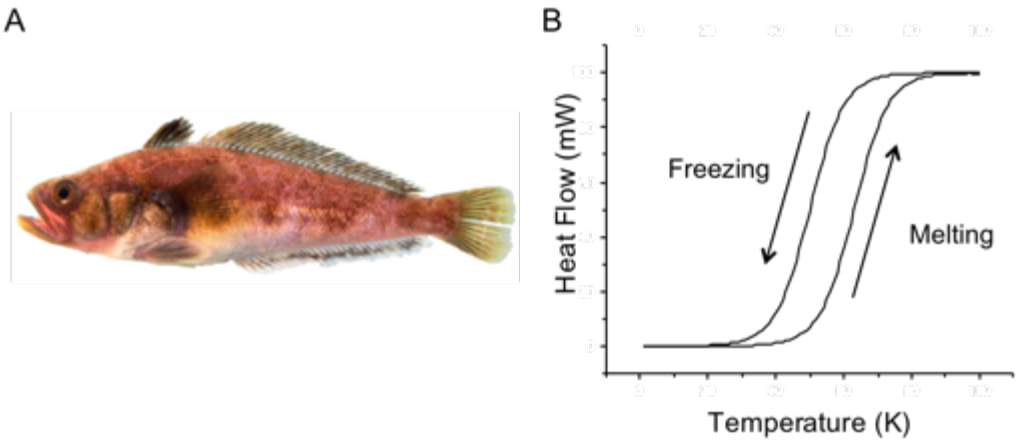

Figure 1.1. Notothenioid Antarctic fish species and associated thermal hysteresis properties. A.) Example notothenioid fish, *Trematomus hansoni*;[13] B.) Thermal hysteresis diagram of ice in the presence of an AFGP showing depressed freezing point with respect to melting point (Endothermic heat flow is shown as positive).

Additional investigation quickly uncovered the presence of several different AFGPs with differing molecular weights, all possessing a remarkably conserved primary sequence.[14-15] Each AFGP consists of varying numbers of repeating alanine-alanine-threonine (AAT) tripeptide units.[16] A complex disaccharide moiety, β-*D*-galactosyl(1→ 3)-α-*N*-acetyl-galactosamine was found to be joined as a glycoside to the hydroxyl group of the threonine residue, Figure 1.2.[17] To date, β-*D*-galactosyl(1→ 3)-α-*N*-acetyl-galactosamine is the only known disaccharide found in naturally occurring AFGPs, highlighting the importance of this specific sugar. Interestingly, this sugar is highly unusual in nature, the only other place where this

disaccharide is common is on a T-antigen associated with many human carcinoma cancers.[18] Further research has found that AFGPs are also found in evolutionary different Arctic cod species, despite being unrelated. This is a rare example of convergent evolution where two species evolve the same gene independently, probably driven by past climate fluctuations in both north and south polar areas.[19-20] More recently, AFGPs with very similar structures have also been discovered in several insect species.[21]

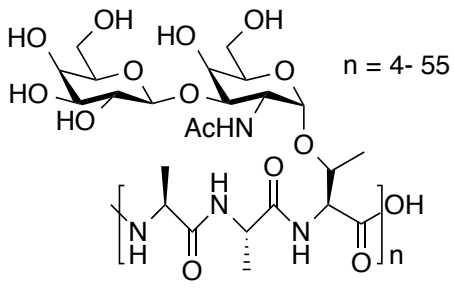

Figure 1.2. Chemical structure of an Antifreeze glycoprotein AFGP. The glycoprotein consists of a repeat unit of AAT peptide with complex disaccharide β-*D*-galactosyl(1→ 3)-α-*N*-acetyl-galactosamine connected to the threonine residue. AFGPs contain between 4 and 55 repeat units.

A large number of different sized AFGPs have been identified and categorised according to their molecular weight. These range from 2.6 kDa (4 repeat units) to 33.7 kDa (55 repeat units), classes 1-5 are usually sub-classified as large, while 6-8 are classified as small. While the large majority have the AAT repeat unit, there can be minor differences in the amino acid sequence, most commonly in classes 6-8 where the first alanine in a small number of the repeat units is replaced by a proline. In

addition, the recent isolation of an AFGP from the Antarctic fish *Pleuragramma antarcticum* suggests that further amino acid substitutions could be tolerated. In this case the AFGP consisted of the amino acids aspartic acid, glutamic acid, glycine, alanine with small amounts of arginine, threonine, valine and leucine and the sugar *N*-acetylglucosamine.[22]

In notothenioid fish species AFGPs have been found to present in virtually all body fluids, with the highest being present in the blood plasma.[23] Their regulation and expression is highly temperature specific, with day length having no effect on expression levels. At temperatures above 1 °C very little AFGP was observed in the blood plasma.[24] The process of AFGP production is both a product of evolutionary and environmental factors, with young Arctic cod, *Gadus morhua* caught in warmer areas found to be able to produce the same amounts of AFGP as those caught further north when kept in the same conditions. This is despite those cod caught further south never having experienced temperatures cold enough for AFGP expression.[25]

A range of techniques have been utilized to elucidate the primary, secondary and tertiary structure of AFGPs. Genetic analysis and various amino acid determination methods were used to ascertain the primary sequence discussed above.[15, 19] Structural information has been investigated using a variety of techniques including circular dichroism (CD), Raman spectroscopy, light scattering and NMR spectroscopy. The first CD study concluded that AFGPs have a random coil conformation,[15] and this was further re-enforced by independent studies using proton and carbon NMR spectroscopy and Raman spectroscopy.[26-27] This was followed by more detailed NMR analysis which suggested that AFGPs contain some turn structure.[28]

The most detailed insight has come more recently using a combination of high field NMR (500 MHz) and Fourier transform infra-red (FTIR) spectroscopies and molecular dynamics (MD) simulation. AFGP 8, a short chain length AFGP with small amounts of proline in its amino acid sequence, was found to display no significant long range order, but possesses a high amount of short chain ordering inducing a type 2 polyproline helical conformation. Using MD techniques to further probe AFGP 8 supported the NMR findings that a polyproline helix is the most probable conformation, although it was also discovered that several other conformations are equally as energetically favorable. Using the same methodology on a mixture of longer chain AFGP 1-5 it was reported that these particular proteins were unordered showing no long or short range ordering.[29-30] This suggests that AFGPs can adopt more than one structural conformation dependent on external conditions. Hydrogen bonding between the protein backbone and the *N*-acetyl groups were also found to play a role in the AFGP's stability.[31] Finally, separate ^{13}C NMR and FTIR analysis of an AFGP from *Arctogadus glacialis* probing its conformation in both solution and freeze-dried states, have further enforced the conclusion that AFGPs are highly flexible being able to access several conformational states.[32]

Despite the range of techniques described above, a three-dimensional structure of an AFGP has yet to be published.[33] The many structural conformations available, the high carbohydrate content and relative flexibility of the peptide backbone make it extremely difficult to produce a definitive structure.

1.2.2. Antifreeze proteins

In addition to the AFGPs described above, a second group of proteins with similar abilities, known as antifreeze proteins (AFPs) were first discovered in the fish species Winter flounder (*Pseudopleuronectes americanus)*.[34] Unlike AFGPs they lack any carbohydrate content. From this initial discovery AFPs have been found in a wide variety of different organisms, including insects, spiders, plants, bacteria and yeast.[35-38] Unlike AFGPs which have a highly conserved primary structure, AFPs have been found that exhibit a wide variety of differing amino acid sequences and defined tertiary structures.

To date, eleven different AFPs have been identified,[39] with four different types discovered in fish species alone (type 1 -4 AFPs).[40] Some species such as Winter flounder, *Pseudopleuronectes americanus* have even been found to express more than one AFP.[41] By investigating the evolutionary origins of these proteins it has been found that they have a very recent evolutionary history and multiple origins. For example type 2 AFPs are evolutionary similar to l-type lectins (sugar binding proteins),[42] while type 4 AFPs are highly similar to plasma apolipoproteins.[43]

Type 1 AFPs are the simplest AFP characterised, and consequently the most widely investigated. In contrast to AFGPs a high resolution crystal structure has been obtained, showing that it exists as a single alpha helical protein (Figure 1.3A).[44] Analysis of the protein sequence revealed that AFP type 1 consists of 37 amino acids, with a high percentage of alanine, and a repeat sequence of 11 amino acids with highly arranged polar and non polar residues.[45] This helical structure results in all the

hydrophobic residues being on one face of the helices, and recent MD simulations investigating this surface suggests that it is these that are involved in ice binding.[46]

Type 2 AFPs are also extremely well studied. They are large globular proteins rich in cysteine and lacking and repetitive amino acid sequences. The structure was solved by NMR spectroscopy and was found to be rich in alpha helices (18 %), beta sheets (38 %) and random coils (44 %),[47] while the cysteine residues play a large role in tertiary structure through disulphide bonding (figure 1.3B). As mentioned above they show similarity to l-type lectins including a binding pocket which appears to bind to ice rather than sugar molecules.[48]

Similarly, type 3 AFPs also possess a globular structure, although lack the cysteine residues characteristic of their type 2 homologues. They characteristically show high amounts of beta sheet, while the ice-binding surface is thought to be a flat amphipathic region (Figure 1.3C).[49] Type 4 AFPs are different yet again, containing high amounts of glutamate and glutamine, and a high helical content as discovered by CD spectroscopy. The tertiary structure was found to consist of a 4 helix bundle orientated with the more hydrophobic surfaces pointing inwards.[50] No one has yet completely solved the three-dimensional structure of a type 4 AFP.

Insects can live in terrestrial environments with lower temperatures (-30 °C) compared to fish (-1.9 °C), so the AFPs need to be significantly more efficient and are often termed hyperactive AFPs. One of the most widely studied of these is found in the moth *Tanebrio molitor,* the crystal structure indicates the presence of 7 different coils, most of which contain β-strands (Figure 1.3D).[51] Furthermore, it has a high amount of disulphide bonding and a regular array of threonine- cysteine- threonine

motifs on one side. This motif is thought to allow the threonine residues to align with both basal and pyramidal planes of an ice crystal, inhibiting growth in both directions, where as fish AFPs only seem to bind to the pyramidal plane.[52]

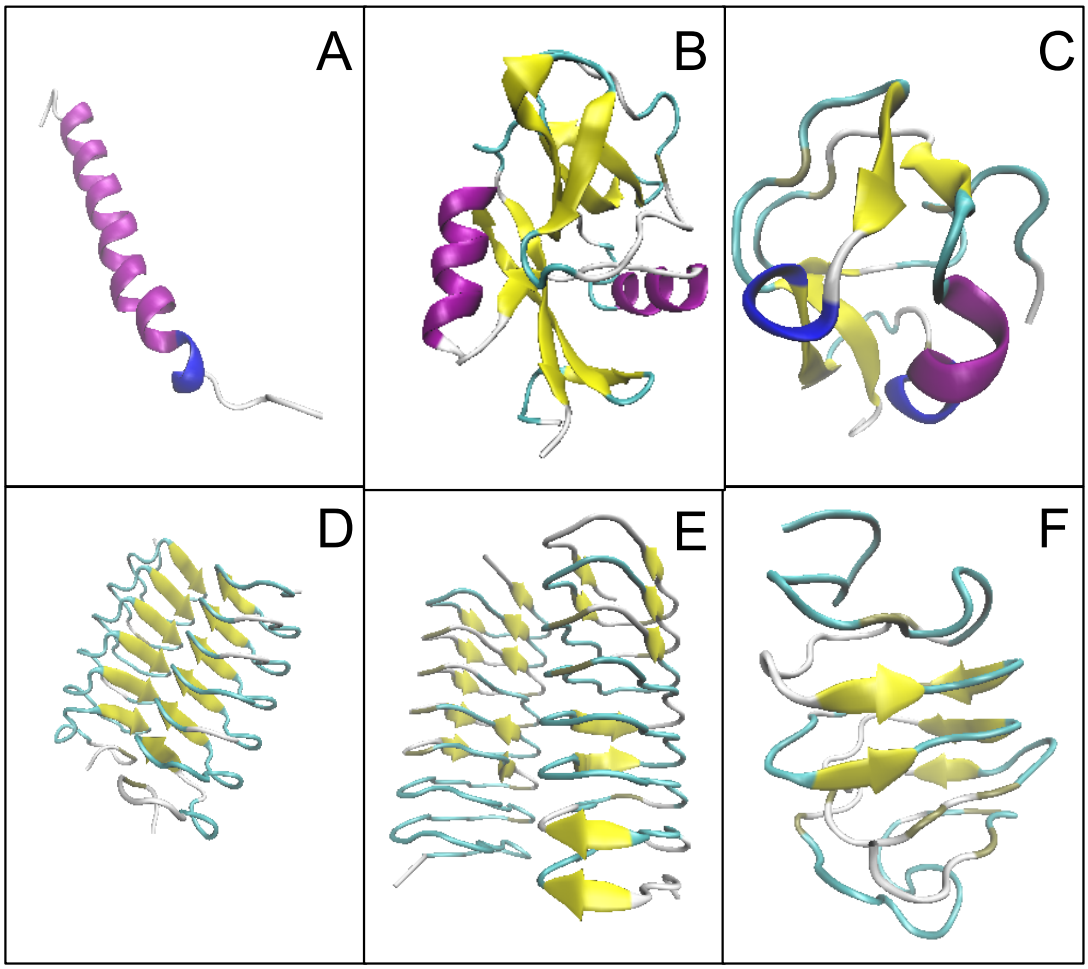

Figure 1.3. Structural representation of various AFPs. (A) Type 1 AFP from shorthorn sculpin, (Kwan *et al*. 2005);[53] (B) Type 2 AFP from herring (Liu *et al*. 2007);[54] (C) Type 3 AFP from ocean pout (Antson *et al.* 2001);[55] (D) Insect AFP from *Tanebrio molitor (*Liou *et al* 2000*)*;[51] (E) Plant AFP from grass Lolium perenne (Middleton *et al.* 2012);[56] (F) Insect AFP from spruce budworm (Graether et al. 2000).[57]

The final group of AFPs discussed here is those produced by plant species. These have been found to contain high amounts of beta sheet, and recent crystallography

data of an AFP from ryegrass *Lolium perenne* suggests that they have the ability to bind to both basal and pyramidal planes (Figure 1.3E).[58] However the irregular spacing of ice binding sites containing serine, threonine and valine means that it has relatively weak activity compared to hyperactive insect AFPs.

To date only one plant AFP has a solved crystal structure, conversely many insect AFPs have been identified, including those recently found from spruce budworm (*Choristoneura fumiferana*) (Figure 1.3F) and snow flea *Hypogastrura nivicola*.[59] It is highly probable that a wide range of highly different plant and insect AFPs similar to those found in fish will be observed in future research. Overall, the wide variety of different AFPs described above highlights the many methods that nature has evolved to overcome the problem of freezing, while also demonstrating that identifying why something has "antifreeze" activity is not trivial.

1.2.3. Other cryo-survival methods

Several non-protein based strategies have also discovered, mainly in amphibians and insects. These strategies involve a mixture of freeze tolerance and freeze avoidance, in contrast to AFGPs and AFPs, which are exclusively the latter.[60] One protein free strategy is the synthesis of large volumes of carbohydrates to prevent freezing; a drop in temperature such as that experienced at the start of winter leads to a metabolic change, resulting in the production of large amounts of one or more small molecules. For example, in many frog species large amounts of glycogen is stored in the liver prior to hibernation and is redistributed around the body as glucose in the event of the skin experiencing freezing temperatures.[61] These cryo-protectant molecules are found in a range of organisms and are commonly polyols and sugars such as

trehalose, glucose, glycerol and sorbitol (Figure 1.4) and are often produced in conjunction with ice nucleation agents such as ice nucleating proteins (INPs), allowing ice to form in a controlled manner.[62]

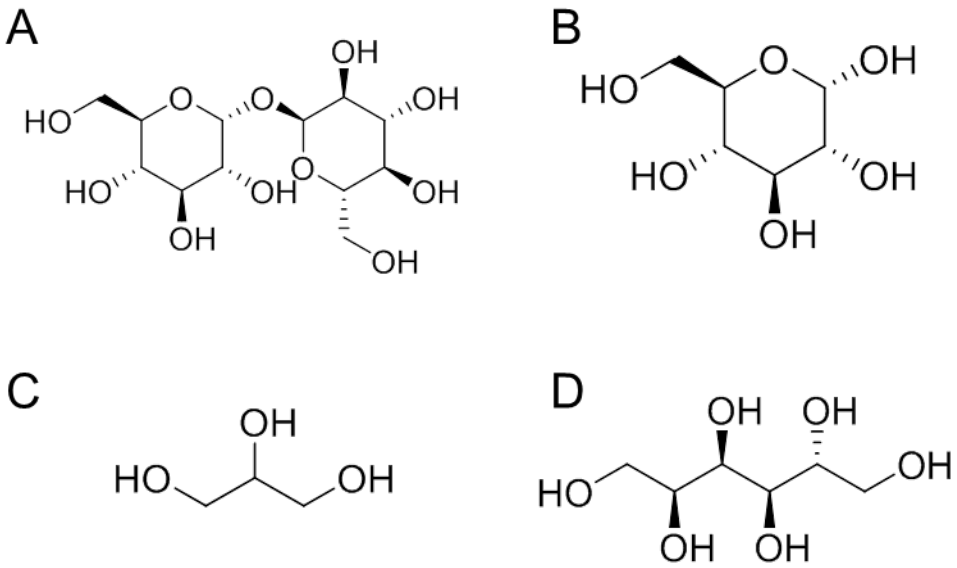

Figure 1.4. Polyols commonly used in cryo-survival. (A) trehalose; (B) glucose; (C) glycerol; (D) sorbitol.

The synthesis of large quantities of polyols can also result in vitrification, a phase transition in which water freezes into a glassy state, rather than a crystalline one. Unlike freezing, vitrified ice is not destructive towards biological material. This is very common in many sub-arctic plants where vitrification of seeds and twigs are key to survival over winter.[63]

While vitrification is highly desirable for many animals, some organisms can survive relatively high amounts of freezing (up to 65 % of total body water).[64] The onset of freezing is highly controlled resulting in a very gradual ice formation occurring over a period of several hours or even days, resulting in dehydration of the intracellular space making ice formation largely extracellular, although studies have shown that

intracellular ice formation can be tolerated in certain larger cell types.[65] Large amounts of carbohydrates are also produced, stabilizing cellular macromolecules and limiting intra-cellular freezing.

A further survival method is that of anhydrobiosis; avoiding the damaging effect of freezing by reducing the amount of water present to miniscule amounts. This is most common in microorganisms, although is also used as a protection method in seeds and spores.[66] Similar to the methods discussed above, several carbohydrates are routinely expressed in order to stabilize cellular and sub-cellular material.[67] While these carbohydrates are widely used to enable life to exist in freezing conditions, the concentrations required are significantly higher than those found for AFPs and AFGPs, meaning the latter are highly appealing for scientific investigation as low concentration inhibitors.

Finally, several sugar molecules containing little or no protein have recently been found to exhibit similar antifreeze activity to an AFP or AFGP. This includes the isolation of a xylomannan carbohydrate macromolecule from the Alaskan beetle, *Upis ceramboides,* figure 1.5.[68] The recognition of the ability of this xylomannan to act as an antifreeze molecule was further enforced by its more recent discovery in several other species including 6 insect, one plant, and one frog species.[69]

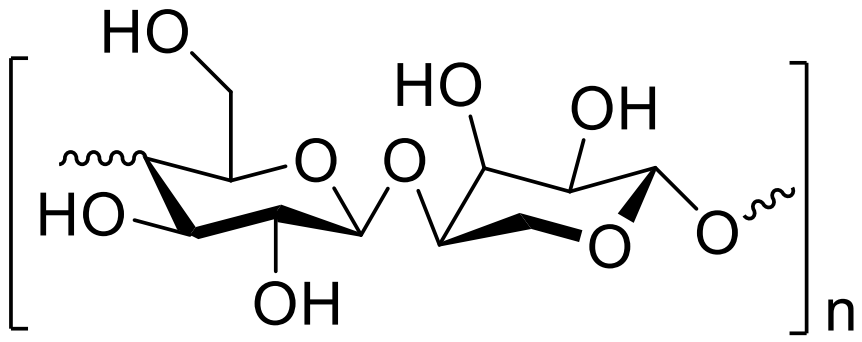

+ Lipid Component

Figure 1.5. Xylomannan disaccharide core strucutre from Alaskan beetle *Upis ceramboides*.[68]

A further polysacharide from the marine bacteria species *Colwellia psychrerythraea* has also been recently discovered. Interestingly, through NMR studies and MD simulation, this polysaccharide exhibits a structure very similar to an AFGP.[70] This vast range of methods and molecules used by organisms to survive in freezing conditions, highlights the importance of this phenomenon and has inspired a range of potential applications. The following sections will expand on the unique antifreeze properties of AFPs and AFGPs rather than polyols since they possess the ability protect an organisms at remarkably low concentrations, making them incredibly appealing for a range of applications.

1.3. Interactions of AFGPs with ice

As described above, AFPs and AFGPs have been discovered to depress the freezing point of water by a much greater amount than would be expected due to colligative effects. This interesting ability signifies that another, active process must be occurring

to account for this. After much investigation, three separate properties have been identified that explain the interactions observed,[71] all of which are described in detail below.

1.3.1. Thermal hysteresis

Thermal Hysteresis (TH) is the depression of a liquid's freezing point relative to that of its melting point. Upon the addition of any solute to a solvent a freezing point depression is observed due to a colligative effect (i.e. a thermodynamic effect similar to that of osmotic pressure or boiling point elevation) whereby the equilibrium point of freezing and thawing is lowered proportionally to the concentration of solute (point at which Gibb's free energy of freezing and thawing are equal.).[71] However, in solutions containing AFGPs, the freezing point can actually be observed to be lower than the melting temperature, Figure 1.6. In some cases this can be up to 1000 times that of the predicted colligative effect. This effect is asymptotically concentration dependent, so after a certain concentration there is no further TH increase.[72] This can be observed experimentally using a nanolitre osmometer to hold an ice crystal in this hysteresis gap. The ice crystal will not grow or melt as long as it is in this range, allowing the precise TH gap to be found. It should be noted that the observation of this property requires high concentrations, typically > 20 $mg.mL^{-1}$.

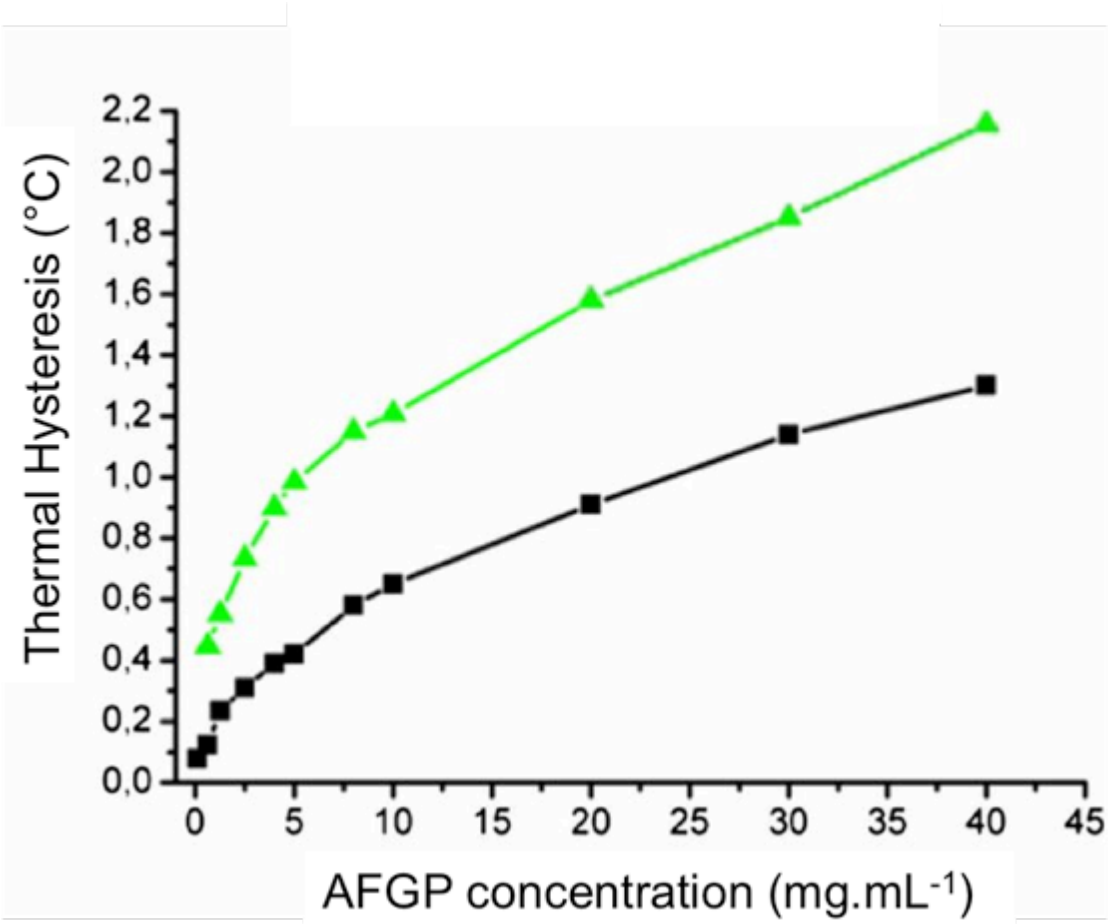

Figure 1.6. Example of concentration dependant thermal hysteresis of AFGP from *Dissostichus mawsoni*. Black data points are TH activity in water, green data points in citrate buffer, adapted from Meister *et al.* 2013.[73]

1.3.2. Dynamic ice shaping

Dynamic ice shaping (DIS) refers to an AFP or AFGP's ability to shape the morphology of a single ice crystal. This is due to the commonly observed preferential binding to the pyramidal faces of the ice crystal as oppose to the basal faces, and results in a spicular shape developing, Figure 1.7.

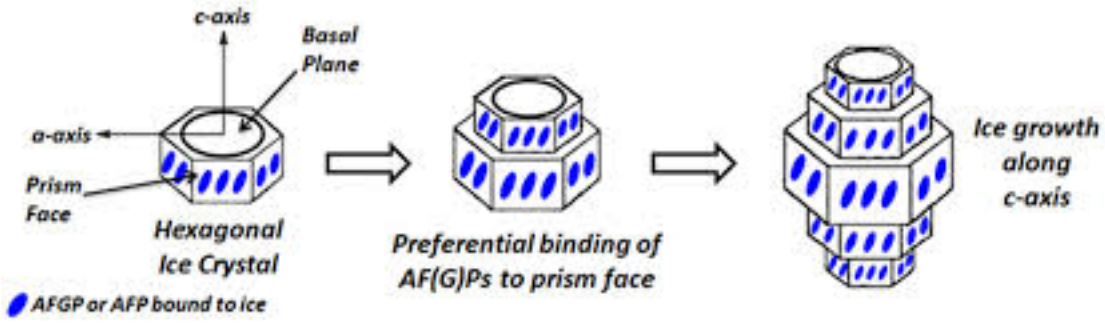

Figure 1.7. Dynamic ice shaping of antifreeze proteins. Growth of the ice crystal is preferentially along the c-axis, due to binding on the pyramidal face. Adapted from Capicciotti *et al.* 2013.[74]

DIS can generally be observed using a nanolitre osmometer holding the crystal as close to freezing point as possible, or in the TH gap between freezing and melting if there is one. Other methods for observing this phenomenon include hemisphere etching and wide-angle x-ray diffraction.

1.3.3. Recrystallization inhibition

The third property that AFGPs possess is recrystallization inhibition (RI), the ability to slow the rate of ice crystal growth. Ice recrystallization can be considered an Ostwald ripening process, whereby small crystals dissolve and larger crystals grow, resulting in a smaller number of bigger crystals, minimizing surface energy. This is usually measured using a "splat assay" developed by Knight *et al*.[75] Briefly, this involves dropping a small droplet of solution from a height of > 1 m onto a surfaced cooled sufficiently that the droplet freezes instantly (< -50 °C). This produces a thin wafer of small crystals typically less than 10 μm diameter, which are annealed on a temperature controlled microscope stage at a desired temperature for a desired amount

of time (typically – 8 °C for 30 minutes), Figure 1.8. The value frequently reported in the literature is usually the mean of the largest dimension for the 10 largest crystals in any wafer. The above method also eliminates the ice nucleation process as a variable, making it highly repeatable and is therefore the method most often used when determining ice recrystallization inhibition (IRI) activity.

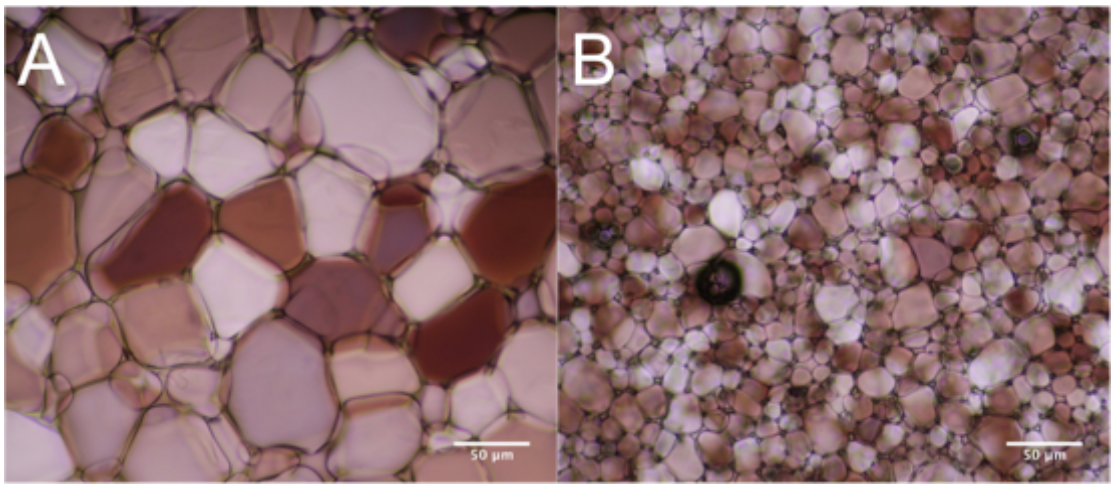

Figure 1.8. Example wafers from splat test method for determining IRI activity. (A) PBS buffer control; (B) PBS with the addition of an IRI inhibitor. Both samples are at the same magnification, images were taken after 30 minutes at -8 °C.

Despite the "splat assay" method being highly repeatable, it is not very high-throughput and consequently several other methods have been introduced, including use of capillary tubes,[76] the addition of high concentrations of solutes such as sucrose,[36, 77] and even the use of microfluidic systems.[78] In a further attempt to increase throughput time of IRI asaays, domain recognition software was recently introduced by Jackman *et al.*,[79] but there remains no truly high throughput system for the identification of IRI activity. As ice crystal growth is a major problem in cellular

cryopreservation, the inhibition demonstrated by AFGPs is of high interest commercially.[80-81]

1.3.4. Structure binding relationships of AFGPs

The exact interaction between an AFGP and ice is not currently totally understood, although several hypotheses have been proposed. To determine the ice-binding point mutations of AFPS and the synthesis of synthetic mimics have been produced to assess the effect of the substitution of amino acid residues and modification to glycans. Initial models assumed that hydrogen bonding was responsible for this interaction based on the facts that threonine and other polar residues can hydrogen bond with water and that the peptide sequence was a repeat unit. Two contrasting models were developed, one in which functional groups tightly bind in a zipper like fashion to the ice surface,[82] and the other which postulates that the functional groups could be incorporated into the ice lattice.[83]

However, more recent studies have cast doubt on this hydrogen bonding mechanism. This includes the substitution of Thr for Val, preserving the methyl group but not the hydroxyl moiety, reducing the ability of the protein to hydrogen bond. The protein containing Val amino acid still retained its activity, thus suggesting that the binding is due more to Van der Waals interactions.[84] This is reinforced by modelling undertaken by Wen and Laursen, which also suggests an active role for Van der Waals interactions possibly in combination with hydrophobic forces.[85]More recently, several investigations involving both experimental and theoretical study, have demonstrated the importance of hydrophobic interactions between the AFGP and ice

and implies that this method of interaction could be most significant in the antifreeze activity of an AFGP or AFP.[46, 86-88]

The first model describing the method of action of an antifreeze molecule was that of Raymond and DeVris, who proposed a mechanism of adsorption and inhibition after observing ice crystals with a distinct hexagonal bipyramid shape, suggesting that growth on the prism faces was being inhibited.[89] It is believed that crystal growth proceeds by propagation of a step across a crystal face. When an AFP or AFGP binds to the crystal surface in the path of a growing step it will only be able to grow in the gaps between the bound molecules in curved fronts, Figure 1.9. The growth of these curved fronts leads to a higher surface energy than that of a flat surface causing the transformation of water into ice to be less favourable therefore reducing the freezing temperature and growth rate of AFP bound crystals. This is known as the Kelvin or Gibbs-Thompson effect.[90-91]

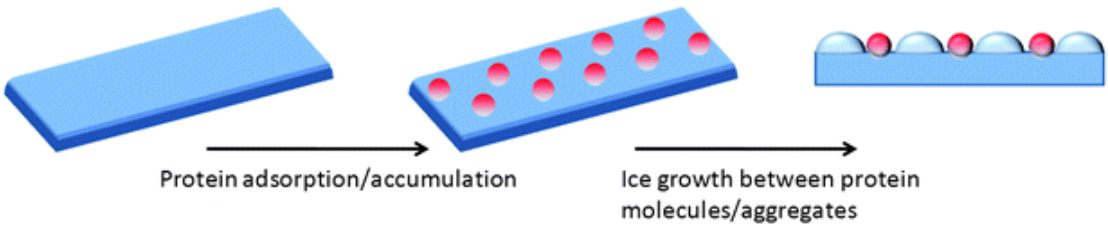

Figure 1.9. Ice growth in curved fronts. Growth of Curved fronts increasing surface energy and therefore decreasing growth rate. Adapted from Gibson, 2010.[71]

Several groups have further developed the adsorption-inhibition model. These include, most notably, the button mattress model of Knight and co-workers and the step- pinning model proposed by Raymond *et al*.[89, 92] The button mattress model

hypothesises that a bound AFP inhibits growth of the ice lattice around it, therefore creating a button-mattress like surface, where as the step-pinning model postulates that the bound antifreeze molecules inhibit growth on the surface by preventing propagation of the step. Both of these models assume that the antifreeze binds irreversibly to the ice surface since desorption would results in rapid crystal growth in the areas where the AFP desorbed.

Although studies by Celik *et al.* and Knight and DeVries investigating the super heating of ice in the presence of an AFP, with support from recent experimentation using microfluidics, strongly suggest that at least some AFPs can bind irreversibly to the ice surface, there has been some criticism of this theory.[78, 93-94] This includes the assumption that the water- ice interface is sharp, despite evidence that the transition from the solid phase to the liquid at the interfaces are gradual and occur over several layers of water molecules, known as the quasi-liquid layer.[88]

In 1999, Hall and Lips proposed an alternative model suggesting that AFPs are adsorbing reversibly to a rough surface, based on the observation that the free energy of adsorption is almost zero. They envisage a layer of AFPs on the crystal surface with a dynamic exchange of molecules at the ice water interface. The AFP would increase the step energy associated with the formation of a 2D nucleus thereby leading to a reduction in freezing point.[95] Despite this model having some success in mathematically describing experimental findings, there are limitations. Recent findings by Celik *et al.*, that surface bound AFPs still inhibit ice crystal growth in a solution depleted of AFPs, showing that a dynamic exchange between free and adsorbed AFPs is unlikely.[78] Overall, there is still currently some disagreement as to

the exact mechanism of binding and inhibition, which remains to be determined by further investigation.

In addition, the molecular mass is also found to play a role in the level of antifreeze activity. In a study by Wu *et al.* it was found that AFGPs could be separated into two distinct classes, those above 13 kDa and those below. Those above showed 3-4 times greater TH activity than those which were smaller.[96]

A further recent hypothesis for the strength of certain hyperactive AFGPs is that the short range binding mechanisms are supplemented by long range interactions. Ebbinghaus *et al.* postulate that this could be due to a large hydration shell formed around the AFGP, as hydration water has a lower freezing point compared to bulk water.[97] In addition, from computer simulation and terahertz absorption spectroscopy of an AFP isolated from the beetle *Dendroides canadensis*, it has been found that protein-water interactions are present up to a distance of 20Å and play an essential role in the strong thermal hysteresis (TH) activity observed.[73]

1.4. Synthetic mimics

AFPs and AFGPs are of much interest in a range of different areas, including cryopreservation, cryosurgery and food technology due to their interesting properties.[98-100] However, there are significant challenges associated with isolating these proteins from their host species and expressing useful amounts using recombinant methods, while there are also potential immunogenic problems with *in vivo* uses. In addition to this, there is still the challenge of identifying which structural motifs provide “antifreeze” activity.

To overcome these challenges several attempts at modifying AFGPs have been reported. A detailed structure-property relationship study on AFGPs was undertaken by Nishimura and co-workers, although it should be noted that only TH and DIS were investigated, Figure 1.10.[101] An important observation was that a single tripeptide motif could influence ice growth while possessing no measureable TH, and that structural changes could be made while still maintaining antifreeze activity. For example, changing the linkage between the sugar and peptide backbone from the native α to its β analogue resulted in no TH activity while maintaining DIS activity. Overall the *N*-acetyl group at the C-2 position on the sugar was found to be essential for TH activity while ice shaping was maintained without it. From circular dichroism it was found that the presence of the *N*-acetyl group was important for forming a polyproline secondary structure. Furthermore the addition of charged moieties resulted in loss of both TH and DIS activity. This suggests that TH requires a certain secondary structure while DIS does not, allowing these properties to be effectively de-coupled.

In 2003, Enaide *et al.* observed that highly simplified glycoproteins retained IRI activity while possessing no TH or DIS activity, suggesting that there could be multiple molecular mechanisms that can lead to the same macroscopic properties, and that it is possible to design molecules that specifically display IRI activity.[102]

Entry	Structure	TH active	Ice Shaping
Peptide Backbone	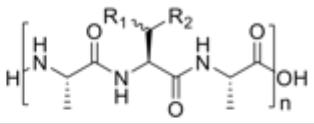	N/A	N/A
1	R_1 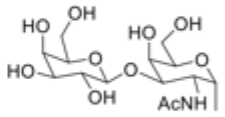 R_2 CH_3	Yes	Yes (pyramidal)
2	R_1 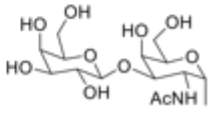 R_2 H	No	Yes (hexagonal)
3	R_1 OH R_2 CH_3	No	No
4	R_1 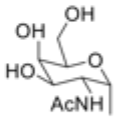 R_2 CH_3	Yes	Yes (pyramidal)
5	R_1 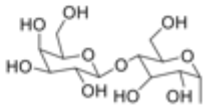 R_2 CH_3	No	Yes (hexagonal)
6	R_1 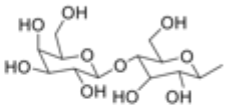 R_2 CH_3	No	No
7	R_1 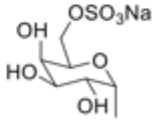 R_2 CH_3	No	No

Figure 1.10. Selection of synthetic AFGPs synthesized by Nishimura and co-workers, demonstrating necessary moieties for TH activity.

Ben and co-workers have shown that it is possible to make reasonably large structural modifications, creating glycopeptides that maintain IRI activity but display no measurable TH activity.[103-104] To explain this phenomenon, they proposed the use of hydration number as a predictive tool.[105] This was defined as the number of tightly bound water molecules divided by the carbohydrate's molar concentration, and was found to correlate well with IRI activity. None of these AFGP mimics possessed the ability to shape ice, which suggests that they are not binding and affecting the growth of the ice crystal itself, leading to the hypothesis that these glycopeptides act at the quasi-liquid layer instead.[104] As the glycopeptide would be excluded from the ice crystal lattice during freezing the concentration in this layer would increase, and consequently the number of hydrated water molecules would also increase. It is postulated that only the free water molecules can add to ice crystals meaning that crystal growth is inhibited.

Several other groups have also investigated the production of synthetic antifreeze mimics, including Heggemann *et al.* who used microwave assisted solid phase peptide synthesis to vary the protein backbone sequence of AFGPs including the insertion of glycine and serine, not normally found in nature.[106] Finally Nishmura and co-workers synthesized cyclic AFGPs which possess strong DIS and TH activity, although IRI activity wasn't investigated.

With recent advances in controlled radical polymerisation and post-polymerisation,[107-108] synthetic polymers have become more appealing as biomimetics for a range of different areas including antimicrobial peptides, cell

signalling and mussel adhesion proteins.[109-111] Despite this, there has been relatively little study into the area of polymers displaying similar properties as AFGPs and AFPs. However there has been some, limited work into polymers that display IRI activity. The first observations that polymers could inhibit ice recrystallization were made by Knight *et al.*, who investigated four polypeptides and 3 vinyl polymers.[112] Specifically they found that poly vinyl alcohol (PVA) (figure 1.11A) was an extremely potent IRI macromolecule, while poly(*L*-Histidine) (figure 1.11B) and poly(hydroxyproline) (figure 1.11C) also acted as inhibitors at relatively low concentrations (< 1 $mg.mL^{-1}$). This is remarkable, given that there is significant differences in structure, both between polymers and to native AFGPs. Poly(*L*-Histidine) is also the first case of any IRI active molecule that does not have large amounts of alcohol units.

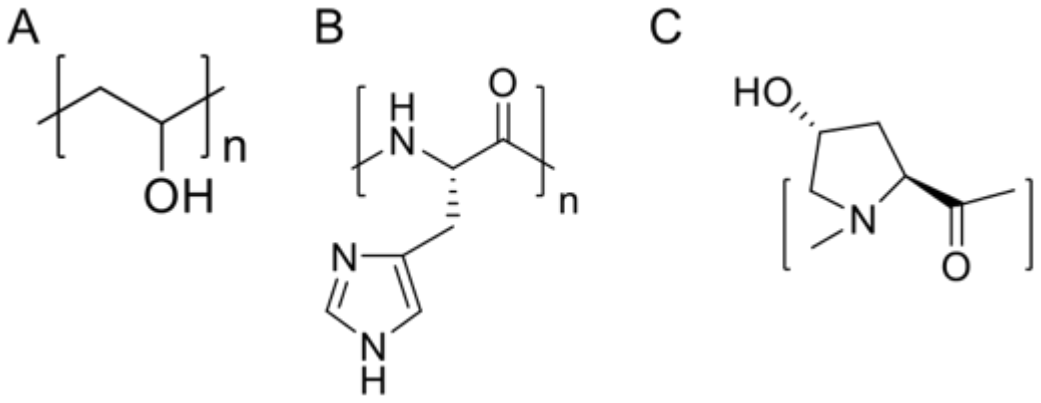

Figure 1.11. Synthetic polymers found to possess IRI activity. (A) Poly vinyl alcohol (PVA); (B) poly(*L*- Histidine); (C) poly(hydroxyproline).

This was followed by a study from Börner and co-workers who synthesized poly(tarter amides), suggesting that some limited TH and IRI activity was present, although in the case of IRI no quantitative measurement was taken.[113] Importantly, they found that the length of backbone spacer played an important role on the

properties of the polymer, demonstrating that the spacing between groups interacting with the ice is important.

Although many polymers were investigated, PVA was the only one found to display IRI activity similar to that of an AFGP or AFP. Inada and co-workers have extensively investigated PVA with respect to it's IRI activity, finding that there is a strong correlation between molecular weight and ice recrystallization inhibition.[114] Likewise the degree of hydrolysis also correlated well with increasing activity, the same group followed this analysis with further investigation demonstrating that PVA exhibits small but measureable DIS and TH activity.[115-116] The above findings were supported by more recent findings by Congdon *et al*. showing that IRI activity is "turned on" when the polymer size increases from 10 to 20 repeat units, Figure 1.12.[117] Furthermore, it was also found that the substitution of the polymer side chains was not well tolerated, although hydrophobic modifications were slightly less inhibitory than hydrophilic, implying that an unbroken chain of hydroxyl groups is important for activity.

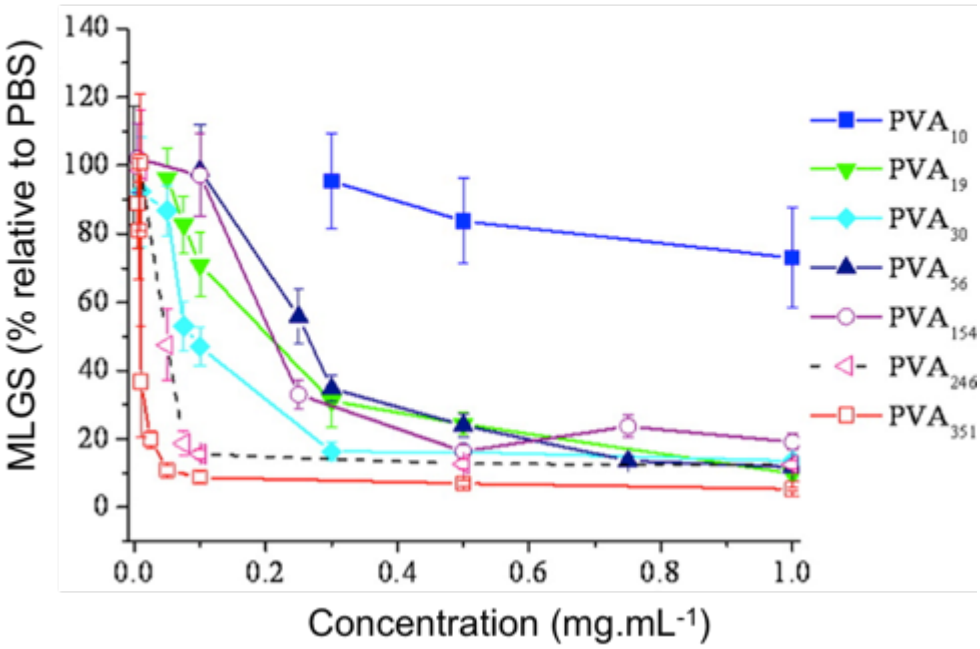

Figure 1.12. IRI activity of PVA with varying repeat units. MLGS (mean largest grain size) is expressed as a percentage relative to PBS buffer. IRI activity is turned on when increasing from 10 to 20 repeat units. Adapted from Congdon *et al.* 2013.[117]

Several further attempts have been made at determining the reason for PVA's remarkable IRI activity despite it bearing little similarity to an AFGP or AFP. Deller *et al*. tested an extensive range of polyols finding that from a large library of saccharides, polymers and small molecules, PVA is the only one to exhibit IRI activity, further suggesting that the spacing of hydroxyl groups and structure of the polymer plays an important role.[118] In addition, polyethylene glycol (PEG) and poly(acrylic acid) (PAA) two other commonly used polymers no activity. Budke and Koop postulated that the hydroxyl groups have very similar spacing to the prism planes of hexagonal ice, suggesting that spacing is critical.[119] However this does not agree with the AFP model, where a hydrophobic face binds to ice raising the possibility of multiple mechanisms for IRI activity.

The use of PVA in cryoprotective applications is highly appealing as, unlike AFGPs and AFPs, it can be synthesized on a large basis for relatively low cost. It is also biocompatible and biodegradable and has the advantage of already being FDA approved.[120-121] However it should be mentioned that a type 3 AFP (named ice shaping protein (ISP) 3) has been found to be non toxic in oral studies, and is currently used by Unilever PLC in ice cream to improve quality and storage lifetime.[122-123] Despite this promise no IRI active molecule is currently used in a clinical setting.

Complexes of zirconium acetate (Figure 1.13A) and zirconium acetate hydroxide (Figure 1.13B) were identified to posses ice shaping properties, similar to those reported for AFGPs and AFPs although only at specific pH values (pH 3-5).[124] The low molecular weight (327 $g.mol^{-1}$) make this particularly interesting as previous studies have observed a positive correlation between size and activity.[33, 117] This was expanded in a study by Mizrahy *et al.* who investigated both TH and IRI activity in addition to ice shaping behaviour, finding that these complexes have negligible TH behaviour, but possess IRI activity in addition to ice shaping ability already found.[125] The authors also surmise that the complexes undergo a relative degree of oligomerization giving activity at certain pH values, and that the functional groups involved in ice binding are acetate and hydroxyl moieties. Although this compound is relatively cheap, making it commercially attractive, it may be undesirable as a cryoprotectant due to the potential toxicity effects associated with high concentrations of metals and would be of more use in material science applications.

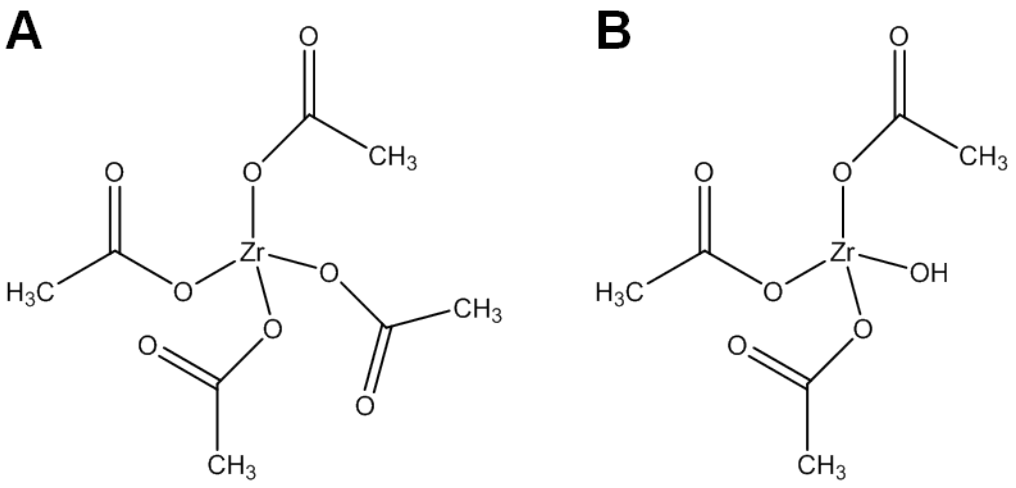

Figure 1.13. Zirconium acetate IRI complexes; (A) Zirconium acetate; (B) Zirconium acetate hydroxide.

Overall the synthetic AFGP/ AFP analogues described above demonstrate the wide variety of different structures that can interact with ice, and there are still significant challenges in understanding the rules of rationally designing an antifreeze molecule, making this an important area for further research. Furthermore with the exception of PVA there is a current lack of potentially commercially viable molecules with antifreeze activity that could be of use as a cryoprotectant.

1.5. Challenges in cryopreservation

While the AFGPs, AFPs and synthetic mimics have numerous potential applications, the focus here will be on cryopreservation due to the huge need for innovative storage methods of biomaterials produced by recent medical advances that currently suffer from longevity issues. This storage can be categorized into four different areas, non-vitrifying (ice crystals present) cryopreservation, vitrifying (ice in glass-like state) cryopreservation, hypothermic storage (> 0 °C) and lyophilisation. Methods of

cryopreservation are described in detail below, together with biological materials of interest that would benefit enormously from reliable cryopreservation.

1.5.1. Overview of current cryopreservation methods

It is clear that there is a wide variety of different biological materials that require cryopreservation to be fully utilized. Cryostorage of these materials requires both optimization of the cryoprotective solution for specific cell types, and the rates at which freezing and thawing is undertaken, and this is discussed in detail below.

1.5.1.1. Cryoprotective compounds

In general there are two types of cryoprotectants, those that penetrate the cell membrane and those that don't. Both types form hydrogen bonds with water and act by regulating the amount of liquid water and solute concentrations. Penetrating cryoprotectants include dimethyl sulfoxide (DMSO), ethylene glycol and glycerol. These are small enough to penetrate the cell membrane and act via a colligative mechanism, replacing water inside the cell. In the 1950s Lovelock developed a theory to explain this cryoprotective mechanism, postulating that due to the molar depression of the freezing point due to the solutes in solution, at any temperature below the ice transition during cooling, increase in salt concentration would be slowed due to the presence of the cryoprotectant (in this case glycerol).[126-127] This effect would prevent toxic concentrations of salts forming and subsequent damage. Likewise the increasingly high viscosity of the cryoprotectant during cooling helps maintain cell shape and slow intracellular ice formation.

Although these cryoprotectants have been used to preserve a variety of cell types such as red blood cells and bacteria, they require relatively high concentrations and show toxicity. Using DMSO as an example to show toxic effects, it has been found that DMSO can cause denaturing of proteins,[128] membrane proliferation[129] and increase the concentration of Ca^{2+} ions in the cytoplasm, which has been linked to depolymerisation and changes within the cytoskeleton.[130] Furthermore it has also been proposed that DMSO can effect RNA splicing.[129] Other penetrating cryoprotectants have also been observed to cause similar toxic effects.[131]

Non-penetrating cryoprotectants include polymers such as polyethylene glycol (PEG) and polyvinylpyrolidone (PVP) and also certain sugars that are too large to enter the cell. They are thought to act by dehydrating the cell before freezing due to high osmotic coefficients, reducing the amount of water the cell has to lose to regain osmotic balance under cooling.[80] Therefore intracellular ice formation becomes less likely, and so provides protection. However, they provide little protection against injuries caused by slow freezing and display significantly weaker activity than penetrating cryoprotectants. Although non-penetrating cryoprotectants show relatively weak activity, they can be added to their penetrating counterparts, reducing the concentrations required and consequently the toxicity effects.[132]

The use of saccharide molecules as cryoprotectants is also appealing as they are highly biocompatible in comparison with DMSO. A selection of sugars have been used in cryopreservation studies, both as a replacement and in addition to traditionally used protectants such as DMSO.[133] These include mono and disaccharides such as glucose, sucrose, fructose and particularly trehalose. In a study of the

cryopreservation and viability of mouse oocytes and zygotes, trehalose was found to substantially increase viability levels,[134] while it has also been shown that a trehalose solution can be used to preserve carrot and tobacco cells.[135] Likewise, the addition of a selection of sugars to an ethylene glycol solution have been found to improve the vitrification properties, shifting the glass transition temperature and improving cryopreservation potential, while also demonstrating low toxicity, Figure 1.14.[136] The optimal concentration and type of different sugars (and cryoprotectants in general) varies between different cell types. Therefore, careful testing and optimization is required for the highest cell survival possible under cryopreservation.

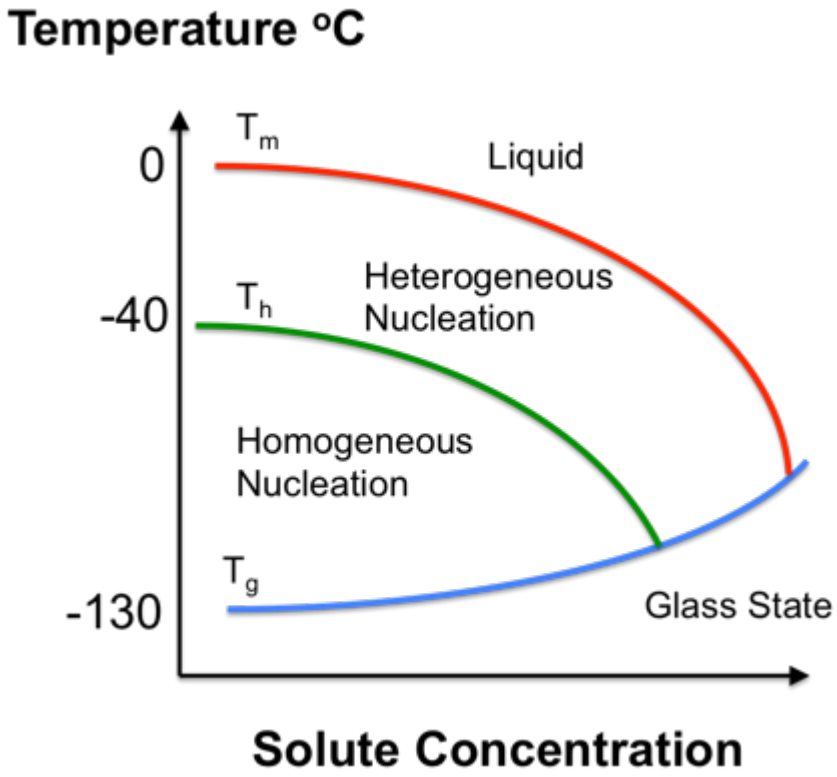

Figure 1.14. Phase diagram of ice showing vitrification as a function of solute concentration.

In addition to a colligative effect, which helps minimize changes in volume as the cell undergoes freezing and rewarming, sugars have also been found to interact with the cell membrane, increasing stability. For example, in a study by Strauss *et al.* it was found that sucrose, trehalose and glucose all stabilize and prevent membrane fusion of simple lipid bilayers under freezing and thawing.[137] The mechanism by which this occurs is thought to be due to hydrogen bonding to the polar phospholipid head groups displacing the water.[138] Furthermore, it has also been suggested that a saccharide can interact with, and stabilize acyl chains present in phospholipids.[139] Finally, sugars may also stabilize proteins, with the hydroxyl groups mimicking hydration, preventing denaturation further improving cryopreservation properties.

Despite the remarkable abilities of AFGPs, AFPs and synthetic analogues discussed above there have been relatively few reported attempts to use these within cryopreservation. Addition of AFGPs to red blood cells (RBCs) provided some cryoprotective effect, although above a certain concentration recovery actually decreased. This is thought to be due to needle like crystals forming due to the DIS activity possessed by the glycoprotein, Figure 1.15.[140] Furthermore, a study that investigated the effect of two AFPs and an AFGP on the viability of mouse spermatozoa, found that survival was decreased upon the addition of an AFP or AFGP, again the authors surmised that this was due to DIS.[141] Several other studies have been undertaken showing conflicting reports on the viability of these proteins as cryprotectants.[142-144]

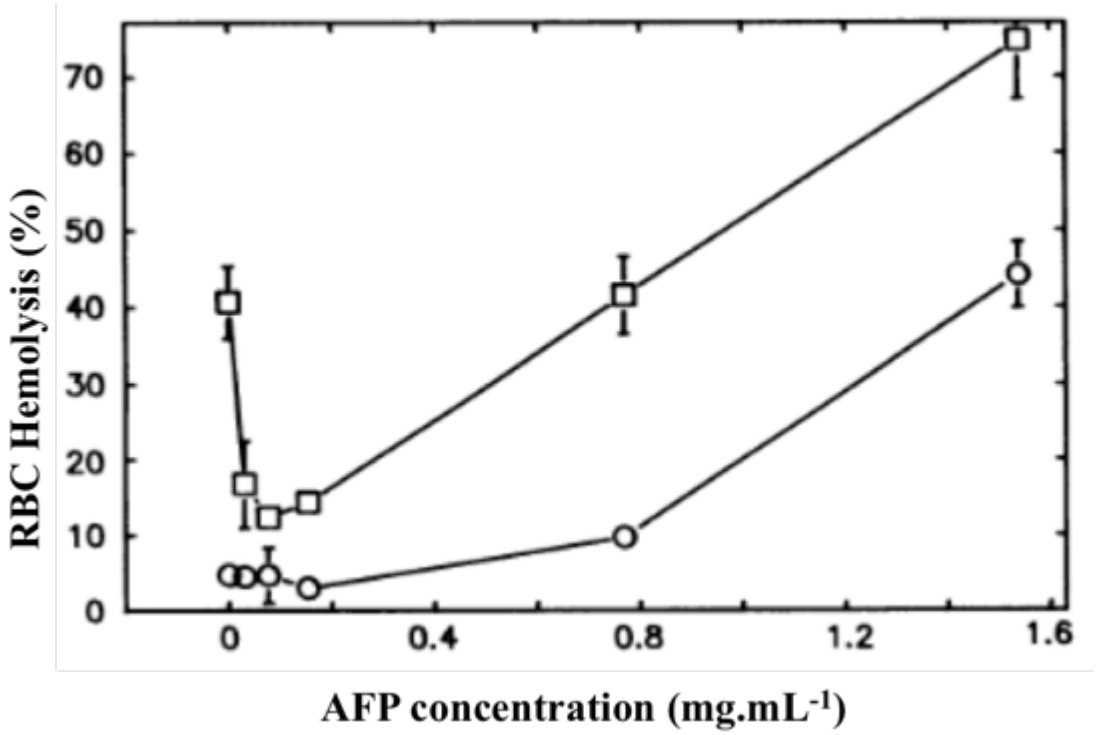

Figure 1.15. AFP concentration dependent hemolysis of red blood cells (RBCs). Percent hemolysis is after freeze, storage at -196 °C and thaw. Adapted from Carpenter and Hansen, 1992.[145]

Interestingly AFPs and AFGPs have been found to effect the cell membrane during hypothermic and cryo-storage. Tomczak *et al*. investigated a type 1 antifreeze protein in the hypothermic storage of chloroplast membranes finding that there is binding of the AFP to the lipid bilayer. This binding was found to inhibit leakage across the membrane and improved cell viability.[146] In a follow up paper the same authors also assessed the role of various AFPs and AFGPs on membrane permeability under freezing. Finding that some proteins such as type 1 AFP described above caused increased membrane leakage while others such as small AFGPs have an inhibitory effect.[147] This membrane binding is thought to be due to the hydrophobic face exhibited by all AFGPs and AFPs and demonstrates an unexpected property that would be highly interesting for cryopreservation applications.

In addition, cryopreservation using synthetic analogues has been attempted on several occasions. This includes the use of a synthetic AFGP with DMSO to preserve islet cells and the use of PVA to enhance the survival of RCBs.[98, 148] Poly(ε-*L*-lysine) modified with between 0 and 100 % hydroxyl groups (Figure 1.16) has also been investigated as a cryoprotectant although no quantitative analysis of IRI activity exists for this polymer.[149] The authors found that between 50 and 70 % carboxylation gave a significant improvement on the recovery of L929 cells when frozen and thawed compared to a DMSO control. Interestingly these polymers could be added at high concentrations (up to 20 wt%), meaning that the addition of other cryoprotectants, such as DMSO could be avoided.

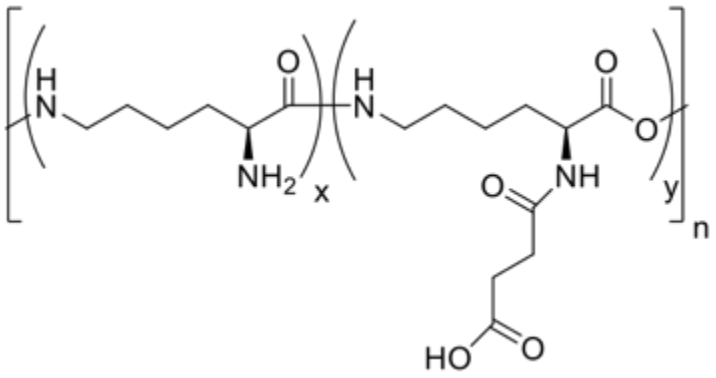

Figure 1.16. Carboxylated Poly(ε-*L*-lysine), functionalized with between 0-90 % carboxyl groups.

Reactive oxygen species (ROS) including hydroxyl radicals (OH) and hydrogen peroxide (H_2O_2) are formed naturally during metabolism within a cell. These can react with cellular constituents such as proteins and lipids to become stable and are required for various cellular processes such as cell signaling. Under normal conditions molecules called antioxidants convert ROS to safe products preventing cell damage,

however, in excess these can cause irreparable damage and lead to cell death,[150] known as oxidative stress. The disruption caused by cryopreservation and subsequent thawing has been found to lead to imbalances of ROS and antioxidants, so there has been a significant amount of investigation into the addition of antioxidants into cryopreservation solutions.[151]

There are two different types of antioxidants, enzymatic and non-enzymatic and both types can prevent harmful build-up of ROS species.[150] Among these antioxidants, several have shown promise for cryopreservation, these include glutathione (GSH) a tripeptide found ubiquitously in living cells, its precursors L-glutamine (L-Glu) and L-cysteine (L-Cys), ascorbic acid and superoxide dismutase and/ or catalase.[152]

The cell type plays a huge role in the optimization of cryopreservation, for example Câmara *et al.* found that the addition of GSH has little effect on the viability of ram spermatozoa, while Gadea and coworkers found that it has a protective effect in the cryopreservation of boar spermatozoa.[151, 153] Furthermore a study into the growth rates of cryopreserved *Rubus* (blackberry) shoots discovered that the addition of GSH improved regrowth by approximately 25 %,[154] demonstrating the challenge in the cryopreservation of a wide variety of cell types.

Finally there has been significant recent investigation into the effect of ice nucleation on cryopreservation and whether the addition of certain additives controlling this process lead to increased cell recovery.[155] As the sample is cooled, supercooling occurs, leading to uncontrollable nucleation, including intracellular nucleation and subsequent damage to the cells. Controlled nucleation has been found to improve

post-thaw viability in numerous cell types including, stem cells, pulmonary endothelial cells and bacteria.[156-158] The production of commercially viable, biocompatible ice nucleating agents are the subject of significant current research,[159] and will be high importance when designing future cryoprotectant mixtures.

1.5.1.2. The effect of freezing and thawing rates on cryopreservation

The survival for a certain cell during cryopreservation can depend on the cooling rate, with all cells exhibiting an optimal cooling rate. If the cooling is too fast or too slow then the level of cell survival will be low. The optimal cooling rate of a particular cell will be different to that of another cell, and so must be determined either through simulation or by experimentation for best cryopreservation.[160-161] While both slow and fast cooling lead to cell death, the mechanisms are different. Generally, slow freezing results in a prolonged exposure to extracellular ice, increasing solute content and causing osmotic problems, while fast freezing causes intracellular ice formation, both causing the death of a cell. The rate of thawing can also lead to decreased cell survival rates if it is not optimised. Overall, it appears that faster warming is preferential to a slower rate. It has found that slower warming can lead to intracellular ice formation, leading to ice recrystallization and cell damage.[162]

Although a faster thawing rate is generally preferred over a slower rate, for cells, which have undergone slow cooling this becomes disputable. Some studies have found that slowly cooled cells show increased survival rates at slower warming speeds, for example Whittingham *et al.* found this to be the case when investigating mouse embryos[163] and Towill and Mazur reported similar findings in plant cells.[164] The reason for this is hypothesised to be due to osmotic shock, since under fast

thawing there is no time to equilibrate.[165] However studies of other types of cell such as mammalian sperm have discovered that slow warming for cells, which have previously been cooled slowly, leads to a lower survival rate than faster warming rates.[166]

After discussion of the various factors involved cryopreservation, several areas of importance are discussed below in greater detail, highlighting where cryostorage is currently viable and the challenges to be overcome if we are to fully to be able to take advantage of recent medical breakthroughs.

1.5.2. Cryopreservation of red blood cells

An area where reliable cryopreservation could be of enormous benefit is the storage of blood. The majority of blood products required in a clinical setting are the red blood cells (RBCs), although platelets and blood plasma are also required. In the United Kingdom approximately 6,000 units of blood (1 unit = 470 mL) are required on a daily basis, with the largest uses being for treatment of anaemia (30%) and in surgery (30%).[167]

Although the demand is relatively constant, the supply is not. During adverse weather, or periods where a large number of people are on holiday, such as around Christmas and New Year the stocks can drop dramatically. This is summarized in figure 1.13, detailing the fluctuations over a 14-week period (figure 1.17A) and showing how different blood groups have differing stocks (figure 1.17B). During adverse weather in February, and at Easter the stocks can be observed to be significantly lower than

normal, while rarer blood groups such as AB negative have worrying low stock levels at the time of writing.

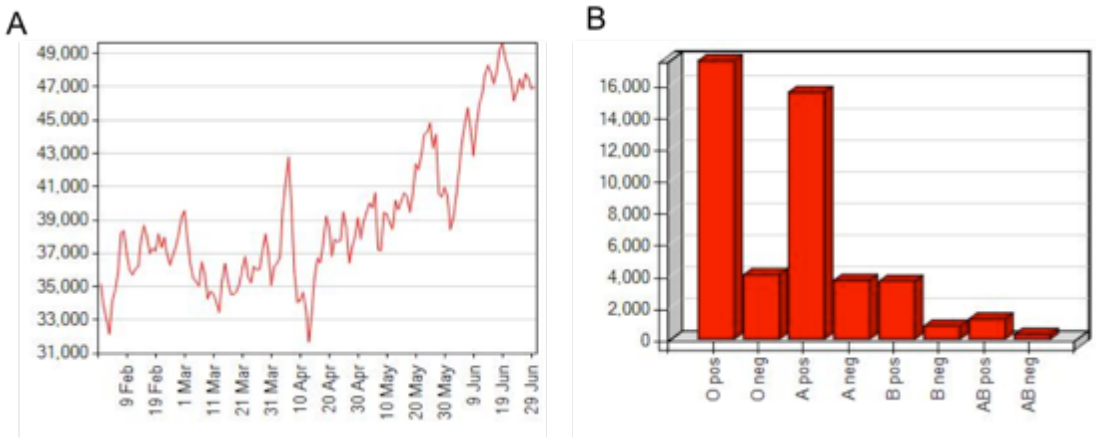

Figure 1.17. Fluctuations of bloodstocks. (A) Overall bloodstocks over a 14-week period in 2015; (B) Differing levels of stocks for various blood types. Figures adapted from NHS blood and transplant.[167]

The fundamental problem is that RBCs can only be stored for 35 days in hypothermic conditions, with platelets having a shelf-life of just 7 days at room temperature.[167] Several storage solutions have been developed, all containing anticoagulants, nutrients and solutes to maintain osmotic pressure. Commonly this involves the addition of compounds such as citrate (anticoagulant), nutrients phosphate and adenine and dextrose.[168] The loss of red blood cells is associated with various factors, collectively known as the "RBC storage lesion", including decrease in pH, decrease in ATP and 2,3-DPG levels and a build up of lactic acid.[169-170] 2,3-DPG is a key regulator in haemoglobin oxygen affinity.[171] This RBC storage lesion is potentially harmful, with the transfusion of older blood resulting in an increased risk of death in certain cases.[172] Other problems associated with hypothermic storage

include the build up of bioreactive substance such as cytokines,[173] and changes to the membrane composition.[174]

In addition to RBCs platelets are of significant importance in the clinical setting. Platelets require storage at 22 °C in contrast to RBCs. As mention above they can only be stored for up to 7 days due to structural lesions, reduced aggregation efficiency and risk of bacterial infection. Hypothermic storage can trigger activation, while also causing modifications in shape and activity.[175]

Current cryopreservation of RCBs requires an array of cryoprotectants, at high concentration and a way of storing samples, usually below -130 °C. The predominant additive in standard cryopreservation is glycerol at concentrations of up to 40 %, which must be removed after thawing as it can induce heamolysis.[176] Despite two methods being developed for the routine storage of RCBs in glycerol,[177] cryopreservation is limited to specific applications where donations are typically limited such as rare blood groups. Addition and removal of glycerol must be highly controlled, requiring specialist equipment and training, while post-thaw cell viability is limited.[178]

In addition to glycerol several cryopreservation techniques using cryoprotectants that are non cell penetrating have been investigated. These include hydroxyethyl starch (HES) and dextran.[179-180] HES has been widely studied as a cryoprotectant and acts to alter solution viscosity, while also acting as an osmolyte reducing intracellular water and helping to reduce potentially damaging ice formation on thawing.[181] Although post-thaw cell viability is generally high, there has been recent concern

about renal toxicity of HES,[182] and this has led to it being recently withdrawn from use in the UK and strictly limited in the USA pending further investigation.[183]

RBCs require optimised cooling and thawing techniques. Focusing on cooling; a range of rates and techniques have been investigated, with the vast majority recommending the immediate immersion in liquid nitrogen cooling the sample rapidly.[180, 184] Although cooling rate has been studied, the critical process for RBC cryopreservation is thawing. Ideally, the thawing process should be fast to prevent ice recrystallization, however RBCs are stored in volumes of 470 mL meaning that differential warming would occur. The cells in the centre would still experience harmful ice growth, while those on the outside may be exposed to high temperature for a relatively long period of time.

Furthermore there has been some limited investigation using AFGPs, AFPs and other IRI active molecules in the cryopreservation of RBCs. Carpenter and Hansen demonstrated that the addition of a type 1 AFP from Winter flounder (*Pseudopleuronectes americanus*) to a HES solution enhanced survival of RBCs,[140] and Chao *et al*. expanded on this, demonstrating that this is an ability of a range of AFGPs and AFPs.[185] More recently Deller *et al*. found that the addition of 1 $mg.mL^{-1}$ PVA to HES provided a similar benefit.[98] In all cases high concentrations of IRI molecule resulted in increased hemolysis, thought to be due to DIS.

1.5.3. Stem cell cryopreservation

Recent advances in stem cell technology has lead to a wide variety of potential uses including bone regeneration, wound treatment and treatment for central nervous

system problems.[186-188] Preservation of these cells enables them to be transported from specialist facilities to elsewhere, and means that they can become more viable as a treatment option. Furthermore, histocompatibility between donor and recipient is a major issue. For example, hematopoietic stem cells, Figure 1.18, used to treat leukaemia are often hard to match, meaning that a large library of different genotypes is required and therefore requiring the highly efficient cryopreservation methods.[189]

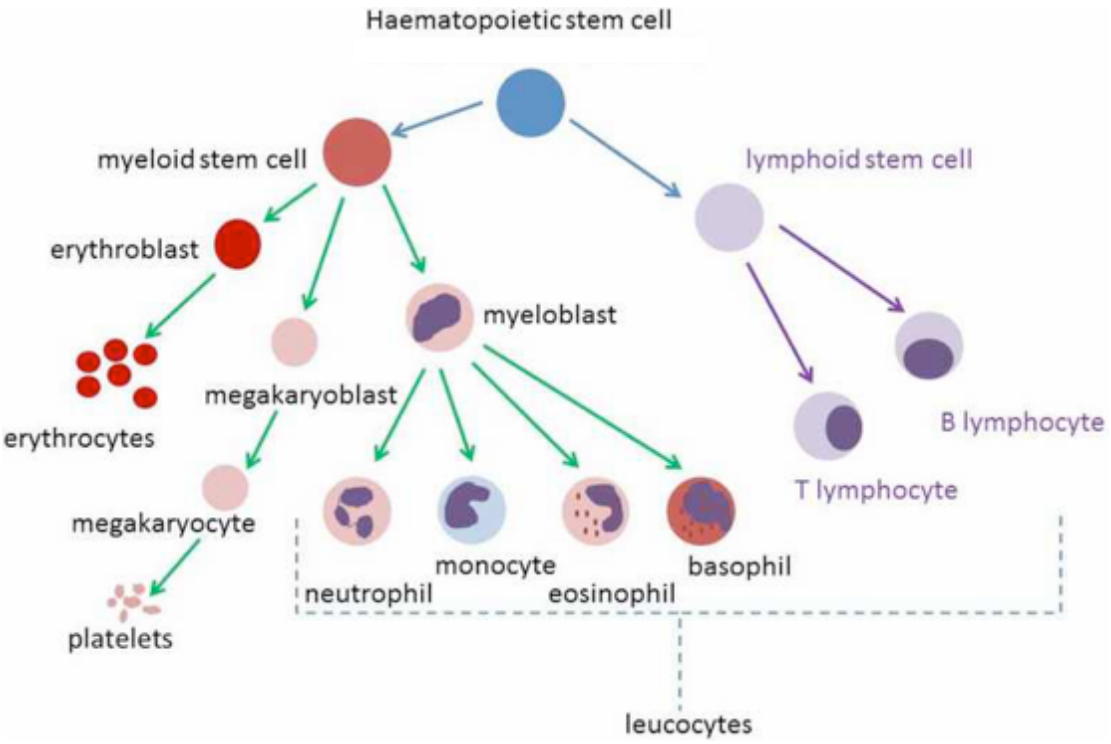

Figure 1.18. Hematopoietic stem cells and associated differentiation. Adapted from Mateos *et al*. 2015.[190]

Stem cell cryopreservation has had some success and current therapeutic strategies rely on good cryostorage. One stem cell line that is successfully stored and used to treat hematologic malignancies such as leukaemia is hematopoietic stem cells.[191] The current best practice for the storage of this cell line involves the use of 10 % DMSO in conjunction with serum albumin and saline.[3] As discussed in section 1.5.1.1,

DMSO has some toxicity issues, so a post-thaw washing stage must be undertaken. Standard cooling procedure involves cooling at a rate of 1-2 °C.min^{-1} to – 40 °C then slightly faster at 5 °C.min^{-1} to -120 °C and then stored in liquid nitrogen. Although fast freezing of hematopoietic stem cells by placing directly in liquid nitrogen, has also been investigated and found to have little detrimental effect.[192] Thawing rates are fast by submerging the samples within a water bath at 37 °C. However, the use of a water bath can lead to problems with sterility and is often not compatible with a clean room or a operating theatre,[193] highlighting the need for an IRI active compound allowing the samples to be thawed at a slower rate without the fear of detrimental ice crystal growth.

Embryonic stem cells and induced pluripotent stem cells have much promise as treatment for a range of genetic diseases, however their extremely fragile nature makes them highly challenging to cryopreserve. Current cryostorage procedure results in recovery of only around 1% and can also induce differentiation.[194] Due to this low yield, several more complex procedures have been introduced, including the addition of Rho-associated kinase (ROCK) inhibitor Y-27632 (protein that inhibits actin depolymerisation and consequently cell death),[195] and the use of very high concentrations of glucose to produce a vitrified solution.[196] Despite these innovative methods no high-yielding method is currently available and therefore cryopreservation of these particular cell lines is highly challenging.

1.5.4. Reproductive medicine

In addition those described above, another area of major importance for cryopreservation is that of reproductive medicine. Relatively recent advances in this

field have lead to the widespread use of *in-vitro* fertilization (IVF) and artificial insemination of domestic species in farming and endangered species.[197] Of all cell types frog and fowl spermatozoa were the first to be successfully cryopreserved and some of the greatest successes to date in cellular cryopreservation have been reported in the field of reproductive medicine.[198]

Reproductive medicine can be split into three cell types, spermatozoa, oocytes and embryos. Spermatozoa arguably the most commonly frozen cell type, typically involving the use of glycerol as the main cryoprotectant instead of DMSO. Although both have been found to have some toxic effect including loss of motility, possibly due to the high osmotic stress so must be removed post-thaw. The optimal freezing and thawing rates are generally thought to be fast, with freezing carried out by placing samples in liquid nitrogen vapour, while thawing is undertaken at 37 °C in a water bath.[199] Typically only low numbers of sperm survive thawing, which can be problematic when cryopreserving samples with low sperm numbers. To improve viability several studies have assessed the addition of AFPs to the cryomixture with mixed results; both enhancement and toxicity were observed.[141, 200]

The cryopreservation of oocytes presents a difficult challenge, due to the unique nature of the cell type. They have a large cellular volume making intracellular ice formation problematic, while also possessing a very complicated microtubule structure due to being locked into the metaphase of meiosis. Furthermore cryopreservation can induce changes in the glycoprotein coat surrounding the oocyte which is critical for fertilization.[201] These challenges mean that typical success rates of live births from cryopreserved embryos remains very low.

Two different approaches are commonly used to cryopreserve oocytes, a slow freezing strategy, whereby samples were frozen to -8 °C at 2 °C.min^{-1} and held at a constant temperature to insure controlled ice nucleation. The temperature was then decreased to -30 °C at 0.3 °C.min^{-1} and finally rapidly cooled at 50 °C.min^{-1} to -150 °C and placed in liquid nitrogen for storage. The cryoprotectants used were 1,2 propanediol (membrane permeable) and sucrose (membrane impermeable).[202] The second method involves fast freezing to produce a vitrified state using either an ethylene glycol, sucrose and human serum albumin mixture,[203] or a solution containing DMSO and PEG.[204] Both fast and slow freezing methods use fast thawing, Figure 1.19.

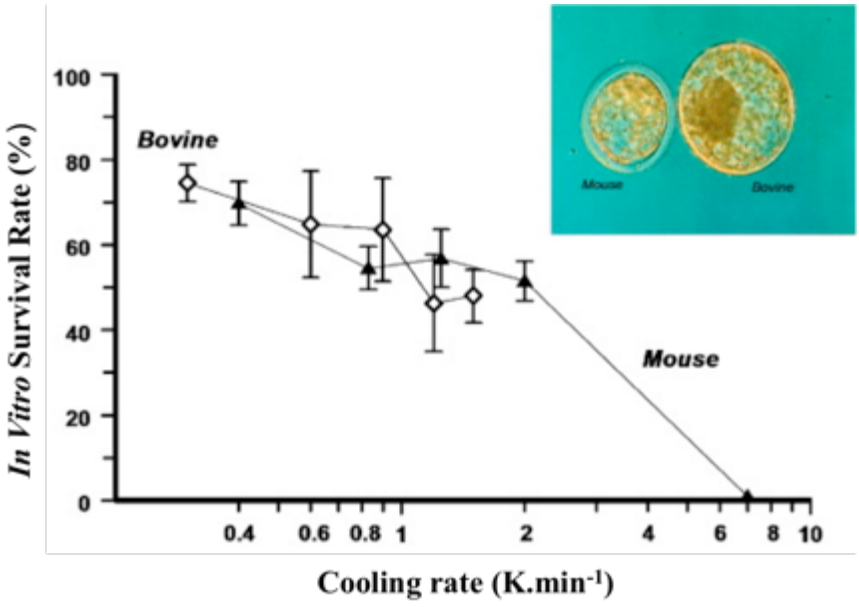

Figure 1.19. Cryopreservation of mouse and bovine oocytes using various freezing rates. Survival based on development into expanded blastocysts, mouse oocytes cryopreservated in DMSO and PEG, bovine oocytes in 1,2 propanediol and sucrose. Adapted from Leibo 2008.[205]

A significant portion of cell damage to oocyte cells during cryopreservation is caused by ice recrystallization, so AFGPs and AFPs or synthetic mimics would be a useful addition to the cryoprotective solution. O'Neil *et al*. prepared a solution of DMSO with the addition of 1 $mg.mL^{-1}$ AFGP and analysed its effect compared to DMSO alone, finding significant improvement in viability although only when added at 4 °C.[206] Likewise, Kim and co-workers reported increased viability upon the addition of a type 3 AFP.[207]

The final area of reproductive medicine involves the cryopreservation of fertilized embryos. As discussed above for oocytes, there is much discrepancy as to whether slow or fast cooling (vitrification) is the optimal method and what the optimal composition of the cryosolution is. Slow cooling methods involve the use of 1,2 propanediol or glycerol with sucrose and requires holding at -7 °C to insure controlled ice nucleation,[208] while fast cooling methods favour glycerol at higher concentrations.[209] Several studies have investigated the effect of IRI active molecules on cryopreservation of embryos in a range of species including zebra fish,[210] rabbit[211] and mice.[212] Despite this initial promise, no current study has investigated the effect of AFPs or AFGPs on the freezing of human embryos, presumably due to ethical concerns.

1.5.5. Transplantation medicine

Cryopreservation techniques have huge potential in the area of transplantation medicine. For example in the USA there are currently over 120,000 people waiting for organ transplants,[213] Table 1.1, and with an aging population this will only increase over time. A wide variety of different cell types are covered under transplant

medicine and the level of complexity can vary from material of one cell type to a whole organ with a variety of different cells present. In addition, unlike RBCs the cells undergoing transplantation must be able to proliferate in the recipient in order to be of benefit. Thus the challenges associated are demanding and require optimization for a particular cell type.

Table 1.1. Transplant waiting list for the USA by organ. Data correct as of August 28th 2015.[213]

Organ	Candidates
Kidney	101,055
Liver	15,159
Pancreas	1,050
Kidney/ Pancreas	1,962
Heart	4,183
Lung	1,537
Heart/ Lung	47
Intestine	256
Total	**122,352**

Although the cryostorage of whole organs has yet to be achieved, there has been some success in the preservation of individual cells lines. One of these is hepatocytes, the primary cell type within the liver. This cell type is used to treat metabolic liver diseases and acute liver failure, while also being useful for toxicology testing.[214] The standard cryopreservation mixture used is known as University of Wisconsin solution

(also known as viaspan). It consists of osmolytes such as lactobionate and raffinose, glutathione and adenosine to maintain cell function, and salts such as potassium phosphate and HES. Usually up to 10 % DMSO is added depending on the cryopreservation procedure used.[215]

In order to achieve successful cryopreservation the cells must be frozen as soon as possible after harvesting, followed by a slow freezing regime of around 1 °C.min^{-1} and then storage in liquid nitrogen. Thawing rate is generally rapid, although after thawing the hepatocytes are cooled down to 4 °C to minimize the toxic effects of DMSO.[216] While this is reasonably successful, hepatocyte function is generally compromised on thawing, for example albumin production is generally only 50 % of that observed in fresh cells. Likewise, a significant percentage of cells fail to attach to the culture substrate.[216] Despite these problems, transplanted hepatocytes have been found to be highly beneficial in clinical trials.[217]

A further primary cell type that is of interest for transplantation given the recent dramatic increase in type 2 diabetes, are islet cells which control insulin levels. Several studies have now shown that islet transplantation can reduce or even eliminate the need for insulin supplementation signifying that a reliable supply would be of enormous therapeutic benefit.[218] General cryopreservation procedure is similar to that of hepatocytes employing slow cooling and fast thawing rates with DMSO as the cryoprotectant. However, a recent study by Stiegler *et al*. found that encapsulation of hepatocytes in sodium cellulose sulphate and frozen with the addition of glycerol resulted in a similar recovery level to DMSO,[219] while further investigations have focused on the use of vitrifying solutions with the addition of polyols such as

propanediol.[220] Furthermore a synthetic AFGP described by Matsumoto *et al*. was found to enhance survival rates of islets cells in comparison to standard the cryosolution by as much as 20 %, which the authors attributed to its IRI activity, thus demonstrating the enormous potential for IRI active molecules in cryopreservation.[221]

AFGPs and AFPs also have the potential to increase the storage lifetime of organs ready for transplantation due to their TH ability. Amir *et al*. showed that rat hearts stored at sub zero temperatures without freezing due to the addition of a type 3 AFP had an extended storage time compared to standard protocols. Although this is not a long term storage method, this limited increase could be crucial in transporting the donor organ to its recipient.[222]

1.5.6. Protein storage

Proteins as therapeutics have also increased dramatically since insulin became the first therapeutic around 30 years ago. Now these materials have the potential as treatments across a whole spectrum of different medical fields, with more than 130 currently in use.[223] The majority of these are unstable for longer periods of time at room temperature, meaning that lyophilisation or cryopreservation is critical. Several problems need to be overcome in order to successfully preserve protein material, including adverse pH shifts and high localized salt concentrations on the removal of water.[224] Membrane proteins are particularly difficult to store successfully.

A variety of different molecules have been used in order to improve the storage of protein materials, including sugars, glycerol, amino acids, polymers and inorganic

salts. A common characteristic of these preservatives is that they seem to be preferentially excluded from contact with the protein in solution.[225] Various physical factors also affect recovery rates, including freezing and thawing rates and protein concentration.[226]

The most common method of cryopreservation is lyophilization in the presence of the disaccharide trehalose (figure 1.3A), which acts to stabilize the protein. Numerous studies have shown the benefit of this particular sugar over a range of proteins.[227-228] In addition, Maynard and co-workers have explored the synthesis of several trehalose glycopolymers as a way of enhancing their protective effect, finding that recovery could be improved by up to 50 % compared to trehalose alone.[229] Despite the success of trehalose in the storage of a range of proteins, there still remains a wide range of other possible therapeutic proteins that are not currently able to be stored long-term, therefore significant further research needs to be undertaken in order to realize the enormous potential in this field of medicine.

1.6. Thesis aims and summary

From considering the above research, this thesis aims to investigate the application of new AFP/AFGP molecules and apply these to cryopreservation. This includes studying the attributes that a molecule must possess in order to possess IRI activity, and whether synthetic, commercially viable AFGP/AFP biomimetics can be made. In addition cryopreservation of several biological materials will be investigated.

Chapter 2 describes how other proteins, not thought of as AFPs although evolutionarily similar can also posses IRI activity in the right conditions, due to various similar structural motifs. Calcium dependant L-type lectins are investigated due to their similarity to type 2 AFPs, while the antimicrobial peptide nisin is considered as it has structural similarity to type 1 AFPs. The identification of these structural similarities is of benefit when designing synthetic mimetics.

After exploring structural features of peptides that possess IRI activity, synthetic mimetics were explored. **Chapter 3** examines polyampholytes as novel IRI molecules, finding that poly(aminoethyl methacrylate) (PAEMA) functionalized with succinic anhydride (SA) forming a polymer with both positive and negative charges (PAEMA-*co*-SA) possessed IRI activity when the ratio of positive to negative charges is around 50 %. The systematic investigation of further polyampholytes including polybetaines and carbohydrate centred oligomers and IRI activity was also considered.

The "splat test" method of identifying IRI activity is robust, but not very high throughput, meaning that the identification of new IRI molecules such as those described in chapters 2 and 3 is a time consuming process. **Chapter 4** details a novel gold nanoparticle based method for quickly and efficiently screening a wide range of materials, while also identifying that serum albumins such as bovine serum albumin (BSA) possess limited IRI activity at concentrations of around 20 $mg.mL^{-1}$.

Chapter 5 investigates the use of amphipathic metallohelicies as potent IRI active molecules. These molecules are intrinsically hydrophobic, demonstrating that hydrophobicity is a desirable property for inhibiting ice crystal growth, while also having a similar helical structure to a type 1 AFP and the benefit over polymeric inhibitors of having a defined molecular weight.

Chapter 6 uses the knowledge that polyampholytes have IRI activity, discovered in chapter 3, in order to create a cheap, non-toxic, commercially viable polyampholyte based on poly(methyl vinyl ether-*co*-maleic anhydride). This is then used in conjunction with HES as a cryopreservative of RBCs, proving that even under sub-optimal slow thawing conditions the addition of an IRI active molecule can have enormous benefit to recovery.

Finally, **Chapter 7** considers the problem of therapeutic protein storage, through the use of IRI active molecules. Using a mixture of PVA and PEG or PAEMA-*co*-SA and PEG, recovery of several proteins was found to be significantly enhanced when frozen at -20 °C and -80 °C. In addition the same mixture was used to successfully

cryo-store antibody IgG, thus demonstrating this mixture as a viable solution to the problem of storing therapeutics.

1.7. References

[1] G. M. Hewitt, *Biol. J. Linn. Soc.* **1996**, *58*, 247-276.

[2] S. Prestrud Anderson, J. I. Drever, N. F. Humphrey, *Geology* **1997**, *25*, 399-402.

[3] D. Berz, E. M. McCormack, E. S. Winer, G. A. Colvin, P. J. Quesenberry, *Am. J. Hematol.* **2007**, *82*, 463-472.

[4] T. Bartels-Rausch, V. Bergeron, J. H. E. Cartwright, R. Escribano, J. L. Finney, H. Grothe, P. J. Gutiérrez, J. Haapala, W. F. Kuhs, J. B. C. Pettersson, S. D. Price, C. I. Sainz-Díaz, D. J. Stokes, G. Strazzulla, E. S. Thomson, H. Trinks, N. Uras-Aytemiz, *Rev. Mod. Phys.* **2012**, *84*, 885-944.

[5] M. Heisig, S. Mattessich, A. Rembisz, A. Acar, M. Shapiro, C. J. Booth, G. Neelakanta, E. Fikrig, *PLoS ONE* **2015**, *10*, e0116562.

[6] J. G. Duman, M. J. Wisniewski, *Environ. Exp. Bot.* **2014**, *106*, 60-69.

[7] M.-L. Sutinen, R. Arora, M. Wisniewski, E. Ashworth, R. Strimbeck, J. Palta, in *Conifer Cold Hardiness, Vol. 1* (Eds.: F. Bigras, S. Colombo), Springer Netherlands, **2001**, pp. 89-120.

[8] P. L. Davies, B. D. Sykes, *Cur. Opin. Struct. Biol.* **1997**, *7*, 828-834.

[9] P. Prestrud, *Arctic* **1991**, *44*, 132-138.

[10] A. L. DeVries, D. E. Wohlschlag, *Science* **1969**, *163*, 1073-1075.

[11] P. F. Scholander, L. van Dam, J. W. Kanwisher, H. T. Hammel, M. S. Gordon, *J. Cell. Comp. Physiol.* **1957**, *49*, 5-24.

[12] S. K. K. DeVries A.L., and R.E. Feeney, *J. Biol. Chem.* **1970**, *245*, 2901–2908.

[13] B. Hathaway*, Vol. 2015*, Yale News, **2012**.

[14] A. L. DeVries, *Science* **1971**, *172*, 1152-1155.

[15] A. L. DeVries, Komatsu, S. K., and Feeney, R. E., *J. Biol. Chem.* **1970**, *245*, 2909–2913.

[16] Y. Lin, J. G. Duman, A. L. DeVries, *Biochem. Biophys. Res. Comm.* **1972**, *46*, 87-92.

[17] M. M. Harding, P. I. Anderberg, A. D. J. Haymet, *Eur. J. Biochem.* **2003**, *270*, 1381-1392.

[18] F. V. D. Akker, E. Steensma, W. G. J. Hol, *Protein Sci.* **1996**, *5*, 1184-1188.

[19] L. Chen, A. L. DeVries, C.-H. C. Cheng, *Proc. Nat. Acad. Sci. U. S. A.* **1997**, *94*, 3817-3822.

[20] F. Franks, E. R. Morris, *Biochim. Biophys. Acta* **1978**, *540*, 346-356.

[21] G. Neelakanta, H. Sultana, D. Fish, J. F. Anderson, E. Fikrig, *J. Clin. Invest.* **2010**, *120*, 3179-3190.

[22] A. P. A. Wohrmann, *Mar. Ecol. Prog. Ser.* **1996**, *130*, 47-59.

[23] J. A. Ahlgren, C.C. Cheng, J.D. Schrag, and A.L Devries, *Comp. Biochem. Physiol. B* **2006**, *144*, 290–300

[24] G. L. Fletcher, M. J. King, M. H. Kao, *Can. J. Zoo.* **1987**, *65*, 227-233.

[25] C. F. Purchase, S. V. Goddard, J. A. Brown, *Can. J. Zoo.* **2001**, *79*, 610-615.

[26] Y. Tomimatsu, J.R. Scherer., Y. Yeh, and R.E Feeney, *J. Biol. Chem.* **1976**, *251*, 2290–2298.

[27] E. Berman, A. Allerhand, and A.L. DeVries, *J. Biol. Chem.* **1980**, *255*, 4407–4410.

[28] J. A. Drewes, K. L. Rowlen, *Biophys. J.* **1993**, *65*, 985-991.

[29] A. N. Lane, L. M. Hays, R. E. Feeney, L. M. Crowe, J. H. Crowe, *Prot. Sci.* **1998**, *7*, 1555-1563.

[30] A. N. Lane, L. M. Hays, N. Tsvetkova, R. E. Feeney, L. M. Crowe, J. H. Crowe, *Biophys. J.* **2000**, *78*, 3195-3207.

[31] D. H. Nguyen, M. E. Colvin, Y. Yeh, R. E. Feeney, W. H. Fink, *Biophys. J.* **2002**, *82*, 2892-2905.

[32] N. M. Tsvetkova, B. Phillips, V.V. Krishnan, and R.E. Feeney, *Biophys. J.* **2002**, *82*, 464–473.

[33] M. M. Harding, P. I. Anderberg, A. D. J. Haymet, *Eur. J. Biochem.* **2003**, *270*, 1381-1392.

[34] J. G. Duman, A. L. Devries, *Nature* **1974**, *247*, 237-238.

[35] N. Hashim, I. Bharudin, D. Nguong, S. Higa, F. Bakar, S. Nathan, A. Rabu, H. Kawahara, R. Illias, N. Najimudin, N. Mahadi, A. Murad, *Extremophiles* **2013**, *17*, 63-73.

[36] M. Smallwood, D. Worrall, L. Byass, L. Elias, D. Ashford, C. J. Doucet, C. Holt, J. Telford, P. Lillford, D. J. Bowles, *Biochem. J.* **1999**, *340*, 385-391.

[37] J. G. Duman, V. Bennett, T. Sformo, R. Hochstrasser, B. M. Barnes, *J. Insect Physiol.* **2004**, *50*, 259-266.

[38] A. Hakim, J. B. Nguyen, K. Basu, D. F. Zhu, D. Thakral, P. L. Davies, F. J. Isaacs, Y. Modis, W. Meng, *J. Biol. Chem.* **2013**, *288*, 12295-12304.

[39] V. Haridas, and S. Naik *RSC Adv.* **2013**, *3*, 14199-14219.

[40] R. S. H. L.A. Graham, G.L. Fletcher, and P.L. Davies *PLoS ONE* **2013**, *8*, 81285-81297.

[41] C. B. Marshall, A. Chakrabartty, P. L. Davies, *J. Biol. Chem.* **2005**, *280*, 17920-17929.

[42] L. A. Graham, S. C. Lougheed, K. V. Ewart, P. L. Davies, *PLoS ONE* **2008**, *3*, e2616.

[43] G. Deng, D. W. Andrews, R. A. Laursen, *FEBS Lett.* **1997**, *402*, 17-20.

[44] D. S. C. Yang, M. Sax, A. Chakrabartty, C. L. Hew, *Nature* **1988**, *333*, 232-237.

[45] R. S. Hobbs, M.A. Shears, L.A. Graham, P.L. Davies, and G.L. Fletcher, *FEBS J.* **2013**, *278*, 3699-3711.

[46] A. Jorov, B. S. Zhorov, D. S. C. Yang, *Prot. Sci.* **2004**, *13*, 1524-1537.

[47] W. Gronwald, M. C. Loewen, B. Lix, A. J. Daugulis, F. D. Sönnichsen, P. L. Davies, B. D. Sykes, *Biochemistry* **1998**, *37*, 4712-4721.

[48] Y. Nishimiya, H. Kondo, M. Takamichi, H. Sugimoto, M. Suzuki, A. Miura, S. Tsuda, *J. Mol. Biol.* **2008**, *382*, 734-746.

[49] A. A. Antson, D. J. Smith, D. I. Roper, S. Lewis, L. S. D. Caves, C. S. Verma, S. L. Buckley, P. J. Lillford, R. E. Hubbard, *J. Mol. Biol.* **2001**, *305*, 875-889.

[50] G. Deng, R. A. Laursen, *BBA - Prot. Struct. Mol.* **1998**, *1388*, 305-314.

[51] Y.-C. Liou, A. Tocilj, P. L. Davies, Z. Jia, *Nature* **2000**, *406*, 322-324.

[52] M. Bar-Dolev, Y. Celik, J. S. Wettlaufer, P. L. Davies, I. Braslavsky, *J. R. Soc. Interface* **2012**, *9*, 3249-3259.

[53] A. H. Kwan, K. Fairley, P. I. Anderberg, C. W. Liew, M. M. Harding, J. P. Mackay, *Biochemistry* **2005**, *44*, 1980-1988.

[54] Y. Liu, Z. Li, Q. Lin, J. Kosinski, J. Seetharaman, J. M. Bujnicki, J. Sivaraman, C. L. Hew, *PLoS One* **2007**, *2*, e548.

[55] A. A. Antson, D. J. Smith, D. I. Roper, S. Lewis, L. S. Caves, C. S. Verma, S. L. Buckley, P. J. Lillford, R. E. Hubbard, *J. Mol. Biol.* **2001**, *305*, 875-889.

[56] A. J. Middleton, C. B. Marshall, F. Faucher, M. Bar-Dolev, I. Braslavsky, R. L. Campbell, V. K. Walker, P. L. Davies, *J. Mol. Biol.* **2012**, *416*, 713-724.

[57] S. P. Graether, M. J. Kuiper, S. M. Gagne, V. K. Walker, Z. Jia, B. D. Sykes, P. L. Davies, *Nature* **2000**, *406*, 325-328.

[58] A. J. Middleton, C. B. Marshall, F. Faucher, M. Bar-Dolev, I. Braslavsky, R. L. Campbell, V. K. Walker, P. L. Davies, *J. Mol. Biol.* **2012**, *416*, 713-724.

[59] R. Gupta, and R. Deswal, *J. Biosci.* **2014**, *39*, 931-935.

[60] K. B. Storey, and J.M. Storey, in *Extremophiles, Vol. 2* (Ed.: C. a. G. Gerday, N.), Eolss Publishers, Oxford, UK, **2005**, pp. 184-215.

[61] T. P. Mommsen, and K.B. Storey, *Gen. Compo. Endocrinol.* **1992**, *87*, 44-53.

[62] K. B. Storey, and J.M. Storey, *Annu. Rev. Physiol. Rev.* **1992**, *54*, 619-637.

[63] A. G. Hirsh, *Cryobiology* **1987**, *24*, 214-228.

[64] D. A. Wharton, W. Block, *Cryobiology* **1997**, *34*, 114-121.

[65] B. J. Sinclair, D. Renault, *Comp. Biochem. Physiol. A: Mol. Int. Physiol.* **2010**, *155*, 14-18.

[66] J. H. Crowe, A. E. Oliver, F. Tablin, *Integr. Comp. Biol.* **2002**, *42*, 497-503.

[67] J. H. Crowe, F. A. Hoekstra, L. M. Crowe, *An. Rev. Physiol.* **1992**, *54*, 579-599.

[68] K. R. Walters, A. S. Serianni, T. Sformo, B. M. Barnes, J. G. Duman, *Proc. Nat. Acad. Sci. U. S. A.* **2009**, *106*, 20210-20215.

[69] K. Walters, Jr., A. Serianni, Y. Voituron, T. Sformo, B. Barnes, J. Duman, *J. Comp. Physiol. B* **2011**, *181*, 631-640.

[70] S. Carillo, A. Casillo, G. Pieretti, E. Parrilli, F. Sannino, M. Bayer-Giraldi, S. Cosconati, E. Novellino, M. Ewert, J. W. Deming, R. Lanzetta, G. Marino, M. Parrilli, A. Randazzo, M. L. Tutino, M. M. Corsaro, *J. Am. Chem. Soc.* **2015**, *137*, 179-189.

[71] M. I. Gibson, *Polym. Chem.* **2010**, *1*, 1141-1152.

[72] J. Barrett, *Int. J. Biochem. Cell Bio.* **2001**, *33*, 105–117.

[73] K. Meister, S. Ebbinghaus, Y. Xu, J. G. Duman, A. DeVries, M. Gruebele, D. M. Leitner, M. Havenith, *Proc. Nat. Acad. Sci. U. S. A.* **2013**, *110*, 1617-1622.

[74] C. J. Capicciotti, M. Doshi, and R.N. Ben, in *Recent Developments in the Study of Recrystallization* (Ed.: P. Wilson), InTech, **2013**, pp. 252-279.

[75] C. A. Knight, J. Hallett, A. L. DeVries, *Cryobiology* **1988**, *25*, 55-60.

[76] M. M. Tomczak, C. B. Marshall, J. A. Gilbert, P. L. Davies, *Biochem. Biophys. Res. Comm.* **2003**, *311*, 1041-1046.

[77] C. Budke, C. Heggemann, M. Koch, N. Sewald, T. Koop, *J. Phys. Chem. B* **2009**, *113*, 2865-2873.

[78] Y. Celik, R. Drori, N. Pertaya-Braun, A. Altan, T. Barton, M. Bar-Dolev, A. Groisman, P. L. Davies, I. Braslavsky, *Proc. Natl. Acad. Sci. U. S. A.* **2013**, *110*, 1309-1314.

[79] J. Jackman, M. Noestheden, D. Moffat, J. P. Pezacki, S. Findlay, R. N. Ben, *Biochem. Biophys. Res. Commun.* **2007**, *354*, 340-344.

[80] A. Fowler, M. Toner, *Ann. N. Y. Acad. Sci.* **2006**, *1066*, 119-135.

[81] C. J. Capicciotti, J.S. Poisson, C.N Boddy, and R.N. Ben., *Cryobiology* **2015**, *15*, 79–89.

[82] K.-C. Chou, *J. Mol. Biol.* **1992**, *223*, 509-517.

[83] C. A. Knight, E. Driggers, A. L. DeVries, *Biophys. J.* **1993**, *64*, 252-259.

[84] A. D. J. Haymet, L. G. Ward, M. M. Harding, C. A. Knight, *FEBS Lett.*, *430*, 301-306.

[85] D. Wen, R. A. Laursen, *Biophys. J* **1992**, *63*, 1659-1662.

[86] F. D. Sönnichsen, C. I. DeLuca, P. L. Davies, B. D. Sykes, *Structure* **1996**, *4*, 1325-1337.

[87] N. Hashim, S. Sulaiman, F. Abu Bakar, R. Illias, H. Kawahara, N. Najimudin, N. Mahadi, A. Murad, *Polar Biol.* **2014**, *37*, 1495-1505.

[88] A. Wierzbicki, P. Dalal, T. E. Cheatham Iii, J. E. Knickelbein, A. D. J. Haymet, J. D. Madura, *Biophys. J* **2007**, *93*, 1442-1451.

[89] J. A. Raymond, A. L. DeVries, *Proc. Nat. Acad. Sci. U. S. A.* **1977**, *74*, 2589-2593.

[90] J. J. De Yoreo, P. G. Vekilov, *Rev. Mineral. Geochem.* **2003**, *54*, 57-93.

[91] Y. Yeh, R. E. Feeney, *Chem. Rev.* **1996**, *96*, 601-618.

[92] C. A. Knight, C. C. Cheng, A. L. DeVries, *Biophys. J.* **1991**, *59*, 409-418.

[93] Y. Celik, L. A. Graham, Y. F. Mok, M. Bar, P. L. Davies, I. Braslavsky, *Proc. Natl. Acad. Sci. U. S. A.* **2010**, *107*, 5423-5428.

[94] C. A. Knight, and A.L DeVries, *Science* **1989**, *245*, 505-507.

[95] D. G. Hall, A. Lips, *Langmuir* **1999**, *15*, 1905-1912.

[96] Y. Wu, J. Banoub, S. V. Goddard, M. H. Kao, G. L. Fletcher, *Comp. Biochem. Physiol. B: Biochem. Mol. Biol.* **2001**, *128*, 265-273.

[97] S. Ebbinghaus, K. Meister, B. Born, A. L. DeVries, M. Gruebele, M. Havenith, *J. Am. Chem. Soc.* **2010**, *132*, 12210-12211.

[98] R. C. Deller, M. Vatish, D. A. Mitchell, M. I. Gibson, *Nat. Commun.* **2014**, *5*, 3244-3251.

[99] K. Muldrew, J. Rewcastle, B. J. Donnelly, J. C. Saliken, S. Liang, S. Goldie, M. Olson, R. Baissalov, G. Sandison, *Cryobiology* **2001**, *42*, 182-189.

[100] M. Griffith, K. V. Ewart, *Biotechnol. Adv.* **1995**, *13*, 375-402.

[101] Y. Tachibana, G. L. Fletcher, N. Fujitani, S. Tsuda, K. Monde, S.-I. Nishimura, *Angew. Chem. Int. Ed.* **2004**, *116*, 874-880.

[102] A. Eniade, A. V. Murphy, G. Landreau, R. N. Ben, *Bioconjugate Chem.* **2001**, *12*, 817-823.

[103] S. Liu, R. N. Ben, *Org. Lett.* **2005**, *7*, 2385-2388.

[104] R. Y. Tam, C. N. Rowley, I. Petrov, T. Zhang, N. A. Afagh, T. K. Woo, R. N. Ben, *J. Am. Chem. Soc.* **2009**, *131*, 15745-15753.

[105] R. Y. Tam, S. S. Ferreira, P. Czechura, J. L. Chaytor, R. N. Ben, *J. Am. Chem. Soc.* **2008**, *130*, 17494-17501.

[106] C. Heggemann, C. Budke, B. Schomburg, Z. Majer, M. Wißbrock, T. Koop, N. Sewald, *Amino Acids* **2010**, *38*, 213-222.

[107] C. Boyer, V. Bulmus, T. P. Davis, V. Ladmiral, J. Liu, S. Perrier, *Chem. Rev.* **2009**, *109*, 5402-5436.

[108] G. Moad, E. Rizzardo, and S.H. Thang., *Aust. J. Chem.* **2006**, *59*, 669–692.

[109] S. Drotleff, U. Lungwitz, M. Breunig, A. Dennis, T. Blunk, J. Tessmar, A. Göpferich, *Eur. J. Pharm. Biopharm.* **2004**, *58*, 385-407.

[110] B. Lee, J. Dalsin, P. Messersmith, in *Biol. Adhes.* (Eds.: A. Smith, J. Callow), Springer Berlin Heidelberg, **2006**, pp. 257-278.

[111] A. Muñoz-Bonilla, M. Fernández-García, *Prog. Polym. Sci.* **2012**, *37*, 281-339.

[112] C. A. Knight, D. Wen, R. A. Laursen, *Cryobiology* **1995**, *32*, 23-34.

[113] Y. E. Yagci, M. Antonietti, H. G. Börner, *Macromol. Rapid Comm.* **2006**, *27*, 1660-1664.

[114] T. Inada, S.-S. Lu, *Cryst. Growth Des.* **2003**, *3*, 747-752.

[115] T. Inada, S.-S. Lu, *Chem. Phys. Lett.* **2004**, *394*, 361-365.

[116] T. Inada, P. R. Modak, *Chem. Eng. Sci.* **2006**, *61*, 3149-3158.

[117] T. Congdon, R. Notman, M. I. Gibson, *Biomacromolecules* **2013**, *14*, 1578-1586.

[118] R. C. Deller, T. Congdon, M. A. Sahid, M. Morgan, M. Vatish, D. A. Mitchell, R. Notman, M. I. Gibson, *Biomater. Sci.* **2013**, *1*, 478-485.

[119] C. Budke, T. Koop, *ChemPhysChem* **2006**, *7*, 2601-2606.

[120] G. Paradossi, F. Cavalieri, E. Chiessi, C. Spagnoli, M. Cowman, *J. Mat. Sci. Mat. Med.* **2003**, *14*, 687-691.

[121] S.-F. Chong, A. A. A. Smith, A. N. Zelikin, *Small* **2013**, *9*, 942-950.

[122] T. Hall-Manning, M. Spurgeon, A. M. Wolfreys, A. P. Baldrick, *Food Chem. Toxicol.* **2004**, *42*, 321-333.

[123] R. W. R. Crevel, K.J. Cooper, L.K. Poulsen, L. Hummelshoj, C. Bindslev-Jensen, A.W. Burks, and H.A. Sampson, *Food Chem. Toxicol.* **2007**, *45*, 79-87.

[124] S. Deville, C. Viazzi, J. Leloup, A. Lasalle, C. Guizard, E. Maire, J. Adrien, L. Gremillard, *PLoS ONE* **2011**, *6*, e26474.

[125] O. Mizrahy, M. Bar-Dolev, S. Guy, I. Braslavsky, *PLoS ONE* **2013**, *8*, e59540.

[126] J. E. Lovelock, C. Polge, *Biochem. J.* **1954**, *58*, 618-622.

[127] J. E. Lovelock, *Biochem. J.* **1954**, *56*, 265-270.

[128] T. R. Henderson, R. F. Henderson, J. L. York, *Ann. N. Y. Acad. Sci.* **1975**, *243*, 38-53.

[129] Y. Murata, T. Watanabe, M. Sato, Y. Momose, T. Nakahara, S.-i. Oka, H. Iwahashi, *J. Biol. Chem.* **2003**, *278*, 33185-33193.

[130] M. Plachinta, T. Zhang, D. M. Rawson, *Cryoletters* **2004**, *25*, 415-424.

[131] T. Arakawa, J. F. Carpenter, Y. A. Kita, J. H. Crowe, *Cryobiology* **1990**, *27*, 401-415.

[132] G. M. Fahy, B. Wowk, J. Wu, S. Paynter, *Cryobiology* **2004**, *48*, 22-35.

[133] B. T. Storey, E. E. Noiles, K. A. Thompson, *Cryobiology* **1998**, *37*, 46-58.

[134] A. Eroglu, J. A. Lawitts, M. Toner, T. L. Toth, *Cryobiology* **2003**, *46*, 121-134.

[135] I. S. Bhandal, R. M. Hauptmann, J. M. Widholm, *Plant Physiol.* **1985**, *78*, 430-432.

[136] L. L. Kuleshova, D. R. MacFarlane, A. O. Trounson, J. M. Shaw, *Cryobiology* **1999**, *38*, 119-130.

[137] G. Strauss, P. Schurtenberger, H. Hauser, *BBA - Biomembranes* **1986**, *858*, 169-180.

[138] C. S. Pereira, P. H. Hünenberger, *J. Phys. Chem. B* **2006**, *110*, 15572-15581.

[139] T. J. Anchordoguy, A. S. Rudolph, J. F. Carpenter, J. H. Crowe, *Cryobiology* **1987**, *24*, 324-331.

[140] J. F. Carpenter, T. N. Hansen, *Proc. Nat. Acad. Sci. U. S. A.* **1992**, *89*, 8953-8957.

[141] C. Koshimoto, P. Mazur, *Cryobiology* **2002**, *45*, 49-59.

[142] S. Qadeer, M. A. Khan, M. S. Ansari, B. A. Rakha, R. Ejaz, A. U. Husna, M. Ashiq, R. Iqbal, N. Ullah, S. Akhter, *Anim. Reprod. Sci.* **2014**, *148*, 26-31.

[143] J.-H. Wang, *Cryobiology* **2000**, *41*, 1-9.

[144] H. Bagis, T. Akkoç, A. Tasş, D. Aktoprakligil, *Mol. Reprod. Dev.* **2008**, *75*, 608-613.

[145] J. F. Carpenter, T. N. Hansen, *Proc. Natl. Acad. Sci. U. S. A.* **1992**, *89*, 8953-8957.

[146] M. M. Tomczak, D. K. Hincha, S. D. Estrada, W. F. Wolkers, L. M. Crowe, R. E. Feeney, F. Tablin, J. H. Crowe, *Biophys. J* **2002**, *82*, 874-881.

[147] M. M. Tomczak, D. K. Hincha, S. D. Estrada, R. E. Feeney, J. H. Crowe, *BBA - Biomembranes* **2001**, *1511*, 255-263.

[148] S. Matsumoto, M. Matsusita, T. Morita, H. Kamachi, S. Tsukiyama, Y. Furukawa, S. Koshida, Y. Tachibana, S.-I. Nishimura, S. Todo, *Cryobiology* **2006**, *52*, 90-98.

[149] K. Matsumura, S.-H. Hyon, *Biomaterials* **2009**, *30*, 4842-4849.

[150] J. C. Kefer, A. Agarwal, E. Sabanegh, *Int. J. Urol.* **2009**, *16*, 449-457.

[151] D. R. Câmara, S. V. Silva, F. C. Almeida, J. F. Nunes, M. M. P. Guerra, *Theriogenology* **2011**, *76*, 342-350.

[152] W. Zhang, K. Yi, C. Chen, X. Hou, X. Zhou, *Anim. Reprod. Sci.*, *132*, 123-128.

[153] J. Gadea, F. García-Vazquez, C. Matás, J. C. Gardón, S. Cánovas, D. Gumbao, *J. Androl.* **2005**, *26*, 396-404.

[154] E. Uchendu, M. Muminova, S. Gupta, B. Reed, *In Vitro Cell. Dev. Biol. - Plant* **2010**, *46*, 386-393.

[155] G. John Morris, E. Acton, *Cryobiology* **2013**, *66*, 85-92.

[156] G. Morris, E. Acton, K. Faszer, A. Franklin, H. Yin, R. Bodine, J. Pareja, N. Zaninovic, and R. Gosden, *Reprod. Biomed. Online* **2006**, *13*, 421-426.

[157] R. Spindler, B. Rusenhahn, and B. Glassmacher, *Cryobiology* **2011**, *63*, 306-307.

[158] F. Fonseca, M. Marin, G. J. Morris, *Appl. Environ. Microbiol.* **2006**, *72*, 6474-6482.

[159] X. Han, H. B. Ma, C. Wilson, J. K. Critser, *Microfluid. Nanofluid.* **2008**, *4*, 357-361.

[160] R. V. Devireddy, D. J. Swanlund, T. Olin, W. Vincente, M. H. T. Troedsson, J. C. Bischof, K. P. Roberts, *Biol. Reprod.* **2002**, *66*, 222-231.

[161] S. Kumar, J. D. Millar, P. F. Watson, *Cryobiology* **2003**, *46*, 246-253.

[162] W. F. Rall, D. S. Reid, J. Farrant, *Nature* **1980**, *286*, 511-514.

[163] D. G. Whittingham, M. Wood, J. Farrant, H. Lee, J. A. Halsey, *J. Reprod. Fertil.* **1979**, *56*, 11-21.

[164] L. E. Towill, P. Mazur, *Plant Physiol.* **1976**, *57*, 290-296.

[165] P. Mazur, *Am. J. physiol.* **1984**, *247*, C125-142.

[166] M. A. Henry, E. E. Noiles, D. Gao, P. Mazur, J. K. Critser, *Fertil. Steril.* **1993**, *60*, 911-918.

[167] NHS*, Vol. 2015*, **2015**.

[168] J. R. Hess, *Blood Trans.* **2010**, *8*, s9-s15.

[169] J. D. R. Kurach, R. Almizraq, B. Bicalho, J. P. Acker, J. L. Holovati, *Transfusion* **2014**, *54*, 1595-1603.

[170] R. L. Sparrow, *Blood Transfus.* **2012**, *10*, s7-s11.

[171] R. MacDonald, *Anaesthesia* **1977**, *32*, 544-553.

[172] D. Wang, J. Sun, S. B. Solomon, H. G. Klein, C. Natanson, *Transfusion* **2012**, *52*, 1184-1195.

[173] I. Chin-Yee, N. Arya, M. S. d'Almeida, *Transfus. Sci.* **1997**, *18*, 447-458.

[174] L. Van de Watering, *Vox Sang.* **2011**, *100*, 36-45.

[175] M. G. Egidi, A. D'Alessandro, G. Mandarello, L. Zolla, *Blood Transfus.* **2010**, *8*, s73-s81.

[176] I. B. Bakaltcheva, C. O. Odeyale, B. J. Spargo, *Biochim. Biophys. Acta* **1996**, *1280*, 73-80.

[177] C. R. Valeri, *Transfusion* **1975**, *15*, 195-218.

[178] T. Peyrard, B. N. Pham, P. Y. Le Pennec, P. Rouger, *Immunohematology / American Red Cross* **2009**, *25*, 13-17.

[179] T. Takahashi, A. Hirsh, E. Erbe, R. J. Williams, *Biophys. J.* **1988**, *54*, 509-518.

[180] M. J. G. Thomas, E. S. Parry, S. G. Nash, S. H. Bell, *Transfus. Sci.* **1996**, *17*, 385-396.

[181] L. E. McGann, *Cryobiology* **1978**, *15*, 382-390.

[182] R. R. Bruno, W. Neuhaus, N. Roewer, C. Wunder, M. A. Schick, *Anesth. Analg.* **2014**, *119*, 570-577.

[183] J. P. Nolan, M. G. Mythen, *Br. J. Anaesth.* **2013**, *111*, 321-324.

[184] A. W. Rowe, E. Eyster, A. Kellner, *Cryobiology* **1968**, *5*, 119-128.

[185] H. Chao, P. L. Davies, J. F. Carpenter, *J. Exp. Biol.* **1996**, *199*, 2071-2076.

[186] R. J. Deans, A. B. Moseley, *Exp. Hematol.* **2000**, *28*, 875-884.

[187] L. K. Branski, G. G. Gauglitz, D. N. Herndon, M. G. Jeschke, *Burns* **2009**, *35*, 171-180.

[188] F. H. Gage, J. Ray, L. J. Fisher, *Annu. Rev. Neurosci.* **1995**, *18*, 159-192.

[189] J. Hanna, A. Hubel, *Organogenesis* **2009**, *5*, 134-137.

[190] M. K. Mateos, D. Barbaric, S.-A. Byatt, R. Sutton, G. M. Marshall, *Transl. Pediatr.* **2015**, *4*, 76-92.

[191] H. Kolb, J. Mittermuller, C. Clemm, E. Holler, G. Ledderose, G. Brehm, M. Heim, W. Wilmanns, *Blood* **1990**, *76*, 2462-2465.

[192] J. P. Lewis, M. Passovoy, S. A. Conti, P. A. McFate, F. E. Trobaugh, Jr., *Transfusion* **1967**, *7*, 17-32.

[193] D. Fountain, M. Ralston, N. Higgins, J. B. Gorlin, L. Uhl, C. Wheeler, J. H. Antin, W. H. Churchill, R. J. Benjamin, *Transfusion* **1997**, *37*, 585-591.

[194] C. B. Ware, A. M. Nelson, C. A. Blau, *BioTechniques* **2005**, *38*, 879-880, 882-873.

[195] S. Mollamohammadi, A. Taei, M. Pakzad, M. Totonchi, A. Seifinejad, N. Masoudi, H. Baharvand, *Hum. Reprod.* **2009**, *24*, 2468-2476.

[196] B. E. Reubinoff, M. F. Pera, G. Vajta, A. O. Trounson, *Hum. Reprod.* **2001**, *16*, 2187-2194.

[197] R. T. Francoeur, *Oryx* **1972**, *11*, 364-366.

[198] C. Polge, A. U. Smith, A. S. Parkes, *Nature* **1949**, *164*, 666.

[199] D. Royere, C. Barthelemy, S. Hamamah, J. Lansac, *Hum. Reprod. Update* **1996**, *2*, 553-559.

[200] J. Beirao, L. Zilli, S. Vilella, E. Cabrita, R. Schiavone, M. P. Herraez, *Biol. Reprod.* **2012**, *86*, 59.

[201] A. Bernard, B. Fuller, *Hum. Reprod. Update* **1996**, *2*, 193-207.

[202] A. Borini, M. A. Bonu, G. Coticchio, V. Bianchi, M. Cattoli, C. Flamigni, *Fertil. Steril.* **2004**, *82*, 601-605.

[203] D. L. Wright, A. Eroglu, M. Toner, T. L. Toth, *Reprod. BioMed. Online* **2004**, *9*, 179-186.

[204] S. J. Paynter, B. J. Fuller, *Methods. Mol. Biol.* **2007**, *368*, 313-324.

[205] S. P. Leibo, *Theriogenology* **2008**, *69*, 37-47.

[206] L. O'Neil, S. J. Paynter, B. J. Fuller, R. W. Shaw, A. L. DeVries, *Cryobiology* **1998**, *37*, 59-66.

[207] J. W. Jo, B. C. Jee, C. S. Suh, S. H. Kim, *PLoS ONE* **2012**, *7*, e37043.

[208] R. Thorat, A. Ingle, *Nat. Protoc.* **2012**, *62*, 1038-1044.

[209] A. M. Van Wagtendonk-De Leeuw, J. H. G. Den Daas, T. A. M. Kruip, W. F. Rall, *Cryobiology* **1995**, *32*, 157-167.

[210] S. Martinez-Paramo, V. Barbosa, S. Perez-Cerezales, V. Robles, M. P. Herraez, *Cryobiology* **2009**, *58*, 128-133.

[211] K. Nishijima, M. Tanaka, Y. Sakai, C. Koshimoto, M. Morimoto, T. Watanabe, J. Fan, S. Kitajima, *Cryobiology* **2014**, *69*, 22-25.

[212] J. M. Shaw, C. Ward, A. O. Trounson, *Hum. Reprod.* **1995**, *10*, 396-402.

[213] HRSA*, Vol. 2015*, US Department of Health and Human Services, **2015**.

[214] R. D. Hughes, R. R. Mitry, A. Dhawan, *Transplantation* **2012**, *93*, 342-347.

[215] J. H. Southard, T. M. van Gulik, M. S. Ametani, P. K. Vreugdenhil, S. L. Lindell, B. L. Pienaar, F. O. Belzer, *Transplantation* **1990**, *49*, 251-257.

[216] C. Terry, A. Dhawan, R. R. Mitry, R. D. Hughes, *Cryobiology* **2006**, *53*, 149-159.

[217] S. C. Strom, R. A. Fisher, M. T. Thompson, A. J. Sanyal, P. E. Cole, J. M. Ham, M. P. Posner, *Transplantation* **1997**, *63*, 559-569.

[218] F. Bertuzzi, S. Marzorati, A. Secchi, *Cur. Mol. Med.* **2006**, *6*, 369-374.

[219] P. B. Stiegler, V. Stadlbauer, S. Schaffellner, G. Halwachs, C. Lackner, O. Hauser, F. Iberer, K. Tscheliessnigg, *Transplant Proc.* **2006**, *38*, 3026-3030.

[220] M. J. Taylor, S. Baicu, *Organogenesis* **2009**, *5*, 155-166.

[221] S. Matsumoto, M. Matsusita, T. Morita, H. Kamachi, S. Tsukiyama, Y. Furukawa, S. Koshida, Y. Tachibana, S.-I. Nishimura, S. Todo, *Cryobiology* **2006**, *52*, 90-98.

[222] G. Amir, L. Horowitz, B. Rubinsky, B. S. Yousif, J. Lavee, A. K. Smolinsky, *Cryobiology* **2004**, *48*, 273-282.

[223] B. Leader, Q. J. Baca, D. E. Golan, *Nat. Rev. Drug Discov.* **2008**, *7*, 21-39.

[224] P. Matejtschuk, in *Cryopreservation and Freeze-Drying Protocols, Vol. 368* (Eds.: J. Day, G. Stacey), Humana Press, **2007**, pp. 59-72.

[225] J. F. Carpenter, J. H. Crowe, *Cryobiology* **1988**, *25*, 244-255.

[226] E. Cao, Y. Chen, Z. Cui, P. R. Foster, *Biotechnol. Bioeng.* **2003**, *82*, 684-690.

[227] A. Hedoux, L. Paccou, S. Achir, Y. Guinet, *J. Pharm. Sci.* **2013**, *102*, 2484-2494.

[228] N. K. Jain, I. Roy, *Protein Sci.* **2009**, *18*, 24-36.

[229] J. Lee, E.-W. Lin, U. Y. Lau, J. L. Hedrick, E. Bat, H. D. Maynard, *Biomacromolecules* **2013**, *14*, 2561-2569.

Chapter 2

2. Latent Ice Recrystallization Inhibition Activity in Non-Antifreeze Proteins; Ca^{2+} Activated Plant Lectins and Cation-Activated Antimicrobial Peptides.

D. E. Mitchell and M. I. Gibson, Biomacromolecules. **2015**, Accepted.

This chapter contains a paper describing ice recrystallization inhibition (IRI) activity of non-antifreeze proteins. Firstly describing the investigation of l-type lectins for their similarity to antifreeze proteins and their ability to inhibit ice crystal growth. This is followed by the examination of the short amphipathic protein nisin A and associated IRI activity. DEM undertook all experimental work. Both authors wrote the manuscript.

2.1. Abstract

Organisms living in polar regions have evolved a series of antifreeze (glyco) proteins (AFGPs) to enable them to survive by modulating the structure of ice. These proteins have huge potential in cellular cryopreservation, ice-resistant surfaces, frozen food and cryosurgery, but are limited by their relatively low availability and questions regarding their mode of action. The identification of new structures and sequences

capable of inhibiting ice growth is crucial to aid our understanding of these. Sequence analysis found that human l-type lectins have high homology to type II AFPs, but these lectins are not widely available. Here we show that calcium binding plant l-type lectins, which have similar biological function to human c-type lectins (glycan recognition), but no sequence homology to AFPs, display potent calcium dependant ice recrystallization inhibition (IRI) activity. This IRI can be 'switched on/off' simply by changing Ca^{2+} concentration. To prove that many proteins may exist with the potential to display IRI, a second motif was considered; amphipathicity. All known AFPs have defined hydrophobic/hydrophilic domains, rationalising this. The cheap and widely used antimicrobial Nisin, was found to have cation-dependant IRI activity, controlled by either acid, or addition of histidine-binding ions such as zinc or nickel, which promote its amphipathic structure. These results demonstrate a new approach to the identification of antifreeze protein mimetic macromolecules and may help shed light on their underlying mechanisms of action as well as developing 'minimum synthetic mimics' of AFPs.

2.2. Introduction

Antifreeze proteins and glycoproteins (AF(G)Ps) are found in a wide variety of different organisms that habitually experience freezing temperatures. They were initially discovered in Arctic and Antarctic fish species but have since been reported in a wide range of plants and insects.[1-5] AFPs provide protection through two main methods, thermal hysteresis and ice recrystallization inhibition (IRI).[6] The former is the depression of the freezing point relative to that of the melting point,[7] while the latter is the slowing of the rate of ice crystal growth (Ostwald ripening) process.[8] The underlying mechanisms for each action are still under investigation and it has

emerged that TH and IRI activities are not necessarily linked. In 2003 Enaide *et al.* reported that simplified AFGPs could retain potent IRI activity while displaying essentially zero TH activity.[9] Furthermore, Ben and co-workers have developed a range of structures that posses only IRI activity including carbohydrate based surfactants, synthetic antifreeze proteins and several small molecules.[10-12] Davies *et al.* have also shown that the magnitude of TH does not always scale with IRI.[13]

IRI-active compounds could have huge application in frozen foods, cryosurgery and cryopreservation.[14-16] For example, ice crystal growth (recrystallization) during thawing has been shown to be a major contributor to cell death during cellular cryopreservation. Carpenter *et al.* showed that AFPs could enhance cryopreservation of red blood cells but benefit was limited by the onset of dynamic ice shaping (DIS), which actually resulted in reduced cell recovery.[17] There are various conflicting results on AF(G)P supplemented cryopreservation showing both benefit and detriment, where detrimental effects are normally due to DIS.[16, 18-19] Despite these challenges, there is an urgent need for new cryopreservatives as alternatives to the current state-of-the-art formulations, which employs (toxic) organic solvents and also for the preservation of cell types which cannot currently be frozen. Ben *et al*. have shown that IRI specific glycopeptides and alkyl glycosides have shown some improvement in cryopreservation.[20] In addition, Gibson *et al.* have demonstrated that IRI-active synthetic polymers dramatically enhance non-vitreous cryopreservation of red blood cells.[21] Despite these structurally diverse IRI mimetics, an understanding of the structural motifs essential for activity remain elusive.

Another outstanding challenge is the development of 'smart' AFP derivatives with switchable activity, enabling them to be activated both spatially and temporally.

Current understanding has revealed that amphiphilicity (segregated hydrophilic and hydrophobic domains) are needed for IRI activity, with most AFPs showing defined regions.[22] Ben *et al.* have shown that hydrophobically modified saccharides have (rather weak) IRI activity associated with their amphiphilicity.[10] Despite this progress, there are still few compounds which are potent IRI inhibitors, which in turn has limited their application and biophysical studies to understand their remarkable properties to slow ice growth.

AFPs display a wide variety of secondary and tertiary structures and amino acid sequences while all binding to the same ice substrate.[23] AFPs have been grouped into several different sub-types based on structure, for example type 1 AFPs consist of a long amphipathic alpha helix,[24] while type 2 AFPs are cysteine rich globular proteins containing several disulphide bonds.[25] In an attempt to understand the evolutionary origins of AFPs, sequence alignment studies have been undertaken. This has revealed strong similarity to other families of proteins such as lectins and apolipoproteins.[26] A defining characteristic of these protein families is that they discriminate between related classes of molecules; for example lectins bind specific carbohydrates. Due to this similarity it may be possible that there exists many protein structures, that subject to the correct evolutionary conditions could have become AFPs and hence might display some latent activity. To this end a c-type lectin from rattlesnake *Crotalus atrox* has been evaluated for specific ice crystal face binding, although not IRI activity.[27]

The aim of this study was to investigate if non-antifreeze proteins can still display ice recrystallization inhibition activity, based on their functional and structural similarities to known AFPs, rather than the traditional chemical biology approaches

based on sequence similarities. The ability to modulate AFP function by application of external stimuli is also studied as a route to 'smart' AFP mimetics.

2.3. Results and Discussion

Inspired by the work of Graham *et al.* and others[25, 28] which unravelled the genetic history of AFPs, sequence alignment of type 2 AFP from the Sea raven, *Hemitripterus americanus* against all known proteins within the protein databank (PBD) was conducted to identify those proteins with high sequencial homology. This search agreed with previous reports, showing that in addition to other type 2 AFPs a range of l-type lectins also had high sequential similarity with the overall sequence identified as a member of the lectin superfamily. c-type lectins most closely related to type 2 AFP include human langerin (c-type transmembrane protein on Langerhans cells), human lithostathine and a rat mannose binding protein, Figure 2.1. Interestingly lithostathine has been found to play a role in the prevention of pancreatic stones by preventing calcite crystal growth, a somewhat similar role to an AFP suggesting there may be common crystallization-inhibiting motifs which has evolved. As reported by Rubinsky *et al.* a c-type lectin from rattle snake *Crotalus atrox* has Ca^{2+} dependent ice shaping activity, but no reports on IRI activity have been made.[27]

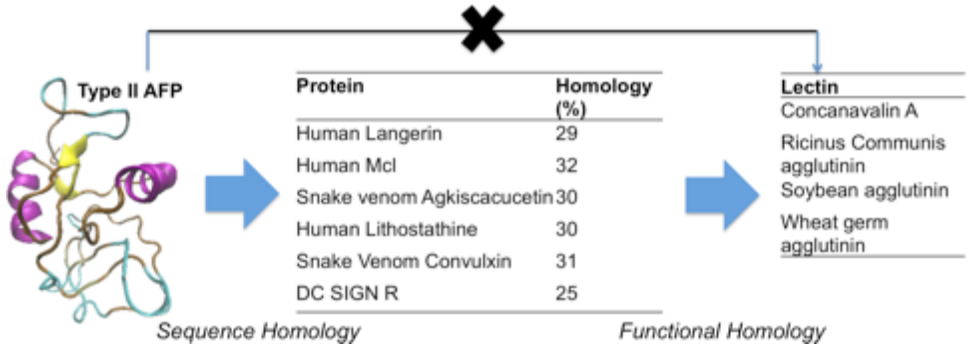

Figure 2.1. Schematic of homology between type 2 antifreeze proteins, c-lectins, and the functional relationship to plant lectins.

While the lectins described above are most sequentially similar to type 2 AFP, they can be challenging to produce in large quantities, requiring (mammalian cell) recombinant expression. Furthermore, the use of human lectins (or rattlesnake venom) in biomedical applications would be limited by immunogenicity and associated problems. Therefore, we decided to move on from sequence similarity, to *functional similarities*. Specifically, the calcium binding l-type lectins found in plants; some plant lectins have found medical applications such as banana lectin in HIV inhibition.[29] These have structural similarities (particularly in the carbohydrate recognition domain; CRD) to the human c-type lectins, but do not have significant relationship to native type 2 AFPs. A range of plant lectins were selected based on them being commercially availability in reasonable quantities; concanavalin A (ConA, Mw 104 kDa), soybean agglutinin (SBA, Mw 120 kDa) and *ricinus communis* agglutinin 120 (RCA_{120}, Mw 120 kDa).

To determine if the lectins demonstrate any antifreeze-protein associated activity, a modified 'splat' assay was employed to screen for ice recrystallization inhibition (IRI). Briefly, buffered 10 μL solutions of the analyte of interest were dropped onto a glass slide chilled to -80 °C to produce a wafer of small ice crystals. These were annealed at -8 °C and the average ice crystal size recorded after a fixed period of time, and compared to a negative control to give the mean largest grain size (MLGS). The smallest size (as a percentage) from this assay is ~ 20 % (as an ice crystal cannot have zero size). HEPES buffer was employed in place of the normal PBS to enable the addition of divalent ions (Ca^{2+}), which cannot be used in PBS (due to calcium phosphate precipitation). Assessment of the IRI activity of ConA at 5 $mg.mL^{-1}$ is shown in Figure 2.2A. As can be seen, ConA showed no activity, being statistically

identical to our negative control, PEG (poly(ethylene glycol)).[30] However, for ConA to bind its native glycans (α-mannose/glucose), it is essential for Ca^{2+} to be present (or similar divalent ions) in the carbohydrate recognition domain inspiring us to repeat the experiment in the presence of $CaCl_2$. Under these conditions, there was definite IRI activity, suggesting that ConA is also a l-type antifreeze protein, which can be 'turned on' (or off) by addition of calcium ions. Calcium dependent ice binding has also been reported for Rainbow smelt and Atlantic herring fish species and the Antarctic bacteria *Marinomonas primoryensis.*[31-32]

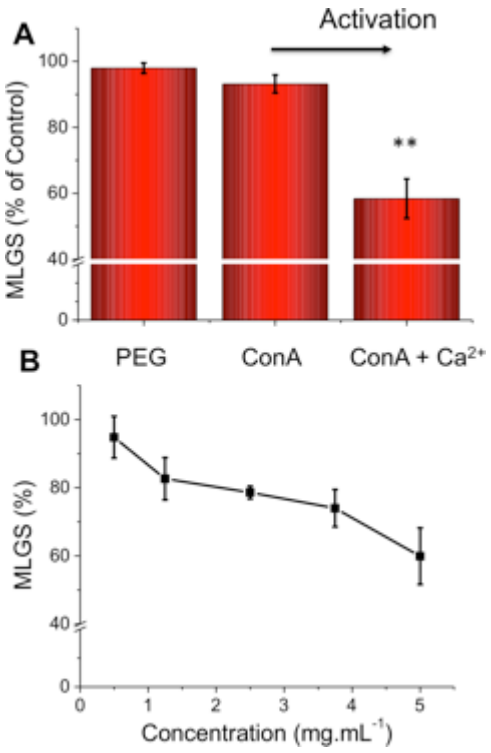

Figure 2.2. IRI activity of ConA in HEPES buffer. (A) Effect of (5 $mg.mL^{-1}$) $CaCl_2$ addition. [ConA] = 5 $mg.mL^{-1}$, [$CaCl_2$] = 5 $mg.mL^{-1}$, [PEG] = 5 $mg.mL^{-1}$; (B). Concentration dependence of ConA with 5 $mg.mL^{-1}$ $CaCl_2$. Error bars represent ± SD from a minimum of 3 repeats. MLGS = mean largest grain size relative to HEPES buffer or HEPES and calcium chloride buffer control. ** Signifies $p < 0.01$ relative to PEG control.

Control experiments of $CaCl_2$ doped buffer revealed the IRI activity was not due to the metal ions (unlike for example ZrAc which has some unique activity to inhibit ice growth) (ESI, Appendix 1).[33] Concentration-dependence of the IRI activity was also measured, Figure 2.2B. Whilst far weaker than native AFPs, PVA, this activity is stronger than synthetic analogues such as poly(ampholytes) which are potent cryopreservation enhancers.[34-36]

ConA exists as a tetramer around pH 7, but at lower pHs it dissociates into its monomeric or dimeric units, providing an accessible route to study the IRI activity in more detail. In pH 5 acetate buffer ConA is a dimer and showed statistically significant, but only slightly enhanced activity relative to the native tetramer measured at pH 7.4 (see ESI, Appendix 1). This implies that the overall tertiary/quaternary structure of the protein might not be essential for activity and that the carbohydrate recognition domain (which has similarity to ice binding domains) is the crucial component. To evaluate if this is a general phenomena, or unique to ConA, the lectins SBA and RCA_{120} were also evaluated by the splat assay, with and without Ca^{2+}, and the results shown in Figure 2.3.

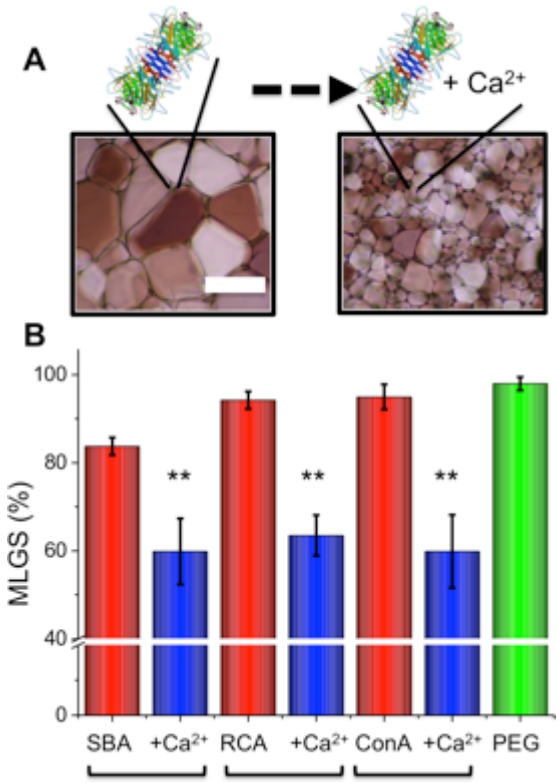

Figure 2.3. IRI activity of l-type lectins with and without 5 mg.mL^{-1} $CaCl_2$. Error bars represent ± SD from a minimum of 3 repeats, MLGS = mean largest grain size relative to HEPES buffer or HEPES and calcium chloride buffer control. ** Signifies $p < 0.01$ relative to PEG control.

Rather remarkably, both SBA and RCA inhibited ice crystal growth at just 5 mg.mL^{-1} with both requiring the addition of Ca^{2+} to 'switch on' the activity, to similar extent to ConA. To rule out this being a non-specific effect, ConA and SBA were both denatured (confirmed by circular dichroism, ESI, Appendix 1) by boiling and re-tested. Pleasingly, this reduced their activity in both cases, confirming it was a specific structural feature of the proteins producing activity not a broad macromolecular effect, Figure 2.4A. In addition the fact that catalase has no activity demonstrates that this is not a common property of all proteins. It should be noted that

heating to 80 °C is not expected to completely denature (and there will be some refolding) hence the MLGS value does not return to 100 %. The results above suggest there are structural features of the lectin, assumed to be related to the carbohydrate recognition domain that generates the IRI activity.

The effect of adding in competing carbohydrate ligands, which will bind the CRD (in presence of Ca^{2+}) was measured and the results shown in Figure 2.4B. There was a very weak enhancement in activity upon addition of the sugars, which in the case of SBA/GalNAc was statistically significant but was only small. This would appear to rule out the CRD (carbohydrate recognition domain) directly binding to the ice (as the sugars would be competing ligands). Alternatively, it might be that the sugar has a similar hydrogen bonding network as the water, and therefore it is tolerated. A detailed site-directed mutagenesis study would be required to undercover this, which is beyond the scope of the present study. No ice shaping was observed (which would imply specific ice face interaction), but this effect is normally only seen at high AFP concentrations (>20 $mg.mL^{-1}$); it was not possible to obtain homogenous protein solutions at these concentrations. Therefore, direct ice interaction cannot be ruled out, but there is building evidence that many (macro)molecules can inhibit ice growth without ice binding by disruption of the quasi-liquid layer/eutectic phase interface.[30, 35, 37]

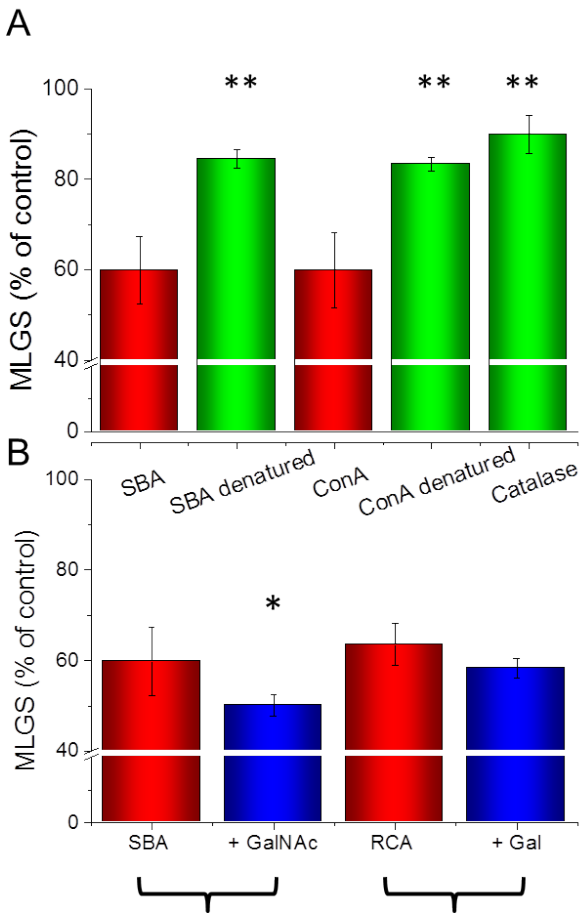

Figure 2.4. IRI inhibition/activation studies of SBA and RCA. (A) Effect of denaturation; (B) IRI effect of the addition of competitive carbohydrates (10 mM). GalNac = N-acetylgalactosamine, Gal = galactose. Error bars represent ± SD from a minimum of 3 repeats, MLGS = mean largest grain size relative to HEPES buffer or HEPES and calcium chloride buffer control. ** signifies $p < 0.01$ relative to respective undenatured sample (or undenatured ConA for catalase) * signifies $p < 0.05$ relative to respective sugar-free lectin solution.

The reasons for the observed activity remains unclear (as with many features of AF(G)Ps), but given the evolutionary origins of type 2 AFPs from lectins, perhaps not surprisingly. Lectins evolved to recognize the difference between sugars and water – a challenging task as both are essentially hydrated –OH groups. An antifreeze protein

could be considered to discriminate between water and ice – a similar problem. The current understanding of antifreeze protein suggests that amphipathic characteristic is required – spatially defined hydrophilic and hydrophobic faces. Our initial analysis of the lectins' crystal structures did not show an obvious amphiphilicity, but crystallography only provides a static, not dynamic, description of protein structure and function.

Inspired by the above observations, we considered the possibility that there might be a wider range of proteins (or peptides), which might have the structural features essential for reproducing IRI properties, but due to a lack of evolutionary stress have never specifically developed into antifreeze proteins. Given the amphipathic structure of AFPs, it would seem that other amphipathic proteins would make good lead molecules. Host-defense, cationic antimicrobial peptides are well-known amphipathic proteins and several are commercially available.[38] To test our hypothesis that latent antifreeze activity might remain, nisin A was selected as a model antimicrobial. Nisin is readily available, low molecular weight (34 amino acids, 3354 $g.mol^{-1}$) and widely used in the dairy industry. It has also been recently reported the *Xodes Scapularis* tick antifreeze glycoprotein has antimicrobial activity proving additional support to the hypothesis of re-purposing antimicrobial peptides.[39] To function as an antimicrobial nisin A requires a sufficiently low pH to protonate histidine 27 and 31, which enforces the correct amphipathic conformation to enable cell membrane disruption/pore formation.[40-42] Figure 2.5 shows a space-filling model illustrating the hydrophilic/hydrophobic domains of nisin A compared to Type 1 AFP from Winter flounder, illustrating the spatiality segregated hydrophilic and hydrophobic domains which we propose is a key component in IRI activity. This peptide provides a

convenient tool to test the amphipathic hypothesis and the IRI activity of nisin A was tested as a function of pH and concentration, Figure 2.6. It should be noted that in Figure 2.6A, activity at each pH is reported relative to a blank of that pH solution.

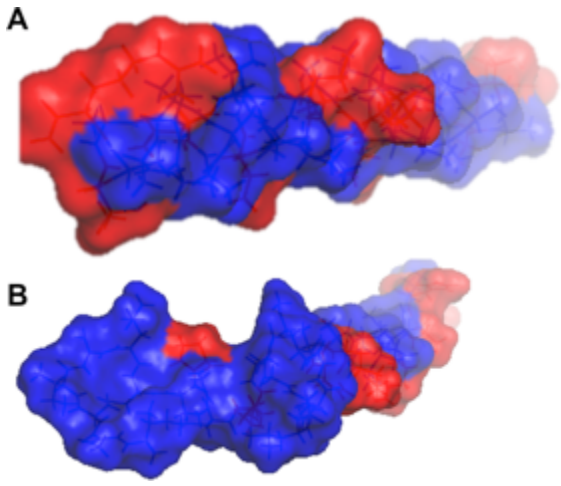

Figure 2.5. Space filling models of peptides with hydrophilic (red) and hydrophobic (blue) domains indicated. A) Winter flounder type I AFP; B) Nisin A.

The results shown reveal that nisin A has clear IRI activity comparable to several other synthetic macromolecules described in the literature.[34-35] Based on its known pH dependent antimicrobial activity, we surmise that protonation of the Histidine residues, (pKa value ~ 6) in the acetate buffer (pH = 5) was the controlling factor. This switchable activity is unique, and may provide a tool for targeted activation of AFP-properties, in applications such as cryo-surgery.[43]

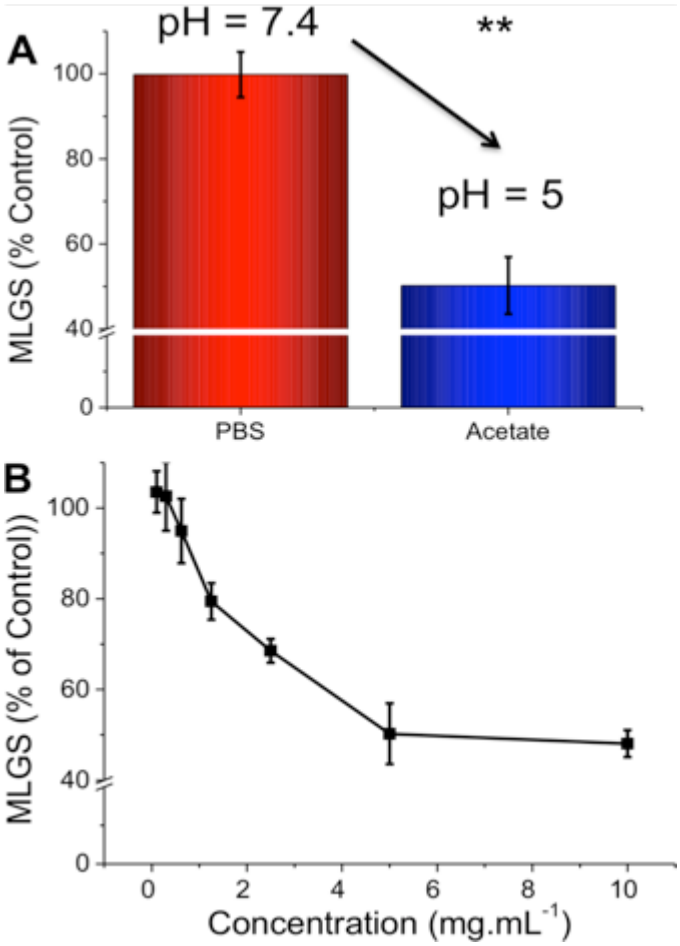

Figure 2.5. IRI activity of nisin A. (A) pH dependence; (B) concentration dependence at pH 5. Error bars represent ± SD from a minimum of 3 repeats, MLGS = mean largest grain size relative to PBS buffer or pH 5 acetate buffer controls. ** signifies $p < 0.01$ relative to control.

However, pH itself may not always be a useful (or desirable) trigger. Histidines are well know to bind to metal ions such as nickel or zinc (forming the basis of His-tag purifications for example),[44] and we therefore reasoned that addition of these ions might also be able to promote the formation of the correct conformation for IRI activity. Figure 2.6 shows IRI activity of nisin A with addition of these metal ions, compared to control solutions containing the metal ions alone.

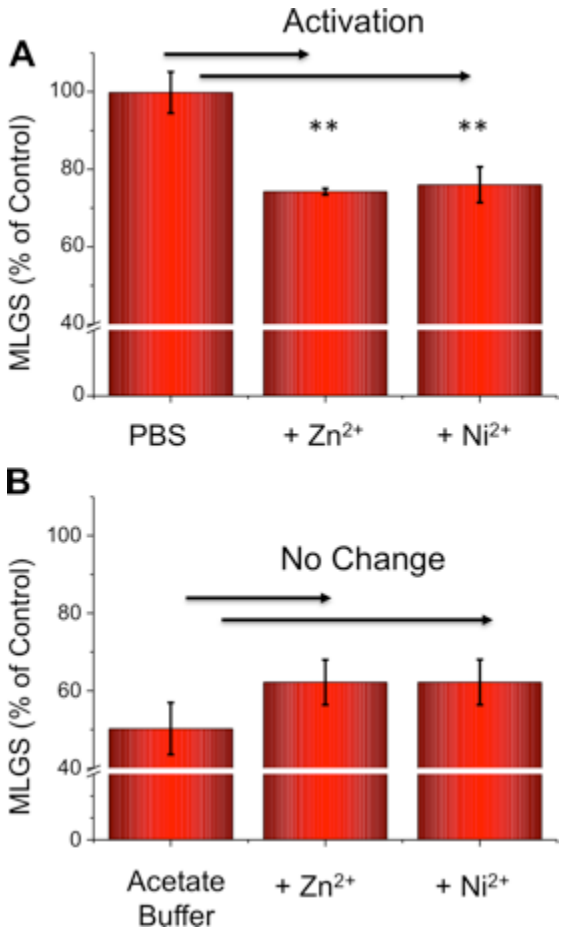

Figure 2.6. Metal ion activation of nisin A IRI activity upon addition of nickel and zinc acetate at 5mg.mL^{-1}. A) In PBS buffer at pH = 7.4; B) Acetate buffer, pH = 5. Error bars represent ± SD from a minimum of 3 repeats, MLGS = mean largest grain size relative to PBS buffer , pH 5 acetate buffer controls or buffer with nickel acetate added only. ** signifies $p < 0.01$ relative to Nisin in PBS buffer only.

For both Zn and Ni additives in PBS (pH 7.4, no protonation of his-residues) there was clear 'switching on' of activity compared to the buffer alone. This demonstrates that metal ions can be used in place of H^+ to induce the conformation changes in nisin A required for activity, although the magnitude of IRI is slightly less. A control experiment conducted at pH 5 (acetate buffer) where histidines were already protonated showed no effect of the metal ions, ruling out other interactions. These

results show that easily available, relatively small, antimicrobial peptides have latent IRI activity that can be activated by the use of specific metal ions providing a new paradigm in AFP biomimetics. Considering the huge progress in the rational design of antimicrobial peptide mimics, it is anticipated that a similar approach will yield new IRI active compounds, without the need to mimic AFP structure. These findings will aid our understanding of ice growth inhibiting macromolecules and aid in the pursuit of cell/tissue cryopreservation for regenerative medicine, in addition to other fields where ice is a problem.

2.4. Conclusions

Here we demonstrate that proteins and peptides with little structural homology to antifreeze proteins can have surprisingly potent ice recrystallization inhibition activity, based upon two motifs. L-type plant lectins, which are widely available and are available at relatively low cost are shown to be calcium-dependent ice recrystallization inhibitors, with their activity easier modulated by the addition of calcium, providing some 'switching' capability. The activity was shown to be present in three different plant lectins, suggesting it is a universal property of lectins. As antifreeze proteins are known to be amphipathic, a second class of peptides was also tested, antimicrobial peptides. The 34 amino acid peptide nisin A was found to have surprisingly strong IRI activity that was activated by a change in pH and consequently, protonation of its histidine residues, again providing a unique switch. To enable antifreeze activity at physiological pH, nickel or zinc ions were employed as the stimulus, which can bind the histidine residues and promote the same conformation change. These results show that new antifreeze protein function can be discovered in non-cold acclimatized species and that this provides a route to

'switchable' antifreeze materials whose function can be tuned by externally applied stimuli, and also eventually leading towards multifunctional macromolecular cryoprotectants.

2.5. Experimental

2.5.1. Materials

Poly (ethylene glycol) (100 kDa), HEPES, sodium acetate, glacial acetic acid, sodium hydroxide pellets, calcium chloride, glyceraldehyde, nisin A, zinc acetate and nickel acetate were purchased from Sigma Aldrich (UK). Lectins; concanavalin A (Con-A), soybean agglutinin (SBA) and *ricinus communis* agglutinin 120 (RCA_{120}) were purchased from Vector Laboratories (USA). Nisin was dialyzed against PBS buffer for 24 hours (5 buffer changes) to ensure that all salts were removed before use. HEPES buffer solution (10 mM) was prepared using solid powder and adjusted to pH 7.4 using sodium hydroxide pellets. Sodium acetate buffer (0.2 M) was prepared by mixing sodium acetate and glacial acetic acid in deionized water and adjusted to pH 5 with sodium hydroxide pellets.

2.5.2. Ice recrystallisation inhibition (splat) assay.

Ice recrystallisation inhibition was measured using a modified splay assay.[45] A 10 μL sample of polymer dissolved in PBS buffer (pH 7.4) was dropped 1.40 m onto a chilled glass coverslip sat on a piece of polished aluminium placed on dry ice. Upon hitting the chilled glass coverslip, a wafer with diameter of approximately 10 mm and thickness 10 μm was formed instantaneously. The glass coverslip was transferred onto the Linkam cryostage and held at -8 °C under N_2 for 30 minutes. Photographs were obtained using an Olympus CX 41 microscope with a UIS-2 20x/0.45/∞/0-2/FN22

lens and crossed polarizers (Olympus Ltd, Southend on sea, UK), equipped with a Canon DSLR 500D digital camera. Images were taken of the initial wafer (to ensure that a polycrystalline sample had been obtained) and after 30 minutes. Image processing was conducted using Image J, which is freely available.[46] In brief, ten of the largest ice crystals were measured and the single largest length in any axis recorded. This was repeated for at least three wafers and the average (mean) value was calculated to find the largest grain dimension along any axis. The average of this value from three individual wafers was calculated to give the mean largest grain size (MLGS). This average value was then compared to that of a PBS buffer negative control providing a way of quantifying the amount of IRI activity.

2.5.3. Analysis of sequence alignment.

Sequences of proteins were analysed using the online BLAST sequence alignment tool[47], while three dimensional structures of proteins were imaged using pymol[48]. A type 2 AFP from Sea raven, *Hemitripterus americanu* (pdb code 2AFP, accession number P05140) was searched against using the protein databank proteins database and blastp algorithm. The sequences of those proteins defined as having significant alignments by BLAST were used for further sequence alignment. Multiple sequence alignment was conducted using Jalview Desktop with Muscle with defaults multiple sequence alignment web service for alignment.[49]

2.5.4. Use of Lectins and nisin.

The lectins used in this study were kept as a solid lyophilized powder until required for testing, then made up in the appropriate buffer in 5mg.mL^{-1} solutions and diluted

as needed. Denaturation of the protein was achieved by incubation of the protein at 80°C for 15 minutes.

2.6. References

[1] J. A. Ahlgren, C.C. Cheng, J.D. Schrag, and A.L Devries, *Comp. Biochem. Physiol. B* **2006**, *144*, 290–300

[2] C. C. Cheng, A. L. DeVries, in *Life Under Extreme Conditions* (Ed.: G. di Prisco), Springer Berlin Heidelberg, **1991**, pp. 1-14.

[3] J. G. Duman, V. Bennett, T. Sformo, R. Hochstrasser, B. M. Barnes, *J. Insect Physiol.* **2004**, *50*, 259-266.

[4] A. J. Middleton, C. B. Marshall, F. Faucher, M. Bar-Dolev, I. Braslavsky, R. L. Campbell, V. K. Walker, P. L. Davies, *J. Mol. Biol.* **2012**, *416*, 713-724.

[5] M. Smallwood, D. Worrall, L. Byass, L. Elias, D. Ashford, C. J. Doucet, C. Holt, J. Telford, P. Lillford, D. J. Bowles, *Biochem. J.* **1999**, *340*, 385-391.

[6] J. Barrett, *Int. J. Biochem. Cell Bio.* **2001**, *33*, 105–117.

[7] Y. Celik, L. A. Graham, Y. F. Mok, M. Bar, P. L. Davies, I. Braslavsky, *Proc. Natl. Acad. Sci. U. S. A.* **2010**, *107*, 5423-5428.

[8] M. I. Gibson, *Polym. Chem.* **2010**, *1*, 1141-1152.

[9] A. Eniade, A. V. Murphy, G. Landreau, R. N. Ben, *Bioconjugate Chem.* **2001**, *12*, 817-823.

[10] A. K. Balcerzak, M. Febbraro, R. N. Ben, *RSC Adv.* **2013**, *3*, 3232-3236.

[11] A. K. Balcerzak, C. J. Capicciotti, J. G. Briard, R. N. Ben, *RSC Adv.* **2014**, *4*, 42682-42696.

[12] A. K. Balcerzak, S. S. Ferreira, J. F. Trant, R. N. Ben, *Bioorg. Med. Chem. Lett.* **2012**, *22*, 1719-1721.

[13] S. O. Yu, A. Brown, A. J. Middleton, M. M. Tomczak, V. K. Walker, P. L. Davies, *Cryobiology* **2010**, *61*, 327-334.

[14] M. Griffith, K. V. Ewart, *Biotechnol. Adv.* **1995**, *13*, 375-402.

[15] H. Koushafar, L. Pham, C. Lee, B. Rubinsky, *J. Surg. Oncol.* **1997**, *66*, 114-121.

[16] H. Chao, Davies, P.L., Carpenter, J.F., *J. Ex. Biol.* **1996**, *199*, 2071-2076.

[17] J. F. Carpenter, T. N. Hansen, *Proc. Natl. Acad. Sci. U. S. A.* **1992**, *89*, 8953-8957.

[18] J. Beirao, L. Zilli, S. Vilella, E. Cabrita, R. Schiavone, M. P. Herraez, *Biol. Reprod.* **2012**, *86*, 59.

[19] J. Lee, S. K. Kim, H. W. Youm, H. J. Kim, J. R. Lee, C. S. Suh, S. H. Kim, *PLoS ONE* **2015**, *10*, e0126252.

[20] C. J. Capicciotti, J.S. Poisson, C.N Boddy, and R.N. Ben., *Cryobiology* **2015**, *15*, 79–89.

[21] R. C. Deller, M. Vatish, D. A. Mitchell, M. I. Gibson, *Nat. Commun.* **2014**, *5*, 3244-3249.

[22] P. L. Davies, C. L. Hew, *FASEB J.* **1990**, *4*, 2460-2468.

[23] P. L. Davies, B. D. Sykes, *Cur. Opin. Struct. Biol.* **1997**, *7*, 828-834.

[24] M. M. Harding, L. G. Ward, A. D. J. Haymet, *Eur. J. Biochem.* **1999**, *264*, 653-665.

[25] W. Gronwald, M. C. Loewen, B. Lix, A. J. Daugulis, F. D. Sonnichsen, P. L. Davies, B. D. Sykes, *Biochemistry* **1998**, *37*, 4712-4721.

[26] K. Ewart, Q. Lin, C. Hew, *Cell. Mol. Life Sci.* **1999**, *55*, 271-283.

[27] B. Rubinsky, Coger, R., Ewart, K.V., Fletcher, G.L., *Nature* **1992**, *360*, 113-114.

[28] L. A. Graham, S. C. Lougheed, K. V. Ewart, P. L. Davies, *PLoS ONE* **2008**, *3*, e2616.

[29] M. D. Swanson, H. C. Winter, I. J. Goldstein, D. M. Markovitz, *J. Biol. Chem.* **2010**, *285*, 8646-8655.

[30] T. Congdon, R. Notman, M. I. Gibson, *Biomacromolecules* **2013**, *14*, 1578-1586.

[31] J. A. Gilbert, P. L. Davies, J. Laybourn-Parry, *FEMS Microbiol. Lett.* **2005**, *245*, 67-72.

[32] K. V. Ewart, D. S. C. Yang, V. S. Ananthanarayanan, G. L. Fletcher, C. L. Hew, *J. Biol. Chem.* **1996**, *271*, 16627-16632.

[33] S. Deville, C. Viazzi, J. Leloup, A. Lasalle, C. Guizard, E. Maire, J. Adrien, L. Gremillard, *PLoS ONE* **2011**, *6*, e26474.

[34] C. J. Capicciotti, M. Leclere, F. A. Perras, D. L. Bryce, H. Paulin, J. Harden, Y. Liu, R. N. Ben, *Chem. Sci.* **2012**, *3*, 1408-1416.

[35] D. E. Mitchell, M. Lilliman, S. G. Spain, M. I. Gibson, *Biomater. Sci.* **2014**, *2*, 1787–1795.

[36] D. E. Mitchell, N. R. Cameron, M. I. Gibson, *Chem. Commun.* **2015**.

[37] R. Y. Tam, C. N. Rowley, I. Petrov, T. Zhang, N. A. Afagh, T. K. Woo, R. N. Ben, *J. Am. Chem. Soc.* **2009**, *131*, 15745-15753.

[38] K. A. Brogden, *Nat. Rev. Micro.* **2005**, *3*, 238-250.

[39] M. Heisig, Nabil M. Abraham, L. Liu, G. Neelakanta, S. Mattessich, H. Sultana, Z. Shang, Juliana M. Ansari, C. Killiam, W. Walker, L. Cooley, Richard A. Flavell, H. Agaisse, E. Fikrig, *Cell Rep.* **2014**, *9*, 417-424.

[40] P. M. Periago, R. Moezelaar, *Int. J. Food Microbiol.* **2001**, *68*, 141-148.

[41] H. S. Rollema, Kuipers, O.P., Both, P., de Vos, W.M., Siezen, R.J. , *Appl. Environ. Microbiol.* **1995**, *61*, 2873–2878.

[42] F. H. Gao, Abee, T., Konings, W.N *Appl. Environ. Microbiol.* **1991**, *57*, 2164-2170

[43] H. Koushafar, L. Pham, C. Lee, B. Rubinsky, *J. Surg. Oncol.* **1997**, *66*, 114-121.

[44] J. A. Bornhorst, J. J. Falke, *Methods Enzymol.* **2000**, *326*, 245-254.

[45] C. A. Knight, J. Hallett, A. DeVries, *Cryobiology* **1988**, *25*, 55-60.

[46] J. Schindelin, I. Arganda-Carreras, E. Frise, V. Kaynig, M. Longair, T. Pietzsch, S. Preibisch, C. Rueden, S. Saalfeld, B. Schmid, J.-Y. Tinevez, D. J. White, V. Hartenstein, K. Eliceiri, P. Tomancak, A. Cardona, *Nat. Meth.* **2012**, *9*, 676-682.

[47] S. F. Altschul, W. Gish, W. Miller, E. W. Myers, D. J. Lipman, *J. Mol. Biol.* **1990**, *215*, 403-410.

[48] L. Schrodinger, *The PyMOL Molecular Graphics System*, 1.3r1 ed., **2010**.

[49] R. C. Edgar, *Nucleic Acids Res.* **2004**, *32*, 1792-1797.

Chapter 3

3. Quantitative Study on the Antifreeze Protein Mimetic Ice Growth Inhibition Properties of Poly(ampholytes) Derived from Vinyl-Based Polymers

D.E. Mitchell, M. Lilliman S.G. Spain and M. I. Gibson, *Biomater. Sci*. **2014**, **2**, 1787-1795.

This chapter contains a paper on the synthesis and testing of poly(ampholytes) as ice recrystallization inhibition (IRI) molecules, aiming to identify the structural motifs and proportion of positive and negative charges required for IRI activity.

DEM synthesized all polymers used here, except carbohydrate centred polymers, which were synthesized by MI. DEM and SGS undertook size exclusion chromatography (SEC) of polymers, while DEM was responsible for characterization through NMR spectroscopy. All IRI testing and dye exclusion assay was carried out by DEM. DEM and MIG prepared the manuscript.

3.1. Abstract

Antifreeze (glyco) proteins (AF(G)Ps) from the blood of polar fish species are extremely potent ice recrystallization inhibitors (IRI), but are difficult to synthesise or extract from natural sources. Despite this challenge, materials which display IRI are appealing due to their ability to enhance cellular cryopreservation, for applications including regenerative and transplantation medicine. Here, poly(ampholytes), which contain a mixture of cationic and anionic side chains are quantitatively evaluated for their IRI activity. Poly(aminoethyl methacrylate), obtained by RAFT polymerization, is functionalised with succinic anhydride to generate the poly(ampholytes). The charge balance of the side chains is shown to be crucial, with only 50 : 50 mixtures having strong IRI activity, which also scales with molecular weight. This is the first example of a non-hydroxylated synthetic polymer with quantifiable IRI activity and raises questions about the mechanism of IRI, as the polymers have no obvious ice-binding motif. The ampholytic structure is shown to be transferable to carbohydrate-centred polymers with activity retained, but poly(betaines) are shown to be inactive.

3.2. Introduction

Since their discovery in the serum of Arctic fish species, antifreeze proteins (AFPs) and antifreeze (glyco)proteins (AF(G)Ps) have attracted significant attention due to their unique ice-interacting properties and their potential applications in cryopreservation, anti-icing surfaces, food storage and more.[1-3] AF(G)Ps have three key macroscopic properties;[4-5] i) Thermal hysteresis (TH) – the non-colligative depression of the freezing point, which does not affect the equilibrium melting point;

ii) Dynamic ice shaping (DIS) where the shape of ice crystals is altered due to specific inhibition of difference faces on the ice surface; iii) Ice recrystallization inhibition (IRI) whereby the AF(G)Ps slow the rate of ice crystal growth (Ostwald ripening). The underlying mechanism of action for each individual property is still under investigation.[6-8] Nishimura and co-workers synthesised several derivatives of AF(G)Ps, varying the carbohydrate and peptide components enabling them to identify the core motifs that were essential to maintain the TH and DIS activity.[9] Combined with previous studies, which have also shown that AF(G)Ps are not tolerant to many structural modifications,[1] it would seem that very particular requirements in terms of functional groups and tertiary structure are essential for AF(G)P activity. However, in most of these studies only TH and DIS were tested for, not IRI meaning its link to structure is less clear. In 2003 Enaide *et al.* observed that dramatically simplified glycoproteins could retain IRI activity but display essentially zero TH or DIS.[10] This observation suggested that there might be multiple molecular mechanisms that give rise to the same macroscopic properties and that it is possible to design new molecules that specifically display IRI activity.[11] Several glycopeptides and even small molecules have since been identified with varying degrees of IRI activity.

Analysis of the process of cellular cryopreservation has revealed that ice growth during thawing is a major contributor to cell death.[12] Consequently, any new materials that can inhibit ice growth (i.e. IRI activity) may find application to enhance the storage of urgently needed donor tissue for transplantation. In 2013 in the USA, 118,000 individuals were on organ waiting lists and demand almost always outstrips supply.[13-14] New regenerative medicines, or drug screening methods, based on stem cells also require improved (cryopreservation) storage methods.[15-16] Attempts at

cryopreservation with AF(G)Ps have reported varying degrees of success. Addition of AF(G)P to erythrocytes gave some cryopreservation enhancement, but above a critical concentration, its benefits stopped, limiting it use.[17] This was found to be due to the formation of needle-like (spicular) ice crystals due to the DIS/TH activity of AF(G)Ps. Subsequent studies on the addition of AF(G)P to sperm resulted led to decreased motility[18] and there is evidence that AF(G)P may be toxic to human cells. [19] There are several other conflicting studies showing both benefits and problems of AF(G)Ps in cryopreservation, normally due to ice shaping, which have prevented their application.[20-21] IRI-specific synthetic glycopeptides showed a marginal benefit in the cryopreservation of human embryonic liver cells.[22]

Due to the difficulties in synthesising glycopeptides,[23] AF(G)P mimics are required, especially if they specifically reproduce only IRI for cryopreservation. Inada *et al*.[24] and Gibson *et al*.[25-26] have shown that poly(vinyl alcohol), PVA, is an extremely potent IRI despite having little or no structural similarity to AF(G)P. PVA with as few as 20 repeat units (M_N = 880 g.mol^{-1}) can inhibit ice growth at concentrations below 1 mg.mL^{-1}. Gibson and co-workers showed that addition of just 1 mg.mL^{-1} PVA to erythrocytes enabled their cryopreservation without the need for any organic solvents,[27] such as glycerol or DMSO, which are themselves cytotoxic at high concentrations and not suitable for transfusion.

Synthetic polymers are particularly appealing as biomimetics due to their scalable synthesis, tuneable structure, and range of different monomers, and have been employed as mimics of mussel adhesive proteins,[28] antibacterial peptides[29] and glycoproteins,[30-31] for example. Despite this appeal, very few synthetic polymers

have been demonstrated (quantitatively) to have IRI activity and it has become clear that simply having a poly(hydroxylated) structure (such as PVA) is not sufficient to guarantee IRI.[32] Hydrophobicity is known to be a crucial component, with crystal structures of native AFPs showing defined hydrophobic and hydrophilic domains.[2, 33] Chemical modification of PVA (hydrophobic/hydrophilic substituents) also removes activity meaning that solution or surface absorbed conformation maybe important and there are few other lead structures to design new IRI-active compounds. Most polymers tested (in our hands) simply have no activity. Intriguingly, Matsumura *et al.* observed that poly(ampholytes) (which have both positive and negative charges) are very effective cryoprotectants, enabling solvent-free cryopreservation of stem cells.[34] They observed that the 50 % carboxylated poly(lysine) had very weak ice shaping effects (DIS). Similar results have been observed for ampholytic polysaccharides and vinyl polymers, but their IRI activity has not been quantitatively studied.[35-36]

The aim of this study was therefore to investigate the poly(ampholyte) structure as a new motif for IRI active polymers which would open the door to a diverse range of non-PVA based AF(G)P mimetic polymers with highly tuneable structures and properties. Such biomaterials will help address the urgent needs of tissue storage, transport and logistics,[13] and lead to real clinical benefits building on our recent observations of the link between IRI and cell survival in cryopreservation

3.3. Results and Discussion

In order to obtain structure-property relationships between mixed charge polymers (polyampholytes) and their ice recrystallization inhibition activity it was necessary to devise a synthetic strategy that was compatible with controlled (radical)

polymerization. The planned synthetic strategy is shown in Scheme 3.1, using poly(aminoethyl methacrylate) (PAEMA) derived from RAFT polymerization as the cationic polymer, as an alternative to poly(lysine). Reaction with succinic anhydride can then produce the mixed charged polymer, inspired by carboxylated poly(lysine), a known cryoprotectant.

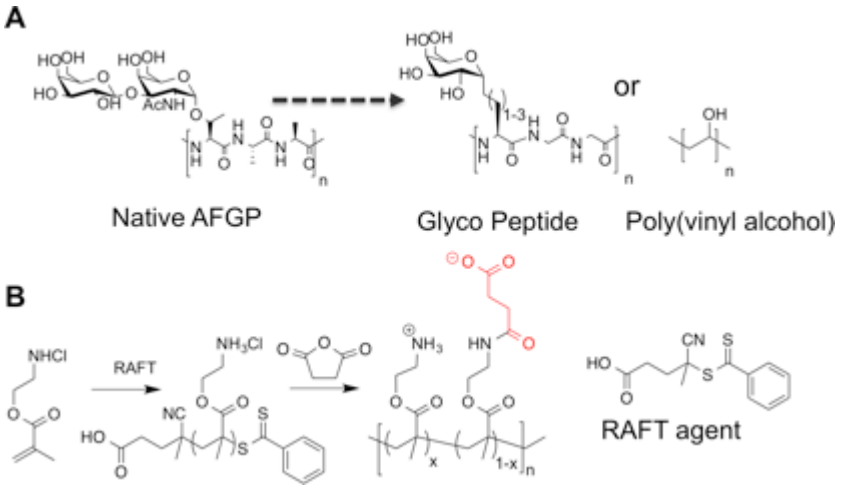

3

Scheme 3.1. IRI active molecules and poly(ampholyte) synthetic method A.) Native AFGP and previously reported IRI active macromolecules; B.) Synthetic method used in this report to obtain poly(ampholytes)

A library of PAEMAs were synthesized using 4-cyanopentanoic acid dithiobenzoate (CTP) as the chain transfer agent, with 4,4′-azobis(4-cyanovaleric acid) (ACVA) as the radical source. A constant [monomer]:[CTA] ratio was employed in all experiments, with the polymerization time being varied to provide control over chain length. The monomer conversion was determined by ^{1}H NMR spectroscopy against an internal mesitylene standard. All polymers were characterized by ^{1}H NMR to provide an estimation of M_n, by comparing the benzylic resonances derived from the RAFT agent to the polymer backbone, Table 3.1. Size exclusion chromatography (SEC) of these polymers was attempted in a range of aqueous buffers, but in all cases

very broad dispersities were obtained, which can be ascribed to the well known self-reactivity of PAEMA which can lead to cross-linking[37]. (ESI, Appendix 2.) To reduce this polymers were not handled in aqueous solution unless essential, and the solutions were acidified to ensure protonation of the amine groups. Previous reports of the polymerization of PAEMA suggest that it is a controlled process under identical RAFT conditions, [38] and the values for M_N extracted by end-group analysis are in agreement with that from conversion, suggesting the RAFT mediating agent is present at the chain ends. From this point on, the molecular weight is defined as that obtained from end group analysis. However, there must be assumed to be error in these measurements which are considered when interpreting data (below).

Table 3.1. **Polymerization of aminoethyl methacrylate**

Entry[a]	Time (hrs)	Conversion (%)	$M_{N,\,Theo}$ [b] (g.mol^{-1})	$M_{N,NMR}$ [c] (g.mol^{-1})
11 k	0.75	8.2	5400	11000
20 k	1	18	11900	20000
23 k	2	35	23100	23000
27 k	3	44	29100	27000
33 k	3.5	52	34400	33000
40 k	5	61	40400	40000
67 k	6	74	49000	67000

(a) [Monomer]:[CTA]:[I] = 400:1:0.2 was used in all polymerizations; (b) Theoretical M_N determined from monomer feed ratio and conversion (^{1}H NMR); (c) Mn determined by end group analysis.

In order to generate mixed-charge polymers with pendant carboxylic acid groups ring-opening of succinic anhydride was employed, Scheme 3.1. All the polymers in Table 3.1 were functionalized in this manner to give approximately 50 mol% (±5%) COOH functionality (ESI, Appendix 2). In order to screen the effect of COOH density on IRI activity (*vide infra*) 33 kg.mol^{-1} PAEMA was functionalized at a range of COOH densities, Table 3.2. The degree of functionalization in each case was estimated by ^{1}H

NMR spectroscopy. 50 mol % carboxylated poly(lysine) was also synthesized from commercial poly(lysine) by the same method as a positive control.

Table 3.2. **Functionalization of PAEMA with succinic anhydride.**

Entry	M_N, PAEMA (kg.mol^{-1})	Succinic Anhydride (mol %)	f_{COOH} (mol %)[(a)]	M_N Copolymer (kg.mol^{-1})
P1	**11**	80	50	15.2
P2	**20**	80	50	27.6
P3	**27**	80	50	37.4
P4	**33**	80	50	45.7
P5	**44**	80	50	60.9
P6	**67**	80	50	92.7
P7	**33**	0	0	33.0
P8	**33**	20	18	37.5
P9	**33**	50	32	41.1
P10	**33**	70	40	43.1
P11	**33**	80	50	45.7
P12	**33**	90	56	47.2
P13	**33**	100	60	48.2
P14	**33**	125	63	49.0
P15	**33**	150	76	52.3
P16	**33**	175	82	53.8

(a) Determined from PAEMA (CH_2-CH_2) to succinic anhydride ratio using ^{1}H NMR

With this large panel of polymers at hand, quantitative 'splat test' measurements were undertaken to correlate polymer structure to ice recrystallization inhibition activity. Briefly, this assay involves dropping a small volume (~10 μL) of phosphate buffered saline containing the polymers onto a $CO_{2(S)}$ cooled glass slide sat on an aluminium plate. This generates large numbers of very small (<10 μm) ice crystals which are allowed to grow at – 6 °C for 30 minutes before being photographed through crossed polarizers. The mean largest grain size (MLGS) is measured and reported relative to a PBS standard, with smaller ice crystal sizes indicating a more active compound. Poly(ethyleneglycol) (PEG, 100 kDa) is used as a negative control polymer as it is well known to have no significant IRI activity.[25-26] The first polymer to be tested was 50 mol % carboxylated poly(lysine), which has been shown to be a useful cryoprotectant but has never been quantitatively assessed for IRI activity, Figure 3.2.

This polymer was shown to only have very weak IRI activity, giving ~ 60 % MLGS at 20 mg.mL^{-1} compared to PEG which gave ~ 75 % MLGS at the same concentration. This is significantly weaker than the most well known polymeric IRI compound, poly(vinyl alcohol) which can inhibit ice growth below 1 mg.mL^{-1}. However, this still represents one of only a handful of polymers with definitive IRI activity and is an interesting lead structure for further investigation especially considering the known cryoprotectant properties of carboxylated poly(lysine) and their significant structure differences to AF(G)Ps. Encouraged by these results, a relatively long PAEMA (**P6**) 67 kg.mol^{-1} with 50 mol % COOH was assessed for activity at a variety of concentrations. Pleasingly, this polymer showed significant IRI activity at concentrations up to 20 mg.mL^{-1}, with an MLGS of ~ 40 %, significantly more active than the corresponding poly(lysine) derivative. Example micrographs of ice wafers grown with **P4** are shown in Figure 3.1, and graphically in Figure 3.2.

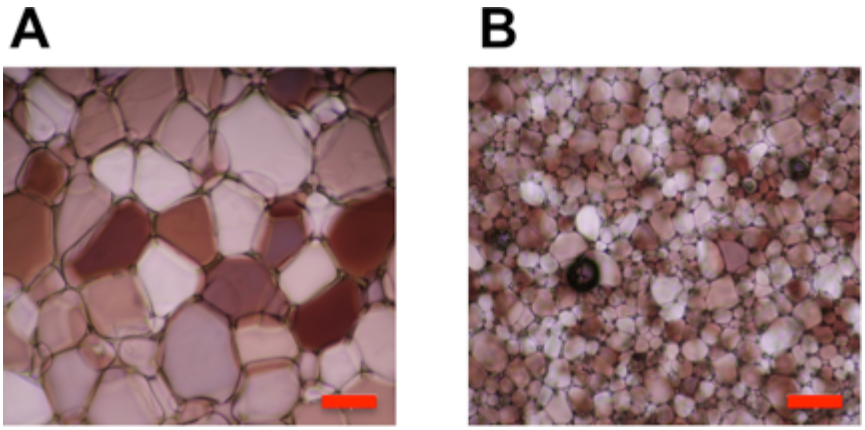

Figure 3.1. Cryomicrographs of ice wafers which have been annealed at -8 °C for 30 minutes. A) PBS control; B) **P4**, 20 mg.mL^{-1}. Scale bar = 100 μm.

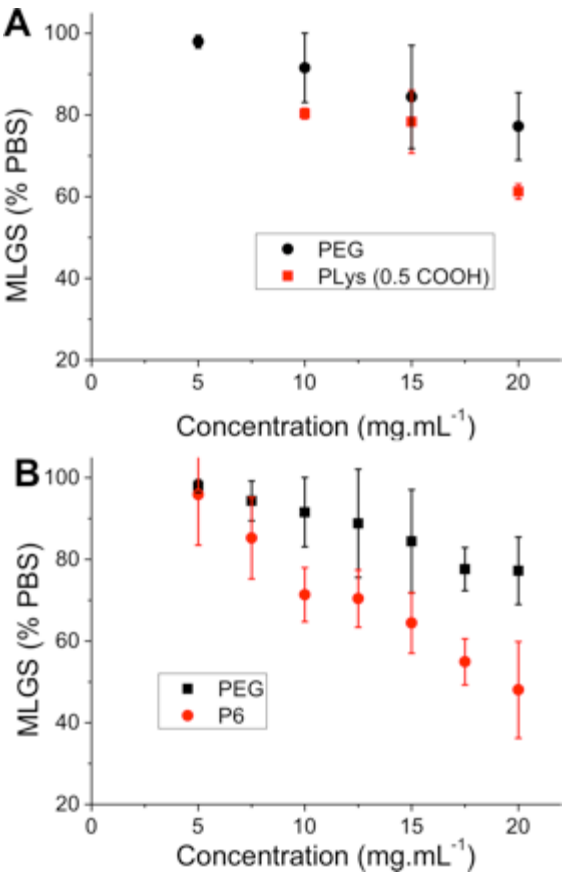

Fig. 3.2. Ice recrystallization inhibition by poly(ampholytes). A) Comparison of PEG and carboxylated poly(lysine); B) Comparison of PEG to PAEMA-co-succinic anhydride (50% functionality), **P6**, Error bars represent ± SD from a minimum of 3 repeats. MLGS = mean largest grain size relative to phosphate buffered saline control.

To ensure that the observed IRI activity was due to the mixed-charge nature of the polymers, **P7** – **P16** with varying degrees of carboxylation were investigated, Figure 3.3. Polymers with 0 to 90 % COOH (the highest achievable using this synthetic method) showed no IRI activity. As the density of COOH groups approached 50 mol% the IRI activity steadily increased (smaller crystals) demonstrating that the ratio of the two side chains is the crucial structural motif for activity. This is rather remarkable, and questions the mechanism of action of IRI-active polymers which are assumed to need defined ice-binding motifs (hydroxyls) which are not present here. Almost all other IRI active materials tested (PVA, native AFGP, carbohydrates) show

a strong molecular weight dependence on activity, with larger polymers having more IRI. Figure 3.3B shows the molecular weight dependency on IRI for the 50 % COOH polymers, **P1 – P6**. The shortest polymer used here (10 kg.mol^{-1}) had essentially zero IRI, and activity steadily increased as molecular weight increased, with the longest polymer (67 kg.mol^{-1}) giving average ice grain sizes half that of the shortest (10 kg.mol^{-1}) (which is equal to 4 fold decrease in ice area).

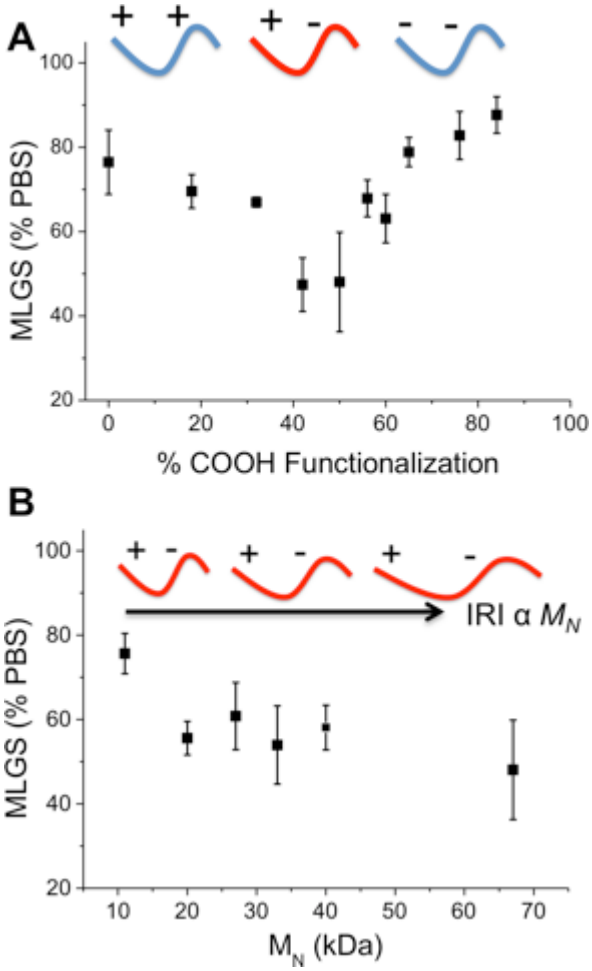

4

Fig. 3.3. Ice recrystallization inhibition activity of PAEMA-derived polymers measured at 20 mg.mL^{-1}; A) effect of degree of carboxylation on activity; B) effect of molecular weight at 50 % carboxylation. Error bars represent ± SD from a minimum of 3 repeats. MLGS = mean largest grain size relative to phosphate buffered saline control.

There are currently no satisfactory models for explaining the mechanism by which IRI active polymers slow ice crystal growth, which has limited their *a priori* design. To test if this mixed–charge motif is a universal method for obtaining IRI polymers, a series of other polymers bearing multiply charged species were investigated. Poly(2-methacryloyloxyethyl phosphorylcholine) (PMPC) and poly([2-(methacryloyloxy) ethyl]dimethyl-(3-sulfopropyl) (PMEDS) ammonium hydroxide) were synthesized by RAFT polymerization of their corresponding monomers, Figure 3.4A. PMPC was obtained with M_N = 25 kg.mol^{-1} and M_W/M_N = 1.12, and PMEDS M_N = 21 kg.mol^{-1} and M_W/M_N = 1.10. These monomers contain cationic and anionic charges on every repeat unit, but of a different nature to the PAEMA derivatives. Quantitative IRI testing revealed that both of these poly(betaines) had essentially zero IRI activity, with their observed MLGS being statistically identical to the negative PEG control at concentrations up to 15 mg.mL^{-1}. At 20 mg.mL^{-1} PMPC had a weak enhancement which was only statistically different from PEG at 95 % confidence. This implies that the distribution and nature (COOH, SO_3) of the charges is crucially important, and will be the subject of future investigations.

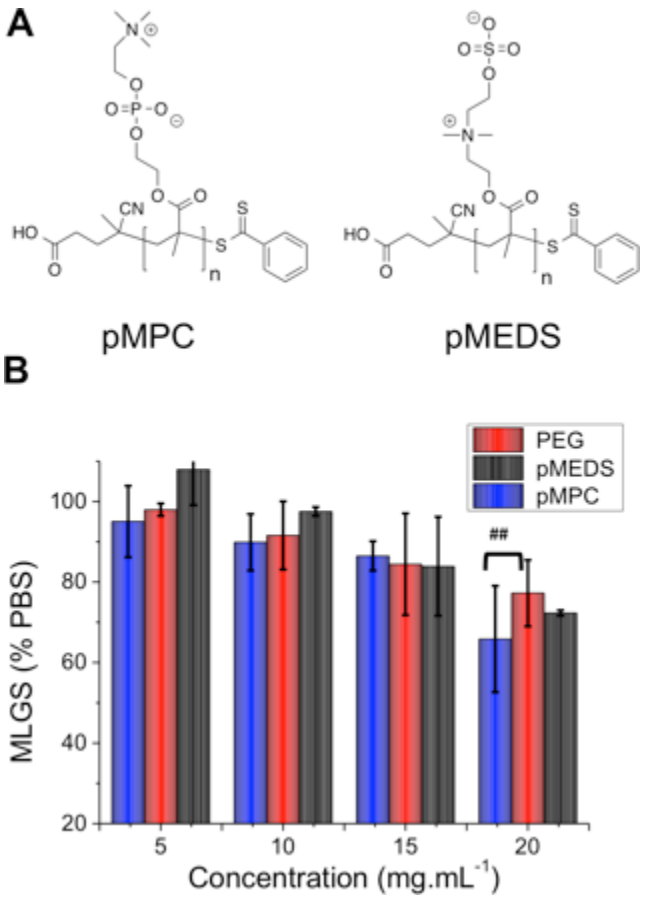

Fig. 3.4. Structure of polymers with multiple charged species and associated IRI activity. A) Structures of PMPC and PMEDS; B) Ice recrystallization inhibition activity. Error bars represent ± SD from a minimum of 3 repeats. MLGS = mean largest grain size relative to phosphate buffered saline control. ## indicates a statistical difference ($p < 0.05$) according to students T-test.

As a final test to determine if the mixed side-chain approach is a universal one, a series of carbohydrate-centred polymers with mixed charges were synthesised (ESI, Appendix 2).[39] Briefly, a series mono, di and tri-saccharides were reacted with methacrylic anhydride to install a reactive methacrylate group on each of the hydroxyls. Addition of L-cysteine to the methacrylated cores by Michael addition ('thiol-ene click') enabled introduction of both an amine and carboxylic acid group at each position ensuring a discrete number of functional groups which is not possible

using radical polymerizations.

Table 3.3. **Carbohydrate-centred poly(ampholytes)**

Core Sugar	Valency	$M_{N, Theo}$ [a] ($g.mol^{-1}$)
Glucose	5	1126
Cellobiose	8	1855
Stachyose	15	2690

(a) Assuming complete functionalization with cysteine.

The two smallest polymers (with either 5 or 8 side chains) displayed very little IRI activity that was statistically identical to PEG. However, the longest oligomer with 12 side chain units gave statistically significant smaller MLGS values compared to PEG and the other carbohydrate-based polymers. Whilst the actual values obtained indicate that these polymers have relatively low activity, it allowed the precise role of valency to be probed, showing that longer polymers are essential when using mixed-charge IRI polymers, but that the concept is a universal one. The structure of these polymers is also desirable as they are composed simply of carbohydrates and amino acids, which is appealing for biomedical applications.

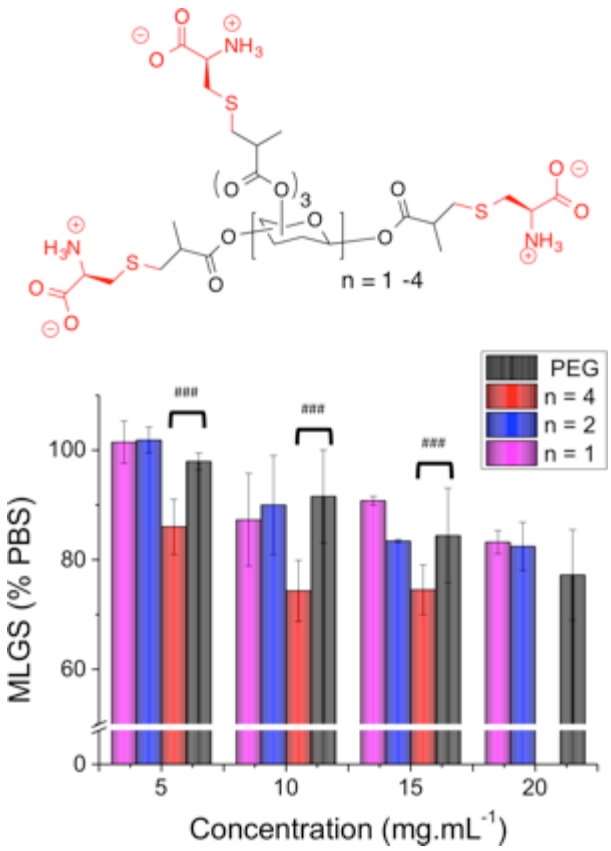

Fig. 3.5. Structure and associated IRI activity of carbohydrate centred poly(ampholytes) A) structure of carbohydrate-centred poly(ampholytes); B) Ice recrystallization inhibition activity. Error bars represent ± SD from a minimum of 3 repeats. MLGS = mean largest grain size relative to phosphate buffered saline control. ### indicates a statistical difference ($p < 0.01$) according to students T-test.

The data presented above clearly demonstrate that mixed charge side chain polymers can inhibit ice growth, but still does not answers the many questions which remain regarding their mode of action. Gibson and Ben have both shown that hydrophobicity, without aggregation, is crucial in the design of new IRIs.[11, 32, 40]. This questions the commonly held theory that hydroxyl groups which are regularly spaced to interact directly with the ice crystal lattice are the crucial motifs to get IRI (or indeed thermal

hysteresis and dynamic ice shaping).[41] Terahertz spectroscopy investigations suggest that AF(G)Ps can disrupt the quasi-liquid layer (interfacial water) prevent exchange of water molecules and hence inhibiting growth.[6, 8] This mechanism would seem to require a hydrophobic domain to either disrupt the water structure or to bind to hydrophobic faces on the ice surface. AFP binding to ice has recently been speculated to be due to anchored clathrate-like water molecules using both hydrophobic interactions as well as crystal-matching.[42] A method to probe hydrophobic domains in polymers is dye inclusion assays. Addition of a hydrophobic dye that does not fluoresce in aqueous solution, but does in non-polar environments allows the ability of a polymer to solubilize hydrophobic compounds to be measured. This is the basis of critical micelle determination for self-assembling amphiphiles, which require a hydrophobic domain. The (polymer) concentration dependant fluorescence of several of the polymers described here were measured and compared to PVA, Figure 3.6. Addition of PVA at less than 10 $mg.mL^{-1}$ lead to significant fluorescence, highlighting its ability to present a hydrophobic domain (and hence its application in colloidal stabilisers[43]). Quantifying the amount of dye incorporation is challenging due to potential self-quenching effects and non-linear fluorescence response, but we would estimate that the PVA can incorporate up to half the dye applied (43 μM) at the highest concentration tested. The non-IRI active PMPC gave rise to fluorescence of ~2500 units at concentrations up to 50 $mg.mL^{-1}$, significantly lower than observed for PVA. **P3** showed essentially no fluorescence enhancement relative to PMPC, suggesting that **P3** does not present a hydrophobic face in solution to solubilise the dye. Dynamic light scattering did not indicate micellisation in any cases. This testing does not rule out specific interactions with an ice surface though, nor does it suggest that that additional hydrophobicity would not enhance activity, but rather than

mechanistically the ampholyte structure does not induce a hydrophobic face. Indeed, studies by Matsumura *et al.* suggest that adding hydrophobicity into poly(ampholytes) can enhance their cryoprotective effect, but the influence of this on IRI has not been determined.[36] The charge-balanced nature of the poly(ampholytes) may be able to disrupt the quasi-liquid layer (or pre-melt layer) at the ice/water interface which is hypothesised to inhibit ice growth, but direct measurements of this challenging interface are non-trivial. Future work will focus on unravelling the structural requirements of IRI activity, and delineating the observable macroscopic properties from the underlying molecular-level mechanisms, as well as probing their application in cryopreservation.

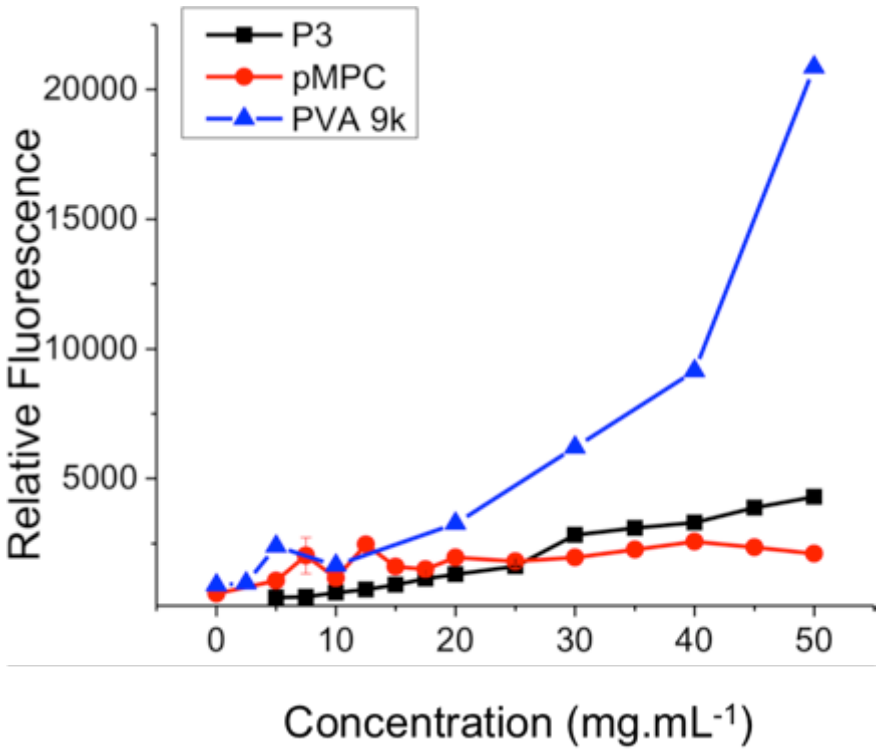

Fig. 3.6. Dye inclusion assay using diphenyl hexatriene. λex = 360 nm λemission at 460 nm.

3.4. Conclusions

This study represents the first detailed analysis of poly(ampholytes) as AF(G)P-mimetic, IRI active polymers. The significance of this work lies in the fact that the poly(ampholyte) structure is synthetically very accessible, but also very different to all previously recorded IRI-active polymers which are thus far limited to poly(hydroxylated) structures. It was demonstrated that the ratio of cationic to anionic groups was crucial, with a 1:1 balance giving maximal IRI activity, and that longer polymers had enhanced activity. The nature of the cation/anion was also found to be important as poly(betaines) showed no appreciable activity.

The remarkable activity of these polymers opens the door to the rational design of new, IRI-active polymers, which are not based on hydroxyl-group presentation and can be obtained from both vinyl and biological backbones. This also questions the underlying mode of action of IRI-active compounds, challenging the paradigm of precise-ice face recognition by hydroxyl groups. Ultimately, the development of IRI active polymers will impact regenerative medicine through enhanced cryopreservation of donor (stem) cells, or even whole organs.

3.5. Experimental Section

3.5.1. Materials

Aminoethyl methacrylate (AEMA), 2-methacryloyloxyethyl phosphorylcholine (MPC), 4-cyanopentanoic acid dithiobenzoate (CTP), 4,4-Azobis(4-cyanovaleric acid) (V-501), succinic anhydride, ethylene sulphate, methacryloyloxy ethyl dimethyl-(3-sulfopropyl)ammonium hydroxide (MEDS) poly-ε-lysine hydrobromide

(30-70 kDa), poly(ethylene glycol) (PEG, 100 kDa size), trehalose, sucrose, diphenylhexatriene (DPH), acetic acid and sodium acetate were purchased from Sigma Aldrich (UK). PEG was dialyzed over 24 hours with 5 water changes, while all other reagents were used as received unless otherwise stated. Phosphate-buffered saline (PBS) solution was prepared using preformulated tablets (Sigma-Aldrich) in 200 mL of Milli-Q water (>18.2 Ω mean resistivity) to give [NaCl] = 0.138 M, [KCl] = 0.0027 M, and pH 7.4.

3.5.2. Physical and analytical methods

^{1}H and ^{13}C NMR spectra were recorded on Bruker DPX-300 and DPX-400 spectrometers using deuterated solvents obtained from Sigma-Aldrich. Chemical shifts in ppm (δ) are reported relative to residual tetramethylsilane (TMS). Fluorescence spectrometry was undertaken using a Synergy HT multi-mode microplate reader (BioTek UK, Bedfordshire, UK).

Aqueous SEC was attempted using two different conditions. The first of these was performed on an Agilent 1260 Infinity Quaternary system utilizing 0.1 M HCl with 0.1 % TFA at a flow rate of 1 $mL.min^{-1}$ while column and detector temperatures were maintained at 35 °C. The instrument was fitted with a PL aquagel guard column (50 × 7.5 mm, 8 μm) and a PSS NOVEMA cationic column (300 X 8.0 mm, 10μm), The data was analyzed using Agilent GPC/SEC software. The second was performed on Cationic (acidic) aqueous GPC was performed on a Shimadzu Prominence UPLC system fitted with a differential refractive index detector. The eluent was 1 M acetic acid containing 0.3 M NaH_2PO_4 (pH 3) at a flow rate of 1 $mL.min^{-1}$ with column and detector cell temperatures maintained at 35 °C. The instrument was fitted with a

Polymer Labs Aquagel-OH guard column (50 × 7.5 mm, 8 μm) followed by a pair of PL Aquagel-OH columns (30 and 40, 300 × 7.5 mm, 8 μm). Column calibration was achieved using narrow poly(2-vinyl pyridine) standards (Polymer Standards Service, Germany) of known molecular weight in the range 0.8-256 kDa. Molecular weights and dispersity values were calculated using Shimadzu LabSolutions software with GPC analysis add-on.

3.5.3. Dye inclusion assay

80 μL Aliquots of 6 kDa PVA, 25kDa pAEMA and pMPC 20 μL of 0.01 $mg.mL^{-1}$ DPH were added to a black solid-bottom (Greiner bio-one) 96-well plate and samples incubated at 25 °C for a minimum of 30 minutes. The fluorescence of each sample was then measured with excitation at 360 nm and emission at 460 nm using top-excitation. Measurements were taken in triplicate.

3.5.4. Ice recrystallisation inhibition (splat) assay

Ice recrystallisation inhibition was measured using a modified splay assay.[44] A 10 μL sample of polymer dissolved in PBS buffer (pH 7.4) was dropped 1.40 m onto a chilled glass coverslip sat on a piece of polished aluminium placed on dry ice. Upon hitting the chilled glass coverslip, a wafer with diameter of approximately 10 mm and thickness 10 μm was formed instantaneously. The glass coverslip was transferred onto the Linkam cryostage and held at −8 °C under N_2 for 30 minutes. Photographs were obtained using an Olympus CX 41 microscope with a UIS-2 20x/0.45/∞/0-2/FN22 lens and crossed polarizers (Olympus Ltd, Southend on sea, UK), equipped with a Canon DSLR 500D digital camera. Images were taken of the initial wafer (to ensure that a polycrystalline sample had been obtained) and after 30 minutes. Image

processing was conducted using Image J, which is freely available.[45] In brief, ten of the largest ice crystals in the field of view were measured and the single largest length in any axis recorded. This was repeated for at least three wafers and the average (mean) value was calculated to find the largest grain dimension along any axis. The average of this value from three individual wafers was calculated to give the mean largest grain size (MLGS). This average value was then compared to that of a PBS buffer negative control providing a way of quantifying the amount of IRI activity. This testing method ensures that positive results are only reported if all ice crystals are inhibited, as opposed to a average per wafer, which would smooth out the presence of rouge ice crystal growth.

3.5.5. Synthesis of poly(amino ethyl methacrylate), PAEMA.

Aminoethyl methacrylate monomer was polymerised by aqueous reversible addition-fragmentation chain transfer (RAFT) polymerisation as previously detailed[38]. The monomer to CTA ratio was 400:1 while CTA to initiator ratio was 5:1. AEMA monomer (825 mg, 5.4 mmol) V-501 (0.7 mg, 0.0025 mmol) and CTP (3.5 mg, 0.013 mmol) were dissolved in 0.6 mL of acetate buffer at pH 5.2 (produced using 0.27 $mol.L^{-1}$ acetic acid and 0.73 $mol.L^{-1}$ sodium acetate) in a 50 ml round bottomed flask, from a stock solution and subsequently diluted to 5ml with the addition of further acetate buffer. The flask was purged with nitrogen for 45 minutes and placed in an oil bath at 70 °C. The reaction was allowed to proceed to produce polymers of varying molecular weight. After the required amount of time (30-540 minutes) the reaction was quenched using liquid nitrogen. Dialysis (membrane size 3.5 kDa) using acetate buffer (24 hours, 5 changes) and lyophilisation were then used to purify the product.

^{1}H NMR (D_2O): δ 4.21 (br, 2H, -OCH2); δ 3.31 (br, 2H, -NH2CH2); δ 1.95 (br, 2H, -CH2); δ 0.83–1.36 (br, 3H, -CH3).

3.5.6. Functionalization of PAEMA with succinic anhydride.

Functionalization of the amino groups present within the PAEMA was used to produce polyampholyte polymers. This was achieved using a method detailed in the literature[46]. Briefly, succinic anhydride was added in a range of ratios to 20 mg of PAEMA and this was dissolved in distilled water. The solution was then placed in an oil bath at 50 °C and allowed to react for 1 hour. Purification of the polymer was then achieved by dialysis using deionized water (24 hours, 5 water changes) and lyophilisation. ^{1}H NMR was used to determine level of functionalization. ^{1}H NMR (D_2O): δ 4.21 (br, 2H, -OCH2); δ 4.05 (br 2H CH_2CH_2COO-) δ 3.50 (br 2H, -$COCH_2CH_2$); δ 3.31 (br, 2H, -NH2CH2); δ 1.95 (br, 2H, -CH2); δ 0.83–1.36 (br, 3H, -CH3).

3.5.7. Polymerization of 2-methacryloyloxyethyl phosphorylcholine (MPC).

MPC was polymerised using RAFT polymerization in an aqueous solution[47] 500 mg (1.7 mmol) of monomer, 7.5 mg (0.017 mmol) of CTP and 3.25 mg (0.003 mmol) of V-501 were dissolved in 5ml deionized water containing 5 wt% (0.6 mmol) $NaHCO_3$ in a 50ml round- bottomed flask equipped with a magnetic stir bar. The mixture was the stirred to ensure dissolution of CTP and V-501 and subsequently purged with nitrogen for 45 minutes. The mixture was then placed in a preheated oil bath at 70°C and the reaction was allowed to proceed for 6 hours. The polymerisation was stopped by quenching in liquid nitrogen and purified using dialysis using deionized water (24 hours, 5 water changes) and lyophilisation. ^{1}H NMR (D_2O): δ 4.26 (br, 4H, -

CH2CH2OP-), δ 4.17 (br, 2H, -COOCH2-), δ 4.03 (br, 2H, -POCH2-), δ 3.52 (br, 2H –CH2N-), δ 3.09 (br, 9H, N(CH3)3), δ 1.95 (br 2H –CH2-), δ 0.9 (br, 3H, -CH3).

3.5.8. Polymerization of methacryloyloxy ethyl dimethyl- (3-sulfopropyl) ammonium hydroxide (MEDS).

MEDS was polymerised using RAFT polymerization in an aqueous solution as undertaken for MPC. 500 mg (1.8 mmol) of monomer, 7.5 mg (0.017 mmol) of CTP and 3.25 mg (0.003 mmol) of V-501 were dissolved in 5 ml deionized water containing 5 wt% (0.6 mmol) $NaHCO_3$ in a 50 ml round- bottomed flask equipped with a magnetic stir bar. The mixture was the stirred to ensure dissolution of CTP and V-501 and subsequently purged with nitrogen for 45 minuets. The mixture was then placed in a preheated oil bath at 70 °C and the reaction was allowed to proceed for 6 hours. The polymerisation was stopped by quenching in liquid nitrogen and the sample purified using dialysis using deionized water (24 hours, 5 water changes) and lyophilisation. ^{1}H NMR (D_2O): δ 4.46 (br, 2H, -OCH2CH2-), δ 3.76 (br, 2H -CH2CH2SO3), δ 3.55 (br, 2H –CH2CH2N-), δ 3.11 (br, 2H, -NCH2CH2-), δ 2.88 (br, 4H, -N(CH2)2-), δ 2.32 (br, 2H, -CH2CH2CH2-), δ 0.94 (br, 3H, -CH3)

3.6. References

[1] M. M. Harding, P. I. Anderberg, A. D. J. Haymet, *Eur. J. Biochem.* **2003**, *270*, 1381-1392.

[2] M. M. Harding, L. G. Ward, A. D. J. Haymet, *Eur. J. Biochem.* **1999**, *264*, 653-665.

[3] A. P. Esser-Kahn, V. Trang, M. B. Francis, *J. Am. Chem. Soc.* **2010**, *132*, 13264-13269.

[4] M. I. Gibson, *Polym. Chem.* **2010**, *1*, 1141-1152.

[5] V. Bouvet, R. N. Ben, *Cell. Biochem. Biophys.* **2003**, *39*, 133-144.

[6] K. Meister, S. Ebbinghaus, Y. Xu, J. G. Duman, A. DeVries, M. Gruebele, D. M. Leitner, M. Havenith, *Proc. Nat. Acad. Sci.* **2013**, *110*, 1617-1622.

[7] K. A. Sharp, *Proc. Nat. Acad. Sci.* **2011**, *108*, 7281-7282.

[8] A. B. Siemer, K.-Y. Huang, A. E. McDermott, *Proc. Nat. Acad. Sci.* **2010**, *107*, 17580-17585.

[9] Y. Tachibana, G. L. Fletcher, N. Fujitani, S. Tsuda, K. Monde, S.-I. Nishimura, *Angew. Chem. Int. Ed.* **2004**, *43*, 856-862.

[10] A. Eniade, M. Purushotham, R. N. Ben, J. B. Wang, K. Horwarth, *Cell. Biochem. Biophys.* **2003**, *38*, 115-124.

[11] C. J. Capicciotti, M. Leclere, F. A. Perras, D. L. Bryce, H. Paulin, J. Harden, Y. Liu, R. N. Ben, *Chem. Sci.* **2012**, *3*, 1408-1416.

[12] A. Fowler, M. Toner, *Annals N.Y. Acad. Sci.* 2005, *1066*, 119 - 135.

[13] A. Opar, *Nat. Med.* **2008**, *14*, 225.

[14] R. A. Wolfe, E. C. Roys, R. M. Merion, *Amer. J. Trans.* **2010**, *10*, 961 - 972.

[15] M. Richards, C.-Y. Fong, S. Tan, W.-K. Chan, A. Bongso, *Stem Cells* **2004**, *22*, 779-789.

[16] J. G. Baust, D. Gao, J. M. Baust, *Organogenesis* **2009**, *5*, 90-96.

[17] J. F. Carpenter, T. N. Hansen, *Proc. Nat. Acad. Sci.* **1992**, *89*, 8953-8957.

[18] C. Koshimoto, P. Mazur, *Cryobiology* **2002**, *45*, 49-59.

[19] S. Liu, W. Wang, E. von Moos, J. Jackman, G. Mealing, R. Monette, R. N. Ben, *Biomacromolecules* **2007**, *8*, 1456 - 1462.

[20] L. O'Neil, S. J. Paynter, B. J. Fuller, R. W. Shaw, A. L. DeVries, *Cryobiology* **1998**, *37*, 59 - 66.

[21] T. Wang, Q. Zhu, X. Yang, J. R. Layne, A. L. DeVries, *Cryobiology* **1994**, *31*, 185-192.

[22] M. Leclere, B. K. Kwok, L. K. Wu, D. S. Allan, R. N. Ben, *Bioconj. Chem.* **2011**, *22*, 1804 - 1810.

[23] B. L. Wilkinson, R. S. Stone, C. J. Capicciotti, M. Thaysen-Andersen, J. M. Matthews, N. H. Packer, R. N. Ben, R. J. Payne, *Angew. Chem. Int. Ed.* **2012**, *51*, 3606-3610.

[24] T. Inada, S.-S. Lu, *Cryst. Growth Des.* **2003**, *3*, 747-752.

[25] M. I. Gibson, C. A. Barker, S. G. Spain, L. Albertin, N. R. Cameron, *Biomacromolecules* **2009**, *10*, 328-333.

[26] T. Congdon, R. Notman, M. I. Gibson, *Biomacromolecules* **2013**, *14*, 1578-1586.

[27] R. C. Deller, M. Vatish, D. A. Mitchell, M. I. Gibson, *Nat. Commun.* **2014**, *5*.

[28] H. Lee, B. P. Lee, P. B. Messersmith, *Nature* **2007**, *448*, 338-341.

[29] K. Lienkamp, G. N. Tew, *Chem. Eur. J.* **2009**, *15*, 11784-11800.

[30] S.-J. Richards, M. W. Jones, M. Hunaban, D. M. Haddleton, M. I. Gibson, *Angew. Chem. Int. Ed.* **2012**, *51*, 7812-7816.

[31] M. W. Jones, L. Otten, S. J. Richards, R. Lowery, D. J. Phillips, D. M. Haddleton, M. I. Gibson, *Chem. Sci.* **2014**, *5*, 1611-1616.

[32] R. C. Deller, T. Congdon, M. A. Sahid, M. Morgan, M. Vatish, D. A. Mitchell, R. Notman, M. I. Gibson, *Biomater. Sci.* **2013**, *1*, 478-485.

[33] S. P. Greather, M. J. Kulper, S. M. Gagnes, V. K. Walker, Z. Jia, B. D. Sykes, P. L. Davies, *Nature* **2000**, *406*, 325-328.

[34] K. Matsumura, S.-H. Hyon, *Biomaterials* **2009**, *30*, 4842-4849.

[35] M. Jain, R. Rajan, S.-H. Hyon, K. Matsumura, *Biomater. Sci.* **2014**, *2*, 308-317.

[36] R. Rajan, M. Jain, K. Matsumura, *J. Biomater. Sci., Polym. Ed.* **2013**, *24*, 1767-1780.

[37] A. Emileh, E. Vasheghani-Farahani, M. Imani, *Eur. Polym. J.* **2007**, *43*, 1986-1995.

[38] A. H. Alidedeoglu, A. W. York, C. L. McCormick, S. E. Morgan, *J. Pol. Sci. A; Polym. Chem.* **2009**, *47*, 5405-5415.

[39] T. Congdon, C. Wilmet, R. Williams, J. Polt, M. Lilliman, M. I. Gibson, *Eur. Polym. J.*, **2015***, 62,* 352-362.

[40] A. K. Balcerzak, M. Febbraro, R. N. Ben, *RSC Adv.* **2013**, *3*, 3232-3236.

[41] C. Budke, T. Koop, *ChemPhysChem* **2006**, *7*, 2601-2606.

[42] C. P. Garnham, R. L. Campbell, P. L. Davies, *Proc. Nat. Acad. Sci.* **2011**, *108*, 7363-7367.

[43] A. Lee, H. Y. Tsai, M. Z. Yates, *Langmuir* **2010**, *26*, 18055-18060.

[44] C. A. Knight, J. Hallett, A. DeVries, *Cryobiology* **1988**, *25*, 55-60.

[45] J. Schindelin, I. Arganda-Carreras, E. Frise, V. Kaynig, M. Longair, T. Pietzsch, S. Preibisch, C. Rueden, S. Saalfeld, B. Schmid, J.-Y. Tinevez, D. J. White, V. Hartenstein, K. Eliceiri, P. Tomancak, A. Cardona, *Nat. Meth.* **2012**, *9*, 676-682.

[46] K. Matsumura, S.-H. Hyon, *Biomaterials* **2009**, *30*, 4842-4849.

[47] B. Yu, A. B. Lowe, K. Ishihara, *Biomacromolecules* **2009**, *10*, 950-958.

Chapter 4

4. Gold Nanoparticle Aggregation as a Probe of Antifreeze (Glyco) Protein-Inspired Ice Recrystallization Inhibition and Identification of New IRI Active Macromolecules

D. E. Mitchell, T. Congdon, A. Rodger and M. I. Gibson. In Revision.

This chapter contains a paper on the analysis of an absorbance based gold nanoparticle assay for the high-throughput screening of ice recrystallization activity. DEM synthesized gold nanoparticles, PAEMA-*co*-SA polymers and undertook all analytical investigation. TC synthesized PVA polymers. DEM and AR carried out circular dichroism spectroscopy and subsequent analysis. DEM and MIG wrote the manuscript.

4.1. Abstract

Antifreeze (glyco)proteins are found in polar fish species and act to slow the rate of growth of ice crystals; a property known as ice recrystallization inhibition. The ability

to slow ice growth is of huge technological importance especially in the cryopreservation of donor cells and tissue, but native antifreeze proteins are often not suitable, nor easily available. Therefore, the search for new materials that mimic this function is important, but currently limited by the low-throughout assays associated with the antifreeze properties. Here 30 nm gold nanoparticles are demonstrated to be useful colorimetric probes for ice recrystallization inhibition, giving a visible optical response and is compatible with 96 well plates for high-throughout studies. This method is faster, requires less infrastructure, and has easier interpretation than the currently used 'splat' methods. Using this method, a series of serum proteins were identified to have weak, but specific ice recrystallization inhibition activity, which was removed upon denaturation. It is hoped that high-throughput tools such as this will accelerate the discovery of new antifreeze mimics.

4.2. Introduction

To survive in the harsh cold environments at high altitude or in the Earth's polar regions, Nature has evolved a series of mechanisms to enable extremophiles to survive, and thrive. One particular method of survival employed by freeze-avoiding[1] (as opposed to freeze tolerant)[2] species is the production of antifreeze proteins and antifreeze glycoproteins (AF(G)Ps).[3] These proteins act to i) lower the equilibrium freezing point in a non-colligative fashion – thermal hysteresis[4] (TH); ii) shape ice crystals (via binding to specific crystallographic faces) – dynamic ice shaping (DIS); iii) inhibit the growth of ice crystals – ice recrystallization inhibition (IRI).[5] The property of IRI is particularly interesting, as ice crystal growth during thawing has been associated with cellular damage during cryopreservation.[6] Considering this, AF(G)Ps have been investigated for their ability to enhance cryopreservation,[6] with

the aim of improving the availability of transplantable materials for regenerative medicine. The results of this have been mixed, with reports of AF(G)Ps both enhancing and reducing cell viability post-thawing.[6-8] This has been attributed to their unwanted effects of DIS/TH, which can promote the formation of needle-like (spicular) ice crystals.[9] There are also concerns about the toxicological and immunological affects of AF(G)PS,[10] along with the inherent cost of producing/purifying them from natural sources.

Therefore, the development of new IRI-specific molecules/macromolecules has been pursued. Ben *et al.* have reported that simplified glycopeptides and glycolipids have potent IRI and can enhance cryopreservation.[11-13] Gibson and co-workers have shown that synthetic polymers can mimic AF(G)Ps function and shown this to enhance red blood cell cryopreservation.[14-16] However, there are still few examples of synthetic AF(G)P mimics, which is in part limited by the time-consuming nature of the assays required to probe their activity. The TH assay requires the growth of single ice crystals in nanolitre droplets, whereas IRI activity is tested by the 'splat' assay; this involves forming many wafers of sub 10 micron ice crystals and monitoring their growth over time.[17] Neither of these assays are suitable for high-throughput analysis, requiring temperature-controlled microscope stages and significant image analysis. To speed the process Ben *et al.* introduced domain recognition software,[18] which aids image processing but the data collection burden is not removed. Several other methods involving capillaries and light scattering have been suggested,[19-21] but these do not give quantitative data or require user 'interpretation' of the results and have not been widely adopted.

Interestingly, Kim *et al.,* [22] suggested that gold nanoparticles could be used to measure thermal hysteresis colourimetrically. Gold nanoparticles show a distinct shift from red to blue colouration upon aggregation and has been employed for a range of bioassays from DNA-sequence comparison,[23] bacteria analysis,[24] viral analysis,[25] glycan analysis,[26] metal detection[27] and more. Kim *et al.*[22] reported that the aggregation of gold particles correlated with the TH activity of an AFP. The mechanism of this was not clear though as freezing then thawing gold nanoparticles should not actually be affected by TH. The macroscopic effect of TH is to lower the freezing point (by circa. 2 °C) but in the reported assays, activity was seen at temperatures significantly below this and using AFP concentrations which are too low for TH activity. We believe these observations actually correlates better with IRI activity, which is maintained at lower concentrations.[28-29] When an aqueous solution is frozen, the ice crystals will grow larger by ice recrystallization, reducing the overall ice surface area. As all solutes are excluded from ice crystal, the gold particles in between will be forced closer together leading to aggregation. Anything that possesses IRI activity would prevent this ice crystal growth, meaning the overall surface area would be larger preventing aggregation from occurring. Despite the previous reports suggesting this is a TH assay, if it can be adapted for IRI the method is very appealing as it could be conducted in multiwell plates, the output can be read by a standard plate-reader (or visually) and only needs a standard – 20 °C freezer. The combination of readily available equipment requirements and multi-well plate compatibility would make this a potential high-throughput assay for testing a diverse range of compounds.

In this manuscript, we report a study into the use of gold nanoparticles (AuNPs) as a simple, and rapid, tool for screening for IRI activity. Using well-defined synthetic polymers, with known IRI activity, but no (or weak) thermal hysteresis we show that the inhibition of gold particle aggregation correlates with IRI. The utility of this in a 96 well plate format is reported to enable higher-throughput screening in comparison to the splat assay.

4.3. Results and Discussion

To test the applicability, if any, of the reversible freezing of colloidal gold as a probe for IRI activity (rather than the previously explored thermal hysteresis)[22] a range of synthetic polymers with known IRI activity were selected. Poly(vinyl alcohol), PVA, was chosen as the positive control due to is well-known IRI activity, which has been investigated in detail.[28] As a negative control poly(ethylene glycol) and poly(*N*-vinyl pyrolidone), PVP, were selected as they have no significant IRI in the relevant concentration range.[30-31] Figure 4.1 shows the results of a 'splat' test, which measures the ripening of ice crystals over time, in both the absence and presence of PVA, highlighting its inhibitory effect on ice crystal growth. Briefly, this assay involves seeding large numbers of small ice crystals and monitoring their growth to obtain the mean largest grain size (MLGS) to quantify activity. Using this assay, it has been shown that concentrations of PVA below 1 $mg.mL^{-1}$ are sufficient to halt ice crystal growth.

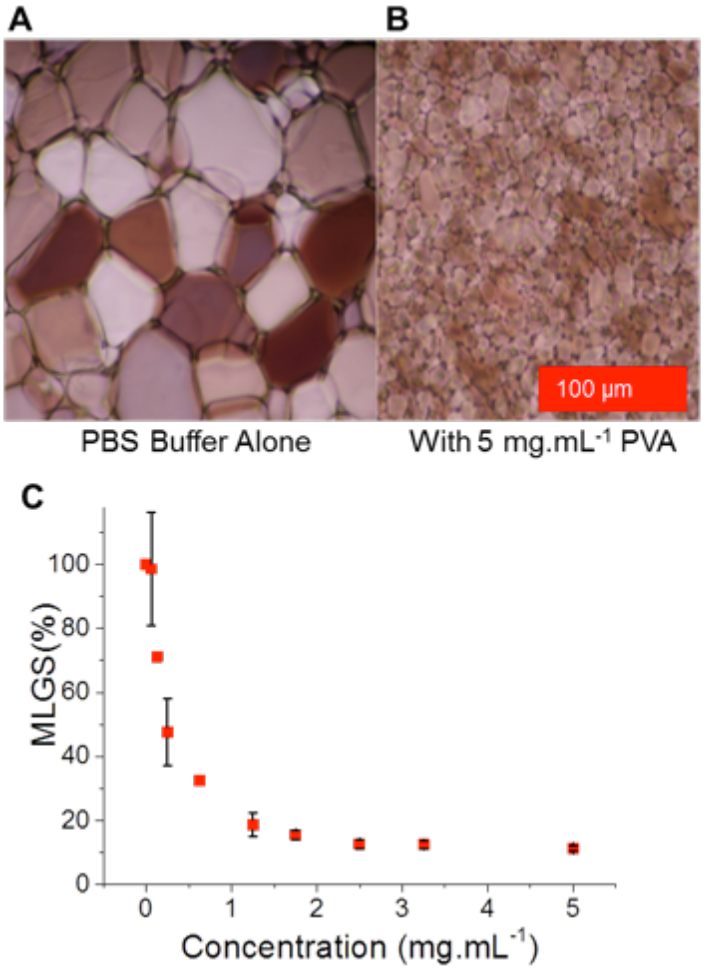

Figure 4.1. Ice recrystallization inhibition activity of PVA; (A) Example micrograph of crystals grown in PBS alone; (B) Example micrograph of crystals grown in 5 mg.mL^{-1} PVA; (C) IRI activity as a function of polymer concentration. MLGS = mean largest grain size relative to a PBS control (%). Error bars represent the standard deviation from at least three measurements. (PVA MW= 6.8 kDa).

30 nm mercaptosuccinic acid (MSA) functionalized gold particles were prepared using literature methods,[22, 32] to assess the viability of this method to measure IRI activity. The gold nanoparticle solutions containing the compounds to be tested for IRI were frozen in 96-well plates at -20 °C for 2 hours in a standard laboratory freezer (-20 °C). The samples were then thawed slowly at 23 °C (ambient temperature) to maximise ice recrystallization, and their UV-visible absorption spectra recorded as

well as optical photographs, as shown in Figure 4.2A. From visual inspection of the samples it was clear that the AuNPs with added PVA were still dispersed (characteristic red colour), but other samples had aggregated. The concentration dependence of AuNPs with PVA was also measured and the success of the assay was found to not depend on gold concentration. A concentration of ~ 80 ug.mL^{-1} is used from this point onwards (ESI, Appendix 3).

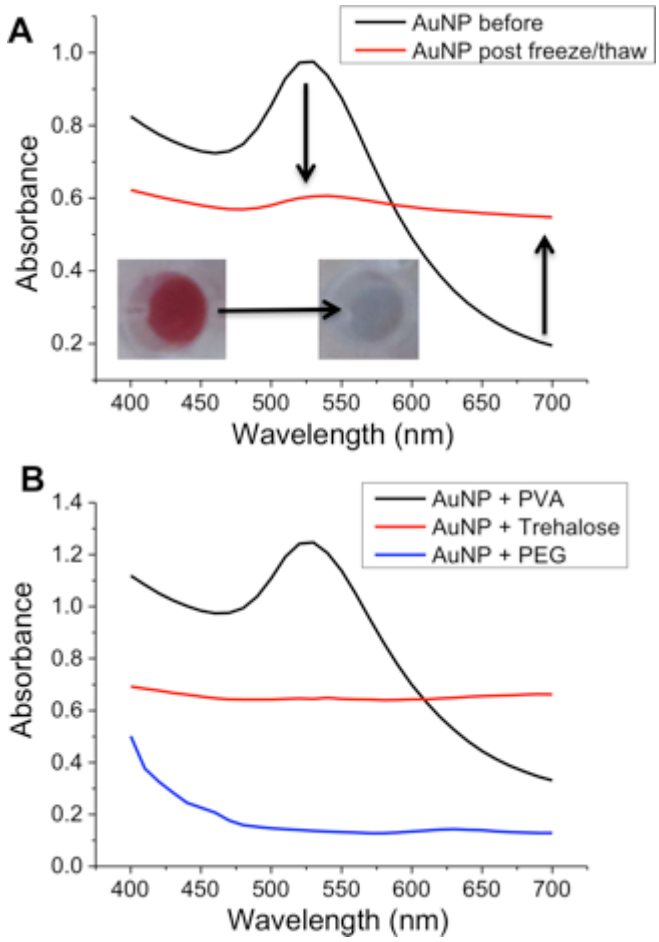

Figure 4.2. Absorbance spectra changes of gold nanoparticles (AuNPs) solutions upon freeze/thawing; (A) Effect of freezing and thawing gold nanoparticle solutions, with decrease in absorbance at 520 nm. Inset photos show colour changes associated with AuNP freeze/thaw; (B) Gold nanoparticle UV-Vis spectra after freeze-thaw in the presence of additives at a concentration of 10 mg.mL^{-1} (PEG MW 4 kDa, PVA MW 6.8kDa). Arrows are to guide the eye in the direction of change.

In order to 'score' the relative degree of aggregation post-thawing, the reduction in the absorbance peaks at 520 nm between pre- and post-thaw were measured to give a qualitative comparison between different additives (ESI, Appendix 3) with higher values indicating less aggregation and hence more IRI activity. To assess the use of this colloidal assay a range of different molecular weight PVAs from 800 – 20000 $g.mol^{-1}$ were synthesised using RAFT/MADIX polymerization[28] (ESI, Appendix 3). The PVA's are labelled according to their degree of polymerization (chain length) from this point. Above 1 $mg.mL^{-1}$ all the PVAs prevented aggregation of the gold particles after a freeze/thaw cycle, in agreement with the 'splat' assay. When the concentration was decreased below 1 $mg.mL^{-1}$ there were clear differences between the polymers of different molecular weight, as shown in the zoomed-in region in Figure 4.3. The largest polymer (PVA_{244}) was capable of inhibiting aggregation as low as 0.1 $mg.mL^{-1}$, but the shortest (PVA_{10}) lead to AuNP aggregation in this concentration range, demonstrating that high molecular weight polymers have increased IRI activity.

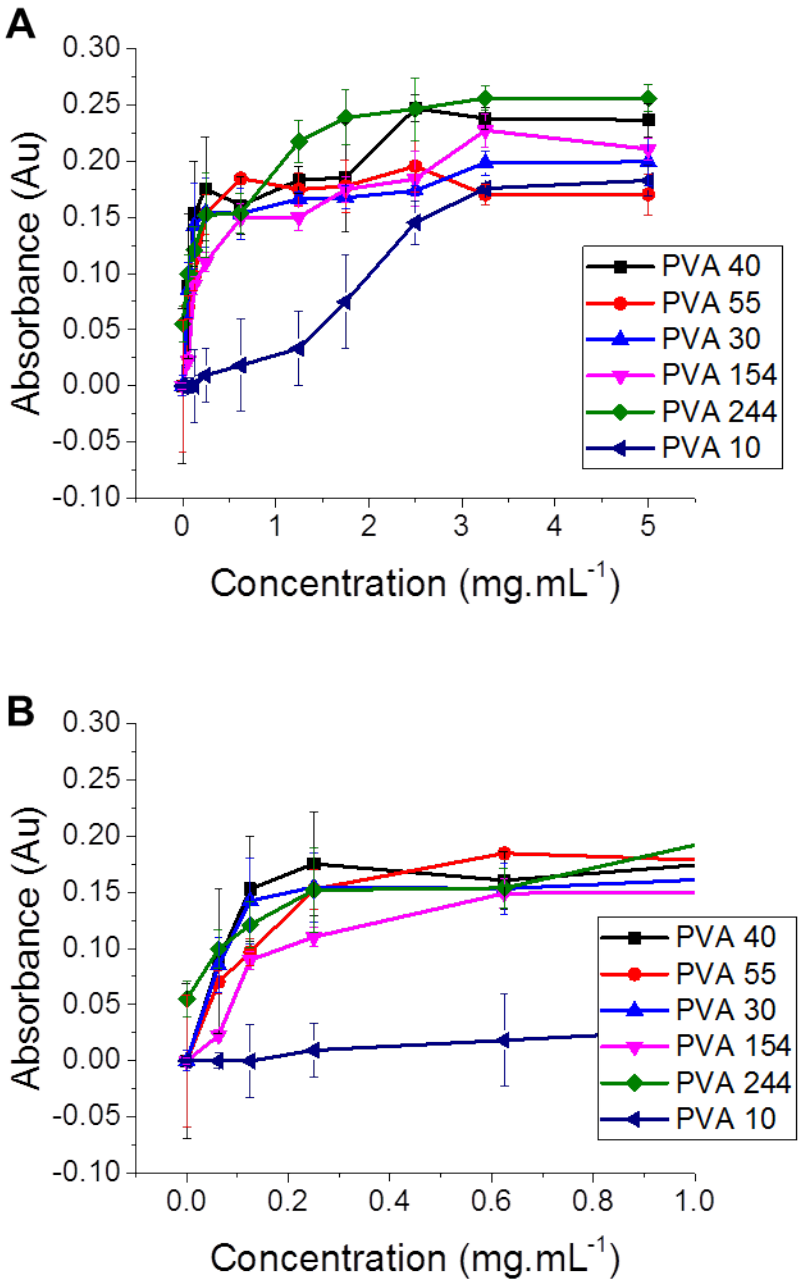

Figure 4.3. Concentration dependence on the absorbance at 520 for different degrees of polymerization of PVA post freeze/thaw. (A) Concentration dependence of IRI activity from 0 to 5 mg.mL^{-1}; (B) Zoomed-in region from 0 to 1 mg.mL^{-1} showing concentration dependence resolution for low concentrations. Error bars represent ± SD from a minimum of 3 repeats.

In an attempt to correlate these observable spectral features with our 'gold standard' splat assay, the whole data set was plotted as Abs_{520} versus MLGS, Figure 4.4. There was a clear correlation between the MLGS and Abs_{520}, with lower absorbance values correlating with smaller MLGS values.

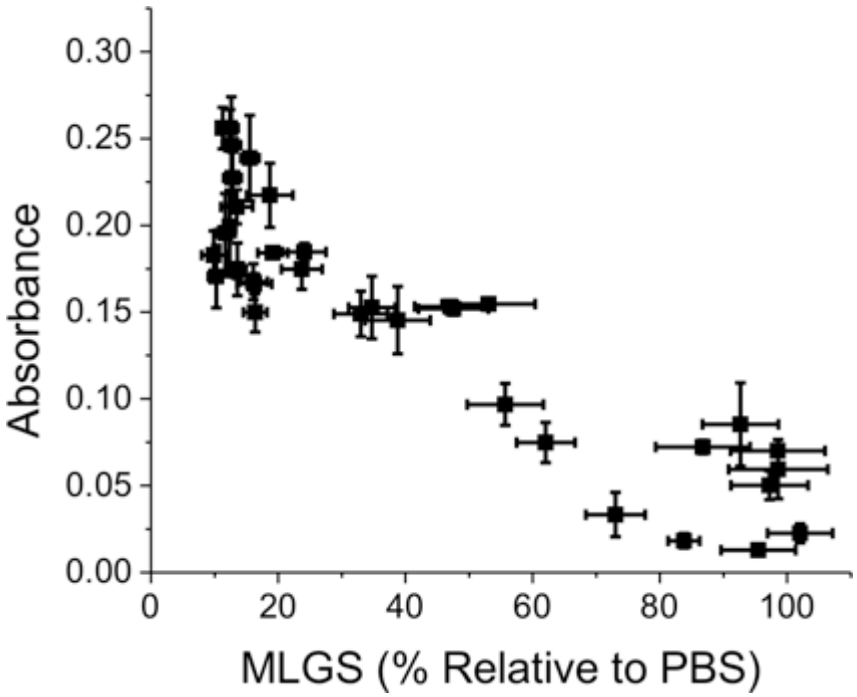

Figure 4.4. Comparison of MLGS values (relative to a PBS control) versus absorbance from all PVA/AuNP aggregation assay. MLGS is expressed as a percentage of PBS buffer control.

Variable volume experiments were also conducted to ensure that this was a recrystallization-specific effect. Briefly, smaller volumes will thaw faster, reducing the opportunities for recrystallization, compared to larger volumes. A short screen of this (ESI, Appendix 3) confirmed that 100 µL total volume per well (in a 96 well plate) lead to aggregation of the gold after freeze-thaw, but lower volumes lead to less

aggregation. This also supports our hypothesis that recrystallization inhibition, not thermal hysteresis is the effect being probed and that the conducting these experiments in 96 well plates, as opposed to 384 well plates may be preferable.

The data presented above suggests that the AuNP method may be a useful screening assay for IRI activity. To probe this, a range of compounds with and without known IRI activity were screened; Poly(amino-ethyl methacrylate) 50 % carboxylated with succinic anhydride, PAEMA-*co*-SA (35 kDa), α-cyclodextrin dextran (40 kDa), trehalose, poly(vinyl pyrolidone) (PVP, MW 40 kDa) and bovine serum albumin (BSA). Of these only PAEMA-*co*-SA is known to have IRI activity and this is significantly less active than PVA, typically requiring concentrations of ~ 20 $mg.mL^{-1}$ to have IRI activity, compared to 1 $mg.mL^{-1}$ for PVA.[33] The IRI activity of trehalose and other sugars has been reported. However, this required concentrations of 220 mM (which is > 50 $mg.mL^{-1}$) to show significant ice inhibition and is only considered to be weakly active, with close to no activity in the concentration range used here.[34] PVP is a well known kinetic hydrate inhibitor, but does not have strong IRI.[35] Figure 4.5 shows the results of screening 6 compounds/macromolecules for IRI using this AuNP based assay.

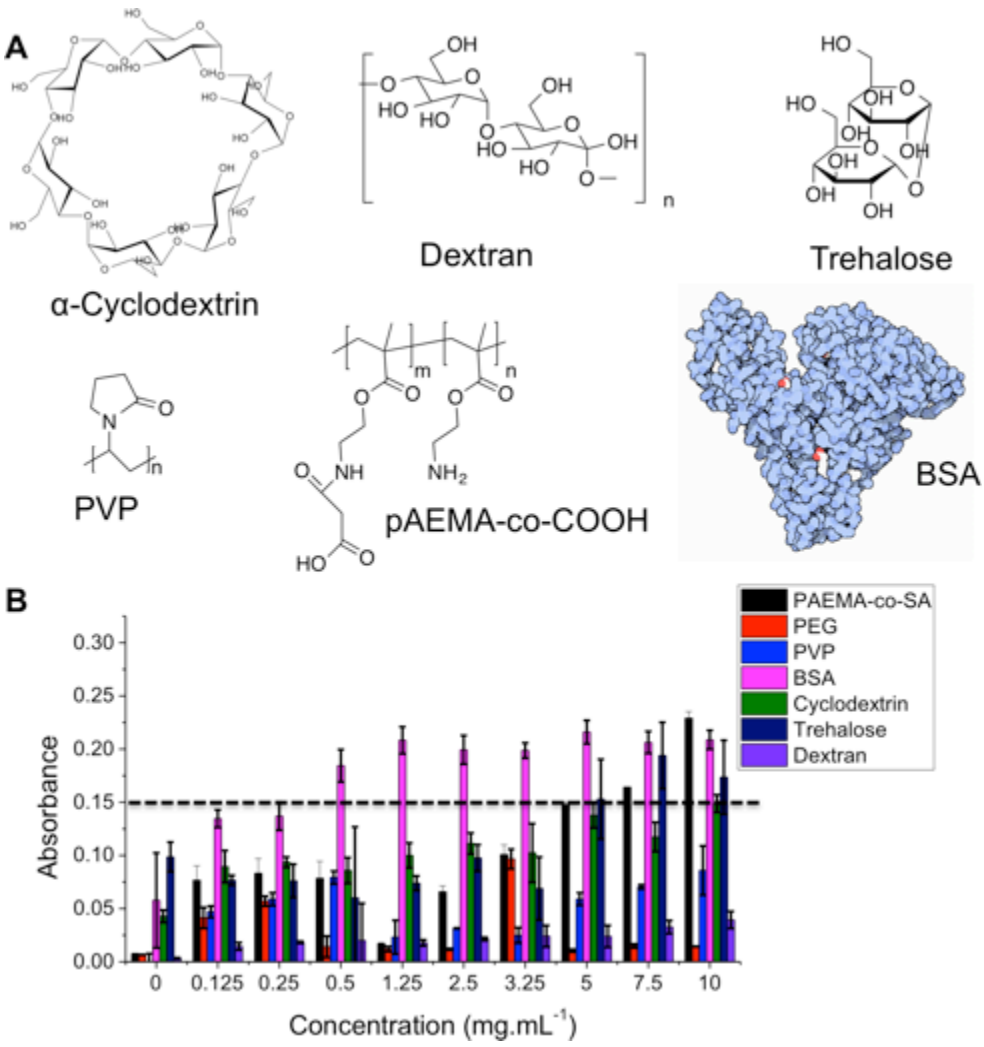

Figure 4.5. Screening for IRI activity using AuNP Assay; (A) Chemical structures of the compounds being interrogated; (B) AuNP colloidal aggregation results. Error bars represent ± SD from a minimum of 3 repeats. Dotted line is to guide the eye – data points above this indicate IRI activity.

As expected, PAEMA-*co*-SA showed a reduction in aggregation across a range of concentrations, in line with its known IRI activity, which correlates well with its MLGS (ESI, Appendix 3). Using dye inclusion assays PAEMA-*co*-SA shows no activity, suggesting that it is not acting as a surfactant, which could provide stabilisation to the AuNPs and is a potential source of false-positives.[30, 33] PVP, dextran and cyclodextrin solutions all aggregated following freeze/thaw for all

concentrations tested. This is in agreement with observations that none of these have IRI activity in the splat test. Most interestingly, BSA gave a result that would indicate IRI activity. This could be interpreted as it stabilising the gold nanoparticle surface (through non-specific absorption) or a real IRI affect. To the best of our knowledge, the IRI activity of BSA has not been quantitatively studied so we set out to investigate this. To ensure that we were probing protein-structure related effects, some of the BSA was denatured by heating (95 °C for 30 minutes). Circular dichroism spectroscopy (Figure 4.6A) confirmed this by the decrease in molar elipticity at 210 and 225 nm. These changes seen in the CD spectra were small, but BSA is known to be quite tolerant to heating and can refold, although not necessarily into the same conformation.[36-37] The native, and denatured forms were then subjected to the splat test as a function of concentration, Figure 4.6B.

The splat test revealed that folded BSA does have real, if not very potent, IRI activity. This is surprising, as in our hands very few synthetic materials or proteins show any appreciable IRI with PAEMA-*co*-SA and PVA being amongst the few. The denatured BSA showed no IRI activity, indicating a remarkable tertiary-structure dependence, which has not been previously explored. This is of particular interest as many cryoprotectant solutions contain large quantities of serum proteins and this data implies that modulation of ice crystal growth may be an unexpected benefit in these systems.

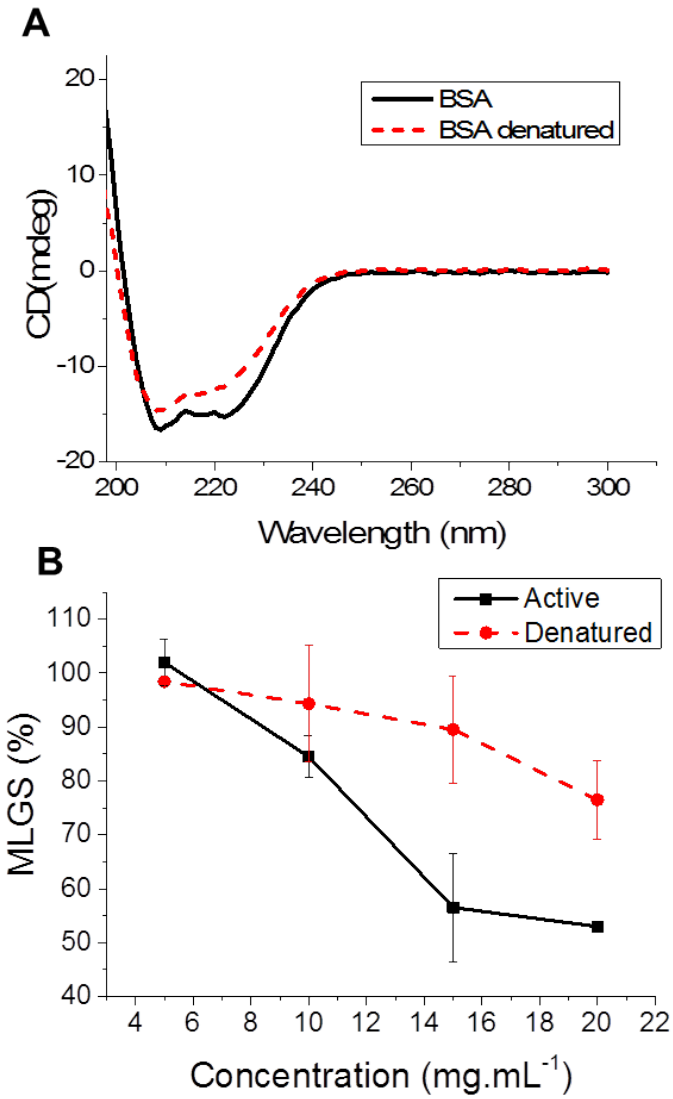

Figure 4.6. IRI activity of BSA. (A) Circular dichroism spectra of BSA at 500 μg.mL^{-1} before and after heat-denaturation; (B) Comparison of active and denatured BSA. Error bars represent ± SD from a minimum of 3 repeats. MLGS = mean largest grain size relative to PBS control.

To determine whether this is a general property of serum proteins, human serum albumin (HSA) and ovine serum albumin (OSA) were also tested using both the AuNP and splat test methods. The AuNP screening method indicated some freeze-thaw resistance and the splat test confirmed that the OSA and HSA both had activity in line with the BSA, Figure 4.7.

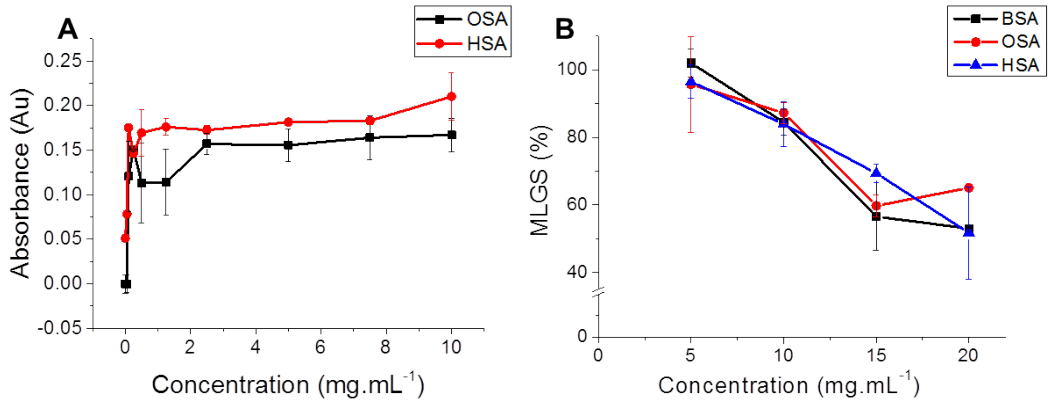

Figure 4.7. IRI activity of serum proteins. A) Gold nanoparticle aggregation assay; B) 'Splat' assay. BSA = bovine serum albumin, OSA = ovine (sheep) serum albumin and HSA = human serum albumin. MLGS = mean largest grain size relative to PBS control. Error bars indicate SD from a minimum of 3 repeats.

BSA is often used as a negative control in antifreeze protein assays (although at lower concentrations than used here) this should be taken into account in the future as it clearly does have activity, although the features that cause this are not clear. One role of serum proteins *in vivo* is as a carrier for various substances such as fatty acids and certain steroids, while also maintaining the oncotic pressure in the blood.[38-39] To carry these substances it possesses several binding domains and hydrophobic regions.[40] This distribution of hydrophobic and hydrophilic regions is a common feature in antifreeze proteins perhaps explaining the reason for its activity.[41] In a small molecule context, Ben *et al.* has shown that addition of increasingly hydrophobic alkyl chains to sugars can result in enhanced IRI which would seem to agree with this hypothesis for BSA activity.[42]

This study shows that AuNP reversible freeze/thaw cycles and the subsequent aggregation appears to be linked to the rate of ice crystal growth (recrystallization) rather than the previously hypothesized TH activity.[22] Our results demonstrate that it may be a useful tool for screening IRI, but that splat tests are still required to confirm activity of newly identified compounds. In particular, this method may be useful when screening structural variations of a single material (e.g. a polymer) where any nonspecific effects (such as particle binding) are common to all the structures, enabling false positives to be removed. The identification of serum albumin activity also suggests that IRI might be a more common property of proteins than previously thought. This opens up the opportunity to identify latent antifreeze-protein activity from non-extremophile organisms.

4.4. Conclusions

Here the application of gold nanoparticles as convenient probes for ice recrystallization inhibition activity has been investigated. During thawing, extensive ice crystal growth occurs, reducing the available surface area for particles, meaning the gold particles are more likely to aggregate if crystal growth occurs. UV-visible spectroscopy can be employed to probe activity by measuring the characteristic red to blue shift of AuNP solutions as they aggregate. The degree of aggregation was found to correlate well with ice recrystallization inhibition activity determined by the (gold standard) splat assay. Previous studies had suggested that this reversible assay was due to freezing point depression (thermal hysteresis), but here synthetic polymers without freezing point depression activity gave strong aggregation inhibition, confirming IRI not TH was the mechanism being probed.

This assay has significant advantages in terms of speed and throughput compared to the splat test, which is the current 'gold standard' for ice recrystallization. This includes compatibility with 96 well plates for automated analysis and the use of a standard – 20 °C lab freezer and easy colourimetric readout. Using this method, the IRI activity of serum proteins was identified for the first time and quantified by the 'splat' test and linked to the tertiary structure/folding of the proteins. At this time, the potential for false positives cannot be ruled out across all chemical space, but this represents a step towards a fully automated IRI activity-screening platform.

4.5. Experimental Section

4.5.1. Physical and analytical methods

^{1}H and ^{13}C NMR spectra were recorded on Bruker DPX-300 and DPX-400 spectrometers using deuterated solvents purchased from Sigma-Aldrich. Chemical shifts are reported relative to residual non-deuterated solvent. Infrared data was recorded on a Bruker Vector 22 GI003097. The THF GPC system comprised of a Varian 390-LC-Multi detector suite fitted with differential refractive index (DRI), light scattering (LS) and ultra-violet (UV) detectors equipped with a guard column (Varian Polymer Laboratories PLGel 5 μm, 50 x 7.5 mm) and two mixed D columns of the same type. The mobile phase was THF with 5 % triethylamine (TEA) eluent at a flow of 1.0 $mL.min^{-1}$, and samples were calibrated against Varian Polymer Laboratories EasiVials linear poly(styrene) and poly(methylmethacrylate) standards (162-2.4 x 10^5 $g.mol^{-1}$) using Cirrus v3.3. Characterization of AuNPs was carried out using differential light scattering (DLS) spectroscopy (Malvern Instruments Zetasizer Nano-ZS). Circular dichroism (CD) spectra were recorded on a spectropolarimeter

(Jasco J-720, Jasco UK) using a data interval of 0.2 nm. Samples were dissolved in PBS buffer diluted two-fold with deionised water, and the spectrum was measured 16 times and averaged. The spectrum of a blank sample containing only buffer was then subtracted giving a final spectrum for each protein. UV-visible spectroscopy was conducted on a microplate reader; Synergy HT multi-mode microplate reader, BioTek UK.

4.5.2. Materials

Hydrogen tetrachloroaurate trihydrate ($HAuCl_4.3H_2O$), sodium citrate dehydrate ($C_6H_5Na_3O_7.2H_2O$), mercaptosuccinic acid (MSA), dextran, α-cyclodextrin (MW 972.84 $g.mol^{-1}$), trehalose, bovine serum albumin (BSA), human serum albumin (HSA), ovine serum albumin (OSA) and poly(ethylene glycol) (PEG) were purchased from Sigma Aldrich. Poly(amino ethyl methacrylate–*co*-succinic anhydride) was synthesized as previously reported[30] and poly(vinyl alcohol) was synthesized as detailed in the ESI. All reagents were of analytical grade. Commercial polymers (PEG, PVP and dextran) were dialysed against deionized water for 24 hours with 5 water changes prior to use against a 3000 MWCO membrane. Phosphate-buffered saline (PBS) solution was prepared using preformulated tablets (Sigma-Aldrich) in 200 mL of Milli-Q water (>18.2 Ω mean resistivity) to give [NaCl] = 0.138 M, [KCl] = 0.0027 M, and pH 7.4.

4.5.3. Synthesis of gold nanoparticles

Gold Nanoparticle (AuNPs) were synthesized according to the literature.[32] Briefly, 6.7 mg of hydrogen tetrachloroaurate was dissolved in 50 mL of distilled water in a 50 mL round bottom flask, equipped with a magnetic stir bar. The solution was then

heated to 100 °C while stirring and 2 mL of sodium citrate solution (2 mM, 17.6 mg) was added. The solution changed colour to purple and then red and the reaction was allowed to proceed for a further 20 minutes. The colloidal suspension was then allowed to cool to room temperature and 2 mL of mercaptosuccinic acid solution (30 mM, 9 mg) was added, and the functionalization was allowed to proceed overnight at room temperature, purification was achieved by centrifugation (7000 g, 10 minutes) and resuspension in deionized water. The resulting concentration of AuNPs was 58 $\mu g.mL^{-1}$. Dynamic light scattering confirmed that the gold particles were ~ 30 nm in size (PDI 0.23).

4.5.4. Freeze-thaw assay

The standard assay involved the addition of 50 μL of test product prepared as a serial dilution from 10 – 0 $mg.mL^{-1}$ (or higher concentrations as needed) in a 96 well plate. To this, 50 μL of as-prepared AuNPs were added. To determine the affect of the solution volume on the assay the quantities of test and AuNP solution were varied although the ratio remained 1:1. All experiments were undertaken in triplicate. Freeze thaw was achieved by placing the plate in a standard domestic freezer for 2 hours at -20 °C and leaving to thaw on the lab bench at room temperature. The UV-vis spectra were corrected for scattering by drawing a straight line between 450 and 680 nm and measuring the absorbance at 520 nm, between this line and the peak. The optimal concentration of gold is 80 $\mu g.mL^{-1}$ (see ESI, Appendix 3).

4.5.5. Ice recrystallization inhibition (splat) assay

Ice recrystallization inhibition was measured using a modified splay assay.[17] A 10 μL sample of polymer dissolved in PBS buffer (pH 7.4) was dropped 1.40 m onto a

chilled glass coverslip sat on a piece of polished aluminium placed on dry ice. Upon hitting the chilled glass coverslip, a wafer with diameter of approximately 10 mm and thickness 10 μm was formed instantaneously. The glass coverslip was transferred onto the Linkam cryostage and held at −8 °C under N_2 for 30 minutes. Photographs were obtained using an Olympus CX 41 microscope with a UIS-2 20x/0.45/∞/0-2/FN22 lens and crossed polarizers (Olympus Ltd, Southend on sea, UK), equipped with a Canon DSLR 500D digital camera. Images were taken of the initial wafer (to ensure that a polycrystalline sample had been obtained) and after 30 minutes. Image processing was conducted using Image J, which is freely available.[43] In brief, ten of the largest ice crystals were measured and the single largest length in any axis recorded. This was repeated for at least three wafers and the average (mean) value was calculated to find the largest grain dimension along any axis. The average of this value from three individual wafers was calculated to give the mean largest grain size (MLGS). This average value was then compared to that of a PBS buffer negative control providing a way of quantifying the amount of IRI activity.

4.6. References

[1] C. C. Cheng, A. L. DeVries, in *Life Under Extreme Conditions* (Ed.: G. di Prisco), Springer Berlin Heidelberg, **1991**, pp. 1-14.

[2] K. B. Storey, J. M. Storey, *Physiol. Rev.* **1988**, *68*, 27-84.

[3] A. L. DeVries, *Comp. Biochem. Physiol., B: Comp. Biochem.* **1988**, *90*, 611–621.

[4] Y. Celik, L. A. Graham, Y. F. Mok, M. Bar, P. L. Davies, I. Braslavsky, *Proc. Natl. Acad. Sci. U. S. A.* **2010**, *107*, 5423-5428.

[5] M. I. Gibson, *Polym. Chem.* **2010**, *1*, 1141-1152.

[6] J. F. Carpenter, T. N. Hansen, *Proc. Natl. Acad. Sci. U.S.A.* **1992**, *89*, 8953-8957.

[7] T. Wang, Q. Zhu, Y. Xiaoping, J. R. Layne Jr., A. L. Devries, *Cryobiology* **2002**, *31*, 185–192.

[8] Chihiro K., M. P., *Cryobiology* **2002**, *45*, 49–59.

[9] L. O'Neil, S. J. Paynter, B. J. Fuller, R. W. Shaw, A. L. DeVries, *Cryobiology* **1998**, *37*, 59-66.

[10] S. R. Payne, J. E. Oliver, G. C. Upreti, *Cryobiology* **1994**, *31*, 180–184.

[11] A. K. Balcerzak, S. S. Ferreira, J. F. Trant, R. N. Ben, *Bioorg. Med. Chem. Lett.* **2012**, *22*, 1719-1721.

[12] L. Corcilius, G. Santhakumar, R. S. Stone, C. J. Capicciotti, S. Joseph, J. M. Matthews, R. N. Ben, R. J. Payne, *Bioorg. Med. Chem. Lett.* **2013**, *21*, 3569-3581.

[13] J. F. Trant, R. A. Biggs, C. J. Capicciotti, R. N. Ben, *RSC Adv.* **2013**, *3*, 26005-26009.

[14] R. C. Deller, M. Vatish, D. A. Mitchell, M. I. Gibson, *Nat. Commun.* **2014**, *5*, 3244-3251.

[15] R. C. Deller, D. A. Mitchell, M. Vatish, M. I. Gibson, *ACS Biomater. Sci. Eng.* **2015**, *10.1021/acsbiomaterials.5b00162*.

[16] D. E. Mitchell, N. R. Cameron, M. I. Gibson, *Chem. Commun.* **2015**, *51*, 12977-12980.

[17] C. A. Knight, J. Hallett, A. L. DeVries, *Cryobiology* **1988**, *25*, 55-60.

[18] J. Jackman, M. Noestheden, D. Moffat, J. P. Pezacki, S. Findlay, R. N. Ben, *Biochem. Biophys. Res. Commun.* **2007**, *354*, 340-344.

[19] M. M. Tomczak, C. B. Marshall, J. A. Gilbert, P. L. Davies, *Biochem. Biophys. Res. Commun.* **2003**, *311*, 1041-1046.

[20] Y. Rabin, M. J. Taylor, J. S. G. Feig, S. Baicu, Z. Chen, *Cryobiology* **2013**, *67*, 264-273.

[21] Y. Celik, R. Drori, N. Pertaya-Braun, A. Altan, T. Barton, M. Bar-Dolev, A. Groisman, P. L. Davies, I. Braslavsky, *Proc. Natl. Acad. Sci. U. S. A.* **2013**, *110*, 1309-1314.

[22] J.-I. Park, J. H. Lee, Y. Gwak, H. J. Kim, E.-S. Jin, Y.-P. Kim, *Biosens. Bioelectron.* **2013**, *41*, 752-757.

[23] H. Li, L. Rothberg, *Proc. Natl. Acad. Sci. U. S. A.* **2004**, *101*, 14036-14039.

[24] S.-J. Richards, E. Fullam, G. S. Besra, M. I. Gibson, *J. Mater. Chem. B.* **2014**, *2*, 1490-1498.

[25] L. Chen, H. Wei, Y. Guo, Z. Cui, Z. Zhang, X.-E. Zhang, *J. Immunol. Methods.* **2009**, *346*, 64-70.

[26] L. Otten, S.-J. Richards, E. Fullam, G. S. Besra, M. I. Gibson, *J. Mater. Chem. B.* **2013**, *1*, 2665-2672.

[27] J.-S. Lee, M. S. Han, C. A. Mirkin, *Angew. Chem. Int. Ed. Engl.* **2007**, *119*, 4171-4174.

[28] T. Congdon, R. Notman, M. I. Gibson, *Biomacromolecules* **2013**, *14*, 1578-1586.

[29] P. Czechura, R. Y. Tam, E. Dimitrijevic, A. V. Murphy, R. N. Ben, *J. Am. Chem. Soc.* **2008**, *130*, 2928-2929.

[30] R. C. Deller, T. Congdon, M. A. Sahid, M. Morgan, M. Vatish, D. A. Mitchell, R. Notman, M. I. Gibson, *Biomater. Sci.* **2013**, *1*, 478-485.

[31] T. Inada, P. R. Modak, *Chem. Eng. Sci.* **2006**, *61*, 3149-3158.

[32] J. Gao, X. Huang, H. Liu, F. Zan, J. Ren, *Langmuir* **2012**, *28*, 4464-4471.

[33] D. E. Mitchell, M. Lilliman, S. G. Spain, M. I. Gibson, *Biomater. Sci.* **2014**, *2*, 1787–1795.

[34] R. Y. Tam, S. S. Ferreira, P. Czechura, J. L. Chaytor, R. N. Ben, *J. Am. Chem. Soc.* **2008**, *130*, 17494-17501.

[35] M. A. Kelland, *Energ. Fuel* **2006**, *20*, 825-847.

[36] G. Barone, C. Giancola, A. Verdoliva, *Thermochim. Acta.* **1992**, *199*, 197–205.

[37] A. Michnik, *J. Therm. Anal. Calorim.* **2003**, *71*, 509-519.

[38] S. Curry, P. Brick, N. P. Franks, *Biochim. Biophys. Acta, Mol. Cell. Biol. Lipids* **1999**, *1441*, 131–140.

[39] G. J. Quinlan, G. S. Martin, T. W. Evans, *Hepatology* **2005**, *41*, 1211-1219.

[40] K. A. Majorek, P. J. Porebski, A. Dayal, M. D. Zimmerman, K. Jablonska, A. J. Stewart, M. Chruszcz, W. Minor, *Mol. Immunol.* **2012**, *52*, 174-182.

[41] A. D. J. Haymet, L. G. Ward, M. M. Harding, *J. Am. Chem. Soc.* **1999**, *121*, 941-948.

[42] A. K. Balcerzak, M. Febbraro, R. N. Ben, *RSC Adv.* **2013**, *3*, 3232-3236.

[43] J. Schindelin, I. Arganda-Carreras, E. Frise, V. Kaynig, M. Longair, T. Pietzsch, S. Preibisch, C. Rueden, S. Saalfeld, B. Schmid, J.-Y. Tinevez, D. J. White, V. Hartenstein, K. Eliceiri, P. Tomancak, A. Cardona, *Nat. Meth.* **2012**, *9*, 676-682.

Chapter 5

5. Antifreeze Protein Mimetic, Supramolecular Metallohelices with Potent Ice Recrystallization Inhibition Activity

D. E. Mitchell, R. A. Kaner, P. Scott and M. I. Gibson, in preparation

This chapter contains a paper on the use of amphipathic metallohelices as ice recrystallization inhibitors. MIG and DEM wrote the manuscript. PS and RK undertook the synthesis of the materials. DEM undertook all ice recrystallization inhibition studies. All others read and contributed to the manuscript.

5.1. Abstract

Antifreeze proteins are produced by extremophile species to control ice formation and growth and have potential applications in many fields. There are few examples of synthetic materials which can reproduce their potent ice recrystallization inhibition property. Here, the first instance of using supramolecular chemistry to generate potent ice recrystallization inhibitors is reported. Self-assembled enantiomerically pure, amphipathic metallohelicies were synthesized, and the most potent compounds fully inhibited ice growth at 20 mM. This opens up a new field of organometallic antifreeze protein mimetics.

5.2. Introduction

Antifreeze proteins (AFPs) found in the blood of cold-acclimatized species have evolved to enable life to flourish in hostile, ice-rich environments. Despite 40 years of study there are still questions about the function of AFPs and their interactions with ice, although recent microfluidic experiments have suggested an irreversible binding process.[1] AFPs posses three key properties; (i) thermal hysteresis (TH)- the non-colligative depression of freezing point relative to that of the melting point;[2] (ii) dynamic ice shaping (DIS)- where the shape of ice crystals is altered due to binding to specific faces on the ice crystal surface;[3] (iii) ice recrystallization inhibition (IRI)- where the rate of ice crystal growth (Ostwald Ripening) is inhibited.[4] Any compound which can control ice growth has huge potential application as frozen food texture modifiers,[5] in cryosurgery,[6] or advanced coatings.[7] The lack of synthetic mimics however, have limited the application of AFPs, except in the case of 'ice structuring proteins' in some ice cream formulations.[8]

In 2001 Ben and co-workers found that short glycopeptides could reproduce the IRI activity found in AFPs,[9] suggesting that there could be a viable synthetic route to new cryoprotectants. Several glycopeptides, glycopolymers and small molecules that posses some level of IRI activity have since been uncovered.[10-12] Many of these require relatively challenging synthesis and their usefulness as cryoprotectants is still under investigation. Gibson *et al.* have shown that synthetic polymers can also show IRI activity, based on either poly(vinyl alcohol) or poly(ampholyte) motifs.[13-14] Both of these have been applied to enhance the non-vitreous cryopreservation of blood, highlighting the potential of synthetic IRIs.[15-16] There is still a lack of understanding of the structural features essential for IRI activity, and the synthesis of a range of new

IRI's tailored to a variety of applications would be possible if fully understood. Structural analysis of AFPs shows that they are all rigid proteins, with many based on an amphiphilic alpha helix.[17-18] This implies that other, synthetic helical materials might be interesting candidates for mimics.

The alpha-helical secondary structure is extremely common in many proteins including those involved in disease, therefore the synthetic design of similar structures is of high interest. Some time ago, Lehn and co-workers noted that helicates; multimetallix and multistrand coordination complexes resemble alpha-helices in terms of their diameter and charge.[19] They have much higher symmetry (commonly D_3) however, and usually lack water solubility/stability and external functionality and are formed as racemates.[20] In contrast we have recently developed ranges of optically pure, water-soluble metallohelical architectures,[21-23] including most recently systems that have directional amphipathic architectures akin to small α-helical peptides.[24] Despite their complexity they are synthesised via self-assembly from small building blocks on a practical scale. Structural integrity and stereoselection are provided by extensive intramolecular π-stacking.[25-26] Interestingly the size and shape corresponds well to that of a type 1 AFP, while the tunability of these organometallic strucutres allows a library of different functional groups to be included, making it possible to accurately assess those strucutral properties required for IRI activity.

In this study we probe the concept that metallohelical structures may behave as AFP mimetics, through the analysis of a library of different ligand structures. Thus

providing a new and unique insight into the properties requires for IRI activity, and a new biomimetic strategy.

5.3. Results and Discussion

The size and shape of a Type I AFP is shown in Figure 5.1A, revealing approximate dimensions of 2.5 x 1.2 nm. Using our previously reported methodology, we assembled ligand L^1 with Fe^{3+} to generate the metallohelix M^1, Figure 5.1B. A comparison of the crystal structure of this helix with the AFP, reveals similar size and dimensions making them good lead molecules as structural AFP mimetics. Crucially, due to the arrangement of the ligands, these complexes have amphipathic character, again relating to the amphiphillic nature of the AFPs, which always have defined hydrophilic and hydrophobic faces. With this complex to hand, we tested for IRI activity using a modified 'splat' assay. Briefly, a small droplet of complex M^1 in PBS buffer was dropped onto a microscope slide at -80 °C to generate a large number of small crystals. These were annealed at -8 °C for 30 minutes, and the mean largest grain size (MLGS) calculated relative to a PBS control. Smaller values indicated more inhibition and hence more activity. Values below 20 % are not possible as this is the relative size of the seed crystals.

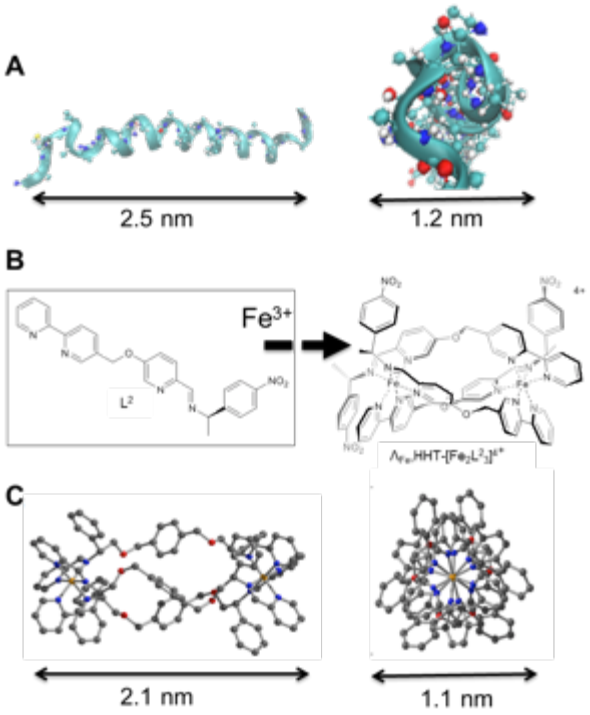

Figure 5.1. Biomimetic approach employed here. A) Crystal structure of Type I AFP with dimensions of the helix highlighted B) Synthesis of compound M^1; C) Crystal structure of compound M^1 and dimensions of the helix indicated. Images obtained using PyMOL.

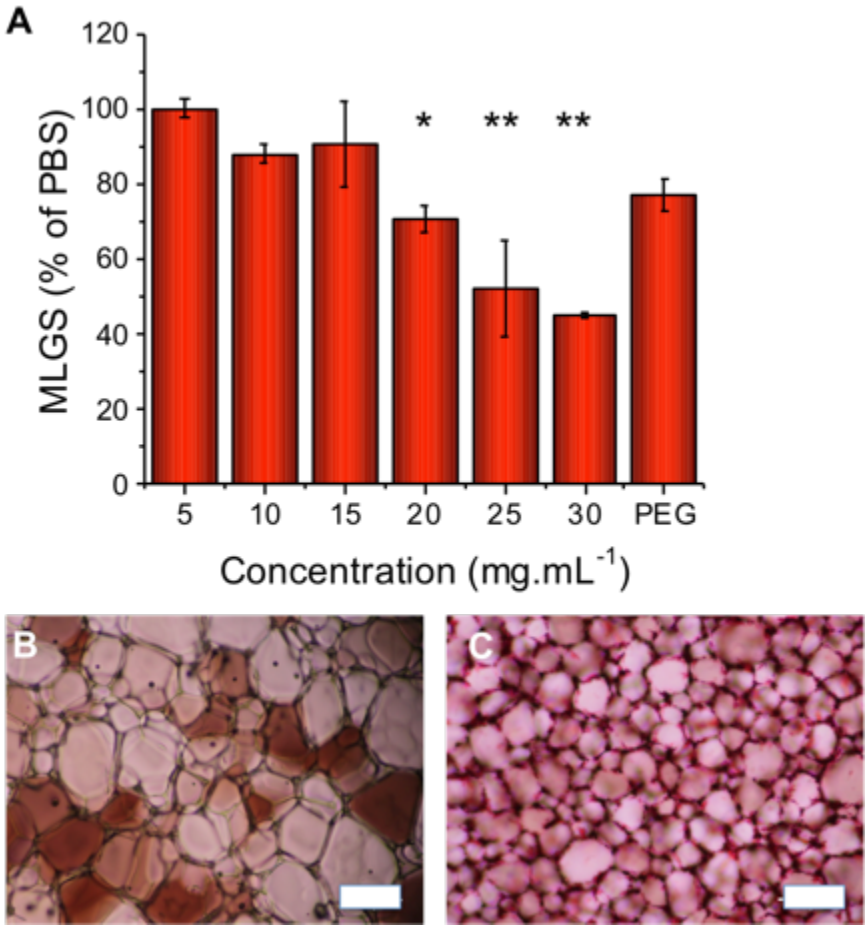

Figure 5.2. IRI activity of compound $M^{1\Lambda}$. A.) Concentration dependence of $M^{1\Lambda}$; B.) Example ice wafer of PBS buffer control; C.) Example wafer of $M^{1\Lambda}$. Error bars represent minimum of three repeats, MLGS = mean largest grain size relative to phosphate buffer saline control. ** represents a significance of $p < 0.01$ relative to poly(ethylene glycol) (PEG, 30 $mg.mL^{-1}$) negative control. Images are of equal magnification, scale bars are 50 μm.

Figure 5.2 clearly shows a dose-dependent decrease in the MLGS as a function of the concentration of compound $M^{1\Lambda}$. Example micrographs show ice crystals grown in PBS (Figure 5.2B) and with 30 $mg.mL^{-1}$ (0.018 M) compound $M^{1\Lambda}$. Note, compound $M^{1\Lambda}$ has a strong red purple color, which accounts for the unusual coloration of the ice wafer. Whilst the absolute activity of this complex in itself is not very high, it is

remarkable in that it is the first example of a self-assembled AFP mimetic, compared to the traditional peptide-based approach.

Encouraged by this remarkable observation, we synthesized a focused library of related compounds, all based on the triplex scaffold. This synthetic strategy produces both enantiomers enabling any chiral (if any) effects to be observed. The ligands used are shown in Table 5.1. All compounds were fully characterized by ^{1}H and ^{13}C NMR along with mass spectrometry and were enantiomerically pure (ESI, Appendix 4). The ease in which this large diversity can be inserted within a common scaffold of similar dimensions highlights the benefits of this chemistry.

Entry	Ligand	Complex Structure	Chirality
$M^{1\Lambda}$	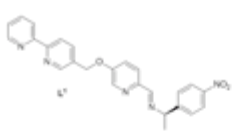	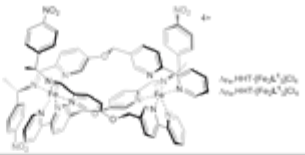	Λ
$M^{1\Delta}$			Δ
$M^{2\Lambda}$	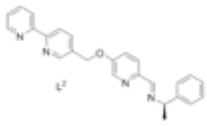	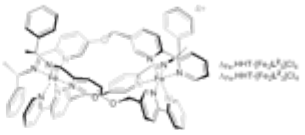	Λ
$M^{2\Delta}$			Δ
$M^{3\Lambda}$	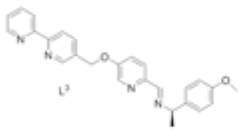	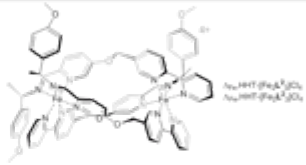	Λ
$M^{3\Delta}$			Δ
$M^{4\Lambda}$	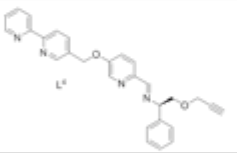	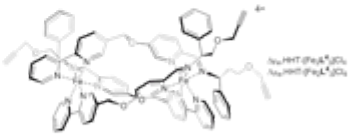	Λ
$M^{4\Delta}$			Δ
$M^{5\Lambda}$	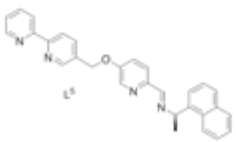	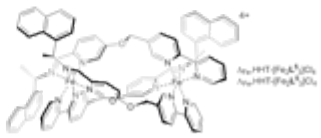	Λ
$M^{5\Delta}$			Δ
$M^{6\Lambda}$	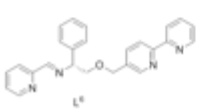	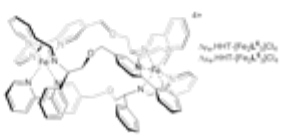	Λ
$M^{6\Delta}$			Δ

Table 5.1. Metallohelix library.

Each of the complexes in Table 5.1 was subsequently tested for IRI activity in the range of 25 – 2 mM using the 'splat' assay. Molar concentrations were used for comparison, due to the slight variation in molar mass between these complexes to ensure a fair comparison. A wide range of activities were observed ranging from zero to complete inhibition demonstrating a structural link to activity.

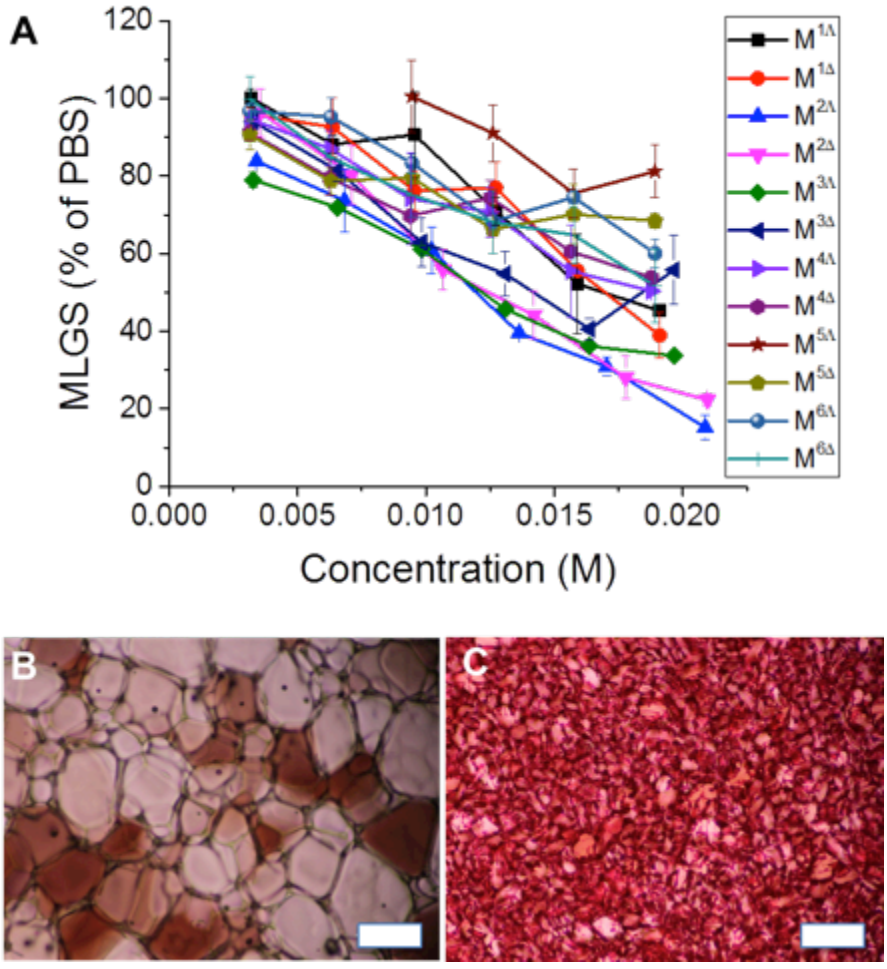

Figure 5.3. IRI activity of metallohelix library. A.) IRI activity concentration dependence of mettallohelices; B.) Example ice wafer of PBS buffer control; C.) Example wafer of $M^{2\Lambda}$. Error bars represent minimum of three repeats, MLGS = mean largest grain size relative to phosphate buffer saline control. Images are of equal magnification, scale bars are 50 μm.

Two compounds $M^{2\Lambda}$ and $M^{2\Delta}$ displayed remarkable activity. They both could completely inhibit all ice growth at 20 mM, but did not show any sign of dynamic ice shaping (unlike AFPs). In comparison to previously reported non-polymer IRI-active small molecules, the metallohelices shown here are more potent than the majority of IRI active carbohydrate based surfactants described in the literature,[12] and significantly better than all small sacchride molecules, with the exception of the sugar; *n*-octyl-β-D-galactopyranoside and a lysine based cationic surfactant, for which similar levels of activity was reported.[10] The other complexes used had varying levels of activity. It has been established that hydrophobicity is essential in IRI specific compounds, but a comparison of hydrophobicity with IRI activity showed no trend. L^5 ligand is the most hydrophobic but yields the least inhibition, while $L^{3,}$; the most hydrophilic is in the middle in terms of potency. There were also no obvious ice-binding groups (i.e. hydrogen bonders). In fact, the individual ligands are only sparing soluble in water, and only become soluble when complexed, and hence they are all intrinsically hydrophobic. Due to this low solubility it was not possible to evaluate the IRI activity of the ligands alone, highlighting that the self-assembly is crucial to activity.

We recently identified that a short peptide Nisin A had IRI activity which appeared to be due to its facially amphiphilic structure;[27] opposing hydrophobic/hydrophilic faces which would be able to disrupt transfer between ice crystals. A comparison of the most active and least active structures, looking along their z-axis revealed that both contain separated regions of more hydrophilicity (oxygen atoms). However, a clear difference relating to their activity was not possible to extract. Part of the

challenge is that these ligands are intrinsically hydrophobic, and hence any hydrophilcity is based on ether linkages, which are difficult to define as hydrophilic. Nonetheless, these complex clearly show that self-assembly of non-biological components can generate potent AFP mimics.

5.4. Conclusions

The above metallohelcies represent the first use of supramolecular chemistry to produce an IRI active molecule. Using this method it was possible to produce compounds, which can completely inhibit ice recrystallization at 20 mM. These complexes are easier to synthesize than glycopeptides, and have the benefit over polymeric inhibitiors in that they have no molecular weight disperstiy. There are also synthetically tractable, which we believe will enable precise-structure activity relationships to be drawn to both understand the fundamentals of ice growth inhibition, but to enable us to obtain ever-more potent IRIs. New synthetic IRI molecules will have huge impact across fields including cryo-medicine, transplantation medicine, frozen food, aqua culture, ice-resistant coatings and more.

5.5. Experimental Section

5.5.1. Materials

All solvents and chemicals purchased from commercial sources (Sigma-Aldrich, Acros, Fisher Scientific or Alfa Aesar) were used without further purification unless otherwise stated. Sodium hydride dispersions in mineral oil were placed in a Schlenk vessel under an inert atmosphere and washed three times with diethyl ether to remove the oil, then dried and stored under argon in an MBraun dry box. Where appropriate,

reactions were carried out under argon using a dual manifold argon/vacuum line and standard Schlenk techniques or in an MBraun dry box. Necessary solvents were dried by heating to reflux for 3 days under nitrogen over the appropriate drying agents (potassium for tetrahydrofuran, sodium/potassium alloy for diethyl ether, and calcium hydride for acetonitrile and pyridine) and degassed before use. Tetrahydrofuran and diethyl ether were additionally pre-dried over sodium wire. Dried solvents were stored in glass ampoules under argon. All glassware and cannulae were stored in an oven at > 375 K.

Deuterated solvents were purchased from Sigma-Aldrich and Cambridge Isotope Laboratories. Phosphate-buffered saline (PBS) solution was prepared using preformulated tablets (Sigma-Aldrich) in 200 mL of Milli-Q water (>18.2 Ω mean resistivity) to give [NaCl] = 0.138 M, [KCl] = 0.0027 M, and pH 7.4.

5.5.2. Physical and analytical methods

NMR spectra were recorded on Bruker Spectrospin 300/400/500 MHz spectrometers. Routine NMR assignments were confirmed by ^{1}H-^{1}H (COSY) and ^{13}C-^{1}H (HMQC) correlation experiments where necessary. The spectra were internally referenced using the residual protio solvent ($CDCl_3$, CD_3CN etc.) resonance relative to tetramethylsilane (δ = 0 ppm). ESI mass spectra were recorded on an Agilent Technologies 1260 Infinity spectrometer or a Bruker Daltonics MicroTOF spectrometer. Infra-Red spectra were measured using a Bruker Alpha-P FTIR spectrometer. Elemental analyses were performed by Medac Ltd. Chobham, Surrey GU24, 8JB, UK or Warwick Analytical Service, Coventry, CV4 7EZ.

Optical rotation measurements were performed on a Perkin Elmer Polarimeter 341 by Warwick Analytical Services, Coventry, UK. In all cases the following parameters were used: solvent: methanol, temperature: 20 °C, pathlength: 100 mm, wavelength: 589 nm.

Thermogravimetric analysis (DSC1-1600 scanning calorimeter) was used to determine the amount of water of crystallisation present in the chloride salts of iron (II) triplex metallohelices.

5.5.3. General synthesis of HHT-[Fe_2L'']Cl_4

Anhydrous iron(II) chloride (2 eq.) was added to a stirred solution of the either the desired R_C-chiral amine (3 eq.) and 5-(2,2'-bipyridin-5-ylmethoxy)picolinaldehyde (3 eq.) or the desired substituted aldehyde (3 eq.) and (R)-2-(2,2'-bipyridin-5-ylmethoxy)-1-phenylethanamine (3 eq.) in methanol (20 ml) at ambient temperature to give a purple solution that was then heated to reflux (65 °C) for 24 – 48 h. The reaction was allowed to cool to ambient temperature, filtered through a celite plug and the solvents were removed *in vacuo* to give the desired dark purple solid (see ESI, Appendix 5 for full synthetic details). Note that the presence of water of crystallisation in these compounds was confirmed by NMR and IR spectroscopy and the absence of other solvents was confirmed also by NMR. The hydration number was then determined by thermogravimetric analysis and the relevant mass loss was correlated with microanalytical data.

5.5.4. Ice recrystallisation inhibition (splat) assay.

Ice recrystallisation inhibition was measured using a modified splay assay.[28] A 10 μL sample of polymer dissolved in PBS buffer (pH 7.4) was dropped 1.40 m onto a chilled glass coverslip sat on a piece of polished aluminum placed on dry ice. Upon hitting the chilled glass coverslip, a wafer with diameter of approximately 10 mm and thickness 10 μm was formed instantaneously. The glass coverslip was transferred onto the Linkam cryostage and held at -8 °C under N_2 for 30 minutes. Photographs were obtained using an Olympus CX 41 microscope with a UIS-2 20×/0.45/∞/0–2/FN22 lens and crossed polarizers (Olympus Ltd, Southend on sea, UK), equipped with a Canon DSLR 500D digital camera. Images were taken of the initial wafer (to ensure that a polycrystalline sample had been obtained) and after 30 minutes. Image processing was conducted using Image J, which is freely available.[29] In brief, ten of the largest ice crystals in the field of view were measured and the single largest length in any axis recorded. This was repeated for at least three wafers and the average (mean) value was calculated to find the largest grain dimension along any axis. The average of this value from three individual wafers was calculated to give the mean largest grain size (MLGS). This average value was then compared to that of a PBS buffer negative control providing a way of quantifying the amount of IRI activity.

5.6. References

[1] Y. Celik, R. Drori, N. Pertaya-Braun, A. Altan, T. Barton, M. Bar-Dolev, A. Groisman, P. L. Davies, I. Braslavsky, *Proc. Natl. Acad. Sci. U. S. A.* **2013**, *110*, 1309-1314.

[2] Y. Celik, L. A. Graham, Y. F. Mok, M. Bar, P. L. Davies, I. Braslavsky, *Proc. Natl. Acad. Sci. U. S. A.* **2010**, *107*, 5423-5428.

[3] M. E. Houston Jr, H. Chao, R. S. Hodges, B. D. Sykes, C. M. Kay, F. D. Sönnichsen, M. C. Loewen, P. L. Davies, *J. Bio. Chem.* **1998**, *273*, 11714-11718.

[4] P. Czechura, R. Y. Tam, E. Dimitrijevic, A. V. Murphy, R. N. Ben, *J. Am. Chem. Soc.* **2008**, *130*, 2928-2929.

[5] M. Griffith, K. V. Ewart, *Biotechnol. Adv.* **1995**, *13*, 375-402.

[6] H. Koushafar, L. Pham, C. Lee, B. Rubinsky, *J. Surg. Oncol.* **1997**, *66*, 114-121.

[7] A. P. Esser-Kahn, V. Trang, M. B. Francis, *J. Am. Chem. Soc.* **2010**, *132*, 13264-13269.

[8] A. Regand, H. D. Goff, *J. Dairy Sci.*, *89*, 49-57.

[9] A. Eniade, A. V. Murphy, G. Landreau, R. N. Ben, *Bioconjugate Chem.* **2001**, *12*, 817-823.

[10] A. K. Balcerzak, S. S. Ferreira, J. F. Trant, R. N. Ben, *Bioorg. Med. Chem. Lett.* **2012**, *22*, 1719-1721.

[11] L. Corcilius, G. Santhakumar, R. S. Stone, C. J. Capicciotti, S. Joseph, J. M. Matthews, R. N. Ben, R. J. Payne, *Bioorg. Med. Chem. Lett.* **2013**, *21*, 3569-3581.

[12] C. J. Capicciotti, M. Leclere, F. A. Perras, D. L. Bryce, H. Paulin, J. Harden, Y. Liu, R. N. Ben, *Chem. Sci.* **2012**, *3*, 1408-1416.

[13] T. Congdon, R. Notman, M. I. Gibson, *Biomacromolecules* **2013**, *14*, 1578-1586.

[14] D. E. Mitchell, M. Lilliman, S. G. Spain, M. I. Gibson, *Biomater. Sci.* **2014**, *2*, 1787–1795.

[15] D. E. Mitchell, N. R. Cameron, M. I. Gibson, *Chem. Commun.* **2015**.

[16] R. C. Deller, M. Vatish, D. A. Mitchell, M. I. Gibson, *Nat. Commun.* **2014**, *5*, 3244-3251.

[17] F. Sicheri, D. S. Yang, *Acta. Crystallogr. D Biol. Crystallogr.* **1996**, *52*, 486-498.

[18] M. E. Daley, L. Spyracopoulos, Z. Jia, P. L. Davies, B. D. Sykes, *Biochemistry* **2002**, *41*, 5515-5525.

[19] J. M. Lehn, A. Rigault, J. Siegel, J. Harrowfield, B. Chevrier, D. Moras, *Proc. Nat. Acad. Sci. U. S. A.* **1987**, *84*, 2565-2569.

[20] S. E. Howson, P. Scott, *Dalton. Trans.* **2011**, *40*, 10268-10277.

[21] S. E. Howson, A. Bolhuis, V. Brabec, G. J. Clarkson, J. Malina, A. Rodger, P. Scott, *Nat. Chem.* **2012**, *4*, 31-36.

[22] V. Brabec, S. E. Howson, R. A. Kaner, R. M. Lord, J. Malina, R. M. Phillips, Q. M. A. Abdallah, P. C. McGowan, A. Rodger, P. Scott, *Chem. Sci.* **2013**, *4*, 4407-4416.

[23] M. Li, S. E. Howson, K. Dong, N. Gao, J. Ren, P. Scott, X. Qu, *J. Am. Chem. Soc.* **2014**, *136*, 11655-11663.

[24] A. D. Faulkner, R. A. Kaner, Q. M. A. Abdallah, G. Clarkson, D. J. Fox, P. Gurnani, S. E. Howson, R. M. Phillips, D. I. Roper, D. H. Simpson, P. Scott, *Nat. Chem.* **2014**, *6*, 797-803.

[25] S. E. Howson, L. E. N. Allan, N. P. Chmel, G. J. Clarkson, R. van Gorkum, P. Scott, *Chem. Commun.* **2009**, 1727-1729.

[26] S. E. Howson, L. E. Allan, N. P. Chmel, G. J. Clarkson, R. J. Deeth, A. D. Faulkner, D. H. Simpson, P. Scott, *Dalton Trans.* **2011**, *40*, 10416-10433.

[27] D. E. Mitchell, Gibson, M.I, *Biomacromolecules*, **2015,** Accepted.

[28] C. A. Knight, J. Hallett, A. L. DeVries, *Cryobiology* **1988**, *25*, 55-60.

[29] C. A. Schneider, W. S. Rasband, K. W. Eliceiri, *Nat. Meth.* **2012**, *9*, 671-675.

Chapter 6

6. Rational, yet Simple, Design and Synthesis of an Antifreeze-Protein Inspired Polymer for Cellular Cryopreservation

D. E. Mitchell, N. R. Cameron and M. I. Gibson, *Chem. Commun.* **2015**, 51, 12977-12980.

This chapter contains a paper on the design and synthesis of a novel polyampholyte polymer. This is subsequently found to inhibit ice recrystallization, be non-cytotoxic and to dramatically enhance cellular survival rates of red blood cells (RBCs) undergoing cryopreservation.

DEM synthesised the polymers and performed all characterisation. Ice recrystallization inhibition, cytotoxicity and cryo-survival assays were performed by DEM. Manuscript was prepared by DEM, NRC and MIG.

6.1. Abstract

Antifreeze (glyco) proteins AF(G)Ps are potent ice recrystallization inhibitors, which is a desiarable property to enhance cryopreservation of donor tissue/cells. Here we present the rational synthesis of a new, biomimetic, ice-recrystallization inhibiting

polymer derived from a cheap commodity polymer, based on an ampholyte structure. The polymer is used to enhance the cryopreservation of red blood cells, demonstrating a macromolecular solution to tissue storage.

6.2. Introduction

In the freezing polar regions of the Earth, Nature has evolved a number of methods to survive. One of these is freeze avoidance[1] (as opposed to freeze tolerance)[2] using antifreeze proteins (AFPs) or antifreeze glycoproteins (AF(G)Ps). Ever since they were discovered in polar fish species AF(G)Ps have attracted interest due to their ability to interact with ice[3] and their potential applications in cryopreservation, cryosurgery, food-storage, anti-icing surfaces and more.[4-7] AF(G)Ps have three key properties; (i) thermal hysteresis (TH) – the non-colligative depression of the freezing point, which does not affect the equilibrium melting point;[8] (ii) dynamic ice shaping (DIS) where the shape of ice crystals is altered due to binding to specific faces on the ice surface;[9] (iii) ice recrystallization inhibition (IRI) whereby the rate of ice crystal growth (Ostwald ripening) is slowed.[10] IRI is a particularly interesting property as it has been found that ice recrystallization during thawing is a major contributor to cell death.[11-12]

New cryoprotectants are urgently needed to improve the availability of cells/tissues/organs to address the needs of a growing and ageing population. For example, blood can only be stored for a maximum of 42 days and stock quantities vary over the course of a year, meaning that there is always a shortage.[13] Emerging regenerative medicine therapies based on stem cells also require efficient cryostorage. The current state-of-the-art cryoprotection involves the addition of large amounts of

organic solvents such as glycerol or DMSO. Whilst successful, these solvents can cause cellular toxicity and, ideally, should not be directly transfused. There are also some cell types for which no effective cryopreservation solution exists.

Considering the above, there have been several attempts at cryopreservation using AF(G)Ps but these have met with mixed results. For example, addition of AFP to erythrocytes gave some cryopreservation enhancement, but above a critical concentration, it actually decreased viability.[14] This was found to be due to the formation of needle-like (spicular) ice crystals due to the DIS/TH activity of AF(G)Ps. There are several other studies demonstrating both benefits and problems of AF(G)Ps in cryopreservation, with the problems normally due to ice shaping, which have prevented their application.[15-16] Furthermore there is some evidence that AF(G)Ps can be toxic to human cells.[17] In 2003 Ben and co-workers demonstrated that short glycopeptides could specifically reproduce IRI, but not TH/DIS suggesting that there may be a synthetic route to new cryoprotectant molecules. [18] Several glycopeptides, glycopolymers and even small molecules have since been identified with varying degrees of IRI activity.[19-22] Some of these are still relatively challenging to synthesize and their cryopreservation activity is still under investigation. As an alternative both Gibson and coworkers and Inada *et al.* have separately investigated synthetic polymers as AF(G)P mimics, in particular the use of poly(vinyl alcohol) (PVA) which has strong IRI activity,[23-24] with very few other polymers reported with this unique property. Polymers are easy to access on a large scale, are highly tunable in terms of composition and architecture and are widely used in personal care and pharmaceutical industries making them appealing additives. Addition of just 0.1 wt % of PVA was found to enhance red blood cell cryopreservation by inhibiting ice

growth.[25] Matsumura and coworkers identified that carboxy-modified poly(ε-lysine) could enhance stem cell cryopreservation although the mechanism was unclear.[26] Gibson and co-workers used controlled radical polymerization to generate well defined poly(ampholytes) with both amino and carboxy side chains with definite IRI activity but that a 1:1 ratio of cationic to anionic groups was required for maximum activity and unambiguously demonstrated that IRI was (in part) the cryoprotective mechanism of poly(ampholytes).[27] To enable exploitation of IRI active polymers, there still exists a need to identify new materials, ensure their availability in quantities needed for application and to demonstrate their biological potential.

This manuscript describes an easy and accessible synthetic route to new poly(ampholytes) with definite IRI activity, derived from the bulk commodity polymer; poly(methyl vinyl ether-*alt*-maleic anhydride) (Gantrez^{TM}) widely used in the coatings industry. The synthetic route ensures perfectly alternating cationic/anionic charges to maximize activity (as opposed to previous routes). This new material was then shown to dramatically enhance red blood cell cryopreservation enabling solvent-free storage of this crucial component of modern medicine.

6.3. Results and Discussion

Previously polyampholytes have been prepared by post-polymerisation functionalization of poly(amines) which intrinsically gives rise to a statistical distribution of the charged groups.[28] Considering Nature requires explicit control over sequence distribution in AFGPs, but tolerates molecular weight distribution, we devised a synthetic strategy to match this. The low cost (< \$20 kg^{-1}), but structurally defined, commodity polymer PMVEMA (Mw = 311 kDa) contains alternating

anhydrides in the main side chain, providing an opportunity to obtain alternative polymers via ring-opening, but has large dispersity as it is obtained by free-radical polymerization (as with most bulk-polymers). The poly(ampholyte) was prepared by nucleophilic ring-opening of the anhydride ring with *N*-Boc-ethanolamine, followed by TFA deprotection in high yield with a minimum of synthetic steps, Figure 6.1. Following exhaustive dialysis, conversion of the anhydrides to esters was confirmed by IR spectroscopy and quantitative incorporation of the ethanolamine group was determined by ^{1}H NMR (Appendix 5).

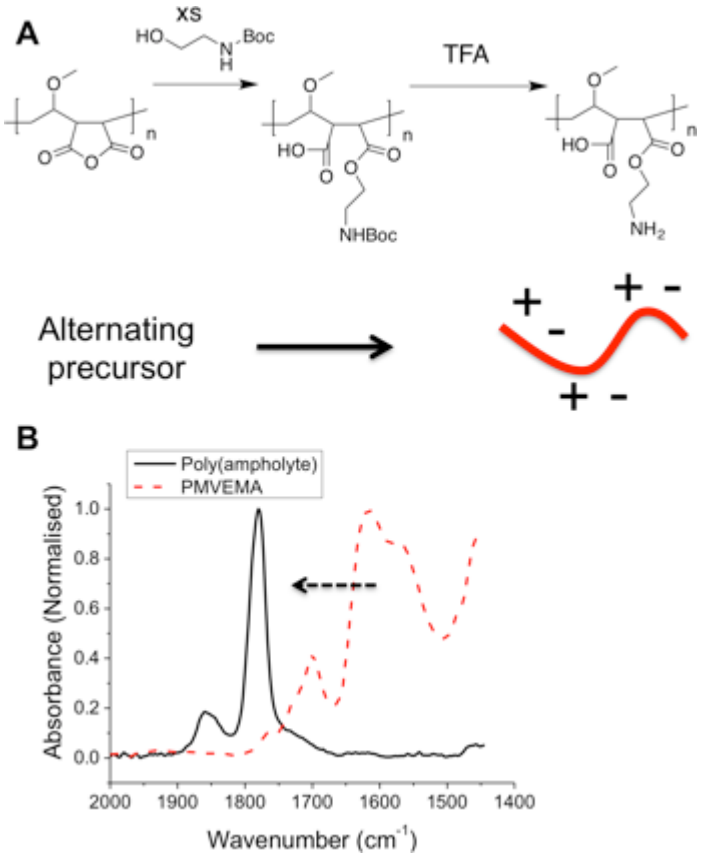

Figure 6.1. Synthesis of new poly(ampholyte) by ring opening of the maleic anhydride units. A) Synthetic route employed; B) IR spectra showing conversion of anhydride into carboxylic acid and ester, confirming substitution.

With this new, low cost, poly(ampholyte) to hand it was necessary to evaluate its IRI activity. A modified splat test was employed, which involves creating a wafer of small ice crystals, which are then allowed to grow at – 8 °C, and then their average crystal sizes are measured, relative to a control (PBS). Small MLGS (mean largest grain size) values indicate increased IRI activity. As a negative control we included a high molecular weight (100 kDa) poly(ethylene glycol), PEG. This PEG was chosen to ensure that any viscosity-related effects (due to high molecular weight) do not bias our measurements. In keeping with reports of other poly(ampholytes), this new polymer was capable of inhibiting 50 % of ice growth at 20 $mg.mL^{-1}$. Whilst this is less active than our positive control, PVA, it is still a definite effect and somewhat surprising given the huge structural differences between this polymer and Native AF(G)Ps, and represents one of only a handful of synthetic polymers with this activity. Inhibiting ice growth at a concentration of 20 $mg.mL^{-1}$ is also relatively low in a cryopreservation context: Up to 40 wt % (~ 400 $mg.mL^{-1}$) is required for tradition organic solvents applied in cryopreservation.

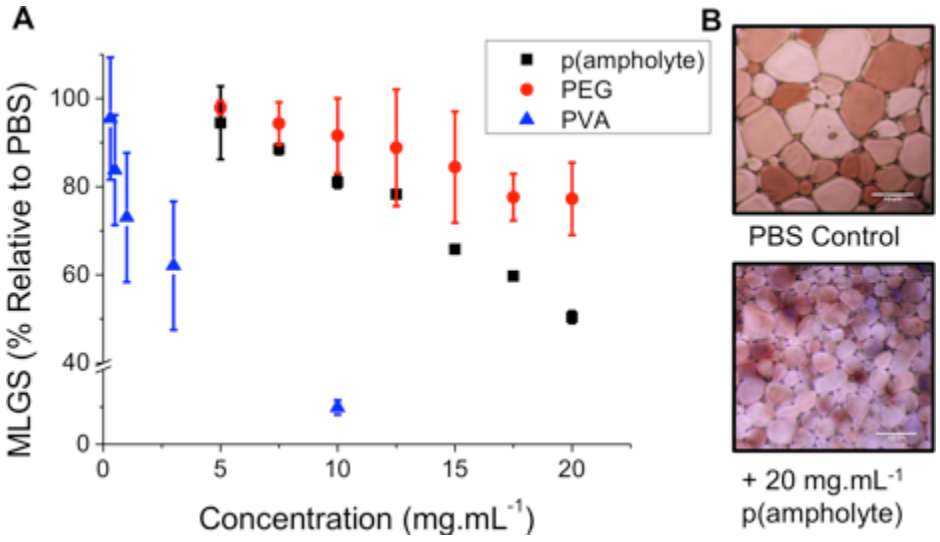

Figure 6.2. Ice recrystallization inhibition of PMVEMA-*co*-EA. A) Comparison with PEG (100 kDa) as a negative control and PVA_{10} as a positive. Mean largest grain size is expressed as a percentage of PBS buffer. Error bars represent ± SD from a minimum of 3 repeats; B) Example micrographs of ice wafers with and without polymeric IRI agent. Both images are of equal magnification, scale bars represent 50 μm.

Our previous studies have shown that addition of PVA to red blood cells dramatically reduces ice-induced damage, but that the level of cell recovery using PVA alone was relatively low (< 40 %).[25] To improve this, hydroxyethyl starch (HES) was selected as a co-cryopreservative – it is non-penetrating macromolecules and does not lead to vitrification, unlike e.g. DMSO. HES is used clinically as a plasma expander, so is ideally suited to blood-contacting applications. Cytocompatibilty of the poly(ampholyte) was evaluated by incubation with fresh ovine red blood cells (RBCs) for 4 hours, after which the degree of haemolysis was measured, Figure 6.3A (cell recovery = 1/haemolysis, see ESI, Appendix 5). At concentrations up to 40 $mg.mL^{-1}$ (above what is needed in later experiments) there was no statistically significant

indication of haemolysis, indicating the polymers were compatible with RBCs. At concentrations as high as 100 $mg.mL^{-1}$, haemolysis was observed, as would be expected for almost any foreign additive at such high concentrations. At these very high (> 50 $mg.mL^{-1}$) concentrations the polymer solution also becomes very viscous, which might contribute to apparent toxicity, due to the challenge of separating undamaged cells. To assess the polymers' cryopreservation enhancement, RBCs were prepared in an isotonic cryopreservation solution containing HES, and different amounts of the poly(ampholyte) were added. Cells were frozen by rapid cooling by placing into liquid nitrogen (-196 °C) and stored in nitrogen vapour for 5 days. Following this time the cells were thawed at room temperature for 1 hour. These thawing conditions are crucial – ice recrystallization is maximised under slow thawing conditions (the property being probed here) and is representative of large volume cryopreservation (e.g. blood bags, or organs) where thermal gradients across the sample lead to ice growth. Control experiments using fast thawing were also conducted, which improves recovery in these low volumes but is challenging in a 'real world' situation (ESI, Appendix 5). It should be noted that differential scanning calorimetry confirmed no vitrification occurred during freezing. The results of the cryopreservation are shown in Figure 6.3B.

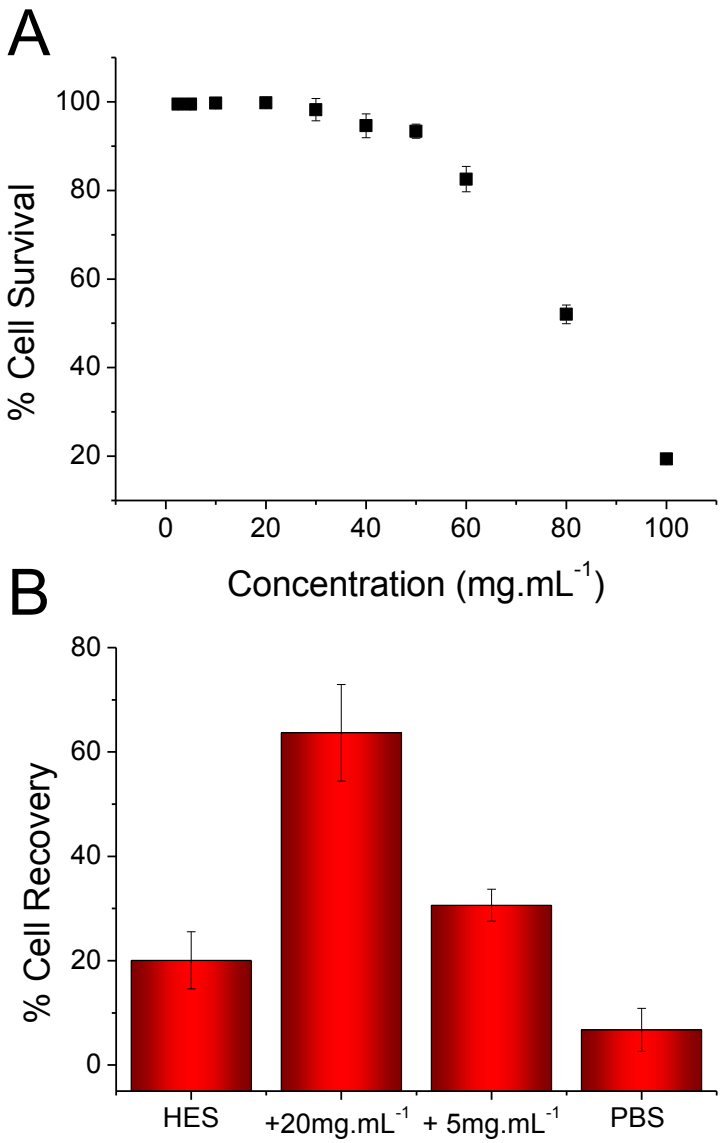

Figure 6.3. Recovery of red blood cells when slow-thawed on the bench top. A) Cytocompatibility assay of RBCs with p(ampholyte) and the working range highlighted in red. Incubation time = 4 hours; B) Cell recovery after freezing (-196 °C, 5 days) and thawing (room temperature, 1 hour). Recovery is expressed as a fraction of an unfrozen positive control, error bars represent ± SD from a minimum of 3 repeats.

Using HES alone, only 20 % of the RBCs were recovered. However, addition of 5 $mg.mL^{-1}$ poly(ampholyte) increased this to 30 %, and addition of 20 $mg.mL^{-1}$ increased it to an impressive 60 %. Higher concentrations could not be tested due to the increased solution viscosity in the cryopreservation solution. The dose-dependence of the cryopreservation correlates well with the observed IRI activity of the polymers and the dose required is far less than was required for a lysine-based poly(amphotyle) when cryopreserving stem cells,[26] which needed > 100 $mg.mL^{-1}$ for cryopreservation. It should again be highlighted that by using slow-thawing conditions, we are maximising potential for cell damage to provide a rigours test – higher levels of recovery could be achieved with fast thawing (~ 80 %) but our aim is to eliminate all recrystallization associated damage. Considering the ease, and scale, of the polymer synthesis and its clear beneficial effect on improving blood cryopreservation this demonstrates that biomimics of AF(G)Ps can have a huge impact on improving the availability of donor cells. The work presented here also demonstrates that the rational design of ice-modifying macromolecules, tuned to their specific application is possible. In the long term, this will enable us to fully understanding how macromolecules (synthetic and biological) control crystallisation processes. Future work will extend to a wide range of cell types and also obtain structure-function relationships to enable an understanding of why certain polymers can inhibit ice growth.

6.4. Conclusions

We have demonstrated a new, facile, biomimetic approach to engineering ice-recrystallization inhibiting polymers, inspired by antifreeze proteins. A region-regular poly(ampholyte) was synthesized from a bulk commodity precursor and shown to

have specific ice recrystallization inhibition activity. The poly(ampholyte) was non-toxic to red blood cells and facilitated a remarkable enhancement in the post-freezing cell recovery by inhibiting ice growth during thawing. This demonstration shows that the identification, and translation of new cryopreservatives is possible, using synthetic, as opposed to biological approaches. It is also a step towards the ability to routinely mimic these proteins, which have a complex function, which will bring benefits both to cryopreservation (and other fields) but to our understanding of interfacial process at ice crystals.

6.5. Experimental Section

6.5.1. Materials

Poly(methyl vinyl ether-*alt*-maleic anhydride) (PMVEMA Mw 311 kDa), ethanol amine, Di-*tert*-butyl dicarbonate (BOC), poly(ethylene glycol) (PEG, 100 kDa size), mannitol, hydroxyethyl starch (HES), sodium chloride, tetrahydrofuran and trifluoroacetic acid were purchased from Sigma Aldrich (UK). Ovine red blood cells in Alserver's solution were purchased from TCS biosciences (UK). Phosphate-buffered saline (PBS) solution was prepared using preformulated tablets (Sigma-Aldrich) in 200 mL of Milli-Q water (>18.2 Ω mean resistivity) to give [NaCl] = 0.138 M, [KCl] = 0.0027 M, and pH 7.4.

6.5.2. Physical and analytical methods

^{1}H and ^{13}C NMR spectra were recorded on Bruker DPX-300 and DPX-400 spectrometers using deuterated solvents obtained from Sigma-Aldrich. Chemical shifts in ppm (δ) are reported relative to residual tetramethylsilane (TMS). FTIR

spectra were acquired using a Bruker Vector 22 FTIR spectrometer with a Golden Gate diamond attenuated total reflection cell. A total of 128 scans were collected on samples in their native (dry) state. Bright and fluorescence microscopy were performed on an Olympus CKX41 with MoticamPro 205C and CoolLed pE-300-W light source, images analysed using Motic Images Advanced 3.2. Cells used were screened, pathogen-free, defibrinated sheep red blood cells in Alsever's solution. All incubations of red blood cells were visualised at 1/10 dilution in PBS, with 2 μL solution on a glass slide with a glass cover slip. Absorbance was measured on a microplate reader (Synergy HT multi-mode microplate reader, BioTek UK).

6.5.3. Synthesis of *N*-boc ethanolamine.

3.57 g Di-*tert*-butyl dicarbonate was added to 1 g ethanolamine (1:1 molar ratio) and reacted at room temperature for 2 hours, producing *N*-boc ethanolamine. ^{1}H NMR ($CDCl_3$): δ 4.92 (br, 1H –ROH); δ 3.74 (br, 2H –OCH_2); δ 3.51 (s, 1H -CH_2NHCOO); δ 3.32 (br 2H– CH_2CH_2NH); δ 1.67 (br, 9H $OC(CH_3)_3$). Mass Spectrometry: m/z (EI^-) calc for $(CH_3)_3COCONHCH_2CH_2OH$, 161.2; found 160.2 $[M]^-$.

6.5.4. Functionalization of PMVEMA with *N*-Boc ethanolamine.

2 g of *N*-boc-ethanolamine was added to 0.4 g PMVEMA (Mw 311 kDa) dissolved in 10 mL THF. The mixture was warmed to 55°C and allowed to react for 24 hours. This was then dialysed against deionized water (7 water changes 48 hours) and lyophilized. Functionalization was confirmed by NMR and FTIR spectroscopy. ^{1}H NMR (D_2O): δ 3.66 (br 2H –OCH_2CH_2); δ 3.47 (br 3H -OCH_3); δ 3.32 (br H –CH_2NHCOO); δ 2.91-

3.12 (br 2H CHCH(COO)CH)); δ 2.62 (br 2H CH_2CH_2NH); δ 1.92 (br 2H -$CHCH_2CH$); δ 1.28 (br 9H -$OC(CH_3)_3$).

6.5.5. Removal of boc protecting group.

0.3 g N-Boc functional-PMVEMA dissolved in methanol was treated with 2 mL trifluoroacetic acid. The mixture was reacted at room temperature for 3 hours. This was followed by dialysis (7 water changes, 48 hours) against deionized water and lyophilisation. To substitute the trifluoroacetate ion for a chloride ion, dialysis against 10 mM sodium chloride (5 water changes) was used followed by dialysis against deionized water (5 water changes) to removal excess salt. ^{1}H spectroscopy was used to determine functionalization. ^{1}H NMR (D_2O): δ 3.66 (br 2H –OCH_2CH_2); δ 3.47 (br 3H -OCH_3); δ 3.32 (br 2H –CH_2NHCOO); δ 2.91- 3.12 (br 2H CHCH(COO)CH)); δ 2.62 (br 2H CH_2CH_2NH); δ 1.92 (br 2H -$CHCH_2CH$);

6.5.6. Ice recrystallisation inhibition (splat) assay.

Ice recrystallisation inhibition was measured using a modified splay assay.[1] A 10 μL sample of polymer dissolved in PBS buffer (pH 7.4) was dropped 1.40 m onto a chilled glass coverslip sat on a piece of polished aluminum placed on dry ice. Upon hitting the chilled glass coverslip, a wafer with diameter of approximately 10 mm and thickness 10 μm was formed instantaneously. The glass coverslip was transferred onto the Linkam cryostage and held at -8 °C under N_2 for 30 minutes. Photographs were obtained using an Olympus CX 41 microscope with a UIS-2 20×/0.45/∞/0–2/FN22 lens and crossed polarizers (Olympus Ltd, Southend on sea, UK), equipped with a Canon DSLR 500D digital camera. Images were taken of the initial wafer (to ensure that a polycrystalline sample had been obtained) and after 30 minutes. Image processing was conducted using Image J, which is freely available.[2] In brief, ten of

the largest ice crystals in the field of view were measured and the single largest length in any axis recorded. This was repeated for at least three wafers and the average (mean) value was calculated to find the largest grain dimension along any axis. The average of this value from three individual wafers was calculated to give the mean largest grain size (MLGS). This average value was then compared to that of a PBS buffer negative control providing a way of quantifying the amount of IRI activity.

6.5.7. Hemolysis testing.

Samples containing 250 μL red blood cells (RBCs) and 250 μL of polymer solution were incubated at 37 °C for 30 minutes prior to testing. After centrifugation to concentrate down the RBCs, 10 μL of the supernatant was added to 90 μL of PBS buffer in a 96 well plate. The absorbance was measured at 450 nm and compared against a PBS buffer positive control (i.e. 100 % recovery) and a deionised water negative control (0 % recovery) to determine the cell survival rate. RBCs leach heme into the supernatant when they die, providing an easily available method of testing cell survival rate. Samples were tested as 6 repeats.

6.5.8. Cryopreservation of RBCs.

A 250 μL aliquot of prepared RBCs (ovine origin, packed cell volume between 32 and 52 %) was added to 250 μL of a standard cryosolution (containing HES (350 $mg.mL^{-1}$), mannitol (30 $mg.mL^{-1}$) sodium chloride (6.5 $mg.mL^{-1}$)) and vortexed gently to ensure mixing. pMVEMA-*co*-EA was added at various concentrations to this cryosolution in order to determine whether any beneficial effect could be seen. These were then rapidly frozen in triplicate by immersion into liquid nitrogen and

stored within a liquid nitrogen container for 5 days. Thawing was either performed at 42 °C for 2 minutes in a water bath, or on the bench top for 1 hour.

6.5.9. Measurement of red blood cell haemolysis and cell recovery.

A 250 μL aliquot of red blood cell / cryoprotectant solution was centrifuged in a 1.5 mL Eppendorf tube for 5 minutes at 6000 rpm. Then 10 μL of the supernatant was removed and added to 90 μL of PBS in a well of a 96-well plate. Absorbance was measured at 450 nm and compared to an unfrozen positive control containing 250 μL prepared RCBs and 250 μL PBS buffer. 100 % hemolysis samples were prepared by adding 250 μL RCBs to distilled water. Cell recovery was calculated by subtracting the attained haemolysis (%) from 100 (%) giving a figure for cell recovery (%).

6.6. References

[1] C. C. Cheng, A. L. DeVries, in *Life Under Extreme Conditions* (Ed.: G. di Prisco), Springer Berlin Heidelberg, **1991**, pp. 1-14.

[2] K. B. Storey, J. M. Storey, *Physiol. Rev.* **1988**, *68*, 27-84.

[3] A. L. DeVries, *Comp. Biochem. Physiol., B: Comp. Biochem.* **1988**, *90*, 611–621.

[4] M. M. Harding, P. I. Anderberg, A. D. J. Haymet, *Eur. J. Biochem.* **2003**, *270*, 1381-1392.

[5] A. P. Esser-Kahn, V. Trang, M. B. Francis, *J. Am. Chem. Soc.* **2010**, *132*, 13264-13269.

[6] K. Muldrew, J. Rewcastle, B. J. Donnelly, J. C. Saliken, S. Liang, S. Goldie, M. Olson, R. Baissalov, G. Sandison, *Cryobiology* **2001**, *42*, 182-189.

[7] M. Griffith, K. V. Ewart, *Biotechnol. Adv.* **1995**, *13*, 375-402.

[8] Y. Celik, L. A. Graham, Y. F. Mok, M. Bar, P. L. Davies, I. Braslavsky, *Proc. Natl. Acad. Sci. U. S. A.* **2010**, *107*, 5423-5428.

[9] M. E. Houston Jr, Chao H., R. S. Hodges, B. D. Sykes, C. M. Kay, F. D. Sönnichsen, M. C. Loewen, P. L. Davies, *J. Bio. Chem.* **1998**, *273*, 11714-11718.

[10] P. Czechura, R. Y. Tam, E. Dimitrijevic, A. V. Murphy, R. N. Ben, *J. Am. Chem. Soc.* **2008**, *130*, 2928-2929.

[11] R. C. Deller, M. Vatish, D. A. Mitchell, M. I. Gibson, *Nat. Commun.* **2014**, *5*, 3244-3249.

[12] A. Fowler, M. Toner, *Ann. N. Y. Acad. Sci.* **2006**, *1066*, 119-135.

[13] A. Ali, M. K. Auvinen, J. Rautonen, Transfusion, **2010**, 50, 584–588.

[14] J. F. Carpenter, T. N. Hansen, *Proc. Natl. Acad. Sci. U. S. A.* **1992**, *89*, 8953-8957.

[15] L. O'Neil, S. J. Paynter, B. J. Fuller, R. W. Shaw, A. L. DeVries, *Cryobiology* **1998**, *37*, 59-66.

[16] T. Wang, Q. Zhu, X. Yang, J. R. Layne Jr, A. L. Devries, *Cryobiology* **1994**, *31*, 185-192.

[17] S. Liu, W. Wang, E. von Moos, J. Jackman, G. Mealing, R. Monette, R. N. Ben, *Biomacromolecules* **2007**, *8*, 1456-1462.

[18] A. Eniade, A. V. Murphy, G. Landreau, R. N. Ben, *Bioconjugate Chem.* **2001**, *12*, 817-823.

[19] A. K. Balcerzak, S. S. Ferreira, J. F. Trant, R. N. Ben, *Bioorg. Med. Chem. Lett.* **2012**, *22*, 1719-1721.

[20] L. Corcilius, G. Santhakumar, R. S. Stone, C. J. Capicciotti, S. Joseph, J. M. Matthews, R. N. Ben, R. J. Payne, *Bioorgan. Med. Chem.* **2013**, *21*, 3569-3581.

[21] C. J. Capicciotti, M. Leclère, F. A. Perras, D. L. Bryce, H. Paulin, J. Harden, Y. Liu, R. N. Ben, *Chem. Sci.* **2012**, *3*, 1408-1416.

[22] M. I. Gibson, C. A. Barker, S. G. Spain, L. Albertin, N. R. Cameron, *Biomacromolecules* **2009**, *10*, 328-333.

[23] T. Congdon, R. Notman, M. I. Gibson, *Biomacromolecules* **2013**, *14*, 1578-1586.

[24] T. Inada, P. R. Modak, *Chem. Eng. Sci.* **2006**, *61*, 3149-3158.

[25] R. C. Deller, M. Vatish, D. A. Mitchell, M. I. Gibson, *Nat. Commun.* **2014**, *5*, 3244-3251.

[26] K. Matsumura, S.-H. Hyon, *Biomaterials* **2009**, *30*, 4842-4849.

[27] D. E. Mitchell, M. Lilliman, S. G. Spain, M. I. Gibson, *Biomater. Sci.* **2014**, *2*, 1787–1795.

[28] M. A. Gauthier, M. I. Gibson, H.-A. Klok, *Angew. Chem. Int. Ed.* **2009**, *48*, 48-58.

Chapter 7

7. A Simple Polymeric Solution to the Challenge of Therapeutic Protein Storage

D. E. Mitchell, R. C. Deller, J. Gutierrez-Marcos and M. I. Gibson, in preparation

This chapter contains a paper on the use of polymers poly(ethylene glycol) and poly(vinyl alcohol) as protectants in the cryo-storage of proteins, including antibodies. DEM undertook freeze-thaw assays of all proteins described below and was responsible for dynamic light scattering and circular dichroism analysis. RCD was involved in initial compound screening using β-galactosidase and JGM assisted in Taq polymerase assay. DEM and MIG wrote the manuscript.

7.1. Abstract

Proteins have many applications as therapeutics or as tools within research, including the rapidly expanding field of antibodies as drug treatments. However the limited stability presents a major issue. Current solutions to this problem involve the addition of large volumes of additives many of which have been found to have an adverse effect on protein activity and potential toxicological concerns for *in vivo* applications. Thus the use of therapeutic proteins has yet to reach its potential due to the limiting

factor of long term storage. Here, a mixture of poly(vinyl alcohol) (PVA) and poly(ethylene glycol) (PEG) has been shown to protect the proteins β- galactosidase (β-Gal), glucose oxidase (GO) and Taq polymerase (Taq) when frozen at -20 °C and -80 °C over a period of several days, by inhibiting ice recrystallization. Furthermore the antibody rabbit IgG was also successfully persevered, showing that this polymer mixture has enormous potential for the long term storage of protein therapeutics. Since both polymers are relatively cheap and non-toxic it is anticipated that they could have applications in both medicine and research.

7.2. Introduction

The use of proteins both as laboratory reagents and as medicines in a clinical setting has become widespread since the adoption of insulin as the first protein therapeutic over 30 years ago.[1] This includes the use of antibodies as therapeutics for the treatment of cancer,[2] Alzheimer's disease,[3] inflammatory diseases[4] and many others, with antibody based drugs currently the fastest growing class of protein therapeutics.[1] The limited storage lifetime presents a major challenge however, with many potentially useful proteins degrading in very short timespans.[5] Adverse conditions such as hot and cold temperatures,[6] sunlight,[7] and dehydration[8] have all previously been found to degrade proteins. Current methods rely on lyophilisation or freezing in solutions containing large concentrations of various additives, including sugars,[9] salts,[10] and osmolytes.[11] Lyophilisation exposes the protein to low temperatures and pressures, dehydration and changes in pH, while freezing in solution requires additives which are often been found to have an adverse effect on protein activity. Sugars such as sucrose and dextran are added in both frozen and lyophilized formulations in order to stabilise the protein and prevent aggregation,[12] while

osmolytes stabilize proteins due to their favourable hydration effects.[13] Currently trehalose, the sugar and osmolyte, is widely used in a range of protein storage formulations.[14] In addition, several polymeric cryoprotectants have been investigated including poly(ethylene glycol) (PEG).[15] Recently Maynard and co-workers, have shown that trehalose glycopolymers can enhance the recovery by up to 50 % over trehalose alone of β-Galactosidase (β-Gal) when lyophilzed,[16] thus demonstrating the potential of polymeric materials. This approach however, requires the synthesis of a protein- polymer conjugate, which has less activity than the natural protein and would require extensive testing to gain FDA approval.

Although Lyophilzation can be effective, limited access to expensive freeze-drying machinery and the difficulty in freeze drying very small amounts of protein, make reliable storage in a standard, widely accessible -20 °C freezer highly appealing. A major hurdle to be overcome in the storage at this temperature is that of ice recrystallization: the growth of ice crystals which can damage and denature biological materials.[17] In nature, many organisms have evolved to thrive at freezing temperatures, due to their ability to express a unique type of protein called an antifreeze (glycol) protein (AF(G)P) which inhibits ice recrystallization.[18] The ice recrystallization inhibition (IRI) property exhibited by these proteins is of immense interest in the field of cryopreservation. However, mixed success has been reported when AF(G)Ps have been added to cryopreservation solutions,[19-20] and to the best of our knowledge there has been no successful storage of proteins using AF(G)Ps, presumably due to the difficulty in separating the proteins post thaw and potential immunogenic effects for *in-vivo* uses. For this reason synthetic mimetics are highly appealing; and therefore Gibson and co-workers and Inada *et al.* have separately

investigated polymers for IRI activity in particularly the use of poly(vinyl alcohol) (PVA) which has strong activity.[21-22] Furthermore, work by Mitchell *et al.* has shown that polyampholyte polymers also possess this ability.[23] Recent studies have also demonstrated the potential of these polymers in the cryopreservation of various cell types,[24-26] however there has been very limited investigation into whether successful storage of proteins is also possible. This manuscript describes the use of IRI active polymers to produce a highly effective cryopreservation solution, and compares this to other widely used cryoprotectants, using a very simple freezing protocol.

7.3. Results and Discussion

β–galactosidase (β-Gal) has previously been found to be a useful enzyme when exploring cryopreservation.[27] Various polymer and / or small molecule solutions were tested to investigate whether they display cryoprotective activity. Samples were frozen at -20 °C and thawed on the bench top, giving a relatively slow freezing and thawing rate, Figure 7.1. This mimics the conditions used in a laboratory or clinical setting, while also is highly suboptimal for maximum recovery, thus providing a robust test of the protective activity shown by the potential cryoprotectants.[28] β-Gal activity was determined using a colourmetric assay based on the hydrolysis of *ortho*-Nitrophenyl-β-galactoside and subsequent colour change.

It appears that only the PEG/ PVA mix and trehalose has a postive effect on the amount of recovery. PVA is well known to inhibit ice recrystallization preventing the growth of harmful ice crystals. Therefore the discovery that PVA alone doesn't have any protective activity suggests that damage by ice crystal growth is not the only factor when considering the reason why freezing and thawing damages β-Gal. It is

also apparent that compounds such as PVP and HES which are commonly added to cryoprotective solutions also result in poor recovery. Both PEG and trehalose are known to stabilize proteins under lyophilization suggesting that this stabilization effect is required in addition to IRI activity.[29-31] Trehalose is also known to aid the formation of a vitrified state,[14] which would mean there would be a lack of damaging ice crystals present. Furthermore, trehalose and PEG can replace water in the hydration shell of a protein reducing damage.[14-15]

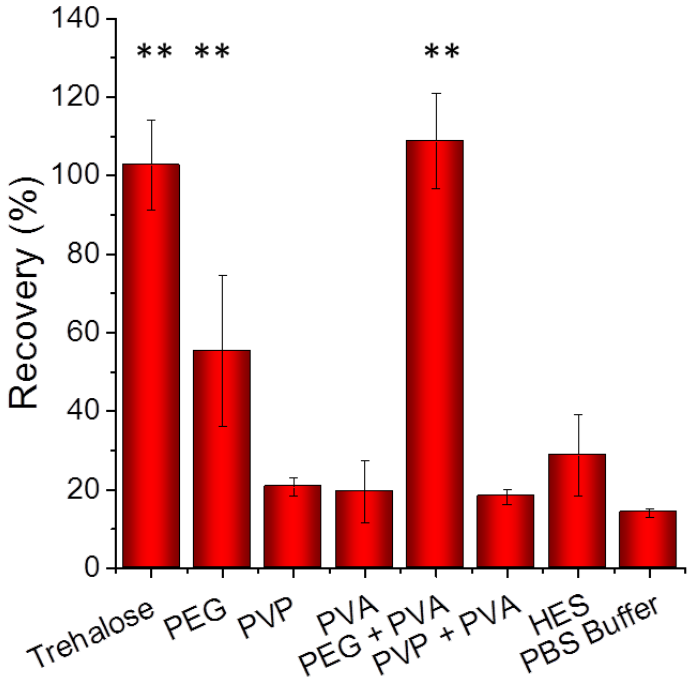

Figure 7.1. **Recovered activity of β-galactosidase after freezing for 3 days at -20 °C and thawing.** Results are expressed as a percentage of fresh, unfrozen protein. Error bars are from a minimum of six repeats, and ** represents $p < 0.01$ relative to PBS buffer control. PEG, PVP, Trehalose and HES at concentration of 100 $mg.mL^{-1}$, PVA at 1 $mg.mL^{-1}$.

The concentrations of PVA, PEG and trehalose were also varied to find optimal and lowest effective concentrations (ESI, Appendix 6). It was found that PEG concentration could be decreased to 40 $mg.mL^{-1}$, with PVA concentration remaining constant. In comparison, trehalose concentration could only be decreased to 75 $mg.mL^{-1}$. Thus when a lower concentration of additive is desirable PEG and PVA would be preferable to trehalose. PVA can still provide significant protection at 0.5 $mg.mL^{-1}$ corresponding well to previous investigation into concentration dependant IRI activity.[32]

Although having an IRI active compound is not sufficient for recovery, it may be the case that it is necessary in non-vitrifying solutions, as seen by the large increase in recovery when PVA is added to PEG in Figure 7.1. To this end another IRI active polymer, poly(aminoethyl methacrylate)-*co*-succinic anhydride (PAEMA-*co*-SA),[23] was tested in a similar manner both with and without PEG, Figure 7.2. It appears that the addition of PAEMA-*co*-SA also results in a dramatic increase in recovery, thus suggesting that IRI activity is the critical factor in protein preservation. Ice recrystallization leads to bigger ice crystals, resulting in reduced total surface area, and consequently the average distance between proteins is significantly reduced. This reduced inter-protein distance means that individual protein molecules are more likely to aggregate together reducing activity. An IRI molecule maintains small crystals and a large surface area reducing the probability of this happening, in addition to preventing the damaging effects of individual ice crystals. Interestingly the activity drops slightly when PVA and PAEMA-*co*-SA are added together to PEG. It is hypothesised that this is due to dynamic ice shaping (DIS) leading to needle like, spicular crystals, a property exhibited by IRI molecules at higher concentrations due

to preferential binding to certain faces of the ice crystal, which has been found to be problematic in cellular cryopreservation studies.[24, 33-34]

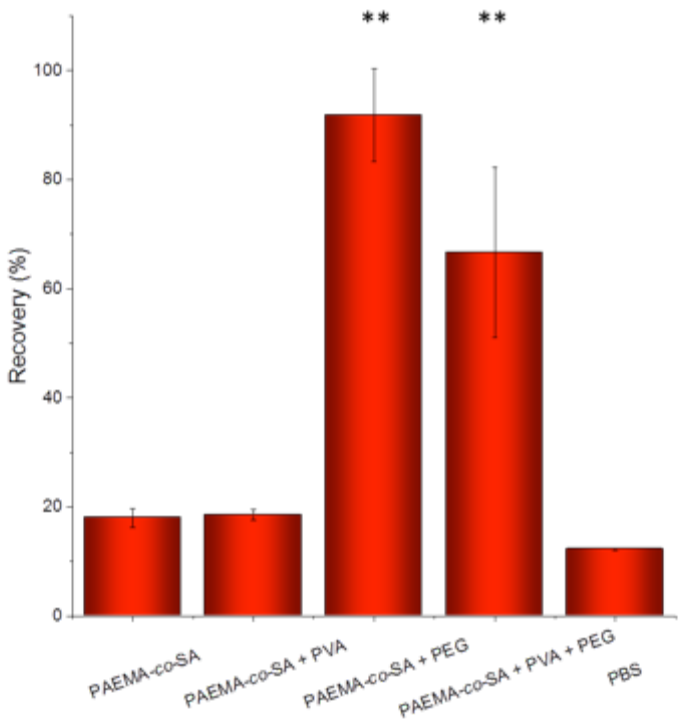

Figure 7.2. Recovery of β-galactosidase with PAEMA-c*o*-SA (20 mg.mL^{-1}) samples frozen for 3 days at -20 °C. Recovery is expressed as a percentage of fresh, unfrozen protein, error bars are from a minimum of six repeats, and ** represents $p < 0.01$ relative to PBS buffer control. PEG concentration 100 mg.mL^{-1}, PVA concentration 1mg.mL^{-1}.

To explore whether the secondary structure of the β-Gal is being damaged via freezing and thawing circular dichroism (CD) was undertaken, Figure 7.3. A general reduction in the spectrum intensity is observed, in addition to a change in spectrum shape. This corresponds to the recovery levels obtained in Figure 7.1, suggesting that

the secondary structure of the protein is being damaged and/or protein aggregation is occurring leading to the observed loss of activity. In addition dynamic light scattering (DLS) showed some level of aggregation occurs when frozen and thawed, with those samples that contain PVA demonstrating less aggregation than those without, although performing DLS of protein-polymer mixes is a significant challenge so it is difficult to draw conclusions from this (ESI, Appendix 6).

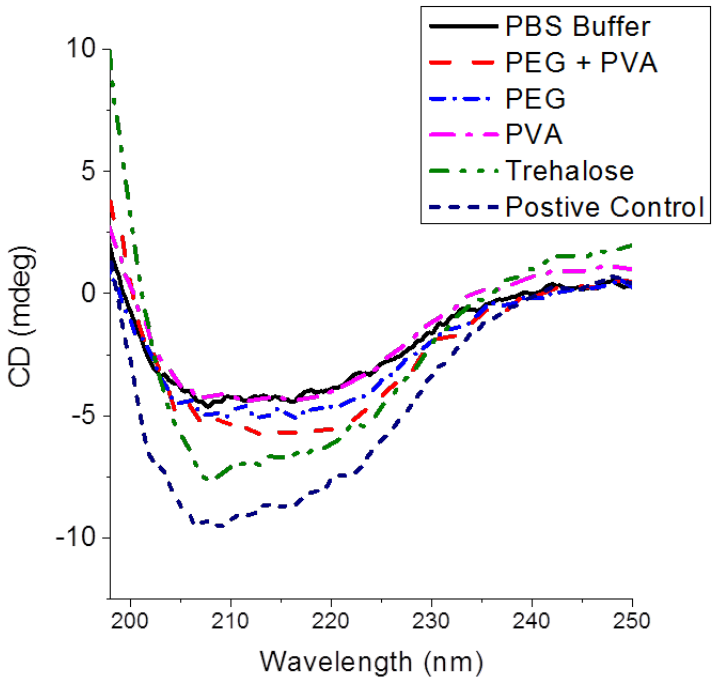

Figure 7.3. **Circular dichroism spectra of freeze thaw samples of β- galactosidase at concentration 150 µg.mL^{-1}.**

In most molecular biology laboratories a -80 °C freezer is used. Therefore the experiment was repeated at this lower temperature. The lower storage temperature reduces ice crystal growth and ensures a single solid phase, thus suggesting that the conditions should be more favourable to storage, but cold induced denaturation could be problematic. PEG and PVA mixture and trehalose by itself were stored at -80 °C

for three days in order to assess the effect of storage at this lower temperature, Figure 7.4. Similar to those samples stored at -20 °C, PEG and PVA together provide a very potent method of protein storage. Again, it seems that they act synergistically and separately there is little protective effect. This suggests that although there would be less ice recrystallization at this lower temperature, it is still an important consideration, possibly due to the slow thawing process.

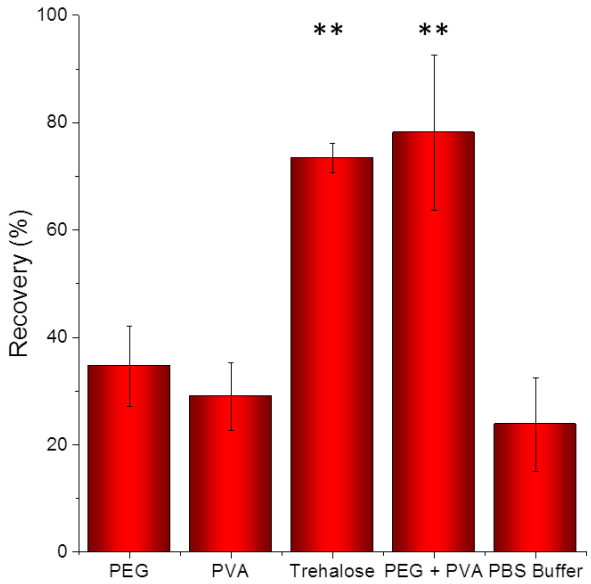

Figure 7.4- Freeze thaw spectra of β-galactosidase frozen at -80 °C for 3 days. Recovery is expressed as a percentage of fresh, unfrozen protein, error bars are from a minimum of six repeats, ** signifies $p < 0.01$ relative to PBS buffer control. (PEG, Trehalose at 100 $mg.mL^{-1}$, PVA at 1 $mg.mL^{-1}$ concentrations.)

For many therapeutic applications longer term storage would be highly appealing, therefore samples were frozen for a period of 1, 2 and 4 weeks, Figure 7.5. The longer term storage will allow time for increased ice recrystallization and any cold induced injury to occur. At -20 °C the level of protection given by the PVA and PEG

combination diminishes as the time period increases, while trehalose still gives recovery levels of near 100 %, Figure 7.5a. In contrast, at -80 °C PVA and PEG still provide a good level of protection, Figure 7.5b. This suggests that storage at -80 °C would be optimal and achievable since the majority of laboratories dealing with biological material are equipped with a -80 °C freezer. It is thought that, this is due to reduction in ice recrystallization at this lower temperature. Even at -20 °C the lifespan of the protein can be extended by over a week making it relevant for many therapeutic uses.

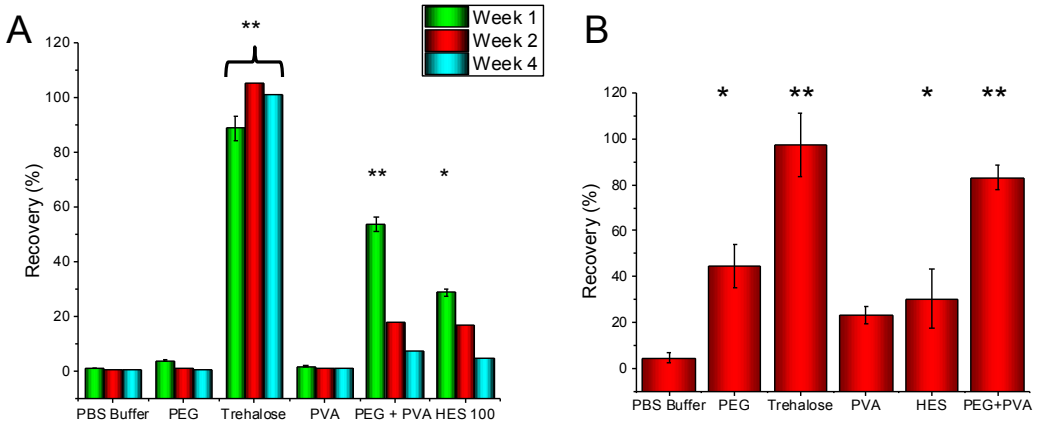

Figure 7.5. **Long term study of the freezing and thawing of β-galactosidase.** (A) Freezing at -20 °C (B) Freezing at -80 °C for 4 weeks. Recovery is expressed as a percentage of fresh, unfrozen protein, error bars are from a minimum of six repeats. ** Signifies $p < 0.01$, * signifies $p < 0.05$ relative to PBS buffer control. PEG, Trehalose, HES were used at 100 $mg.mL^{-1}$ PVA at 1 $mg.mL^{-1}$.

As some widely used cryoproctants such as glycerol have been found to have a detrimental effect on the activity of proteins,[35] it is important to ascertain whether the protective solutions described here are having a negative effect on protein activity prior to freezing. If there is a negative effect then the level of recovery could never

reach 100 % and the storage mixtures would have limited use. Samples were tested prior to freezing against a positive control of PBS buffer only, which has no negative effect on the protein.[27] For comparison purposes 10 and 20 wt% glycerol solutions were also tested, Figure 7.6. The solutions described here were found to display no negative effect on the assay, in contrast to glycerol, which reduces the activity quite dramatically. This demonstrates that the PEG and PVA mix would likely be more beneficially in formulations where glycerol is currently used. Trehalose also gave a small decrease in activity, highlighting the benefit of polymers.

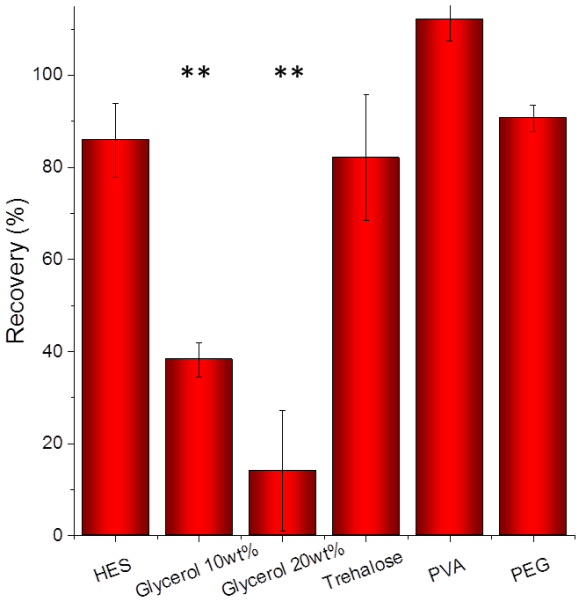

Figure 7.6. **Recovery of unfrozen control β-galactosidase samples in the presence of various additives.** Recovery is expressed as a percentage of fresh, unfrozen protein, error bars are from a minimum of six repeats. HES, treholse, PEG at 100mg.mL^{-1} and PVA 1mg.mL^{-1}. ** Represents $p < 0.01$ with respect to positive PBS buffer control. Value over 100 % is due to the relative absorbance between positive control and PVA sample.

In addition to the protection given to β-Gal when frozen and thawed, other proteins were examined to determine whether this a generally applicable method. Taq polymerase (Taq) is an extremely important protein due to its high thermal stability and ability to amplify sequences of DNA. It allows polymerase chain reaction (PCR) to be applied to a range of DNA based molecular biology and without it DNA analysis would be extremely difficult. Unfortunately, the freezing of Taq results in almost total loss of activity, unless large amounts of glycerol is added, making it an interesting target for the previously discussed polymer solutions. To this end samples of Taq were stored at -20 °C for 3 days as for β-Gal, thawed and tested using quantitative PCR (QPCR). QPCR was used to detect differences between samples, as it provides numerical data on the efficiency of the Taq, Figure 7.7. Briefly, QPCR involves the use of a DNA binding fluorescent dye, which provides a fluorescent reading of how many DNA helices have been polymerised by the Taq. The more efficient the Taq, the more DNA strands, and the greater the level of fluorescence. As glycerol is normally added as a cryoprotectant in commercially available Taq a sample with this present was also tested for comparison. The number of cycles taken to reach a threshold fluorescence was used as an indication of how good the recovery was, i.e. the lower the number of cycles the more efficient the Taq. The Taq sample in buffer alone gave no measurable activity.

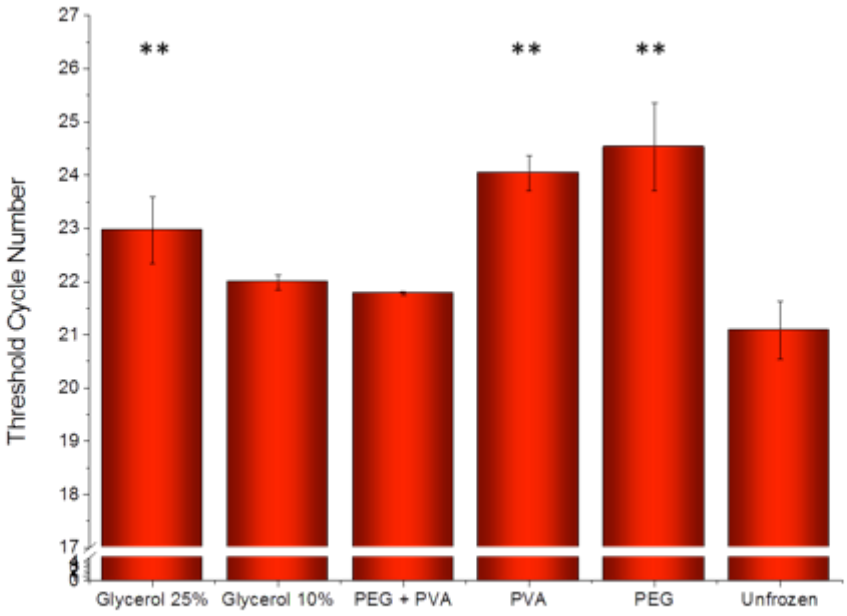

Figure 7.7. **QPCR cycle threshold data for various samples frozen at -20 °C for 5 days.** Error bars were found from a minimum of three repeats, ** represents $p < 0.01$ relative to unfrozen control. Glycerol w/w%, PEG at 100 $mg.mL^{-1}$ and PVA 1 $mg.mL^{-1}$. Initial DNA concentration was 20 $ng.mL^{-1}$.

The PEG/PVA mix seems to be the best cryoprotectant, while increasing the glycerol concentration appears to have a slightly detrimental effect. This correlates well with the results discussed above for β-Gal and suggests that PEG and PVA mixed together provide a viable way of the cryostorage of a range of proteins.

To further probe the cryoprotectivity of PEG and PVA, glucose oxidase (GO) was tested in the same manner. Similar polymer samples were produced and placed in a -20 °C freezer for 7 days. They were then thawed and tested with unfrozen samples acting as positive controls. As observed for Taq and β-Gal the addition of polymers

provides an increase level of protection (ESI, Appendix 6). In PBS buffer only, activity drops dramatically showing that the damage caused by freezing and thawing is common amongst proteins and PEG and PVA mixed together provides a viable method of cryostorage.

Antibodies have attracted widespread interest due to their ability to treat a wide range of medical issues, such as many cancers and the Ebola virus.[36-37], and are forcast to have a market value of over $2.5 Billion by 2019.[38] However, therapeutic antibodies are limited by storage lifetime. Rabbit IgG was stored at -20 °C for 4 days using the PEG and PVA mixture described above to determine whether this mixture would be a viable solution to this problem, Figure 7.8.

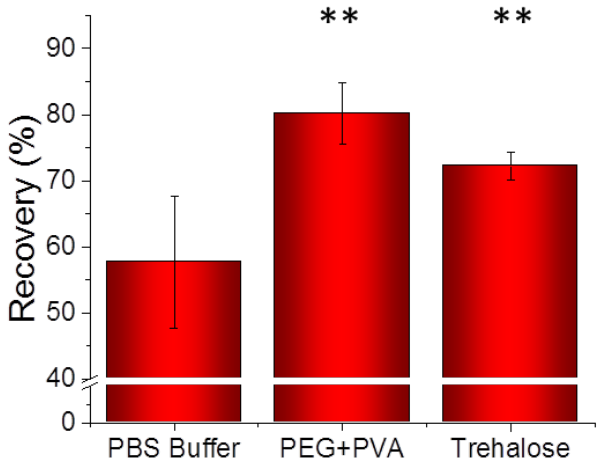

Figure 7.8. Recovered activity of rabbit IgG when stored at -20 °C for 4 days. ** represents $p < 0.01$, error bars are from a minimum of 6 repeats. PEG and trehalose were used at a concentration of 100 $mg.mL^{-1}$ while PVA was used at 1 $mg.mL^{-1}$

Recovery in the PEG/ PVA mix is significantly enhanced when compared to PBS buffer alone and also provided a slight enhancement over trehalose. This demonstrates that this mixture is a viable method of storing antibodies, potentially helping to address the stability issues in the use of antibody therapeutics which currently hold back this emerging and highly promising field.

7.4. Conclusions

Overall, the polymer combination of PVA/ PEG has been found to be an effective combination in the cryoprotection of proteins, as found for β-Gal, Taq and GO. It is hypothesised that PVA is required to inhibit ice recrystallization (IR) and this is reinforced by the data shown here for a mixture of PAEMA-*co*-SA and PEG. PEG is known to stabilize proteins, so this may be required to increase stability in proteins which undergo cold deformation. Over longer periods of time trehalose appears to perform better than the PEG/ PVA mix, possibly due to vitrification, although molar concentrations are significantly higher which may be a worry for applications where higher concentrations are an issue. Furthermore PEG and PVA have been found to be more beneficial than glycerol, which is currently widely used.

The successful freezing storage of an antibody demonstrates that this particular mix would be of benefit in the storage of antibody therapeutics a problem that is currently limiting their widespread use in a clinical setting. Therefore, it is anticipated that the polymer solutions described here can help provide a method of the storage of proteins and antibodies, and expand the range of currently available therapeutics and laboratory reagents.

7.5. Experimental Section

7.5.1. Materials

β-galactosidase (β-Gal), glucose- oxidase (GO), o- dianosidine, glucose, horse radish peroxidase (HRP), o-nitrophenyl-β-D-galactoside (ONPG), ethanol, poly(ethylene glycol) (PEG, 2.5 kDa), poly(vinyl pyrolidone) (PVP, 5 kDa), succinic anhydride, aminethyl methacrylate rabbit IgG and trehalose were purchased from Sigma Aldrich. EvaGreen dye was purchased from VWR chemicals while M13 primers, dNTPs PCR buffer (including $MgCl_2$) were purchased from Invitrogen. Rabbit IgG assay kit and Taq polymerase was purchased from Life technologies. CDNA was provided by the lab of Jose Gutierez-Marcos (University of Warwick Life Sciences department) Phosphate-buffered saline (PBS) solution was prepared using preformulated tablets (Sigma-Aldrich) in 200 mL of Milli-Q water (>18.2 Ω mean resistivity) to give [NaCl] = 0.138 M, [KCl] = 0.0027 M, and pH 7.4. Taq polymerase was dialysed against glycerol free taq buffer prior to use using Amicon 0.5ml centrifugal filters (Merck, Irl) [Tris-HCL] = 10 mM, [KCl] = 100 mM, [DTT] = 1mM, [EDTA] = 0.1 mM, 0.5 wt% Tween 20, 0.5 wt% Triton X. Poly(vinyl alchol) (PVA, 5.1 kDa) and poly(aminoethyl methacrylate) (PAEMA, 32 kDa) functionalised with approximately 50 % COOH groups (PAEMA-co-SA) were synthesized as detailed previously.[23, 32] All reagents were used as received unless otherwise stated.

7.5.2. Physical and analytical methods

Absorbance spectroscopy was undertaken using a Synergy HT multi-mode microplate reader (BioTek UK, Bedfordshire, UK). Quantitative polymerase chain reaction (QPCR) was carried out on a real-time PCR detection system while a thermocycler

was used for standard PCR reactions. PCR was undertaken using the following protocol, initiation at 94 °C for 1 minute, denaturation at 94 °C for 20 seconds, annealing at 56 °C for 20 seconds and elongation at 72 °C for 30 seconds. Twenty-five cycles were used and followed by a final elongation at 72 °C for 5 minutes.

Circular Dichroism (CD) spectra were recorded on a spectropolarimeter (Jasco J-720, Jasco UK) using a data interval of 0.2 nm. The spectrum was measured 16 times and averaged. The spectrum of a blank sample containing only buffer or the appropriate cryoprotectant was then subtracted giving a final spectrum for each protein. Dynamic light scattering was undertaken on a Malvern Zetasizer Nano ZS, and size was measured using intensity particle size distribution.

7.5.3. β-galactosidase assay

β-Gal activity was determined by a colorimetric assay involving the use of ONPG. Briefly aliquots of 30 μL of 4 $mg.mL^{-1}$ ONPG were added to wells of a 96 well plate containing 50 μL of 20 $\mu g.mL^{-1}$ β-Gal solution. This was then incubated at room temperature for 5 minutes and quenched by addition of 50 μL of 1M Na_2CO_3 solution. Absorbance was measured at 420 nm.

7.5.4. Glucose oxidase assay

Activity of GO was determined using the oxidation of o-dianosidine through a peroxidase-coupled reaction[39]. Briefly 2.5 mg of o-dianosidine was dissolved in 2 mL of ethanol, which was further diluted by the addition of 8 mL of PBS buffer resulting in a 10 mL stock solution. A Horseradish peroxidase (HRP) stock solution of 100 $\mu g.mL^{-1}$ was prepared by dissolving HRP into a solution of 18 % w/w glucose

in distilled water, while GO samples were prepared at a concentration of 2 $\mu g.mL^{-1}$. 30 µL of GO sample was added to 30 µL of HRP solution into separate wells of a 96 well plate, then 150 µL of o-dianosidine was added and the mixture was incubated for 3 minutes. Finally absorbance was measured at 450 nm.

7.5.5. Quantitative polymerase chain reaction assay

Cryoprotectants at required concentrations were added to Taq in the appropriate buffer solution in 20 µL volumes. QPCR was undertaken using standard protocols. EvaGreen dye was used as the DNA-binding fluorescent dye, sample volumes were 20 µL. Briefly, samples of 2.5 µL PCR buffer, 1 µL dNTPs, 1.5 µL Eva Green fluorescent dye, 1 µL forward and reverse primers, 1 µL of Taq at 1.25 $U.\mu L^{-1}$ and 12 µL PCR water, were prepared. Samples were tested in triplicate with three dilutions of template DNA at 20, 10 and 5 ng, with appropriate positive and negative controls.

7.5.6. Rabbit IgG assay

Activity of rabbit IgG was determined using an "Easy-Titer rabbit IgG assay kit" (Life technologies). 125 µL Solutions of 125 $\mu g.mL^{-1}$ of IgG were prepared and frozen for 4 days. Upon thawing, 20 µL of IgG sensitized beads were pipetted into wells of a 96 well plate and 20 µL of IgG solution was added. The plate was then incubated under shaking for 5 minutes at room temperature after which 100 µL of blocking buffer was added and the plate was incubated for a further 5 minutes. Absorbance was measured at 405 nm using a plate reader, and samples were compared to a freshly made up positive control.

7.5.7. Freeze-thaw methodology

Samples were made in triplicate at the appropriate concentrations and frozen by placing in a freezer either at -20 °C or -80 °C. The samples were then held at this temperature within the freezer for the appropriate amount of time and then thawed on the bench top.

7.6. References

[1] B. Leader, Q. J. Baca, D. E. Golan, *Nat. Rev. Drug Discov.* **2008**, *7*, 21-39.

[2] A. M. Scott, J. D. Wolchok, L. J. Old, *Nat. Rev. Cancer* **2012**, *12*, 278-287.

[3] R. B. DeMattos, K. R. Bales, D. J. Cummins, J.-C. Dodart, S. M. Paul, D. M. Holtzman, *Proc. Nat. Acad. Sci. U. S. A.* **2001**, *98*, 8850-8855.

[4] S. Kotsovilis, E. Andreakos, *Methods mol. biol.* **2014**, *1060*, 37-59.

[5] J. Vlasak, R. Ionescu, *mAbs* **2011**, *3*, 253-263.

[6] R. Hough, M. Rechsteiner, *Proc. Nat. Acad. Sci. U. S. A.* **1984**, *81*, 90-94.

[7] B. M. Greenberg, V. Gaba, O. Canaani, S. Malkin, A. K. Mattoo, M. Edelman, *Proc. Nat. Acad. Sci. U. S. A.* **1989**, *86*, 6617-6620.

[8] S. D. Allison, T. W. Randolph, M. C. Manning, K. Middleton, A. Davis, J. F. Carpenter, *Arch. Bioch. Biophys.* **1998**, *358*, 171-181.

[9] L. Chang, D. Shepherd, J. Sun, D. Ouellette, K. L. Grant, X. C. Tang, M. J. Pikal, *J. Pharm. Sci.* **2005**, *94*, 1427-1444.

[10] S. D. Arntfield, E. D. Murray, M. A. H. Ismond, *J. Food Sci.* **1986**, *51*, 371-377.

[11] J. K. Kaushik, R. Bhat, *J. Biol. Chem.* **2003**, *278*, 26458-26465.

[12] Y. Han, B. S. Jin, S. B. Lee, Y. Sohn, J. W. Joung, J. H. Lee, *Arch. Pharm. Res.* **2007**, *30*, 1124-1131.

[13] P. H. Yancey, *Amer. Zool.* **2001**, *41*, 699-709.

[14] N. K. Jain, I. Roy, *Protein Sci.* **2009**, *18*, 24-36.

[15] S. Rawat, C. Raman Suri, D. K. Sahoo, *Biochem. Biophys. Res. Commun.* **2010**, *392*, 561-566.

[16] J. Lee, E.-W. Lin, U. Y. Lau, J. L. Hedrick, E. Bat, H. D. Maynard, *Biomacromolecules* **2013**, *14*, 2561-2569.

[17] J. F. Carpenter, T. N. Hansen, *Proc. Natl. Acad. Sci. U. S. A.* **1992**, *89*, 8953-8957.

[18] S. Venketesh, C. Dayananda, *Crit. Rev. Biotechnol.* **2008**, *28*, 57-82.

[19] J. Beirao, L. Zilli, S. Vilella, E. Cabrita, R. Schiavone, M. P. Herraez, *Biol. Reprod.* **2012**, *86*, 59.

[20] H. Chao, Davies, P.L., Carpenter, J.F., *J. Ex. Biol* **1996**, *199*, 2071-2076.

[21] M. I. Gibson, C. A. Barker, S. G. Spain, L. Albertin, N. R. Cameron, *Biomacromolecules* **2009**, *10*, 328-333.

[22] T. Inada, P. R. Modak, *Chem. Eng. Sci.* **2006**, *61*, 3149-3158.

[23] D. E. Mitchell, M. Lilliman, S. G. Spain, M. I. Gibson, *Biomater. Sci.* **2014**, *2*, 1787–1795.

[24] R. C. Deller, M. Vatish, D. A. Mitchell, M. I. Gibson, *Nat. Commun.* **2014**, *5*, 3244-3251.

[25] K. Matsumura, S.-H. Hyon, *Biomaterials* **2009**, *30*, 4842-4849.

[26] D. E. Mitchell, N. R. Cameron, M. I. Gibson, *Chem. Commun.* **2015**.

[27] K. A. Pikal-Cleland, N. Rodríguez-Hornedo, G. L. Amidon, J. F. Carpenter, *Arch. Biochem. Biophys.* **2000**, *384*, 398-406.

[28] E. Cao, Y. Chen, Z. Cui, P. R. Foster, *Biotechnol. Bioeng.* **2003**, *82*, 684-690.

[29] N. K. Jain, I. Roy, *Curr. Protoc. Protein Sci.* **2010**, *Chapter 4*, Unit 49.

[30] S.-H. Chao, S. S. Matthews, R. Paxman, A. Aksimentiev, M. Gruebele, J. L. Price, *J. Phys. Chem. B* **2014**, *118*, 8388-8395.

[31] L. L. Y. Lee, J. C. Lee, *Biochemistry* **1987**, *26*, 7813-7819.

[32] T. Congdon, R. Notman, M. I. Gibson, *Biomacromolecules* **2013**, *14*, 1578-1586.

[33] J. F. Carpenter, J. H. Crowe, *Cryobiology* **1988**, *25*, 244-255.

[34] M. E. Houston Jr, H. Chao, R. S. Hodges, B. D. Sykes, C. M. Kay, F. D. Sönnichsen, M. C. Loewen, P. L. Davies, *J. Bio. Chem.* **1998**, *273*, 11714-11718.

[35] W. J. Armitage, *Cryobiology* **1986**, *23*, 116-125.

[36] J. L. Rubenstein, J. Kim, T. Ozawa, M. Zhang, M. Westphal, D. F. Deen, M. A. Shuman, *Neoplasia* **2000**, *2*, 306-314.

[37] T. Maruyama, L. L. Rodriguez, P. B. Jahrling, A. Sanchez, A. S. Khan, S. T. Nichol, C. J. Peters, P. W. H. I. Parren, D. R. Burton, *J. Virol.* **1999**, *73*, 6024-6030.

[38] Markets and Markets, http://www.marketsandmarkets.com/MarketReports /antibody-production-market-181543091.html, **2015.**

[39] Worthington Biochemical Corperation*, Vol. 2014*, Worthington Biochemical Corperation, http://www.worthington-biochem.com/GOP/default.html, **2014**.

Chapter 8

8. Conclusions

Since their discovery antifreeze proteins (AFPs) and antifreeze glycoproteins (AFGPs) have been of great interest due to their unique properties, particularly ice recrystallization inhibition (IRI). Molecules possessing this property have potential benefits in many areas, including cellular cryopreservation, therapeutic protein storage, frozen food and ice resistant surfaces. However these are severely limited by lack of understanding of their method of action, relatively low availability and potential immunogenic issues.

The identification of new structures that posses IRI activity is crucial to understanding and overcoming these challenges. To this end, proteins which show some sequential or structural homology to AFPs were investigated for this effect. L-type lectins, which show some evolutionary similarity to type 2 AFPs, were shown to be surprisingly potent, calcium-dependant ice recrystallization inhibitors. Their activity was found to be modulated by the addition of calcium providing the first-reported case of 'switchable' activity. Furthermore the addition of a sugar competing with ice for the binding site was actually beneficial, slightly increasing IRI activity, suggesting that IRI activity is more complicated than just the possession of an 'ice recognition domain'. This activity was shown in three different l-type lectins suggesting that it is a universal property.

As many antifreeze proteins are known to be amphipathic a second class of peptides where also investigated; antimicrobial peptides. Nisin A, an antimicrobial was also found to have surprisingly potent activity at acidic pH, which corresponds with protonation of its two histidine residues. Furthermore, to enable antifreeze activity at physiological pH, nickel and zinc ions, which can bind histidine residues causing the same conformational change, were added. This also switched on IRI activity in a similar manner to the addition of Ca^{2+} to l-type lectins, further demonstrating the switchability of these proteins.

The use of antifreeze proteins or other IRI active proteins is limited by the difficulty obtaining large quantities and potential immunogenic effects. Conversely, the development of synthetic polymers that mimic biological activity is highly appealing due to their scalability, tunable structures and huge monomer scope. Despite this, very few synthetic molecules have been identified which display IRI activity. It has been shown here that poly(ampholytes) inhibit ice recrystallization and that approximately a 1:1 ratio between positively and negatively charged side chains is optimum. This structure is the first reported that does not have a poly(hydroxylated) structure, and opens the possibility of a new class of IRI active molecules, while questioning the hypothesis that molecules must have a precise, hydroxyl based ice recognition face in order to possess IRI activity.

While the identification of IRI molecules above has been relatively successful, it is currently limited by low throughput assays associated with this property. The application of gold nanoparticles (AuNPs) has been investigated as a potential high throughput method. As ice recrystallization leads to the growth of larger ice crystals

and hence reduced surface area, the AuNPs are forced closer together, and a colour change from pink to blue is observed. By using UV-Vis spectroscopy (or by eye), this colour change was found to be well correlated with IRI activity. As this can be performed in a 96 well plate, identification can be sped up dramatically. Using this method, serum proteins were also identified for the first time as having some IRI activity at higher concentrations.

In addition to polymeric AFP mimics, this thesis has shown that metallohelical structures constructed from iron coordination complexes to resemble alpha helical structures, which in terms of diameter and charge, are similar to a type 1 AFPs. Thus providing a range of compounds which could be investigated for IRI activity. It was found that amphipathic metallohelices do possess IRI activity, although unfortunately, they could not be screened using the above gold nanoparticle assay due to the strong purple colour of solution when dissolved. These also have the benefit of having a defined molecular weight unlike polymers, which have some dispersity, allowing more precise structural-activity investigation to be achieved. Their similarity to a type 1 AFP demonstrates that a structural or biomimetic approach to identifying features required for IRI activity and new IRI molecules is achievable.

After investigating the design, synthesis and identification of IRI active molecules the potential applications in a clinical setting was explored. As a cryprotectant, an IRI active molecule would have enormous benefit, preventing highly damaging ice crystal growth. Building from previous work on poly(ampholytes), the polymer poly(methyl vinyl ether-alt-maleic anhydride) functionalized with ethanolamine to give an alternating positive and negative side chain structure was found to be a potent

cryoprotection agent in the storage of red blood cells (RBCs). This polymer is low cost, highly scalable and non-cytotoxic making it highly interesting for a range of cryopreservation challenges.

Finally, the storage of proteins and antibodies was investigated. The polymers poly(vinyl alcohol) (PVA) and poly(ethylene glycol) (PEG) when mixed to together, were found to be highly efficient in the recovery of several proteins. PVA has previously been found to be IRI active, while PEG provides a stabilizing effect on the protein. The importance of an IRI active molecule was reinforced by the addition of an IRI active poly(ampholyte) to PEG providing the same recovery levels. The PEG and PVA mixture is also shown to be highly efficient in the protection of antibodies. As protein therapeutics and in particular antibodies have enormous potential in a clinical setting, for example the treatment of cancer and Alzheimer's disease, the viable long term storage of these materials is paramount and the solution presented here provides a novel, viable method of achieving this.

In uncovering a range of different IRI active molecules it is possible to rank them in terms of relative activity. The current best remains natural hyperactive AFPs followed, by other AFPs and AFGPS and PVA, all of which are extremely potent, working at concentrations less than 1 $mg.mL^{-1}$. The antimicrobial peptide nisin and l-type lectins are relatively equal in active concentration, while the metalohelicates require higher concentrations but inhibition is greater. Finally the polyampholytes described here are the least affective. It is important to consider possible applications however, and with this in mind the ampholytes are useful as cheap, biocompatible materials, something which may be an issue for protein based IRI active compounds. Furthermore, by using any IRI active compound in cryopreservation, the volume of

other potentially harmful additives can be reduced, meaning that providing they are biocompatible any IRI active compound is of benefit.

Ultimately, it is hoped that the research presented here will lead to the rational design of a range of novel synthetic antifreeze protein mimics, and to a greater understanding of the interactions occurring at the ice water interface. In addition, it is anticipated that the IRI active materials will have tremendous impact on the field of regenerative medicine through enhanced cryopreservation of stem cells, transplantation medicine and the use of proteins as therapeutics.

Appendices

Appendix 1

Appendix 1: Supplementary Information for "Latent Ice Recrystallization Inhibition Activity in Non-Antifreeze Proteins; Ca^{2+} Activated Plant Lectins and Cation-Activated Antimicrobial Peptides".

Sequential comparison of l-type lectins and type 2 antifreeze proteins

The sequence from type 2 AFP (pdb code 2AFP) from Sea raven, *Hemitripterus americanu* was analyzed against the protein databank (PDB) database for similarity. It was found to be a member of the l-type lectins superfamily and various animal l-type lectins were found to display similarity, figure S1.1.

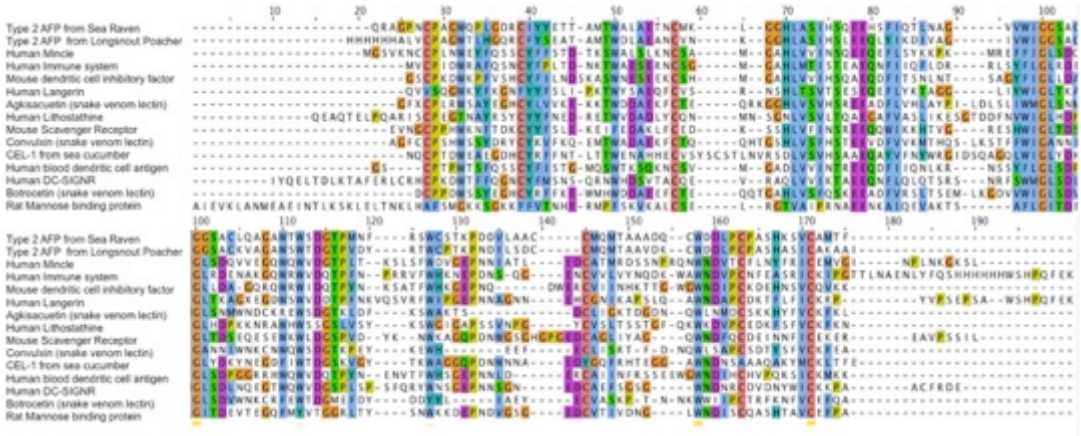

Figure S1.1. Sequence alignment of type 2 AFPs and most closely related lectins. Similar or identical amino acid residues are highlighted. Lectins are ordered downward in terms of level of sequential similarity with type 2 AFP from sea raven shown as the top entry.

Plant lectins are significantly cheaper and easier to obtain in large quantities, and have less potential immunogenic and toxicity issues than human lectins or snake venom, while still displaying the same sugar binding function despite being less sequentially similar. Therefore, it was decided that these would be used instead of mammalian lectins. Comparing lithostathine, a l-type lectin found in figure S1.1 to be highly similar to type 2 AFP with several plant lectins there was some sequential similarity. Figure S1.2 gives a comparison of lithostathine, several plant lectins and type 2 Sea raven AFP.

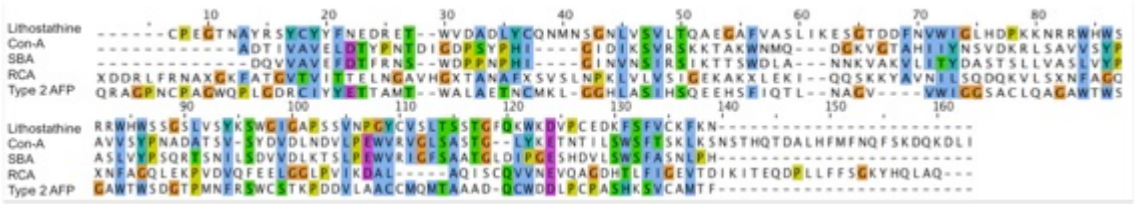

Figure S1.2. Sequence alignment of lithostathine, type 2 AFP and L-type plant lectins.

The pH dependence of ConA on IRI activity

In order to assess the effect pH has on IRI activity, ConA was evaluated in pH 4.7 acetate buffer (with added calcium) and compared to its activity at pH 7.4 (in HEPES buffer). MLGS was recorded as a percentage of the appropriate buffer control.

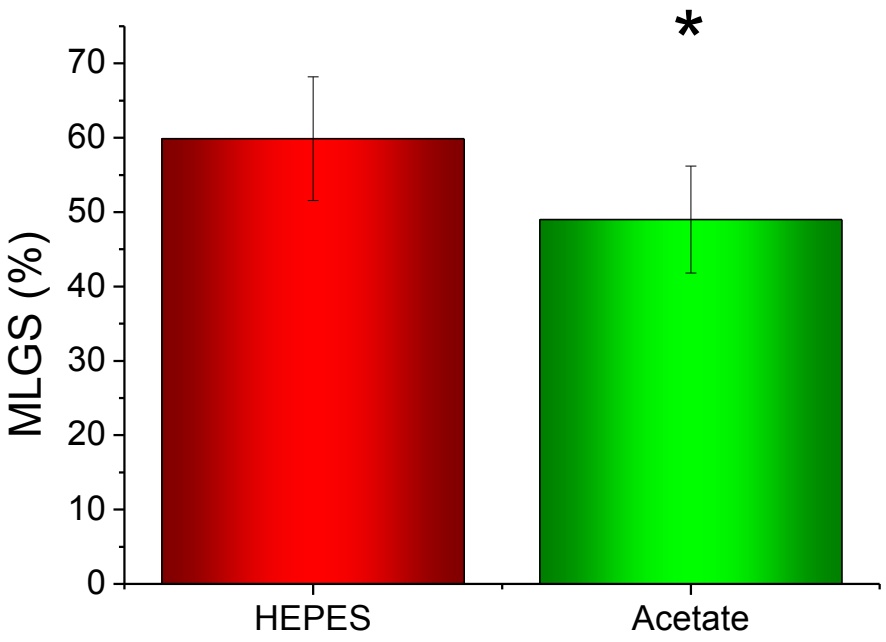

Figure S1.3. Comparison of IRI activity of ConA in acetate and HEPES buffer (concentration 5 mg.mL^{-1}). Error bars represent ± SD from a minimum of 3 repeats, MLGS = mean largest grain size relative to HEPES and calcium chloride or Acetate and calcium chloride buffer control. * signifies $p < 0.05$ relative to ConA in HEPES Buffer.

Changing the pH provides a significant improvement in IRI activity; it is thought that this is because ConA exists as a dimer at lower pH, suggesting that the quaternary structure also plays a role in its activity.

CD Spectra of lectins before and after heat denaturation

By heating at 80 °C the protein was denatured, as seen in figure S1.4 by the change to a more random coil secondary structure.

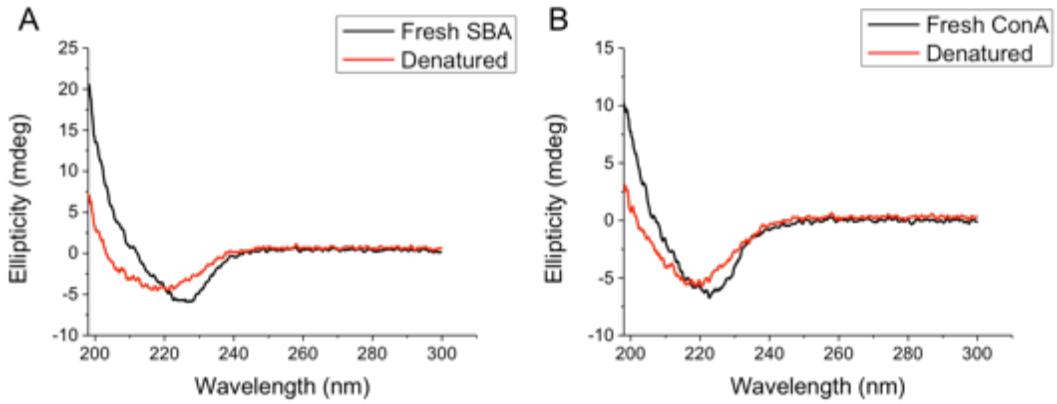

Figure S1.4. CD Spectra of lectins before and after denaturation by incubation at 80 °C. (A) CD spectra of soybean agglutinin (SBA); (B) CD spectra of concanavalin A (ConA).

CD Spectra of nisin at different pH

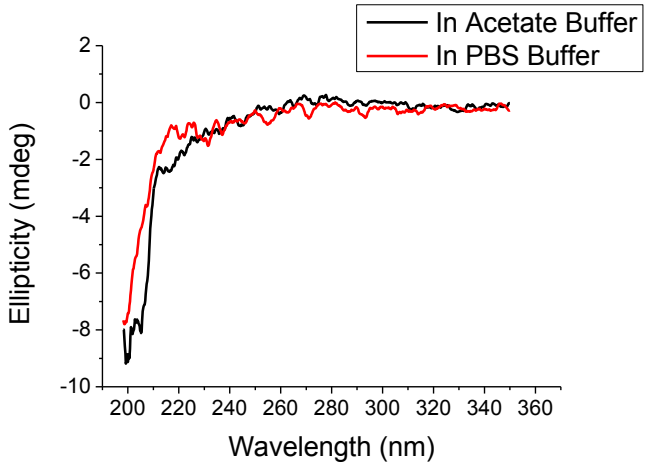

Figure S1.5. Circular dichroism spectra of nisin A in PBS and acetate buffer. CD spectra was taken at nisin concentration 500 μg.mL^{-1} and buffers were diluted 2 fold from those detailed in the methods section with deionized water.

It appears that there is a very minor change to the confirmation on nisin A when the pH is changed. As its antimicrobial activity dependents on its interaction with the cell membrane, it may be the case that the structure does not dramatically change in solution.

MLGS of various buffers and negative controls used in this study

To insure that the change in mean largest grain size was not a result of the change of buffer alone, all buffers formulations used here were also assessed for any IRI activity. As PBS is the standard buffer used for the "splat test" the other buffers are tested in comparison to this, Figure S1.6.

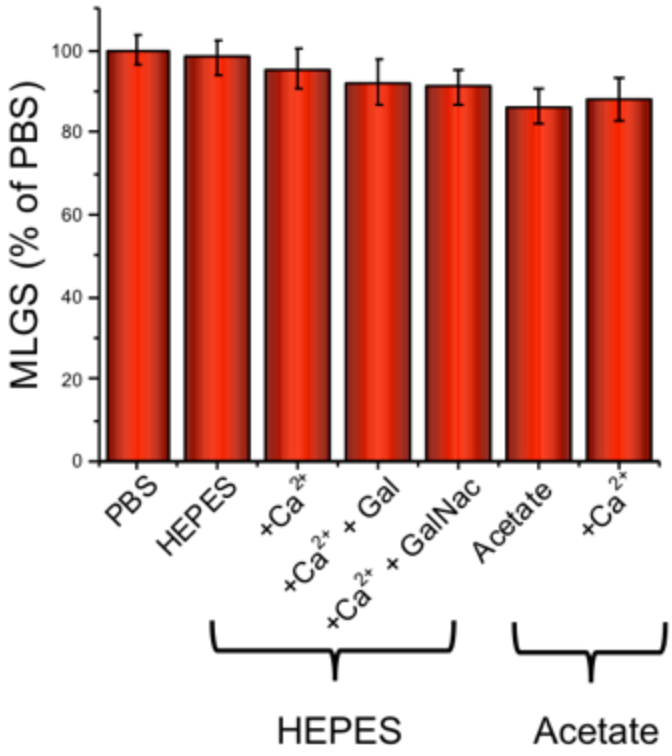

Figure S1.6. MLGS of buffers used in this study. Error bars represent ± SD from a minimum of 3 repeats, MLGS = mean largest grain size relative to PBS buffer sample shown in the first column. Both [$CaCl_2$] = 5mg.mL^{-1}, Cabohydrates Gal = galactose, GalNac = N-acetylgalactosamine were at concentration 10 mM.

Appendix 2

Appendix 2: Supplementary Information for "Quantitative Study on the Antifreeze Protein Mimetic Ice Growth Inhibition Properties of Poly(ampholytes) Derived from Vinyl-Based Polymers"

SEC analysis of poly(aminoethyl methacrylate)

Below are representative traces for the SEC of the PAEMAs. Molecular weights below that expected from NMR/conversion were observed, as discussed in the main manuscript. This was ascribed to a combination of polymer 'sticking' to the column and internal amidation by backbiting of the amine onto the ester, which is a well-known side reaction for PAEMA upon storage in aqueous solution.

Figure S3.1 shows the SEC trace obtained for $PAEMA_{11k}$ showing two peaks at molecular weights significantly below that expected from conversion and end-group analysis. Similarly, Figure S3.2 shows SEC for $PAEMA_{35k}$ showing a similar bimodal

distribution at very small molecular weights. Further evidence that these molecular weights are incorrect is that the polymers could be dialysed (in acidic media to prevent amidation) against 10 kDa MWCO dialysis tubing, without significant mass loss.

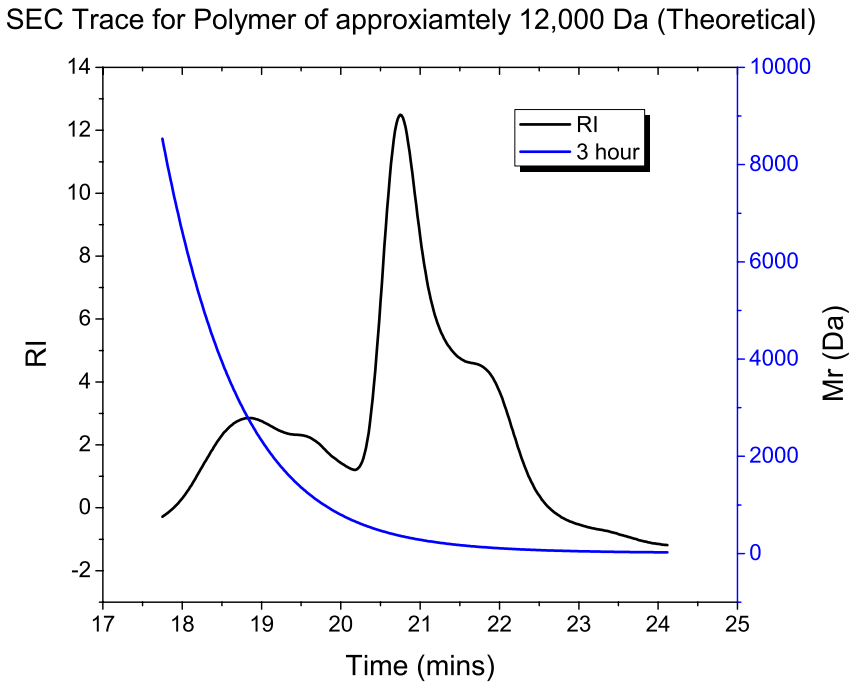

Figure S2.1. SEC trace of PAEMA M_N = 11 kg.mol^{-1} (by NMR).

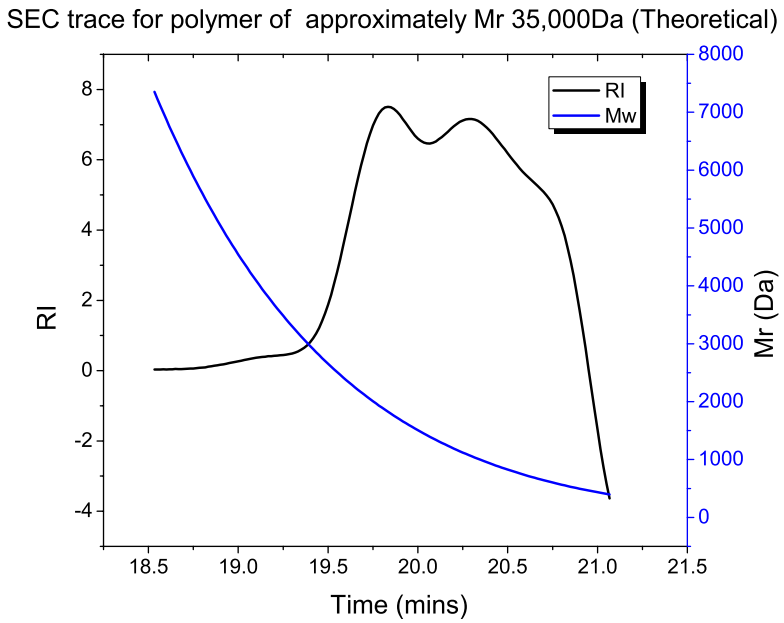

Figure S2.2. **SEC trace of PAEMA M_N = 35 kg.mol^{-1} (by NMR).**

It was also attempted to functionalize the amine side chains, to obtain a non-reactive polymer. This was done by addition of Boc-anhydride, and the obtained SEC (in THF) trace is shown below. A rather disperse, but mono-modal peak is obtained at ~ 20 kg.mol^{-1}, which is in line with the NMR measurements, suggesting the polymer does have the anticipated chain length. The dispersity can be accounted for by the incomplete functionalization of the amine groups, leaving some cationic groups which still have strong column interactions.

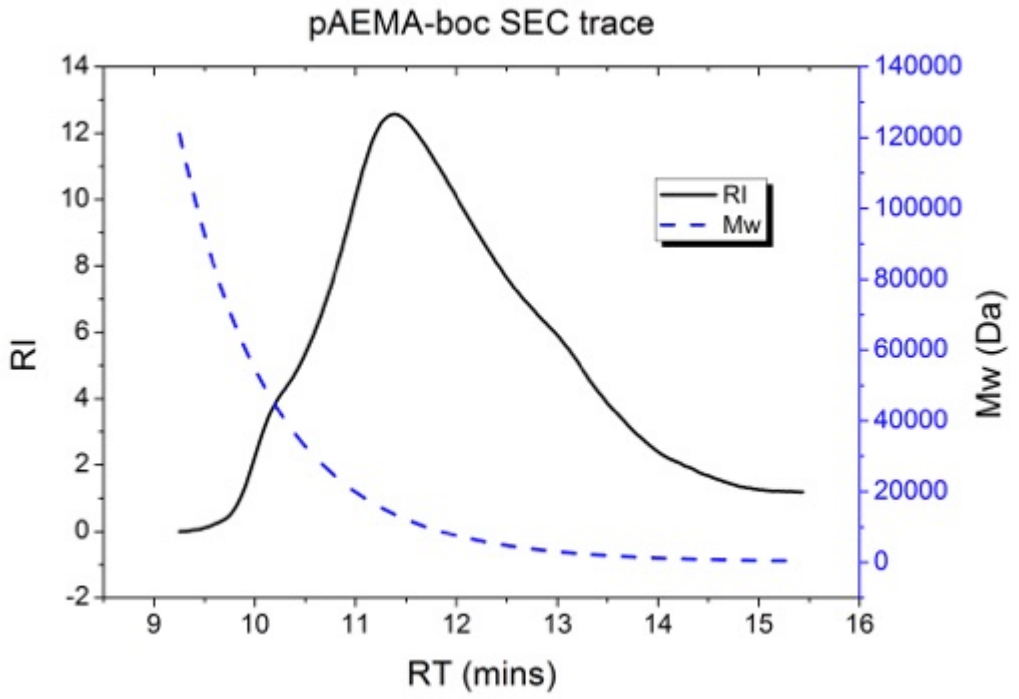

Figure S2.3. **SEC (THF) of Boc-PAEMA.** M_N **= 33 kg.mol^{-1} (by NMR).**

Synthesis of carbohydrate-centered poly(ampholytes)

The reaction scheme is shown in Figure S3.4, below, and full synthetic details are also included.

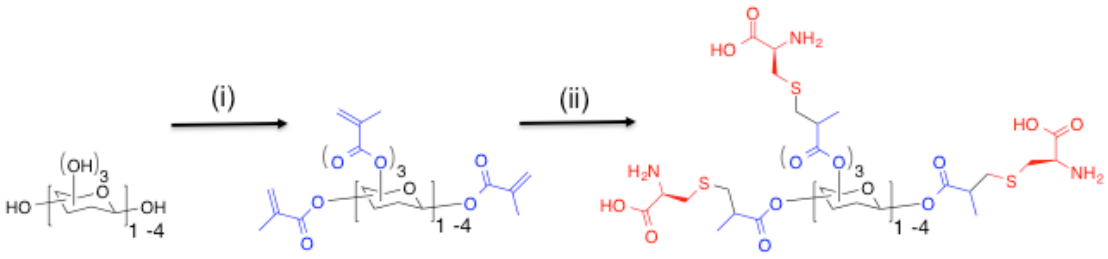

Scheme S2.1. Synthesis of carbohydrate poly(ampholytes) (i) Methacrylic anhydride/pyridine; (ii) Boc-Cys, then TFA/DCM.

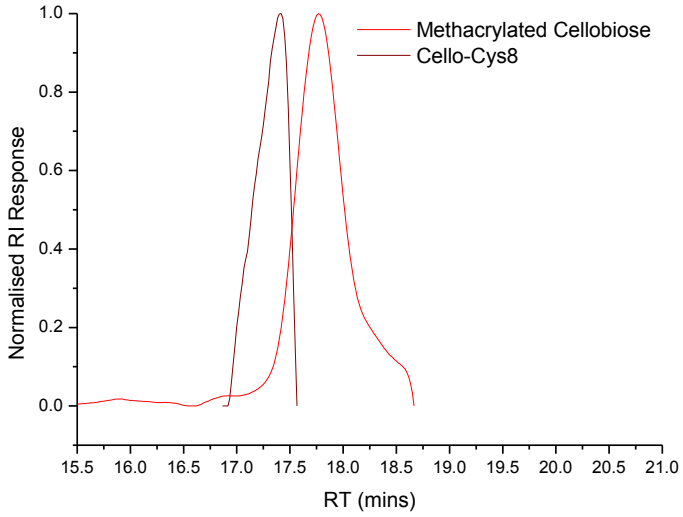

Figure S2.4. SEC (DMF) showing decrease in retention time upon addition of boc-cysteine.

Synthetic procedures.

All reactions were undertaken in a similar manner. Representative example using glucose core is described.

Glucose pentamethacrylate

Glucose (5.0500 g, 27.75 mmol, 1 eq), methacrylic anhydride (21.5252 g, 0.14 mol, 5.1 eq) and pyridine (125 mL) were stirred at room temperature overnight before being heated to 60 °C for 3 hours. Upon cooling, dichloromethane (50 mL) was added and the product washed with 0.1M HCl (40x50 mL), water (2x50 mL), brine (50 mL) and saturated $NaHCO_3$ (2x50 mL) before being dried with $MgSO_4$. The solvent was then removed under vacuum at 40 °C to yield a clear sticky product which was purified from THF and water (2.9101 g, 20 % yield). ^{1}H NMR ($CDCl_3$, 400 MHz) δ (ppm): 6.45 (d, *J*=3.8 Hz, 0.5H, β anomer), 6.27-6.03 (m, 5H, C=H_1H_2), 5.87 (d, J=8.0 Hz, 0.5H, α anomer), 5.76-5.44 (m, 6H, 5 C=H_1H_2, 1 C$H_{glucose}$), 5.39-5.09 (m, 2H, C$H_{glucose}$), 4.44-4.15 (m, 3H, C$H_{glucose}$, C$H_{2\ glucose}$), 2.01-1.84 (m, 15H, CH_3); ^{13}C

NMR ($CDCl_3$, 600MHz, PENDANT) δ (ppm) 166.9-164.9 (*C*=O), 135.7-134.8 (R_2C=CH_2), 128.2-126.4 (R_2C=CH_2), 92.3-92.1 (β anomer), 89.8-89.7 (α anomer), 76.1-68.2 ($CH_{glucose}$), 62.8-62.0 ($CH_{2\ glucose}$), 18.2-18.0 (CH_3); IR υ (cm^{-1}) 1721 (s, C=O ester), 1637 (m, C=C), 1453 (m, CH_2/CH3 bend), 1317 (m, CH_3 bend), 1292 (m, alkyl C-H), 1140 (s, C-O stretch); ESMS (positive mode) m/z 475.1 $[M(4mer)+Na]^+$ $C_{22}H_{28}O_{10}$, m/z 543.2 $[M(5mer)+Na]^+$ $C_{26}H_{32}O_{11}$; GPC (DMF) M_n 432, M_w 442, M_w/M_n 1.02.

Penta-cysteine glucose methacrylate.

Methacrylated glucose (0.0521 g, 96 μmol, 1eq), Boc-cysteine (0.1143 g, 250 μmol, 2.6 eq), tributyl phosphine (drop, catalytic) and benzylamine (drop, catalytic) were dissolved in DCM (3ml) and stirred at 45 °C for 72 hours. DCM (10 mL) was then added and the product washed with water (2x20 mL) and brine (20 mL) before the solvent was removed under vacuum. The product (Gluco-Cys5) was then purified in THF and water. IR υ (cm^{-1}) 2960 (m, O-H), 2927 (m, C-H stretch), 1720 (s, C=O ester), 1637 (m, C=C), 1454 (m, CH_2/CH3 bend), 1318 (m, CH_3 bend), 1160 (s, C-O stretch), 751 (m, C-S); GPC (DMF) M_n 946 Da, M_w 1190 Da, M_w/M_n 1.26. The product was then dissolved in DCM, and TFA (4 drops) added to remove the boc protecting group. The product was then dialysed and the water removed by freeze-drying to yield a sticky solid (0.0072 g, 7 % yield)

Cellobiose core

GPC (DMF) M_n = 2126 Da, M_w = 2153 Da, M_w/M_n 1.01.

Stachyose core

GPC (DMF) M_n = 2467 Da, M_w = 2575 Da, M_w/M_n 1.04.

Ice recrystallization assay

Some example micrographs are shown below. The COOH degree of functionalization is indicated, with 50 % clearly have smaller grains compared to the others. Micrographs are for **P7, P11, P16** respectively at 15 mg.mL^{-1}.

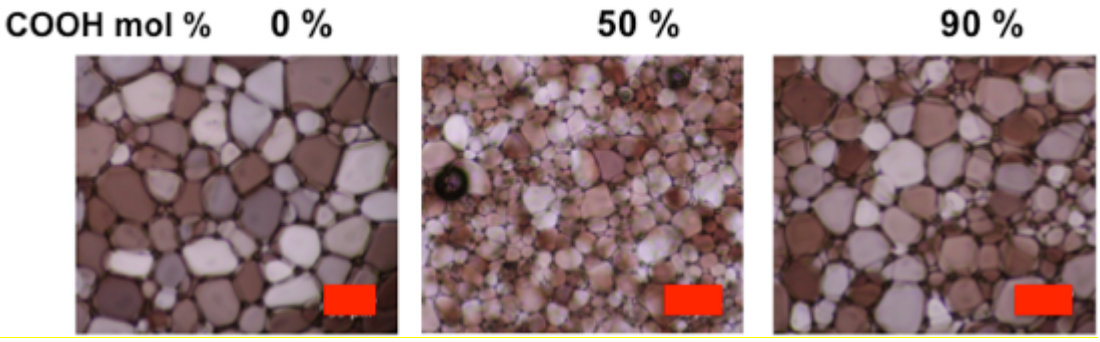

Figure S2.5. **Example ice recrystallization assay micrographs for (left to right) P7, P11, P16 at 15 mg.mL^{-1}, after 30 minutes annealing at -8 °C.**

Appendix 3

Appendix 3: Supplementary Information for "Gold Nanoparticle Aggregation as a Probe of Antifreeze (Glyco) Protein-Inspired Ice Recrystallization Inhibition and Identification of New IRI Active Macromolecules"

Synthesis and characterisation of Poly(vinyl alcohol), PVA.

The synthesis of PVA used in this study, was conducted as described in Congdon *et al*[1]. The method is explained below and shown in Scheme S3.1. Table S3.1 provides characterization details of the polymers selected for this study

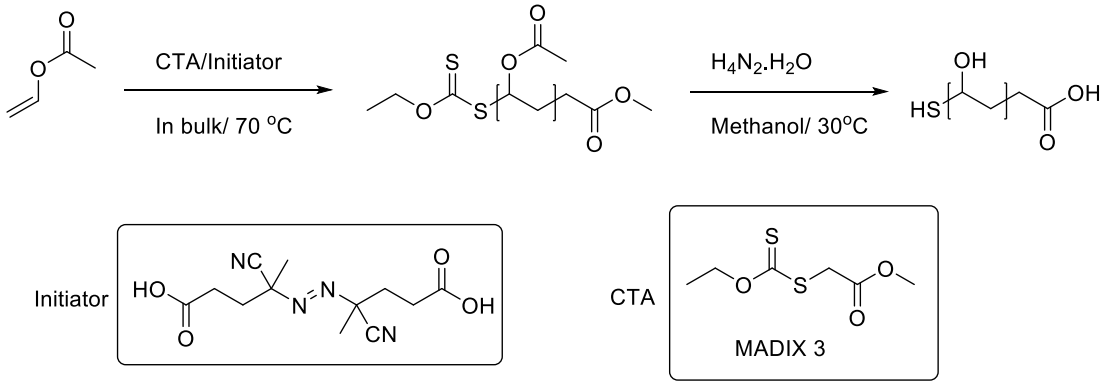

Scheme S3.1. Schematic of the synthesis of PVA using RAFT polymerisation.

Table S3.1. Details of polymers used in this study.

Entry	[M]/ [CTA][(a)]	Conv[(b)] %	$M_{n,theo}$ [(c)] g.mol^{-1}	$M_{n,NMR}$ [(d)] g.mol^{-1}	$M_{n,SEC}$ g.mol^{-1}	Đ [(e)]	DP_N [(b)]	PVA[(g)]
$PVAc_{10}$	10	83.2	860	900	870	1.18	10	**PVA_{10}**
$PVAc_{30}$	50	60.0	4300	2580	2700	1.45	30	**PVA_{30}**
$PVAc_{56}$	100	54.7	8600	4700	5100	1.23	56	**PVA_{56}**
$PVAc_{154}$	200	73.8	17200	12700	13800	1.45	154	**PVA_{154}**
$PVAc_{246}$	300	80.1	25800	20660	21700	1.39	246	**PVA_{246}**

(a) Monomer to RAFT agent ratio; (b) Determined by ^{1}H NMR spectroscopy; (c) Theoretical M_n determined from monomer to RAFT agent ratio; (d) Determined by ^{1}H NMR; (e) Determined by SEC in THF using PMMA standards; (f) Number-average degree of polymerization; (g) Corresponding PVA prepared by hydrolysis of the respective PVAc polymer.

Synthesis of methyl(ethoxycarbonothioyl)sulfanyl acetate (MADIX 2)

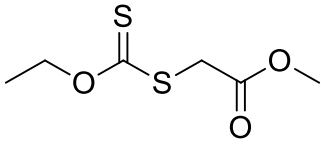

Ethanol (70 mL) was added to a round bottom flask equipped with a stir bar. Potassium hydroxide (11.45 g, 0.2 mol) was added and left to dissolve for 1 h. Carbon disulphide (12.1 mL, 0.2 mol) was added dropwise, forming a yellow solution, which was left for 5 h. Methyl bromoacetate (6.5 mL, 0.06 mol) was added dropwise and the solution left to stir overnight. The solution was filtered and washed with cold ethanol and concentrated *in vacuo*. The crude product was partitioned in DCM and sat. brine solution and the organic fraction concentrated *in vacuo*. The residue was washed through a column of basic alumina using pure ethyl acetate as the eluent. The fractions were concentrated *in vacuo* and then dried under vacuum. Yield 5.25 g 46 %. ^{1}H NMR ($CDCl_3$): δ = 1.42 (2H, t, J=7.2, CH_3CH_2), 3.76 (3H, s, CH_3O), 3.92 (2H, d, J=7, SCH_2), 4.64 (3H, q, J=7.2, CH_3CH_2). ^{13}C NMR ($CDCl_3$): δ = 14.0 (CH_2–CH_3), 37.7 (CH_2), 61.0(CO_2CH_3), 70.4 (CH_2–CH_3), 167.7 (C=O), 212.4 (C=S).

Polymerisation of vinyl acetate using MADIX 2

As a representative example, MADIX 2 (0.21 g, 0.99 mmol), vinyl acetate (4.67 g, 2.64 mmol), and ACVA (4,4′-azobis(4-cyanovaleric acid); 0.013 g) were added to a stoppered vial. The solution was thoroughly degassed under a flow of N_2 for 20 min, and the reaction mixture was then allowed to polymerize at 68 °C for typically 15 h. The yellow solutions were then cooled to room temperature. Poly(vinyl acetate) was then recovered as a yellow sticky solid after precipitation into hexane. The hexane was then decanted and the poly(vinyl acetate) was redissolved in THF, which was then concentrated *in vacuo* and thoroughly dried under vacuum at 40 °C for 24 h, forming a white solid. Representative characterization data for $PVAc_{56}$: ^{1}H NMR (400 MHz, $CDCl_3$) δ 4.61 (−C*H*O–CH_2, br, 1H), 1.74 (−CO–C*H*$_3$, br, 3H), 1.53 (−C*H*$_2$–, br, 2H); M_n^{SEC}(THF) = 5100 Da, M_w/M_n = 1.23.

Hydrolysis of poly(vinyl acetate) to poly(vinyl alcohol)

As a representative example, poly(vinyl acetate) (1.5 g, 3300 Da, M_n/M_w = 1.22) was dissolved in a methanol (20 mL) and hydrazine hydrate solution (15 mL, 80 % in water) in a round-bottom flask. The reaction mixture was stirred at 30 °C for 2 h. The reaction mixture was then dialyzed using distilled water and poly(vinyl alcohol) was recovered as a spongy white solid by freeze-drying the dialysis solution. Deacetylation was determined by ^{1}H NMR. Representative characterization data for PVA_{56}: ^{1}H NMR (400 MHz, $CDCl_3$) δ 4.00 (−C*H*OH–, br, 1H), 1.68–1.60 (−C*H*$_2$–, br, 2H).

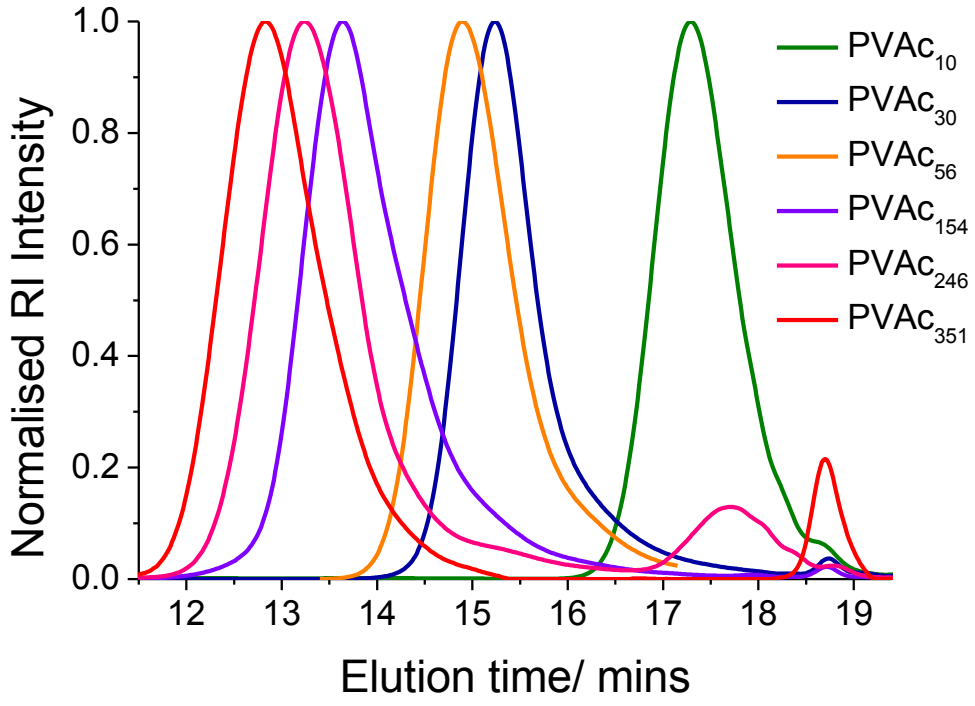

Figure S3.1. SEC traces of PVA of various molecular weights showing clear differences in size and low polydispersities.

Determining extent of aggregation

The change in absorbance at 520 nm was identified as the simplest measurement of aggregation in this study. To account for scattering of aggregated samples, we conveniently measured the difference between the actual absorbance at 520 nm and that of a baseline define between 450 and 680 nm as show in Figure S3.2.

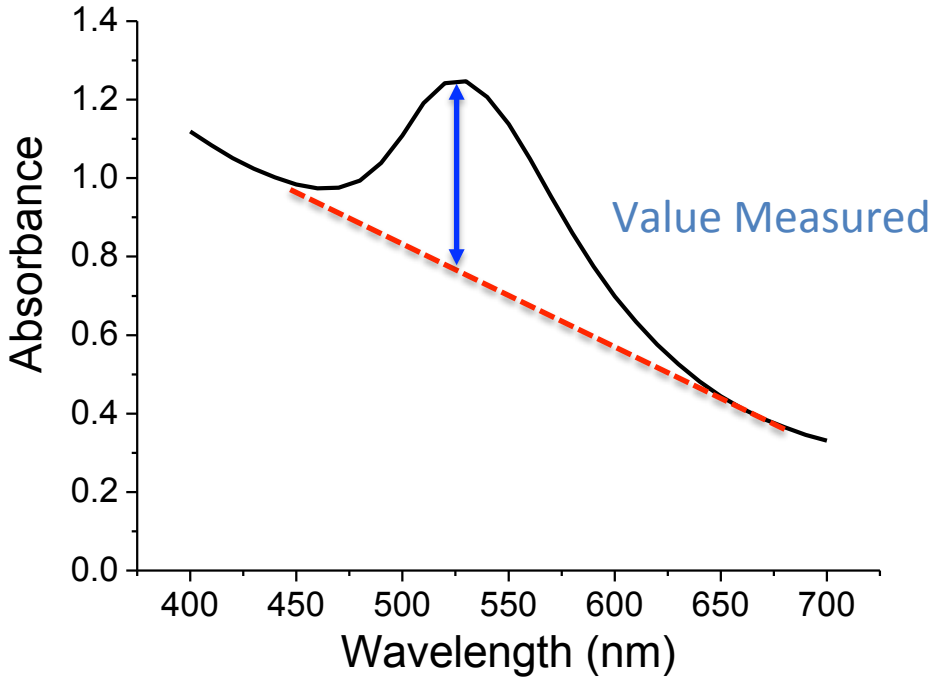

Figure S3.2. Measurement of absorbance used here.

Variable volume gold particle aggregation experiments

An advantage of the AuNP method is that samples can be tested at a range of different volumes. The rationale for this was that larger volumes would take longer to freeze/thaw, which should increase the amount of ice recrystallization inducing more aggregation and enabling optimization so that there are clear differences between IRI active and non-active compounds. Furthermore, the standard 'splat' assay only uses 10 μL of liquid, which is far from the volumes employed in applications such as cryopreservation, and therefore larger volumes may provide a more predictive test for the additives ultimate application. To this end samples of 50, 100, 200, 500, 1000 and 2000 μL where prepared in 96 and 24 well plates and subjected to the same freeze/thaw cycle as detailed within the paper. The sample depth (which is crucial for freezing rate) verses the volume of the samples is plotted in Figure S3.3.

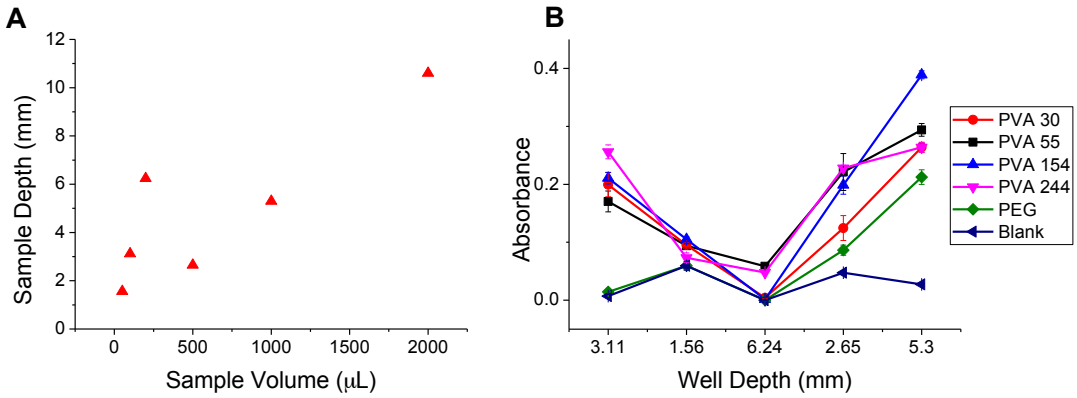

Figure S3.3. Effect of well depth. (A) Depth of well compared to volume of sample, a 24 well plate is substituted for a 96 well plate for samples volumes greater than 200 μL; (B) Absorbance dependence on the well depth.

From Figure S3.3, samples with lower well depth provide a generally lower absorbance probably due to the decreased distance for the light to pass through. At the highest depth, 6.24 mm there is very little absorbance at 520 nm compared to background scatter, possibly due to the increased thawing time and increased ice recrystallization. The depth-dependence also suggests that this assay is probing ice recrystallization and not ice shaping, which was previously suggested. Overall the clearest difference between IRI active and no active compounds is found at a well depth of 3.118 mm, which corresponds to 100 μL in a 96 well plate. It is therefore recommended that 50 μL of sample to 50 μL of AuNPs making an overall volume of 100 μL be used to investigate the IRI activity of compounds.

Comparison of absorbance change to mean largest grain size for poly(Amino ethyl methacrylate)-*co*-succinic anhydride

Since PAEMA-*co*-SA has also been shown to exhibit IRI activity the absorbance has been plotted here against mean largest grain size (MLGS) (as a percentage of PBS buffer negative control), Figure S3.4.

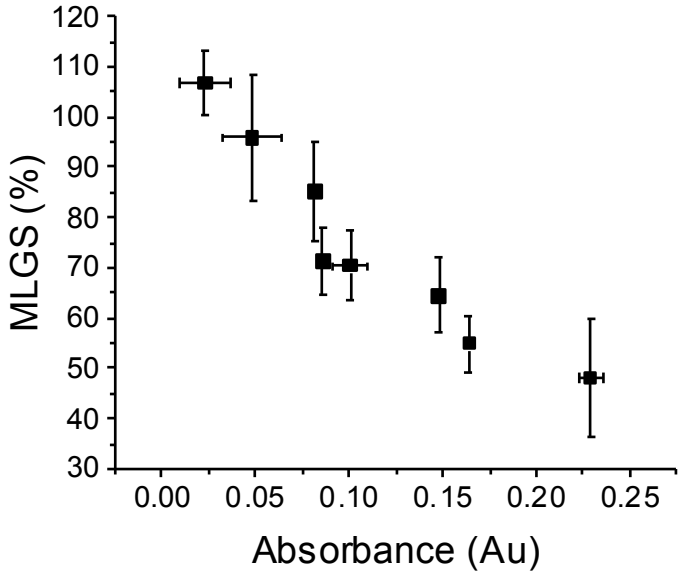

Figure S3.4. Comparison of PAEMA-*co*-SA polymers mean largest grain size (MLGS) and absorbance at 20 mg.mL^{-1}. MLGS = mean largest grain size relative to a PBS control, expressed as %. Error bars represent ± SD from a minimum of 3 repeats.

Plotting the MLGS absorbance change against each other on the same graph shows a linear correlation and reinforces the premise that the AuNP method is probing the same phenomenon as the "splat test" namely ice recrystallization inhibition.

Concentration dependence of AuNPs with PVA

To assess how the concentration of AuNPs affects the assay, a serial dilution was performed in the presence of 5mg.mL^{-1} PVA, figure S3.5.

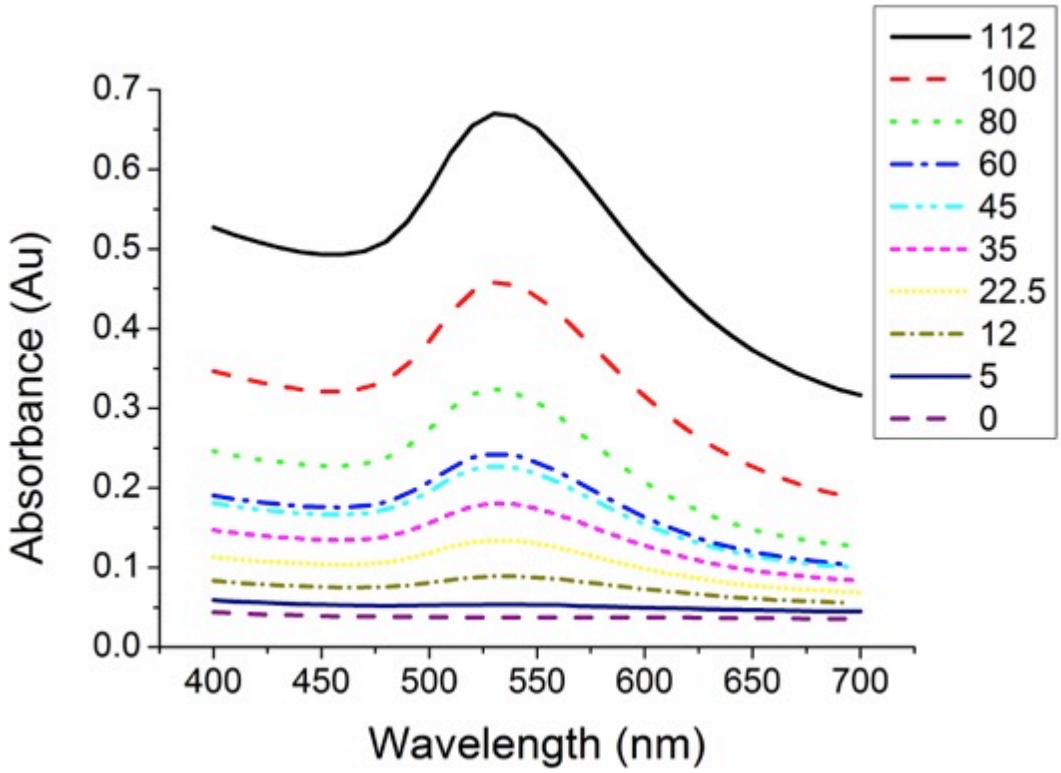

Figure S3.5. Spectra of AuNPs frozen in the presence of 5mg.mL^{-1} PVA. Values given in the key are concentration in μg.mL^{-1}.

From Figure S3.5 it can be seen there is a reduction in absorbance across the whole spectra as AuNP concentration decreases. However the peak at around 550 nm remains at all concentrations showing that PVA prevents the aggregation of AuNPs. Furthermore if no PVA is added, this 550 nm peak disappears at all concentrations of AuNPs. To maximize the difference between 520 nm and 650 nm a minimum AuNP concentration of 80 μg.mL^{-1} is optimal to avoid wastage and still function in the assay.

References.

[1] T. Congdon, R. Notman, M. I. Gibson, *Biomacromolecules* **2013**, *14*, 1578-1586.

Appendix 4

Appendix 4: Supplementary Information for "Antifreeze Protein Mimetic, Supramolecular Metallohelices with Potent Ice Recrystallization Inhibition Activity".

Synthesis

The compounds 5-(chloromethyl)-2,2'-bipyridine,[1] [2]hydroxypicolinaldehyde,[3] phenylglycinol,[4] 1-phenyl-2-(prop-2-ynyloxy)ethanamine[5] and pyrazine-2-carboxaldehyde[6] were synthesised by known methods, and are described briefly below.

5-methoxypicolinaldehyde

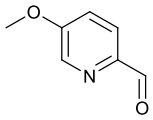

5-hydroxypicolinaldehyde (2.0 g, 1 eq.), methyl iodide (2.3 g, 1 mL, 1 eq.), and potassium carbonate (2.69 g, 1.2 eq.) were dissolved in acetonitrile (50 mL) and heated at reflux (85 °C) for 18 h, allowed to cool to ambient temperature and filtered through a silica plug. Solvents were removed under reduced pressure and the crude material was dissolved in dichloromethane (20 mL), filtered and solvents were removed under reduced pressure to give the desired compound as white solid.

Yield = 1.2 g, 72 %.

^{1}H NMR (300 MHz, 298 K, $CDCl_3$) δ_H 9.92 (1H, s, CHO), 8.36 (1H, d, $^{4}J_{HH}$ = 3.0 Hz), 7.90 (1H, d, $^{3}J_{HH}$ = 8.5 Hz), 7.24 (1H, dd, $^{3}J_{HH}$ = 8.5 Hz, $^{4}J_{HH}$ = 2.5 Hz, Py), 3.89 (3H, s, OCH_3).

$^{13}C\{^{1}H\}$ NMR (75 MHz, 298 K, $CDCl_3$) δ_C 192.1 (CHO), 159.1, 146.4, 138.7, 123.5, 120.0 (Py), 56.0 (OCH_3).

MS (ESI) m/z 138 $[M+H]^+$, 160 $[M+Na]^+$.

IR ν cm^{-1} 3099 w, 3052 w, 3033 w, 2984 w, 2947 w, 2831 w, 1692 s, 1572 s, 1489 m, 1452 m, 1380 w, 1308 m, 1261 m, 1222 m, 1117 m, 1007 s, 898 m, 852 s, 750 m, 734 m.

Elemental analysis found (calculated for $C_7H_7NO_2$) % C 61.00 (61.31), H 4.98 (5.14), N 10.00 (10.21).

(*S*)-1-phenyl-2-(prop-2-ynyloxy)ethanamine

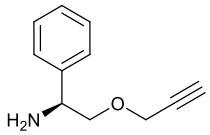

(*S*)-1-phenyl-2-(prop-2-ynyloxy)ethanamine was synthesised using the procedure described for 5-methoxypicolinaldehyde, substituting iodomethane for 3-bromoprop-1-yne (80% in toluene) and (*R*)-phenylglycinol for (*S*)-phenylglycinol. Distilled under high vacuum at 110 °C.

Yield 1.03 g, 81 %.

^{1}H NMR (400 MHz, 298 K, $CDCl_3$) δ_H 7.45-7.20 (5H, m, Ph), 4.26-4.16 (3H, m, CH, CH_2), 3.68 (1H, dd, $^{3}J_{HH}$ = 9.0 Hz, $^{4}J_{HH}$ = 4.0 Hz), 3.47 (1H, t, $^{3}J_{HH}$ = 9.0 Hz, CH_2), 2.43 (1H, t, $^{4}J_{HH}$ = 2.5 Hz, CH), 1.70 (2H, s, NH_2).

$^{13}C\{^{1}H\}$ NMR (101 MHz, 298 K, $CDCl_3$) δ_C 142.1, 128.3, 127.3, 126.7 (Ph), 79.4 (C), 74.4 (CH), 60.2, 58.3 (CH_2), 55.2 (CH).

MS (ESI) m/z 159 $[M\text{-}NH_2]^+$, 176 $[M+H]^+$

IR υ cm^{-1} 3286 w, 2855 w, 1087 s, 861 m, 759 s, 699 s.

Elemental analysis found (calculated for $C_{11}H_{13}NO$) % C 74.92 (75.40), H 7.56 (7.48), N 7.92 (7.99).

Optical rotation +65.74 ° (3.10 g/ 100 mL)

(*R*)-1-phenyl-2-(prop-2-ynyloxy)ethanamine

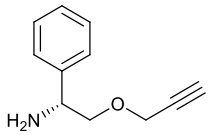

(*R*)-1-phenyl-2-(prop-2-ynyloxy)ethanamine was synthesised using the procedure described for 5-methoxypicolinaldehyde, substituting iodomethane for 3-bromoprop-1-yne (80 % in toluene). Distilled under high vacuum at 110 °C.

Yield 0.37 g, 28 %.

^1H NMR (400 MHz, 298 K, $CDCl_3$) δ_H 7.43-7.22 (5H, m, Ph), 4.25-4.17 (3H, m, CH, CH_2), 3.68 (1H, dd, $^3J_{HH}$ = 9.0 Hz, $^4J_{HH}$ = 4.0 Hz), 3.47 (1H, t, $^3J_{HH}$ = 9.0 Hz, CH_2), 2.43 (1H, t, $^4J_{HH}$ = 2.5 Hz, CH), 1.68 (2H, s, NH_2).

$^{13}C\{^1H\}$ NMR (101 MHz, 298 K, $CDCl_3$) δ_C 142.7, 128.5, 127.5, 126.8 (Ph), 79.6 (C), 74.6 (CH), 60.4, 58.4 (CH_2), 55.4 (CH).

MS (ESI) m/z 159 $[M\text{-}NH_2]^+$, 176 $[M+H]^+$

IR υ cm^{-1} 3285 w, 2855 w, 1088 s, 859 m, 759 s, 699 s.

Elemental analysis found (calculated for $C_{11}H_{13}NO$) % C 74.82 (75.40), H 7.60 (7.48), N 7.81 (7.99).

Optical rotation -81.60 ° (3.12 g/ 100 mL) [Lit. -32.11 ° (6.08 g/100 mL)]

5-(benzyloxy)picolinaldehyde

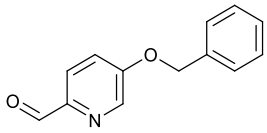

5-hydroxypicolinaldehyde (2.0 g, 1 eq.), benzyl bromide (0.73 g, 0.5 ml, 1.05 eq.), and potassium carbonate (2.69 g, 1.2 eq.) were dissolved in acetonitrile (50 mL) and heated at reflux (85 °C) for 18 h, allowed to cool to ambient temperature and filtered through a silica plug. Solvents were removed under reduced pressure and the crude material was dissolved in dichloromethane (20 mL), filtered and solvents were removed under reduced pressure to give the desired compound as yellow solid.

Yield = 0.67 g, 77 %.

^{1}H NMR (300 MHz, 298 K, $CDCl_3$) δ_H 9.99 (1H, s, CHO), 8.52 (1H, d, $^{4}J_{HH}$ = 2.5 Hz), 7.96 (1H, d, $^{3}J_{HH}$ = 8.5 Hz), 7.43 (6H, m, Ar), 5.21 (2H, s, CH_2).

$^{13}C\{^{1}H\}$ NMR (75 MHz, 298 K, $CDCl_3$) δ_C 192.1 (CHO), 158.2, 139.2, 135.2, 129.0, 128.8, 127.7, 127.1, 123.5, 121.1 (Ar), 70.78 (CH_2).

MS (ESI) m/z 236 $[M+Na]^+$.

IR ν cm^{-1} 2836 w, 1698 s, 1571 s, 1501 w, 1477 w, 1462 w, 1452 m, 1387 m, 1370 w, 1310 s, 1262 m, 1209 s, 1130 m, 1045 w, 1032 w, 1012 w, 996 w, 912 w, 872 w, 835 m, 790 w, 740 s, 696 s.

Elemental analysis found (calculated for $C_{13}H_{11}NO_2$) % C 72.67 (73.23), H 5.38 (5.20), N 6.36 (6.57).

(S)-2-(2,2'-bipyridin-5-ylmethoxy)-1-phenylethanamine

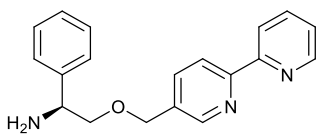

S-Phenylglycinol (1.00 g, 1 eq.) was dissolved in dry tetrahydrofuran (20 mL) and was added dropwise to a stirred suspension of sodium hydride (0.36 g, 2 eq.) in dry

tetrahydrofuran (10 mL). The solution was stirred for 1 h at ambient temperature before a solution of 5-(bromomethyl)-2,2'-bipyridine (1.82 g, 1 eq.) in dry tetrahydrofuran (20 mL) was added dropwise. The solution was stirred for a further 1 h at ambient temperature. The reaction mixture was then heated to reflux (65 ˚C) for 2 h, allowed to cool the ambient temperature, and quenched with the addition of brine (40 mL). The dichloromethane extracts (4 × 60 mL) were dried over sodium sulphate and the solvent was removed to leave a dark yellow oil. This crude product was purified by Kügelrohr distillation (excess phenylglycinol removed at 120°C under high vacuum) to give a yellow oil that solidifies on standing.

Yield 1.25 g, 56 %.

^{1}H NMR (300 MHz, $CDCl_3$) δ_H 8.61-8.59 (1H, m), 8.56 (H, d, J_{HH} 2.0 Hz), 8.33-8.29 (2H, m), 7.76-7.67 (2H, m), 7.33-7.16 (6H, m, Ar), 4.54 (2H, s, CH_2), 4.19 (1H, dd, $^{3}J_{HH}$ = 9.0 Hz, $^{4}J_{HH}$ = 4.0 Hz, CH), 3.58 (1H, dd, $^{3}J_{HH}$ = 9.0 Hz, $^{4}J_{HH}$ = 4.0 Hz), 3.44 (1H, t, $^{3}J_{HH}$ = 8.5 Hz, CH_2).

$^{13}C\{^{1}H\}$ NMR (75 MHz, $CDCl_3$) δ_C ppm 156.0, 155.7, 149.3, 148.6, 142.3, 137.0, 136.4, 133.7, 128.5, 127.6, 126.9, 123.8, 121.1, 120.9 (Ar), 76.9 (CH_2), 70.7 (CH_2), 55.6 (CH).

MS (ESI) 306 $[M+H]^{+}$.

IR ν cm^{-1} 3361 w, 3296 w, 3055 w, 3027 w, 2902 w, 2860 w, 1589 w, 1574 w, 1558 w, 1490 w, 1459 m, 1434 w, 1414 w, 1387 w, 1349 w, 1257 m, 1098 m, 1038 w, 1022 m, 991 w, 936 w.

Elemental analysis found (calculated for $C_{19}H_{19}N_3O$) % C 74.75 (74.73), H 6.13 (6.27), N 13.67 (13.76).

Optical rotation +15.41 ° (1.65 g /100 mL MeOH).

The *R* enantiomer was synthesised in an identical manner but starting from *R*-Phenylglycinol.

Yield 1.34 g, 60 %.

Optical rotation -14.04 ° (1.64 g /100 mL MeOH).

5-(2,2'-bipyridin-5-ylmethoxy)picolinaldehyde

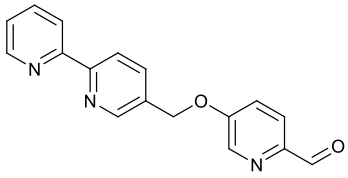

5-(hydroxy)-picolinaldehyde (2.0 g, 1.0 eq.) was dissolved in acetonitrile (50 mL). Potassium carbonate (2.65 g, 1.2 eq.) followed by 5-(chloromethyl)-2,2'-bipyridine (3.32 g, 1.0 eq.) were added and the solution was stirred at reflux (80 °C) for 16 h. The reaction mixture was filtered through a silica plug and the solvent was removed under reduced pressure. The crude product was taken up in dichloromethane (50 mL), filtered and the solvent was removed under reduced pressure to give the desired 5-(2,2'-bipyridin-5-ylmethoxy) picolinaldehyde, a pale brown solid.

Yield 3.67 g, 79 %.

^{1}H NMR (400 MHz, 298 K, $CDCl_3$) δ_H 9.94 (1H, s, CHO), 8.69 (1H, d, $^{3}J_{HH}$ = 2.0 Hz), 8.62 (1H, d, $^{3}J_{HH}$ = 4.5 Hz), 8.47 (1H, d, $^{3}J_{HH}$ = 2.5 Hz), 8.40 (1H, $^{3}J_{HH}$ = 8.0 Hz), 8.34 (1H, d, $^{3}J_{HH}$ = 8.0 Hz), 7.91 (1H, d, $^{3}J_{HH}$ = 8.5 Hz), 7.84 (1H, dd, $^{3}J_{HH}$ = 8.5 Hz, $^{4}J_{HH}$ = 2.5 Hz), 7.77 (1H, td, $^{3}J_{HH}$ = 8.0 Hz, $^{4}J_{HH}$ = 2.0 Hz), 7.34 (1H, dd, $^{3}J_{HH}$ = 8.0 Hz, $^{4}J_{HH}$ = 3.0 Hz), 7.27 (1H, m, Py), 5.21 (2H, s, CH_2).

$^{13}C\{^{1}H\}$ NMR (75 MHz, 298 K, $CDCl_3$) δ_C 192.1 (CHO), 149.4, 148.6, 139.0, 138.1, 137.2, 1366, 131.9, 130.9, 124.3, 124.2, 123.5, 122.7, 121.4, 121.2 (Py), 68.1 (CH_2).

MS (ESI) m/z 292 $[M+H]^+$, 314 $[M+Na]^+$.

IR ν cm^{-1} 2811 w, 1701 s, 1567 s, 1455 m, 1204 s, 788 s, 736 s, 590 s.

Elemental analysis found (calculated for $C_{17}H_{13}N_3O_2$) % C 69.82 (70.09), H 4.66 (4.50), N 14.01 (14.42).

General synthesis of HHT-$[Fe_2L''']Cl_4$

Anhydrous iron(II) chloride (2 eq.) was add to a stirred solution of the either the desired R_C-chiral amine (3 eq.) and 5-(2,2'-bipyridin-5-ylmethoxy)picolinaldehyde (3 eq.) or the desired substituted aldehyde (3 eq.) and (R)-2-(2,2'-bipyridin-5-ylmethoxy)-1-phenylethanamine (3 eq.) in methanol (20 mL) at ambient temperature to give a purple solution that was then heated to reflux (65 °C) for 24 – 48 h. The reaction was allowed to cool to ambient temperature, filtered through a celite plug and the solvents were removed *in vacuo* to give the desired dark purple solid. Note that the presence of water of crystallisation in these compounds was confirmed by NMR and IR spectroscopy and the absence of other solvents was confirmed also by NMR. The hydration number was then determined by thermogravimetric analysis and the relevant mass loss was correlated with microanalytical data.

R_c,Λ_{Fe},HHT-$[Fe_2L^1{}_3]Cl_4.13H_2O$

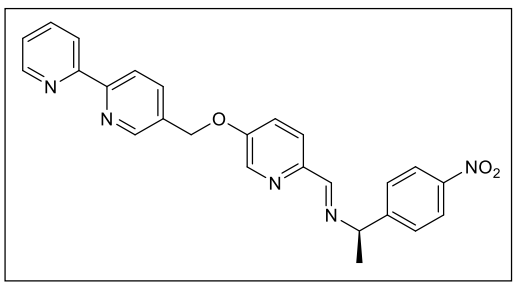

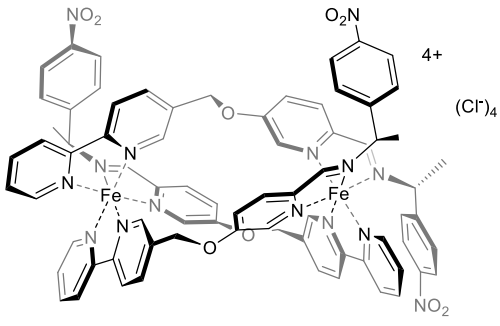

Yield 0.36 g, 99 %.

MS (ESI) m/z 357 $[Fe_2L_3]^{4+}$

IR v cm^{-1}: 3352 br s, 3035 m, 1602 m, 1561 m, 1216 m, 1344 s, 1232 s, 1011 m, 853 m, 788 w, 753 w.

Elemental analysis found (calculated for $C_{75}H_{63}Cl_4Fe_2N_{15}O_9.13H_2O$) % C 48.88 (49.88), H 4.31 (4.97), N 10.65 (11.63).

S_c,Δ_{Fe},HHT-$[Fe_2L^1_3]Cl_4.13H_2O$

Data as for *R*-enantiomer

Yield 0.33 g, 0.021 mmol, 90 %

Elemental analysis found (calculated for $C_{75}H_{63}Cl_4Fe_2N_{15}O_9.13H_2O$) % C 50.15 (49.88), H 4.35 (4.97), N 10.89 (11.63).

R_c,Λ_{Fe},HHT-$[Fe_2L^2_3]Cl_4.11H_2O$

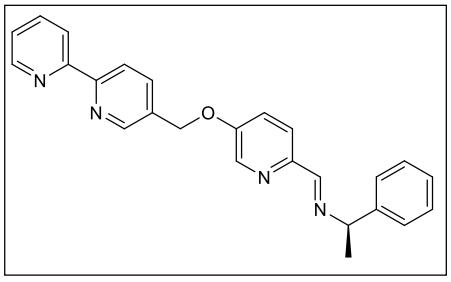

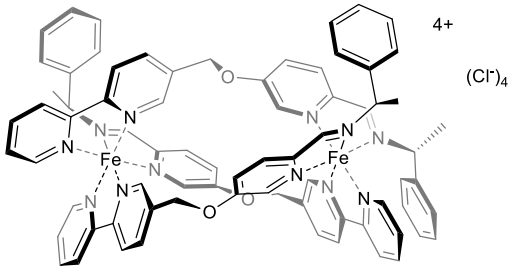

Yield 0.31 g, 96 %.

$^{13}C\{^1H\}$ NMR (126 MHz, 298 K, MeOH) δ_C 171.1, 170.8, 170.3 (CHN), 161.1, 160.9, 160.8, 160.5, 160.3, 160.0, 159.4, 158.7, 158.4, 157.2, 156.6, 155.1, 153.9, 153.8, 153.7, 142.1, 141.4, 140.8, 140.7, 140.5, 140.5, 139.7, 139.75, 139.6, 136.7, 136.6, 136.6, 133.5, 132.7, 132.5, 130.3, 130.2, 130.2, 129.9, 129.8, 129.6, 129.1, 128.9, 128.7, 128.6, 128.5, 127.6, 126.1, 126.0, 125.3, 125.0, 124.9, 124.7 (Ar), 70.5, 70.5, 69.6, 69.6, 69.5, 69.3 (CH/CH_2), 26.4, 25.6, 25.2 (CH_3).

MS (ESI) m/z 323 $[Fe_2L_3]^{4+}$.

IR ν cm^{-1} 3358 br, s, 3001 w, 1555 m, 1467 w, 1233 m, 759 w, 701 m.

Elemental analysis found (calculated for $C_{75}H_{66}Cl_4Fe_2N_{12}O_3.11H_2O$) % C 54.70 (55.09), H 4.76 (5.42), N 9.67 (10.28).

S_c,Δ_{Fe},HHT-$[Fe_2L^2_3]Cl_4.11H_2O$

Data as for *R*-enantiomer

Yield 0.32 g, 96 %.

Elemental Analysis Found (calculated for $C_{75}H_{66}Cl_4Fe_2N_{12}O_3.11H_2O$) % C 55.02 (55.09), H 4.99 (5.42), N 10.04 (10.28).

R_c,Λ_{Fe},HHT-$[Fe_2L^3_3]Cl_4.14H_2O$

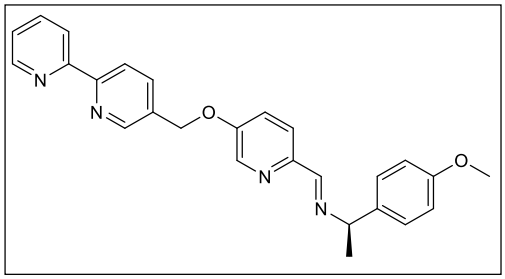

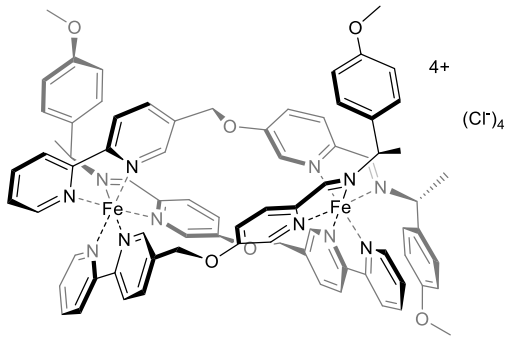

Yield 0.33 g, 94 %.

$^{13}C\{^1H\}$ NMR (126 MHz, 298 K, MeOH) δ_C 170.6, 170.9, 169.7 (CHN), 161.8, 161.1, 161.0, 160.9, 160.6, 160.5, 160.4, 160.2, 160.0, 159.4, 158.6, 158.3, 157.2, 156.6, 155.0, 154.0, 153.9, 153.8, 140.5, 139.7, 139.6, 136.7, 136.6, 133.3, 133.1, 132.6, 132.5, 131.3, 129.8, 129.1, 129.0, 128.5, 127.4, 127.4, 125.9, 125.3, 125.0, 124.9, 124.5, 115.6, 115.4, 115.2, 114.9 (Ar), 70.5, 70.0, 69.6, 69.5, 69.0, 68.7 (CH/CH_2), 56.0, 55.9, 55.9, (OCH_3), 26.3, 25.5, 25.1 (CH_3).

MS (ESI) m/z 346 $[Fe_2L_3]^{4+}$

IR ν cm^{-1} 3359 br s, 2968 m, 1607 w, 1510 m, 1301 m, 1235 s, 1023 m, 834 m.

Elemental analysis found (calculated for $C_{78}H_{72}Cl_4Fe_2N_{12}O_6.14H_2O$) % C 51.97 (52.65), H 5.33 (5.67), N 9.29 (9.45).

S_c,Δ_{Fe},HHT-[$Fe_2L^3_3$]Cl_4.14H_2O

Data as for *R*-enantiomer

Yield 0.32 g, 96 %.

Elemental analysis found (calculated for $C_{78}H_{72}Cl_4Fe_2N_{12}O_6.14H_2O$) % C 52.83 (52.65), H 5.48 (5.67), N 9.43 (9.45).

Λ_{Fe},HHT-[$Fe_2L^4_3$]Cl_4.9H_2O

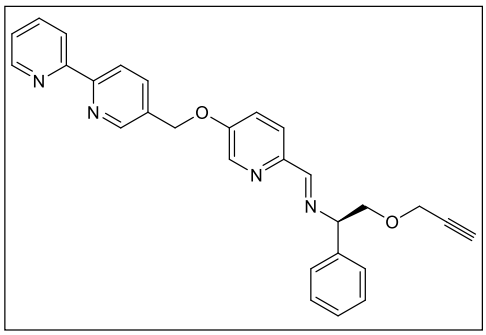

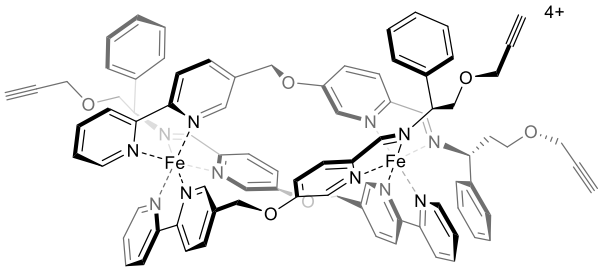

Λ_{Fe},HHT-[Fe_2**L**$^4_3$]Cl_4 was synthesised using the procedure described for Λ_{Fe},HHT-[Fe_2**L**$^3_3$]Cl_4, substituting (*R*)-1-phenylethan-1-amine for (*S*)-1-phenyl-2-(prop-2-ynyloxy)ethanamine.

Yield 0.243 g, 80 %.

$^{13}C\{^1H\}$ NMR (126 MHz, 298 K, MeOH) δ_C 172.0, 171.8, 171.3 (CHN), 161.1, 160.9, 160.8, 160.5, 160.3, 160.0, 159.4, 158.8, 158.2, 157.7, 157.1, 155.0, 153.8, 153.7, 153.5, 140.4, 139.8, 136.8, 136.6, 135.8, 135.1, 134.9, 133.8, 133.0, 132.6, 130.5, 130.3, 130.0, 130.0, 129.7, 129.6, 129.5, 129.1, 128.8, 128.4, 127.5, 127.4, 127.3, 127.1, 125.8, 125.3, 125.1, 125.0, 124.8, 124.7 (Ar), 77.6, 77.2, 77.0 (CH_2),

73.5, 73.3, 72.7 (CH), 71.9, 71.7, 71.3 (CH_2), 70.7, 69.6, 69.4 (C*C*H), 59.7, 59.5, 59.4 (*C*CH).

MS (ESI) m/z 364 $[Fe_2L_3]^{4+}$, 449 $[L+H]^+$.

IR υ cm^{-1} 3362 br s, 3024 m, 1556 m, 1434 w, 1233 m, 1082 m, 700 m.

Elemental analysis found (calculated for $C_{84}H_{72}Cl_4Fe_2N_{12}O_6.9H_2O$) % C 57.69 (57.29), H 4.89 (5.15), N 9.39 (9.54).

Δ_{Fe},HHT-[$Fe_2\mathbf{L}^{\mathbf{4}}{}_3$]$Cl_4$.9$H_2O$

Δ_{Fe},HHT-[$Fe_2\mathbf{L}^{\mathbf{4}}{}_3$]$Cl_4$ was synthesised using the procedure described for Λ_{Fe},HHT-[$Fe_2\mathbf{L}^{\mathbf{4}}{}_3$]$Cl_4$, substituting (*R*)-1-phenyl-2-(prop-2-ynyloxy)ethanamine for (*S*)-1-phenyl-2-(prop-2-ynyloxy)ethanamine.

Yield 0.222 g, 74 %.

MS (ESI) m/z 364 $[Fe_2L_3]^{4+}$, 449 $[L+H]^+$.

IR υ cm^{-1} 3355 br s, 3027 m, 1556 w, 1486 w, 1233 m, 1082 m, 700 m.

Elemental analysis found (calculated for $C_{84}H_{72}Cl_4Fe_2N_{12}O_6.9H_2O$) % C 56.68 (57.29), H 4.85 (5.15), N 9.29 (9.54).

Λ_{Fe},HHT-[$Fe_2\mathbf{L}^{\mathbf{5}}{}_3$]$Cl_4$

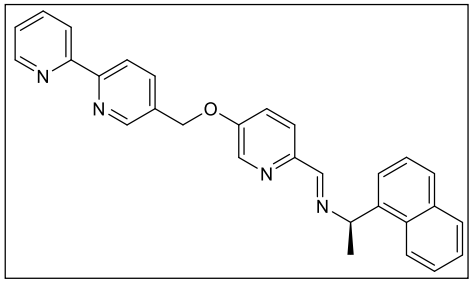

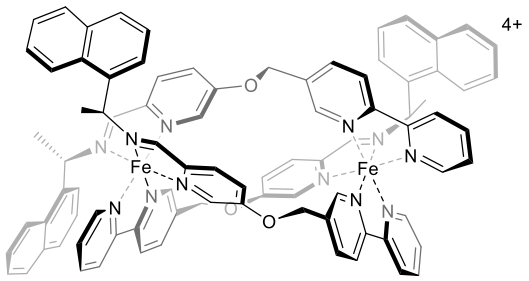

Λ_{Fe},HHT-[$Fe_2\mathbf{L}^{\mathbf{5}}{}_3$]$Cl_4$ was synthesised using the procedure described for Λ_{Fe},HHT-[$Fe_2\mathbf{L}^{\mathbf{3}}{}_3$]$Cl_4$, substituting (*R*)-1-phenylethan-1-amine for (*R*)-1-(naphthalen-1-yl)ethan-1-amine.

Yield 0.267 g, 89 %.

$^{13}C\{^{1}H\}$ NMR (126 MHz, 298 K, MeOH) δ_C 172.7, 172.2, 171.7 (CHN), 161.1, 161.9, 160.5, 160.4, 160.0, 159.7, 158.9, 157.7, 156.5, 155.4, 153.6, 153.4, 151.8, 149.5, 148.6, 148.5, 148.4, 148.3, 147.9, 147.4, 144.7, 142.8, 142.3, 141.2, 141.0, 140.6, 140.2, 140.0, 137.2, 137.1, 136.9, 136.6, 134.0, 133.4, 132.9, 130.6, 129.9, 129.6, 129.0, 128.9, 127.6, 127.5, 126.9, 125.2, 125.1, 125.1, 124.9, 124.8, 124.7, 124.4, 123.3, 122.8, 122.4 (Ar), 70.5 (CH_2), 69.8 (CH), 69.6, 69.5 (CH_2), 68.8, 68.7 (CH), 27.1, 25.9, 25.0 (CH_3).

MS (ESI) m/z 467 $[L+Na]^+$, 493 $[Fe_2L_3][Cl]^{3+}$

IR υ cm^{-1} 3364 br s, 2973 m, 1568 w, 1510 w, 1228 m, 1074 m, 702 w, 621 w.

Δ_{Fe},HHT-$[Fe_2\mathbf{L}^{5}_{3}]Cl_4$

Δ_{Fe},HHT-$[Fe_2\mathbf{L}^{5}_{3}]Cl_4$ was synthesised using the procedure described for Λ_{Fe},HHT-$[Fe_2\mathbf{L}^{5}_{3}]Cl_4$, substituting (*R*)-1-phenylethan-1-amine for (*S*)-1-phenylethan-1-amine.

Yield 0.211 g, 77 %.

MS (ESI) m/z 467 $[L+Na]^+$, 493 $[Fe_2L_3][Cl]^{3+}$

IR υ cm^{-1} 3356 br s, 2975 m, 1567 w, 1531 m, 1229 m, 1074 m, 702 w, 621 w.

R_c,Δ_{Fe},HHT-$[Fe_2\mathbf{L}^{6}]Cl_4.9H_2O$

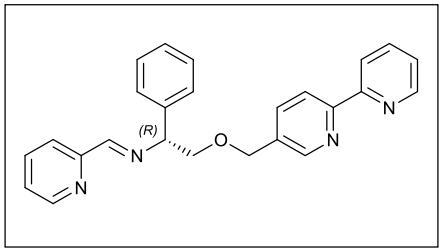

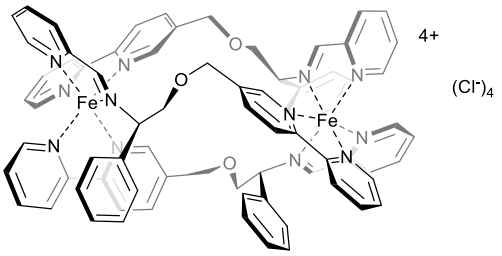

Yield 0.68 g, 87 %.

$^{13}C\{^{1}H\}$ NMR (126 MHz, 298 K, MeOH) δ_C 174.7, 174.6, 174.0 (CHN), 161.0, 160.4, 160.3, 160.0, 159.9, 159.9, 159.5, 159.3, 158.9, 158.7, 156.4, 155.7, 155.4, 154.8, 154.4, 154.2, 141.6, 141.4, 140.5, 140.0, 139.8, 138.8, 138.6, 138.3, 135.3, 133.8, 133.5, 132.7, 132.0, 131.4, 130.6, 130.3, 130.2, 130.1, 129.9, 129.7, 129.6, 129.2, 129.0, 128.9, 128.7, 127.0, 125.8, 125.1, 125.1, 124.2, 123.6 (Ar), 74.5, 74.4, 72.6 (CH), 70.9, 70.8, 70.5, 69.9 (CH_2).

MS (ESI) m/z 323 $[Fe_2L_3]^{4+}$.

IR ν cm^{-1} 3331 br, 3023 w, 1604 m, 1493 m, 1438 m, 1403 w, 1360 w, 1318 w, 1242 m, 1102 m, 1073 s, 1010 w, 936 m, 866 w, 836 w.

Elemental analysis found (calculated for $C_{75}H_{66}Cl_4Fe_2N_{12}O_3 \cdot 9H_2O$) % C 56.52 (56.33), H 5.31 (5. 92), N 10.68 (10.51)

S_c,Λ_{Fe},HHT-$[Fe_2L^6]Cl_4.9H_2O$

Data as for *R*-enantiomer

Yield 0.64 g, 82 %.

MS (ESI) m/z 323.7 $[Fe_2L_3]^{4+}$.

Elemental analysis found (calculated for $C_{75}H_{66}Cl_4Fe_2N_{12}O_3 \cdot 9H_2O$) % C 56.02 (56.33), H 5.22 (5.29), N 10.34 (10.51).

NMR Spectra

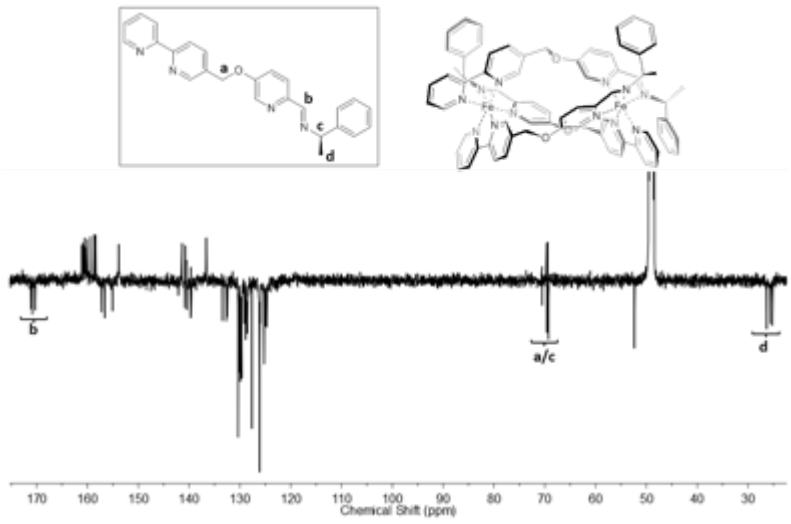

Figure S4.1. $^{13}C\{^{1}H\}$ (126 MHz) NMR spectrum of R_c,Λ_{Fe},HHT-$[Fe_2L^1{}_3][ClO_4]_4$ in d^4-methanol at 298 K with key assignments. Residual solvent δ_C 49.00 (δ_C 52.35 free amine).

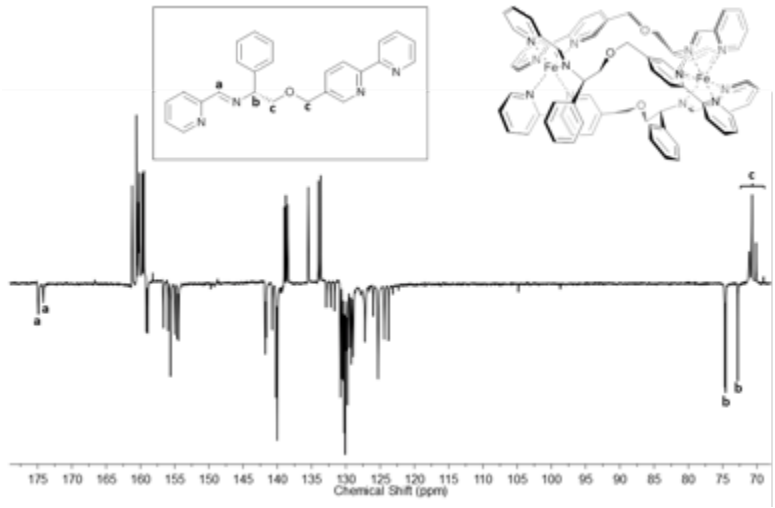

Figure S4.2. $^{13}C\{^{1}H\}$ (126 MHz) NMR spectrum of R_c,Δ_{Fe},HHT-$[Fe_2L^6{}_3][ClO_4]_4$ in d^4-methanol at 298 K with key assignments.

Thermogravimetric analysis

Thermogravimetric analysis was used to determine the amount of water of crystallisation present in the chloride salts of iron (II) triplex metallohelices. An accurately weighed 40 µl aluminium crucible was heated from 25 to 400 °C at 10 °C.min^{-1} under dinitrogen in a DSC1-1600 scanning calorimeter. The mass lost was plotted against temperature (see below) and the % mass loss from 70-120 °C (loss of water) was calculated.

R_c,Λ_{Fe},HHT-[$Fe_2\mathbf{L}^{\mathbf{1}}$]$Cl_4$

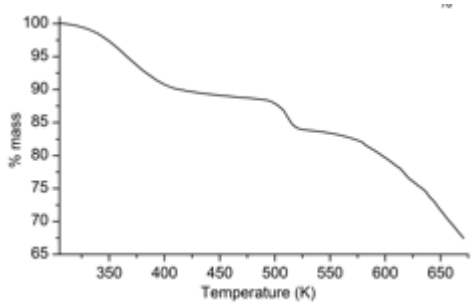

S_c,Δ_{Fe},HHT-[$Fe_2\mathbf{L}^{\mathbf{1}}$]$Cl_4$

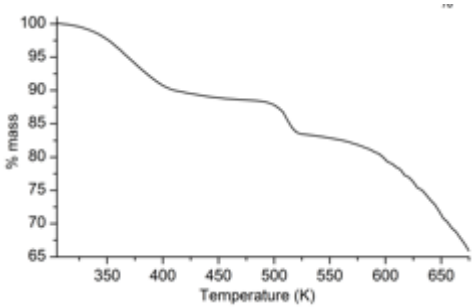

R_c,Λ_{Fe},HHT-[$Fe_2\mathbf{L}^{\mathbf{2}}$]$Cl_4$

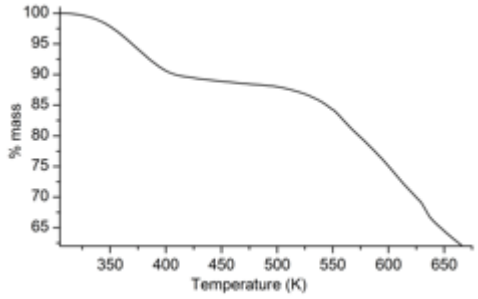

S_c,Δ_{Fe},HHT-[$Fe_2\mathbf{L}^{\mathbf{2}}$]$Cl_4$

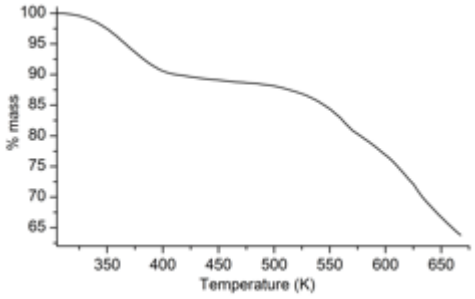

R_c,Λ_{Fe},HHT-[$Fe_2\mathbf{L}^{\mathbf{3}}$]$Cl_4$

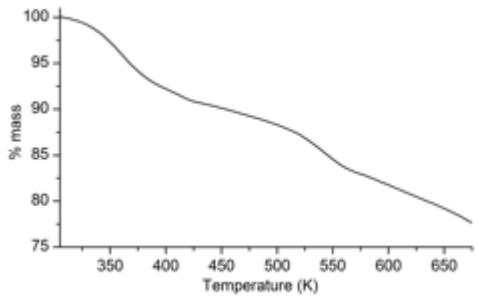

S_c,Δ_{Fe},HHT-[$Fe_2\mathbf{L}^{\mathbf{3}}$]$Cl_4$

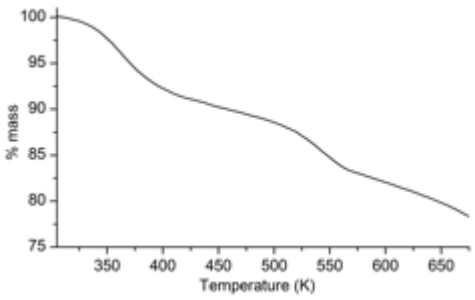

R_c,Δ_{Fe},HHT-$[Fe_2\mathbf{L^6}]Cl_4$ S_c,Λ_{Fe},HHT-$[Fe_2\mathbf{L^6}]Cl_4$

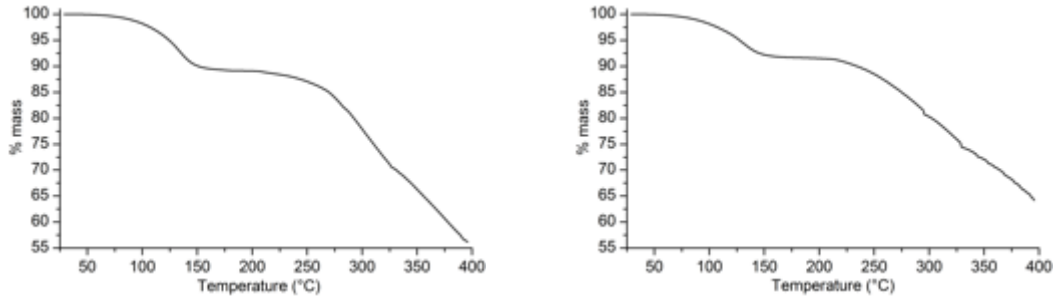

Figure S4.3. Example thermogravimetric analysis of triplex metallohelices. Indicating mass lost due to water of crystallisation and thermal decomposition.

Circular dichroism spectroscopy

Spectra were measured on a Jasco J-815 spectrometer, calibrated conventionally using 0.060 % ACS a holmium filter. Measurements were collected using a 1 cm path-length quartz cuvette. The parameters used were; bandwidth 1 nm, response time 1 sec, wavelength scan range 200 – 750 nm, data pitch 0.2 nm, scanning speed 100 $nm.min^{-1}$ and accumulation 4.

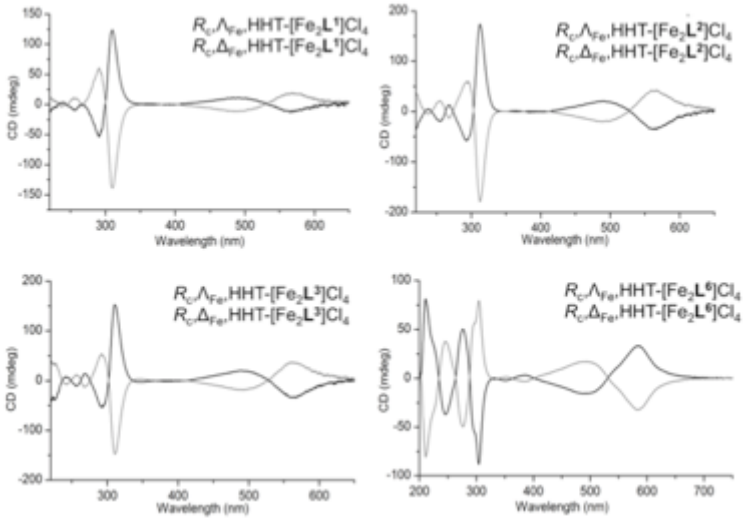

Figure S4.4. Example CD spectra of pairs of enantiomers of triplex metallohelices (0.03 mM in water); each enantiomer shows an equal and opposite spectrum to its pair.

References

[1] P. Das, A. Ghosh, M. K. Kesharwani, V. Ramu, B. Ganguly, A. Das, *Eur. J. of Inorg. Chem.* 2011, *2011*, 3050-3058.

[2] C. Dallaire, I. Kolber, M. Gingras, in *Organic Syntheses*, John Wiley & Sons, Inc., 2003.

[3] M. Seredyuk, A. B. Gaspar, V. Ksenofontov, Y. Galyametdinov, J. Kusz, P. Gütlich, *J. Am. Chem. Soc.* 2008, *130*, 1431-1439.

[4] Y. Hsiao, L. S. Hegedus, *J. Org. Chem.* 1997, *62*, 3586-3591.

[5] S. E. Howson, A. Bolhuis, V. Brabec, G. J. Clarkson, J. Malina, A. Rodger, P. Scott, *Nat. Chem.* 2012, *4*, 31-36.

[6] O. Branytska, L. J. W. Shimon, R. Neumann, *Chem. Commun.* 2007, 3957-3959.

Appendix 5

Appendix 5: Supplementary Information for "Rational, yet Simple, Design and Synthesis of an Antifreeze-Protein Inspired Polymer for Cellular Cryopreservation"

Additional data

^{1}H NMR spectrum of *N*-boc ethanolamine

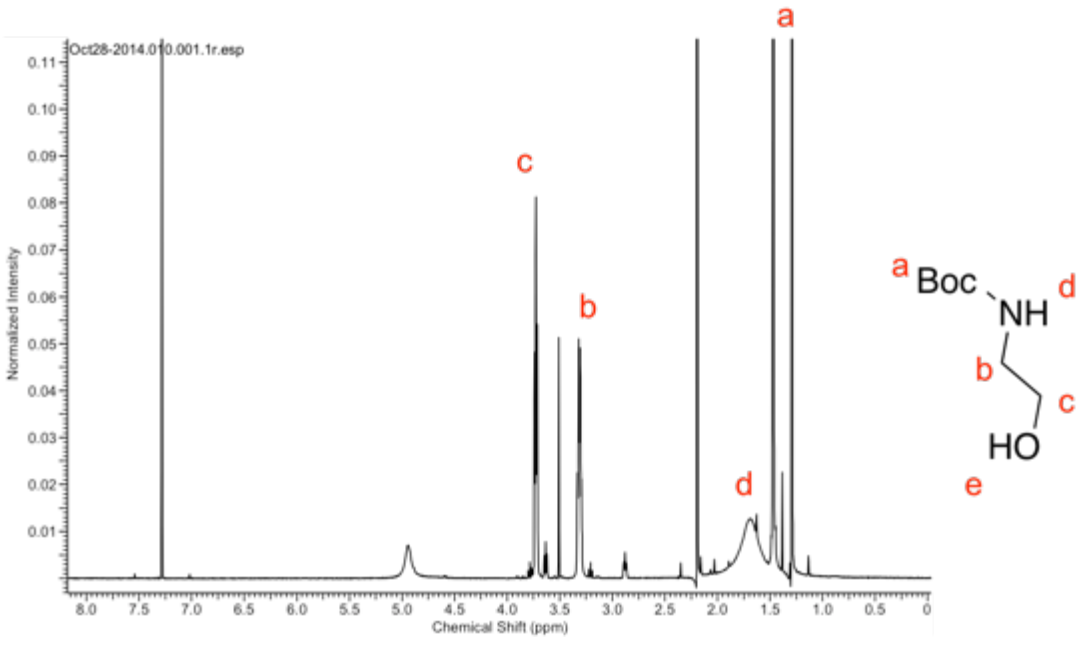

Figure S5.1. ^{1}H NMR of *N*-boc ethanolamine (400 MHz, $CDCl_3$).

Mass-spectroscopy spectrum for *N*-boc ethanolamine

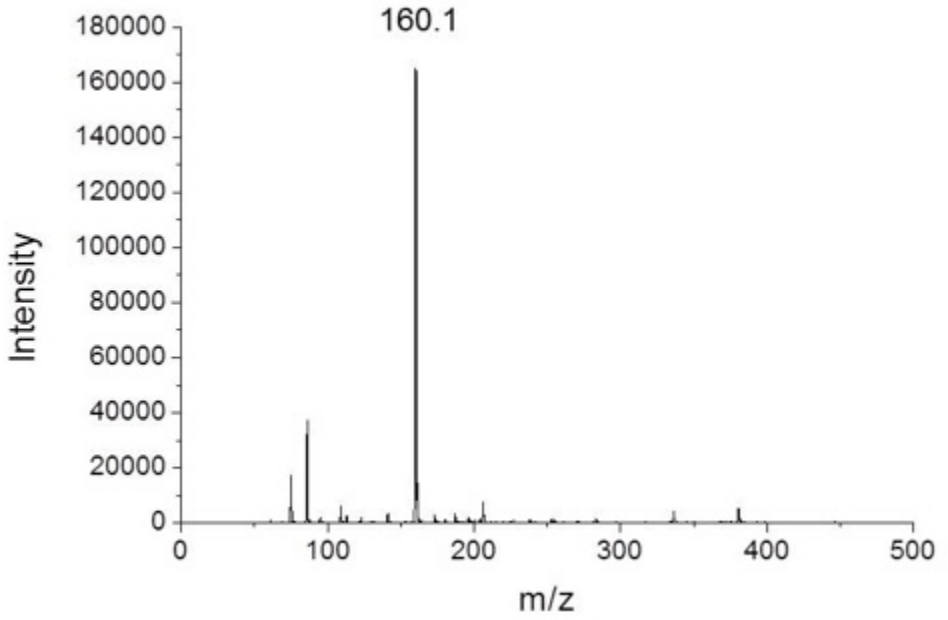

Figure S5.2. EI Mass-spectrometry spectra of *N*-boc ethanolamine.

^{1}H NMR spectrum of poly(methyl vinyl ether-*alt*-maleic anhydride)

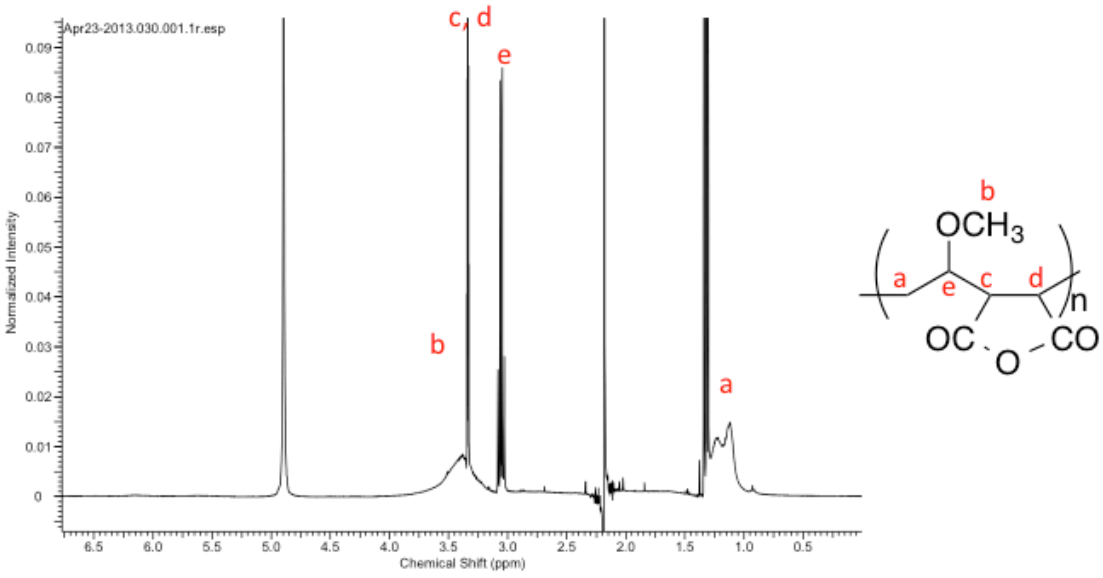

Figure S5.3. ^{1}H NMR of poly(methyl vinyl ether-*alt*-maleic anhydride).

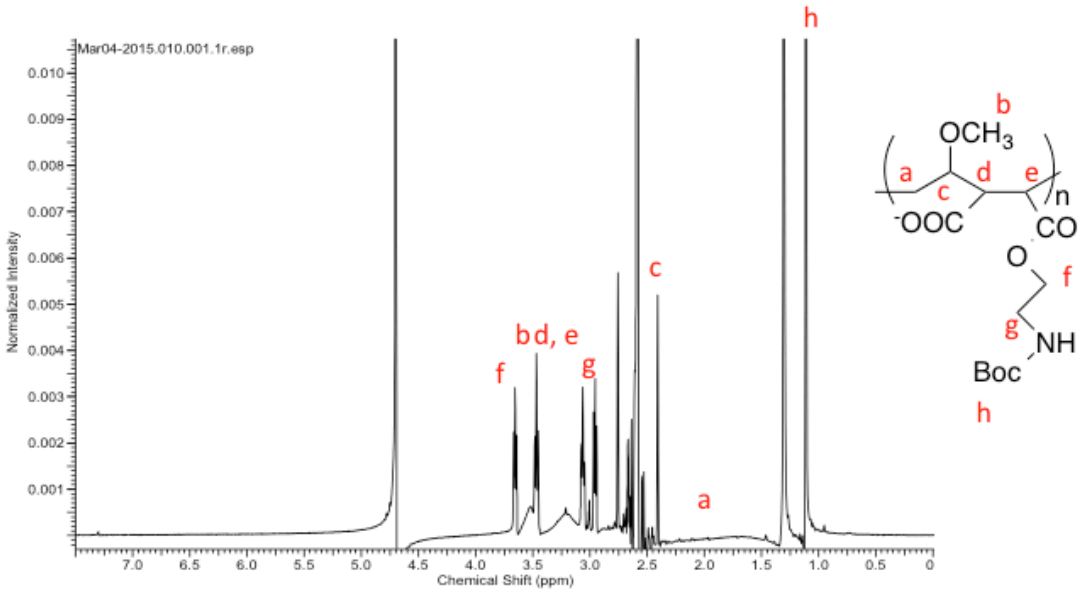

Figure S5.4. ^{1}H NMR functionalized PMVEMA with boc protected ethanol amine.

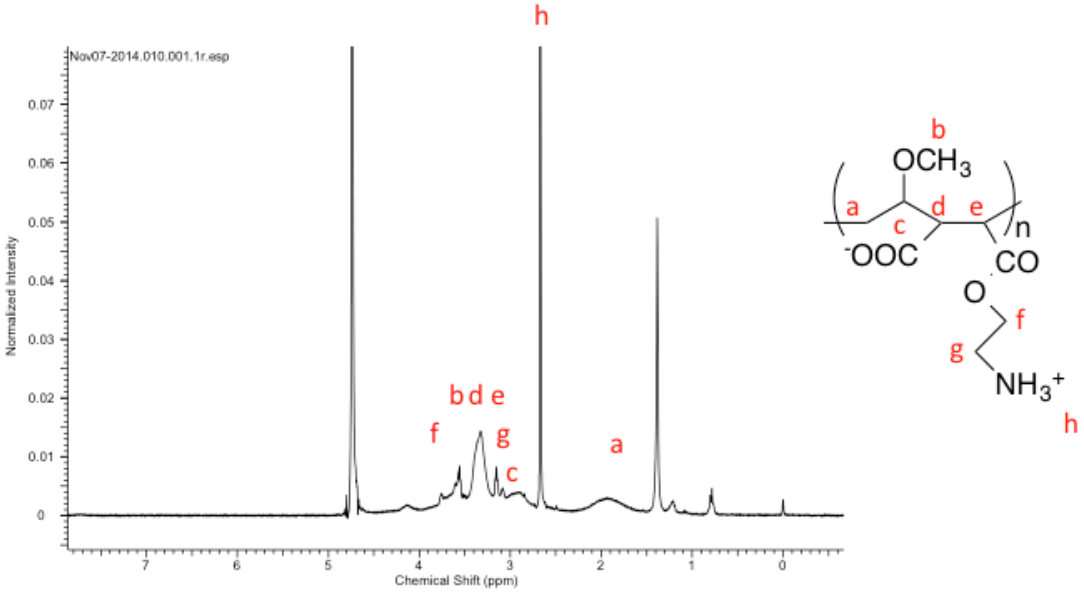

Figure S5.5. **^{1}H NMR functionalized polymer deprotected with TFA.**

Differential scanning calorimetry of HES and PMVEMA-*co*-EA

In order to ascertain that the cryosolution does not vitrify differential scanning calorimetry (DSC) was used, Figure S5.6. As seen in Figure S5.6, there is a sharp peak at around –14 °C which is characteristic of crystallization.

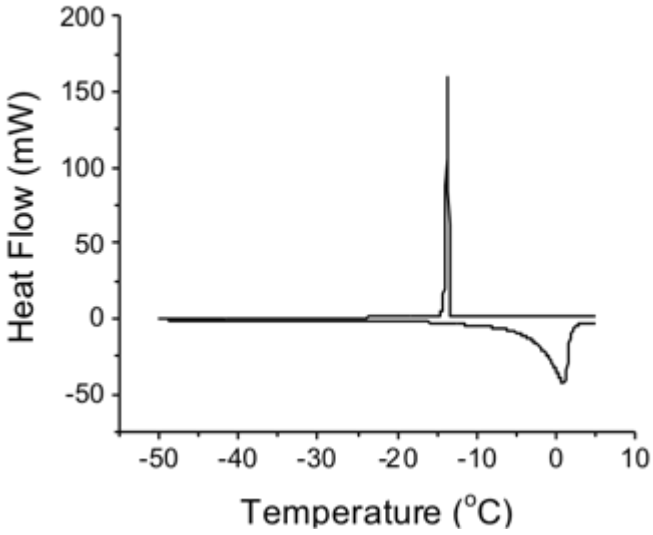

Figure S5.6. DSC of HES and PMVEMA-*co*-EA. Cooling rate was 2 °C per minute, heating rate was 10 °C per minute.

IRI activity of PMVEMA-*co*-EA dialyzed against sodium chloride

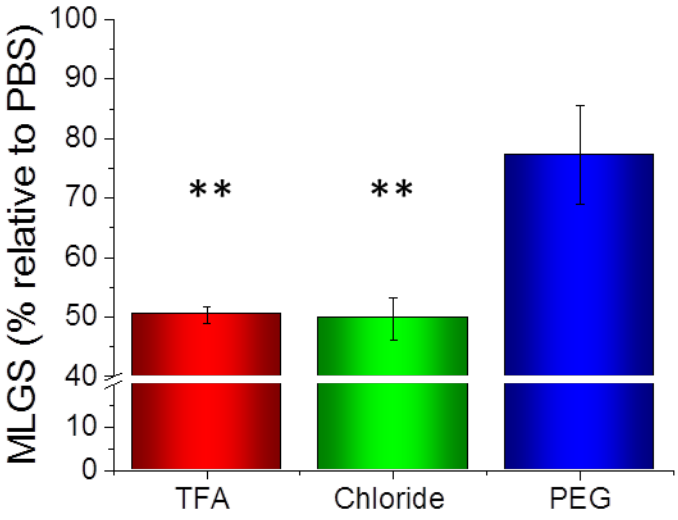

Figure S5.7. Ice recrystallization inhibtion of PMVEMA-*co*-EA with chloride counter ion compared to trifluoracetate counter ion. Mean largest grain size (MLGS) expressed as a percentage of PBS buffer control, all samples were at 20 $mg.mL^{-1}$. Error bars represent ± SD from a minimum of 3 repeats.

Cryopreservation using fast thaw methodology

Samples were frozen in liquid nitrogen, stored for 5 days then thawed at 37 °C in a water bath. The rapid level of thawing limits the time in which ice recrystallization can occur and limits damage to cells, figure S5.8 shows greater recovery for all samples, and a very limited improvement from adding PMVEMA-*co*-EA. However, the volumes of blood stored would likely be scaled up in commercial storage, meaning that differential warming rates would occur making the slow warming methodology more relevant for cryoprotective applications.

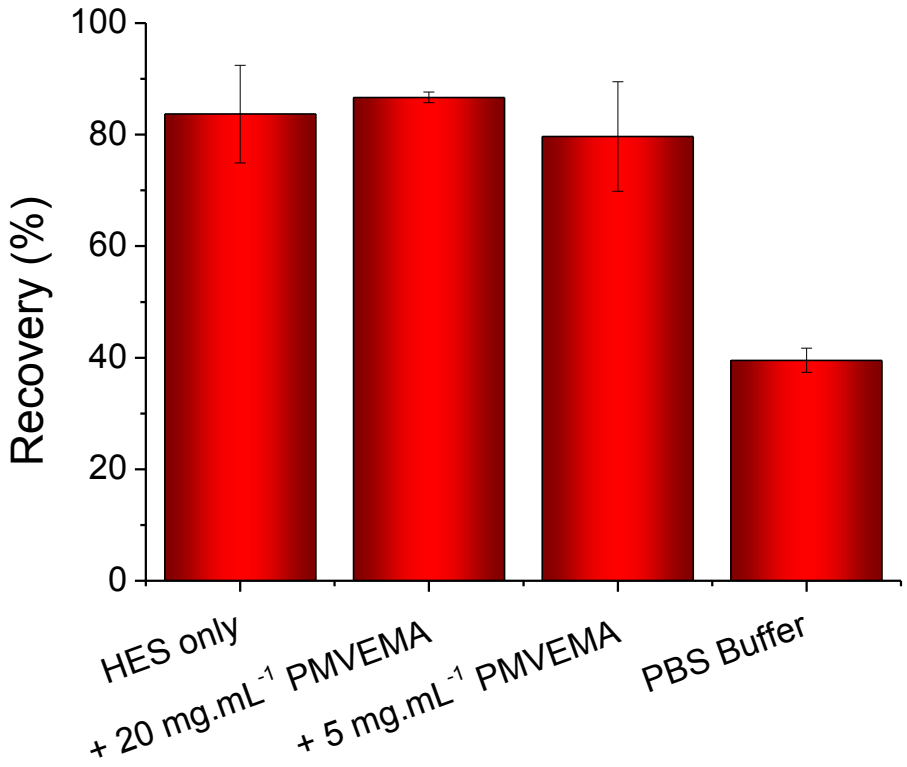

Figure S5.8. Recovery from fast thawing of red blood cells. Standard Cryomix contained containing HES (350 mg.mL^{-1}), mannitol (30 mg.mL^{-1}) sodium chloride (6.5 mg.mL^{-1}) with PMVEMA-*co*-EA added. Error bars represent ± SD from a minimum of 3 repeats.

Appendix 6

Appendix 6: Supplementary information for "A Simple Polymeric Solution to the Challenge of Therapeutic Protein Storage".

Serial dilutions of cryoprotectants

In order to determine the optimal concentrations of the cryoprotectant mixtures used, serial dilutions were made, Figure S6.1. It seems that recovery drops significantly when PEG concentration is reduced below 40 $mg.mL^{-1}$, while there is little benefit over the 3 day period of increasing concentration over 50 $mg.mL^{-1}$. In addition the PVA concentration can be reduced as low as 0.5 $mg.mL^{-1}$, before recovery drops below a significant level. Furthermore increasing the concentration of either PEG or PVA from 100 $mg.mL^{-1}$ and 1 $mg.mL^{-1}$ used in the main manuscript results in no significant benefits. A serial of dilution of trehalose was also undertaken for comparison, figure S6.2.

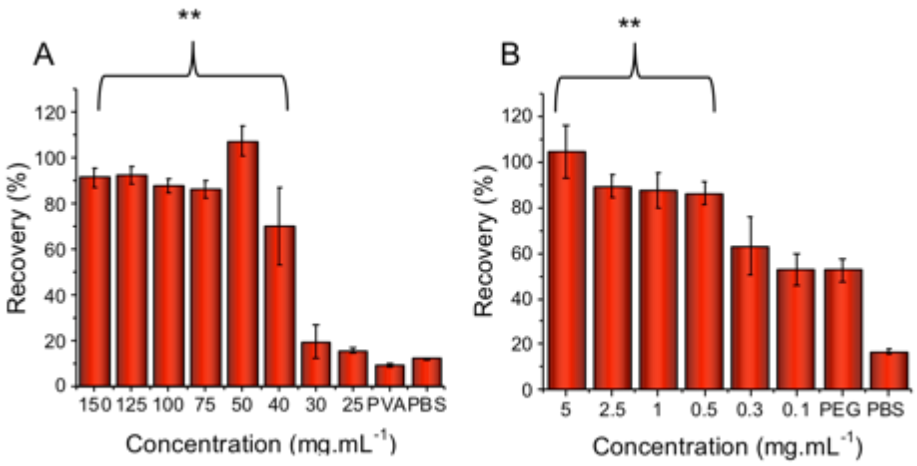

Figure S6.1. **Dilutions of PEG and PVA frozen and stored for 3 days at -20 °C.** A.) Serial dilution of PEG, with 1 mg.mL^{-1} PVA; B.) Serial dilution of PVA, with 100 mg.mL^{-1} PEG. ** Represents $p < 0.01$ relative to PBS buffer, error bars are calculated from minimum of 6 repeats. Recovery expressed as a percentage of fresh unfrozen β-Gal.

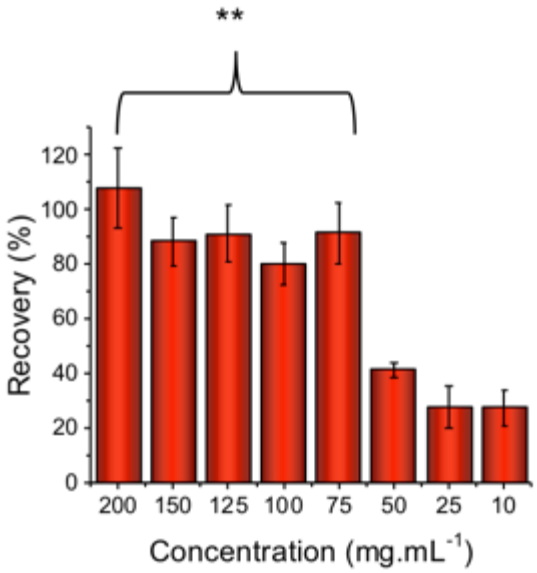

Figure S6.2. **Serial dilution of trehalose, frozen and stored for 3 days at -20 °C.** ** Represents $p < 0.01$. Error bars are calculated from a minimum of 6 repeats, recovery is expressed as a percentage of unfrozen β-Gal.

The ability of trehalose to protect β-Gal under freezing drops significantly below 75 $mg.mL^{-1}$. In comparison to PEG and PVA, which still provides significant recovery at 40 $mg.mL^{-1}$ and 1 $mg.mL^{-1}$ respectively, a higher concentration. This is appealing as all additives can have potentially negative effects on biological materials when added in high concentration.

Aggregation induced damage caused by freezing and thawing

As ice crystals grow by an Ostwald ripening process, whereby larger ice crystals grow at the expense of smaller ones, overall surface area reduces over time resulting in proteins being forced closer together and consequently are more likely to aggregate, Figure S6.3A-B. To assess whether this was occurring and whether it was having a detrimental effect on the protein, dynamic light scattering was used to investigate the size of β-Gal particles before and after freezing, figure S6.3C.

It appears that PVA and PEG / PVA mix stops aggregation due to freezing and thawing when compared to a PBS buffer control as seem in Figure S6.3C. As PEG and PVA together seem to provide a greater level of protection when compared to PVA alone, it is surmised that the stabilizing effect of the PEG is required in addition to the IRI activity exhibited by the PVA, but due to the difficulty in undertaking DLS on protein-polymer mixtures, these results should not be viewed as conclusive proof.

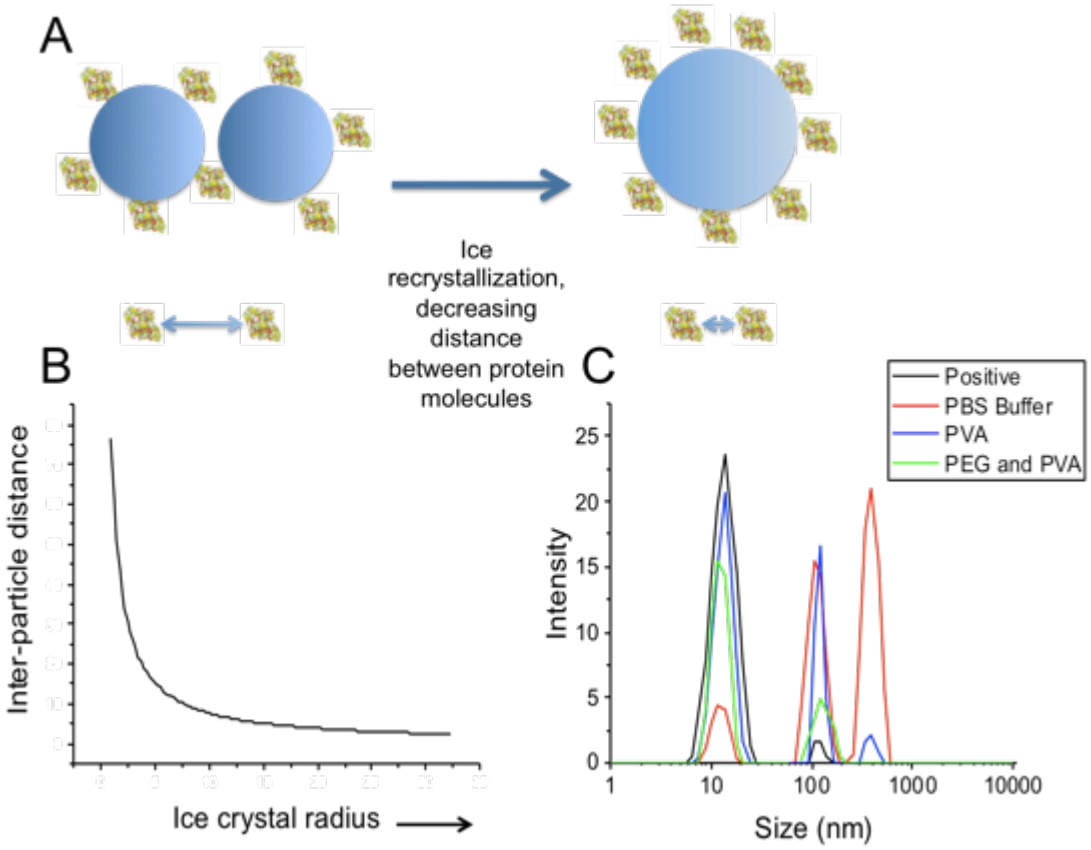

Figure S6.3. Freeze-thaw induced aggregation of β-Gal. A.) Schematic showing reduction in inter-particle distance; B.) Ice crystal radius against inter-particle distance; C.) Dynamic light scattering plot of β-Gal. Positive control is sample of unfrozen protein, β-Gal was made in solution at 3 $mg.mL^{-1}$, PVA at 0.8 $mg.mL^{-1}$, PEG at 80 $mg.mL^{-1}$.

Assessment of Taq polymerase through PCR

As a preliminary test to determine whether PEG and PVA together provide an efficient method of protection, PCR was used, and the resulting products imaged on a 1 % agarose gel, Figure S6.4.

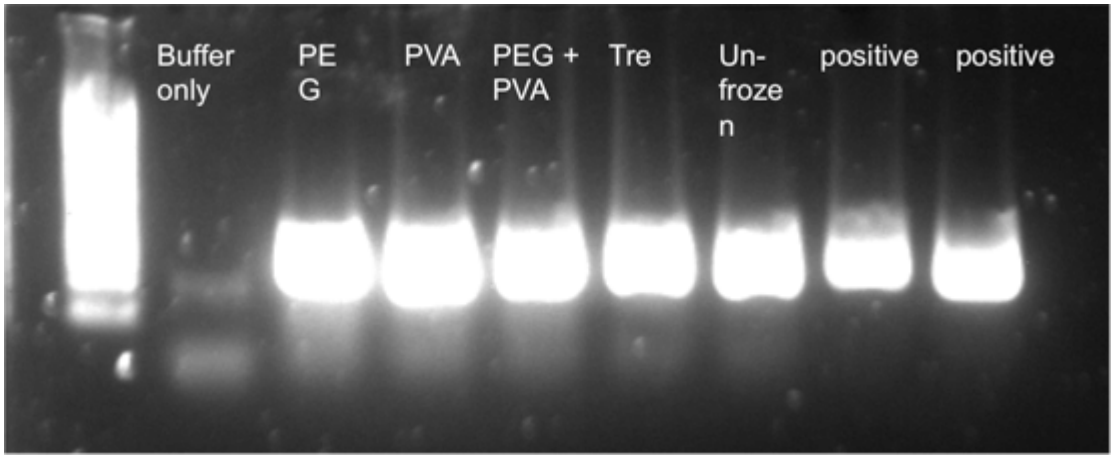

Figure S6.4. PCR products of Taq samples protected using various cryoprotectants. Positive controls are measured using commercially available Taq stored in glycerol. Unfrozen sample was measured using fresh dialysed Taq. Samples were frozen for 5 days at -20 °C.

While this initial test proved inconclusive, the sample frozen in just buffer exhibited no activity, demonstrating that damage is caused by the freezing process and that QPCR would provide a good method of differentiating the level of recovery achieved by different protective mixtures.

Freezing and thawing of glucose oxidase

Glucose oxidase was also stored at -20 °C in order to determine whether the PEG and PVA mixture worked for a range of proteins, Figure S6.5. The recovery was found to be significantly increased when the polymer mix was added with respect to PBS buffer only, therefore it suggests that this mix can be used as a general cryoprotection solution.

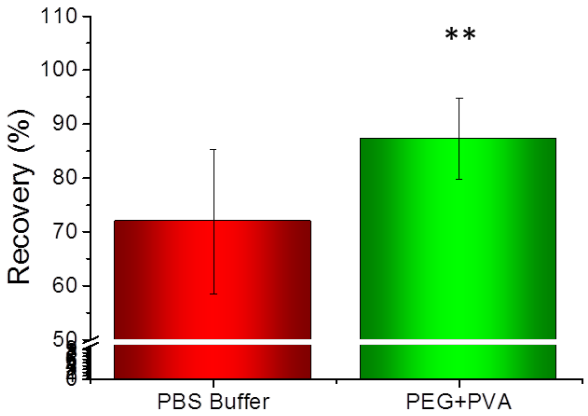

Figure S6.5. **Recovery of glucose oxidase after freezing and thawing at -20 °C for 7 days.** Recovery is expressed as a percentage of fresh, unfrozen protein, error bars are from a minimum of six repeats, ** represents $p < 0.01$ relative to PBS buffer.

Curriculum Vitae

Daniel E. Mitchell

daniel.mitchell@warwick.ac.uk

MOAC DTC, University of Warwick
Gibbet Hill Road
Coventry
West Midlands, CV4 7AL
0044 247 6573550

Education

2012- present **PhD Student in Mathematical Biology and Biophysical Chemistry**, University of Warwick. Expected submission data, September 2015.
Thesis Title: "The Rational Design and Applications of Synthetic Antifreeze protein mimics".
Supervisor: Dr Matthew Gibson.

2012 **MSc Mathematical Biology and Biophysical Chemistry (Distinction)**, University of Warwick.

2011 **BEng Civil Engineering (1st Class Honours)**, University of Bristol.

Research Experience

2012- present Department of Chemistry and School of Life Sciences, University of Warwick. Investigation of antifreeze proteins, their synthetic mimics and uses in cryopreservation of biological material.

Bursaries and Awards

2015 Biochemical Society student travel bursary.
2015 RSC Macro group student travel bursary.

Publications

- **D.E. Mitchell**, M. Lilliman, S.G. Spain, and M.I. Gibson, *Biomater. Sci.*, 2014, **2**, 1787-1795. "Quantitative Study on the Antifreeze Protein Mimetic Ice Growth Inhibition Properties of Poly(ampholytes) Derived from Vinyl-Based Polymers"
- **D.E. Mitchell**, T.R Congdon, A. Rodger, M.I Gibson. In Revision. "Gold Nanoparticle Aggregation as a Probe of Antifreeze (Glyco) Protein-Inspired Ice Recrystallization Inhibition and Identification of New IRI Active Macromolecules".

- **D.E. Mitchell**, M.I Gibson. *Chem. Commun.,* 2015, 51, 12977-12980. "Rational, yet simple, design and synthesis of an antifreeze-protein inspired polymer for cellular cryopreservation."
- **D.E. Mitchell** and M.I. Gibson, *Biomacromolecules*, 2015, Accepted. "Latent Ice Recrystallization Inhibition Activity in Non-Antifreeze Proteins; Ca^{2+} Activated Plant Lectins and Cation-Activated Antimicrobial Peptides".
- **D.E. Mitchell**, R. Kaner, P. Scott and M.I. Gibson, In preparation for: "Metallohelices Mimic the Ice Recrystallization Inhibition Activity of Helical Antifreeze Proteins".
- **D.E. Mitchell**, R.C. Deller, J. Gutierrez-Marcos, M.I. Gibson, In preparation for: "A simple polymeric solution to the challenge of therapeutic protein storage".

Teaching Experience

2012- present: Mentoring of undergraduate project students within a research laboratory setting.
2013 Laboratory Demonstrator.

Additional Training

2014 Circular and linear dichorism summer school, University of Warwick.
2014 Fast track cell culture course, University of West of England.

Technical Skills

- Polymer chemistry and associated techniques, encompassing RAFT polymerization, NMR spectroscopy, mass spectroscopy, size exclusion chromatography and FTIR spectroscopy.
- Microbiology techniques, including PCR, quantitative PCR, protein expression and purification and plasmid transformation.
- Analytical chemistry, including CD spectroscopy, differential scanning calorimetric, dynamic light scattering spectroscopy and UV/vis spectroscopy.
- Computational chemistry skills, C, Tcl and python programming languages, NAMD, DLPOLY molecular dynamics programs, VMD, pymol and ImageJ molecular visualization programs.
- Cell biology, including cell culture techniques and cryopreservation of cellular material

Research Interests

- Design and synthesis of polymers that mimic properties possessed by antifreeze proteins.
- The evolutionary basis of antifreeze proteins.
- Study of ice crystal growth inhibition using molecular dynamics simulations.
- Cryo-storage of biological material.
- Design and synthesis of antimicrobial polymers.

Conference Presentations

Oral- Biochemical Society, Carbohydrate enzymes in medicine and biotechnology, University of St Andrews, UK. August 2015. “L-type lectins structural and functional similarities to antifreeze proteins.”

Oral - Inter-DTC Conference June 2014, University of Warwick, “Extremophile engineering- polymeric mimics of antifreeze proteins”.

Oral- Molecular mechanisms seminar workshop, University of Warwick- “Searching for antifreeze-protein function in non- antifreeze protein”

Poster- Challenges in chemical biology, Zurich. Switzerland. June 2015. “Novel cryoprotectants and the origin of antifreeze proteins.”

Poster- RSC Younger Members Symposium, University of Birmingham, June 2014, “Extremophile engineering- polymeric mimics of antifreeze proteins”.

Poster- Internatational Conference on Materials Chemistry July 2013, University of Warwick, "Investigating Polymers as Antifreeze molecules".

Poster- RSC Biomaterials Group annual meeting, Sheffield Hallem University, January 2013, “Antifreeze proteins and synthetic mimics”

Academic Community Involvement

2013- present: Representative on departmental student staff liaison committee.

2014- present: University of Warwick public engagement network member.

References

- Dr Matthew Gibson, Department of Chemistry, University of Warwick, UK. m.i.gibson@warwick.ac.uk.
- Prof. Alison Rodger, Department of Chemistry, University of Warwick, UK. a.rodger@warwick.ac.uk.
- Elizabeth Fullam, School of Life Sciences, University of Warwick, UK. e.fullam@warwick.ac.uk.